Volume 1, Number 3

September-October, 1960

KINETICS AND CATALYSIS

КИНЕТИКА И КАТАЛИЗ/KINETIKA I KATALIZ

TRANSLATED FROM RUSSIAN

CONSULTANTS BUREAU

KINETIKA I KATALIZ
EDITORIAL BOARD:

A. A. Balandin
G. K. Boreskov *(Editor)*
V. T. Bykov
I. V. Kalechits
A. A. Koval'skii
V. N. Kondrat'ev
K. I. Matveev *(Secretary)*
S. Z. Roginskii
M. G. Slin'ko
V. V. Voevodskii *(Acting Editor)*
N. N. Vorozhtsov

KINETICS AND CATALYSIS

A translation of KINETIKA I KATALIZ,
a publication of the Academy of Sciences of the USSR

© 1961 CONSULTANTS BUREAU ENTERPRISES, INC.
227 West 17th Street, New York 11, N. Y.

Volume 1, Number 3 September-October, 1960

CONTENTS

	PAGE ENG.	PAGE RUSS.
The Relation Between the Lower Limit of Autoignition of Hydrogen-Oxygen Mixtures and Composition. O. A. Ivanov and A. B. Nalbandyan	311	337
The Kinetic Features of the High-Temperature Cracking of Isopentane. A. M. Brodskii, K. P. Lavrovskii, and Su Wei-Hang	314	340
The Mechanism of Formation of Methyl Alcohol During the Oxidation of Hydrocarbons. M. B. Neiman, V. Ya. Efremov, and N. K. Serdyuk	319	345
The Isotopic Exchange of Hydrogen on Specimens of n- and p-Type Germanium. V. L. Kuchaev and G. K. Boreskov	330	356
The Mechanism of the Acid Decomposition of Hydroperoxides. Yu. A. Shlyapnikov	339	365
Mechanism of Homogeneous Catalytic Activity of Molecular Hydrogen. V. K. Bykhovskii and O. N. Temkin	347	374
Effect of Cathodic and Anodic Polarization on the Catalyst for Ammonia Synthesis and Its Activity. L. M. Dmitrenko, S. S. Lachinov, and R. F. Sibyakova	352	379
Catalytic Activity of Nickel Catalysts. II. Effect of Additions of Transition Metals. G. D. Lyubarskii, L. N. Ivanovskaya, G. G. Isaeva, D. I. Lainer, and N. M. Kagan	358	385
The Activation of Fused Iron Fischer-Tropsch Catalysts Under the Influence of the Reaction Mixture. Yu. B. Kagan, A. N. Bashkirov, E. V. Kamzolkina and S. M. Loktev	365	393
Characteristics of the Kinetics of the Isomerization of Allylbenzene on Platinum Films at High Temperatures. V. I. Shimulis, V. M. Gryaznov, and A. E. Cherkashin	372	401
Investigation of the Kinetics of the Oxidation of Sulfur Dioxide Over Platinum Catalyst Under Equilibrium Conditions. V. A. Roiter, N. A. Stukanovskaya, G. P. Korneichuk, N. S. Volinkovskaya, and G. I. Golodets	379	408
A Study of Orthoxydrogen–Parahydrogen Conversion Over Solid Catalysts. II. Reaction in the Liquid Phase. R. A. Buyanov	389	418
An Isotopic Study of the Surface Heterogeneity of Oxide Catalysts for Decomposition of Isopropyl Alcohol. 1. Calcium Oxide. O. V. Krylov and E. A. Fokina	392	421
Modifying of Catalysts for Hydrocarbon Oxidation. E. Kh. Enikeev, O. V. Isaev, and L. Ya. Margolis	402	431
Decomposition of Formic Acid and Esterification of Acetic Acid in the Vapor Phase on the Ion-Exchange Resin KU-2. T. I. Andrianova and B. P. Bruns	410	440
Selective Hydrogenation of Butynediol into Butenediol on a Nickel Skeleton Catalyst. L. Kh. Freidlin, A. A. Balandin, and I. F. Zhukova	416	447

Annual Subscription: $150 **Single Issue: $35** **Single Article: $12.50**

Note: The sale of photostatic copies of any portion of this copyright translation is expressly prohibited by the copyright owners.

CONTENTS (continued)

	PAGE	RUSS. PAGE
Investigation of the Adsorption Characteristics of Chromia–Alumina–Potassium Paraffin Dehydrogenation Catalysts. A. M. Rubinshtein, K. I. Slovetskaya, and T. R. Brueva	424	455
The Effect of Restriction of Internal Diffusion on the Kinetics of Ethylene Hydrogenation. A. Ya. Rozovskii, V. V. Shchekin, and E. G. Pokrovskaya	432	464
The Effect of the Pore Structure of Catalysts on Catalytic Activity and on the Kinetic Parameters of Cracking Reactions. K. V. Topchieva, T. V. Antipina, and Li He-Suyan	438	471
On The Question of the Wall Heat Transfer Coefficient in Pakced Tubes. M. E. Aerov and Ya. F. Batishchev,	445	478
REPORT		
Second European Symposium on the Processes of Chemical Technology. G. K. Boreskov and M. G. Slin'ko	450	483

THE RELATION BETWEEN THE LOWER LIMIT OF AUTOIGNITION OF HYDROGEN–OXYGEN MIXTURES AND THEIR COMPOSITION

O. A. Ivanov and A. B. Nalbandyan

Institute of Chemical Physics, Academy of Sciences of the USSR
Translated from Kinetika i Kataliz, Vol. 1, No. 3, pp. 337-339, September-October, 1960
Original article submitted January 20, 1960

We have measured the lower limit for autoignition of hydrogen-oxygen mixtures as a function of composition for three temperatures, in a vessel treated with potassium tetraborate. The lower limit values obtained were very small, so that reaction was occurring in the kinetic region. It was shown that, in accordance with N. N. Semenov's theory of the lower limit, the initiating active centers were hydrogen atoms in mixtures containing 5 to 50% of oxygen. A value was obtained for the branching constant of $H + O_2 = OH + O$, the activation energy was determined, and it was established that hydrogen atoms were probably removed on the surface of the reactor treated with potassium tetraborate.

* * *

In 1937 one of the authors, together with A. Biron [1], showed that in accordance with N. N. Semenov's theory [2] for the lower limit of autoignition, the product of the lower limit (P_{lim}) and the proportion of oxygen γ in the hydrogen–oxygen mixture remained approximately constant at constant temperature, in a fused pyrex vessel which had been treated with flashes. As γ altered from 0.1 to 0.5, i.e., by a factor of 5, the product $P_{lim} \cdot \gamma$ only altered from 0.06 to 0.07.

In connection with the production of new more precise data, relating to the separate elementary reactions and leading to a detailed mechanism for the chain oxidation of hydrogen, it became necessary to carry out a careful check on this important aspect of the theory, based on the deduction that in hydrogen-rich mixtures the concentration of hydrogen atoms should be considerably greater than the concentrations of OH radicals or O atoms. This deduction led us to conclude that, in considering the conditions determining the lower ignition limit, it was only necessary to consider the loss of hydrogen atoms on the reaction vessel walls and that the loss of other chain carriers (OH and O) could be neglected, although the loss of OH radicals was considerably more probable than that of H atoms.

The objects of the present paper were to determine precisely the application range of the simple formula $P_{lim} \cdot \gamma$ = constant, and to investigate the probability of H atom adhesion to the reaction vessel walls and its variation with temperature, under the conditions that the reaction vessel had been washed out with hydrofluoric acid and then treated with potassium borate.

The experiments were carried out in a cylindrical quartz vessel, 5.8 cm in diameter and 10 cm long. In order to obtain the minimum P_{lim} values, the vessel was first washed out with warm concentrated hydrofluoric acid, then washed repeatedly with distilled water, and finally treated with a 2% solution of potassium tetraborate. The ignition limit was determined from the change in pressure, using a membrane manometer of sensitivity 104 mm of scale for 1 mm Hg.

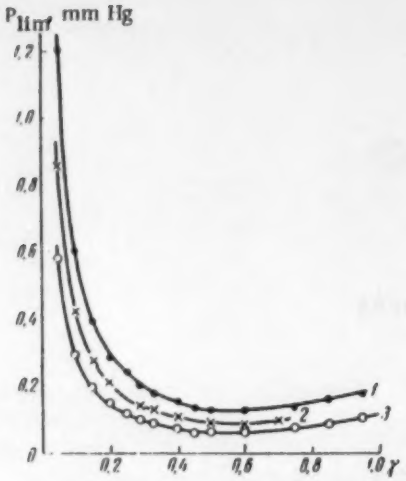

Fig. 1. The variation of the lower ignition limit of a hydrogen–oxygen mixture with its oxygen content at: 1) 430°; 2) 470°; 3) 520°.

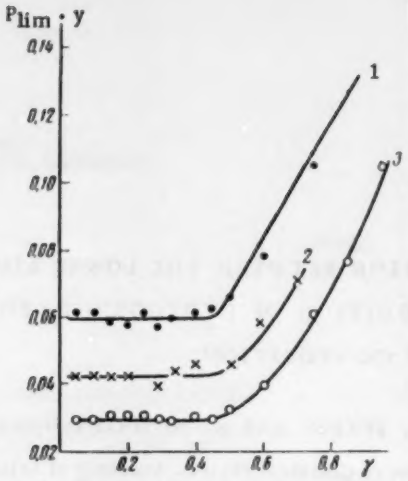

Fig. 2. The variation of $P_{lim} \cdot \gamma$ with γ at: 1) 430°; 2) 470°; 3) 520°.

Figure 1 shows the results of these measurements relating P_{lim} and γ, for γ values from 0.05 to 0.95. Th low P_{lim} values obtained in this series of experiments indicate that the probability (ϵ_H) of H atom adhesion to the wall was very small, and that the reaction was limited by kinetic factors. Figure 2 shows the relation betwe $P_{lim} \cdot \gamma$ and γ, recalculated from the data in Fig. 1. It is apparent that, at all three temperatures, the product $P_{lim} \cdot \gamma$ remained constant to a high degree of precision over the γ range 0.05 to 0.5. This demonstrates that the simple formula $P_{lim} \cdot \gamma$ = constant, based on the assumption that H atoms were removed preferentially because their concentration was considerably greater than those of other chain carriers, was valid for all hydrogen-rich mixtures up to an equimolecular hydrogen–oxygen mixture. It only ceased to be valid with $\gamma > 0.5$. Clearly, for oxygen-rich mixtures, it is also necessary to assume loss of OH radicals. The data of Fig. 1 was used to determine the probability of loss of hydrogen atoms on the reactor walls and its variation with temperature, under our experimental conditions, i.e., a quartz vessel previously washed out with hydrofluoric acid and treated with potassium tetraborate.

Using the approach described above, the conditions for the lower limit is that the rate of chain branching, 2) $H + O_2 = OH + H$, is equal to the rate of chain breaking, 4) $H \xrightarrow{\text{wall}} \frac{1}{2} H_2$, so that

$$2k_2[O_2] = k_4, \qquad (1)$$

Here, k_2 is the velocity constant for reaction 2), which has been determined precisely over a wide temperature range by Karmilova, Nalbandyan, and Semenov [3]; $k_4 = \epsilon_H \cdot U_H / d$ is the velocity constant for reaction 4); ϵ_H is the probability of H atom adhesion to the wall; U_H is its thermal velocity; $\underline{d}$ is the vessel diameter.

Substituting this value for k_4 in (1), and assuming that $[O_2] = \gamma \cdot P_{lim}$, we obtain the following expression for ϵ_H:

$$\epsilon_H = \frac{2k_2 \cdot \gamma \cdot d \cdot P_{\text{пред}}}{U_H}. \qquad (2)$$

Let us calculate the value of ϵ_H at 430° for a mixture containing 95% H_2 and 5% O_2 ($\gamma = 0.05$). At this temperature

$$k_2 = 1{,}86 \cdot 10^{-15} \text{ cm}^3/\text{sec};$$

$$P_1 = 1{,}2 \text{ mm Hg} \quad = 1{,}2 \cdot \frac{10^{19}}{T} \text{ mole/cm}^3;$$

$$U_H = 4{,}18 \cdot 10^5 \text{ cm/sec};$$

$$d = 5{,}8 \text{ cm}$$

Substituting these values in equation (2), we obtain $\epsilon_H = 4.38 \times 10^{-5}$. Similar calculations give $\epsilon_H = 5.24 \times 10^{-5}$ and 6.36×10^{-5} at 470 and 520°, respectively. As would be expected, almost identical values for ϵ_H are obtained using other values of $\gamma < 0.5$. It is known [4] that the temperature variation of ϵ_H is given by the expression $\epsilon_H = \epsilon_0 e^{-E_{\epsilon_H}/RT}$ E_{ϵ_H} can thus be determined easily from the values of ϵ_H at the three different temperatures. Calculation shows that $E_{\epsilon_H} \simeq 4.6$ kcal/mole.

SUMMARY

1. A quartz vessel, washed with hydrofluoric acid and treated with potassium tetraborate, has been used at three temperatures for the careful measurement of the lower autoignition limit of hydrogen–oxygen mixtures as a function of the oxygen content of the mixture.

2. It has been found that the simple formula $P_{lim} \cdot \gamma$ = constant, based on Semenov's theory of the lower ignition limit with the assumption of preferential loss of hydrogen atoms at the wall surface, is strictly obeyed for mixtures containing 5 to 50% of oxygen.

3. Values have been obtained for the probability of hydrogen atom removal at the walls of a quartz reactor, washed with hydrofluoric acid and treated with potassium tetraborate, and its variation with temperature.

LITERATURE CITED

1. A. Biron and A. B. Nalbandyan, Zhur. Fiz. Khim. 9, 132 (1937).
2. N. N. Semenov, Chain Reactions [in Russian] (GTTI, Moscow, 1934).
3. L. V. Karmilova, A. B. Nalbandyan, and N. N. Semenov, Zhur. Fiz. Khim. 32, 1193 (1958).
4. A. B. Nalbandyan and V. V. Voevodskii, The Mechanisms of Oxidation and Combustion of Hydrogen [in Russian] (Izd. AN SSSR, Moscow, 1949).

THE KINETIC FEATURE OF THE HIGH-TEMPERATURE CRACKING OF ISOPENTANE

A. M. Brodskii, K. P. Lavrovskii, and Su Wei-Hang

Institute of Petrochemical Synthesis, Academy of Sciences of the USSR
Translated from Kinetika i Kataliz, Vol. 1, No. 3, pp. 340-344,
September-October, 1960
Original article submitted February 23, 1960

A study has been made of the kinetics of the high-temperature cracking of isopentane in a vacuum apparatus at 700-850° and a pressure of 110 mm Hg. The detailed composition of the products formed was determined by a chromatographic method. It has been shown that the reaction involved in the cracking of isopentane at high temperature follows first order kinetics. The phenomenon of spontaneous retardation of the reaction with increase in the degree of decomposition, which is familiar at lower temperatures, was not observed under the conditions studied, up to extremely high degrees of conversion. The value of the activation energy up to 800° was found to be 60.5 kcal/mole with a pre-exponential coefficient of 10^{14} sec^{-1}.

We have made a detailed study of the over-all kinetics of the cracking of isopentane in the temperature range 700-840°, in order to examine the kinetic features of the high-temperature cracking of isoparaffins and to compare the results of thermal cracking and catalytic dehydrogenation of isopentane. The study of the cracking process in this little-studied temperature range is of considerable theoretical interest and of some practical importance in connection with the development of processes for the pyrolysis of gasoline fractions to produce olefins [1]. Literature data on the regular features of isopentane cracking are available only for lower temperatures [2, 3] and the analysis of the products in these cases was insufficiently accurate.

The increase in temperature and the corresponding sharp decrease in the duration of the reaction to several hundredths of a second, made it necessary to use the special experimental procedure suggested in [4]. In this method the raw material for cracking is heated sufficiently rapidly, and the temperature maintained constant along the reaction zone, by making use of intensive heat-exchange with a turbulent layer [5, 6] of powdered heat-carrier, which in this case consisted of corundum. The gases from the cracking process were analyzed by a chromatographic method [7]. The chromatographic analysis data for the isopentane used as starting material showed the presence of only 0.01% impurity (n-pentane).

A diagram showing the basic features of the apparatus is given in Fig. 1. The isopentane was supplied to the reaction vessel through a capillary and the rate of supply was measured with a rotameter. The temperature in the upper and lower regions of the turbulent layer of heat-carrier, and at the reactor outlet, was measured with platinum–platinorhodium thermocouples. The thermocouple readings were recorded by means of a rapid-action electronic potentiometer with an error of ±3°. All the experiments were carried out at a pressure of 110 ± 2 mm Hg. The pressure in the reaction vessel was set up by means of a special valve (7). Before the experiment the apparatus was evacuated to a pressure of 10^{-4} mm Hg. At the start of the experiment the "blank" line was switched in and the pressure in the reaction vessel was then lower than the pressure in the valve. After working conditions had been established, the blank line was switched out, the pressure in the reaction vessel was raised, the valve was opened automatically, and the gas stream was directed into the line of "working" traps.

Temp. °C	P, mm Hg	t, sec	α	$\frac{C_0}{\alpha C}$	Composition of outlet gas, mole %														
					iso-C_5H_{12}	n.-C_5H_{12}	α-C_4H_8	β-C_4H_8	iso-C_4H_8	C_4H_6	n.-C_4H_{10}	iso-C_4H_{10}	C_3H_6	C_3H_8	C_2H_2	$C_2H_4+C_2H_6$	CH_4	H_2	Coke (CO_2)
735	110	0,035	1,2	1,28	63,0	—	0,3	2,7	2,8	0,2	—	—	4,1	0,1	—	6,5	9,1	6,1	0,1
	111	0,037	1,23	1,31	61,9	0,2	0,4	4,5	4,7	0,2	—	—	4,6	0,1	—	3,3	11,6	8,1	0,1
	112	0,033	1,21	1,23	64,5	—	0,6	3,4	3,3	0,2	0,1	0,1	4,7	0,1	—	4,3	10,4	8,2	0,1
740	112	0,031	1,21	1,25	66,9	—	0,4	2,4	3,7	0,2	0,1	0,1	4,5	0,2	—	4,7	10,4	6,3	0,1
	110	0,033	1,36	1,34	55,8	—	0,5	3,4	3,7	0,3	0,1	0,1	6,3	0,2	—	6,5	13,8	9,2	0,1
	103	0,018	1,18	1,13	70,5	—	0,4	2,4	2,6	0,2	—	—	3,8	0,2	—	3,2	10,3	6,3	0,1
	111	0,017	1,16	1,15	73,0	—	0,4	2,5	2,9	0,2	0,1	0,1	4,4	0,1	—	4,2	6,9	4,1	0,1
745	111	0,03	1,24	1,3	65,5	—	0,4	2,5	2,8	0,2	0,1	0,1	6,4	0,2	—	6,9	8,7	6,1	0,1
780	103	0,027	1,79	1,62	34,3	—	0,6	4,6	6,0	0,4	0,1	0,1	9,3	0,2	—	10,2	20,1	14,0	0,1
	103	0,022	1,7	1,46	39,7	—	0,7	4,4	4,8	0,4	0,2	0,1	8,6	0,3	—	8,8	18,6	13,3	0,1
	109	0,013	1,63	1,42	42,0	—	0,6	4,6	5,0	0,4	0,1	0,1	8,0	0,4	—	8,1	18,6	12,0	0,1
	110	0,015	1,6	1,37	44,4	—	0,5	3,9	3,8	0,3	0,1	0,1	6,9	0,3	0,1	7,5	18,3	13,7	0,1
	111	0,011	1,53	1,3	51,2	—	0,5	3,4	4,7	0,3	0,1	—	7,7	0,3	—	7,7	13,7	10,0	0,2
	110	0,035	1,97	1,9	26,0	—	0,5	3,9	5,4	0,4	0,2	0,1	10,7	0,4	—	12,5	23,2	15,6	0,1
	109	0,03	1,85	1,72	31,5	—	0,6	3,6	5,0	0,4	0,2	0,1	10,1	0,4	—	11,3	21,7	15,0	0,1
820	109	0,015	2,03	2,36	19,0	—	0,7	6,0	5,6	0,4	0,4	0,1	12,4	0,4	0,2	16,0	23,1	17,0	0,2
	108	0,013	2,12	2,71	17,9	—	0,5	5,1	4,4	0,3	0,3	0,1	11,8	0,4	0,2	19,0	23,3	16,5	0,4
	110	0,023	2,2	3,22	14,2	—	0,5	6,2	5,5	0,3	0,4	0,1	11,6	0,5	0,2	18,0	24,1	17,2	0,4
	109	0,012	2,06	2,18	23,3	0,2	0,6	5,0	5,2	0,4	0,2	0,1	10,0	0,6	0,1	17,8	21,0	15,2	0,3
	109	0,009	1,71	1,83	32,0	0,6	0,6	4,7	6,0	0,4	0,2	0,1	9,7	0,6	0,1	11,7	19,4	14,5	0,4
840	109	0,019	2,52	4,23	9,5	—	0,8	7,7	6,8	0,5	0,4	0,1	13,1	0,4	0,2	17,5	26,3	16,5	0,2
	111	0,017	2,22	3,92	11,8	—	0,8	7,5	6,5	0,5	0,4	0,1	12,2	0,4	0,2	18,3	26,7	14,1	0,2

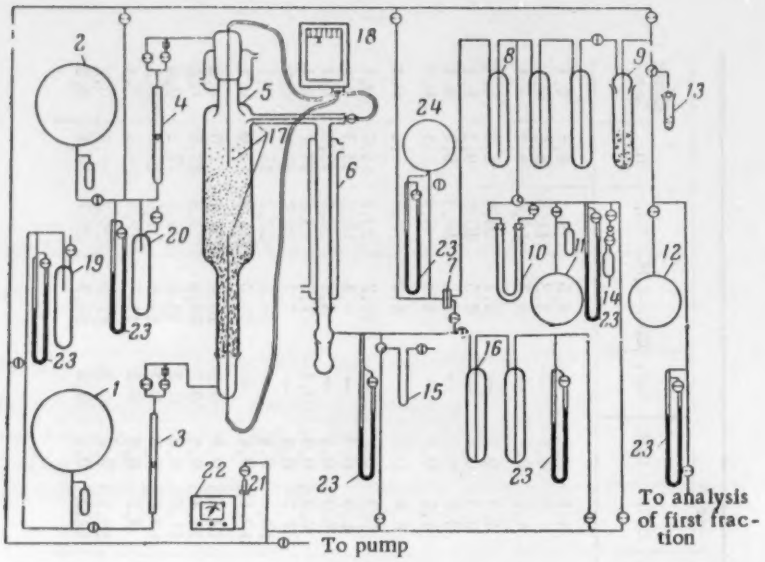

Fig. 1. Diagram of apparatus. 1) Flask for storing the isopentane; 2) flask for storing the carbon dioxide; 3,4) rotameters; 5) reaction vessel; 6) condenser; 7) valve; 8) traps; 9) trap with activated carbon; 10) tube with ascarite; 11,12) flasks for storing gases obtained; 13) finger with activated carbon; 14) pipet; 15) U-tube; 16) trap in "blank" line; 17) thermocouples; 18) potentiometer; 19,20) traps; 21) thermocouple lamp; 22) vacuum gauge; 23) manometer; 24) valve flask.

The table gives the composition of the products of cracking at the temperatures studied for different reduced times of contact equal to $t = VT_0P\epsilon/WTP_0\alpha$, where V is the volume of the turbulent layer, cm^3; W is the rate of supply of gas, cm^3/sec; T_0 is the room temperature, °K; P_0 is 760 mm Hg; P is the pressure in the reaction vessel, mm Hg; α is the expansion coefficient for the increase in the number of moles during the reaction; and ϵ is the porosity coefficient.

Since the reaction was carried out under conditions ensuring complete mixing, and the composition of the outlet gases was the same as the composition in the reaction zone, which is uniform throughout the length of the zone, it is sufficient, for the determination of the final concentrations, to set up the conservation equation. For isopentane this equation has the form

$$C_0v_0F = CvF + kCV\epsilon, \tag{1}$$

where k is the rate constant of the cracking process, C_0 is the isopentane concentration at the inlet of the reaction vessel, C is its concentration at the outlet of the reaction vessel, v_0 and v are the respective rates of the gas stream at the inlet and outlet of the reaction vessel, and F is the cross-sectional area of the reaction vessel.

Equation (1) can be rewritten in the form

$$z = \frac{C_0}{\alpha C} = 1 + kt. \tag{2}$$

Figure 2 shows the relationship z(t) for three temperatures. The value of k was found to be 8.33 sec^{-1} at 540°, 26 sec^{-1} at 780°, and 95 sec^{-1} at 820°. The data obtained at 840° are not given in the graph since they correspond to extensive degrees of conversion where secondary processes begin to play a significant part. The figure shows that the reaction involved in the cracking of isopentane at high temperatures follows first order kinetics and that the phenomenon of spontaneous retardation of the reaction with increase in the degree of decomposition is not observed up to very high degrees of conversion.

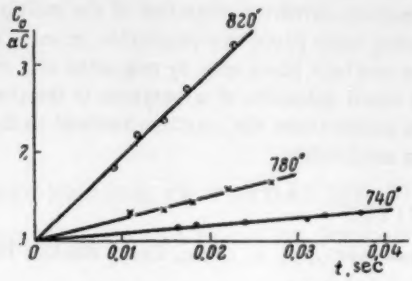

Fig. 2. Relationship between $\frac{C_0}{\alpha C}$ and the contact time $\underline{t}$ at 740, 780, and 820°.

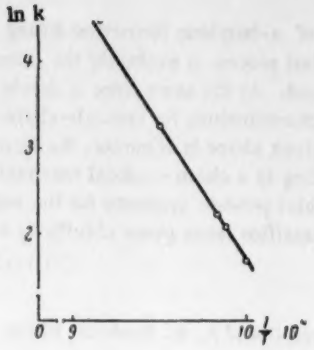

Fig. 3. Relationship between the logarithm of the rate constant and 1/T.

Figure 3 shows the relationship between ln k and 1/T. The value of the activation energy

$$E = -R\frac{d\ln k}{d\,1/T}$$

up to a temperature of 800°, proves to be equal to 60.5 ± 2 kcal/mole, with account taken of all possible errors, and the value of the pre-exponential factor is 10^{14} sec^{-1}.

Frey and Hepp [3] estimated the value of the activation energy for this reaction at a lower temperature (below 600°) and obtained the value 58 kcal/mole. From this it follows that the value of the experimental activation energy increases slightly with increase in temperature. At the same time it should be noted that the value obtained for the activation energy is lower than the activation energy for the cracking of isopentane, inhibited by NO, which according to [2] has the value $E_{inhib.}$ = 70 kcal/mole. It is interesting to compare this result with the previously-found increase in the activation energy for the cracking of ethane with increase in the temperature to 900° (see also [4]).

The following point may be made with reference to the composition of the products formed. Although in [3] good agreement is noted between the composition of the cracking products of normal C_4-C_6 hydrocarbons and the results predicted by Rice's scheme, such agreement was not observed in our case, and this scheme does not explain, even qualitatively, the composition of the cracking products, particularly the ratios of C_4 olefins.

Under the conditions in question, rupture of the C–C bonds predominates over all other reactions and practically no dehydrogenation of isopentane takes place. Without going into the details of the mechanism, we can represent the high-temperature cracking of isopentane by the following over-all scheme:

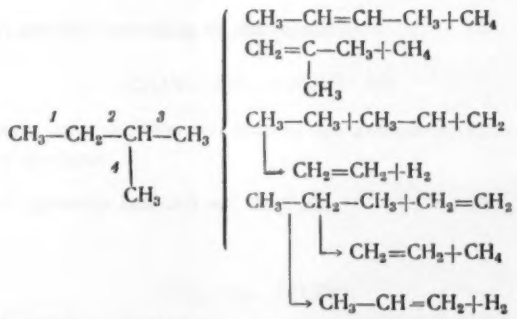

The probability of the isopentane cracking reaction leading to the formation of C_2 and C_3 is much greater than the probability of the reaction leading to the formation of butylenes. The formation of β-butylene may be attributed to the fact that during rupture of the C–C bonds 3 and 4, the secondary hydrogen atom may split off from the carbon atom more readily than the primary hydrogen atom, so that β-butylene and methane are formed.

The possibility of α-butylene formation during the cracking of isopentane is low. When the C–C bond 1 is broken, the easiest process is evidently the removal of a hydrogen atom from the tertiary carbon atom, and isobutylene is formed. At the same time it should be noted that the reaction involving migration of the multiple bond, which is characteristic for radical–chain mechanism, apparently takes place to a negligible extent. Thus if the scheme given above is accurate, the formation of α-butylene can take place only by migration of a multiple bond according to a chain–radical mechanism. The relatively small quantities of α-butylene in the cracking products (see table) provide evidence for the suggestion that at high temperatures the reaction involved in the cracking of isoparaffins takes place chiefly by a molecular reaction mechanism.

LITERATURE CITED

1. K. P. Lavrovskii and A. M. Brodskii, Khim. Nauka i Prom. 2, 189 (1957); M. A. Dalin, Khim. Nauka i Prom. 3, 259 (1956).
2. M. C. Peard, F. J. Stubbs, and C. N. Hinshelwood, Proc. Roy. Soc. Lond. A 214, 330 (1952).
3. F. E. Frey and H. J. Hepp, Ind. Eng. Chem. 25, 441 (1933).
4. A. M. Brodskii, et al., Doklady Akad. Nauk SSSR, 116, 289 (1957).•
5. K. P. Lavrovskii and A. L. Rozental', Khim. Tekh. Topliva i Masel 2, 27 (1956).
6. A. M. Brodskii, R. A. Kalinenko, K. P. Lavrovskii, and V. B. Titov, Zhur. Fiz. Khim. 33, 2457 (1959).
7. K. P. Lavrovskii, et al., Khim. Tekh. Topliva i Masel 3, 30 (1959).

• Original Russian pagination. See C. B. translation.

THE MECHANISM OF FORMATION OF METHYL ALCOHOL DURING THE OXIDATION OF HYDROCARBONS

M. B. Neiman, V. Ya. Efremov, and N K. Serdyuk

Chemical Physics Institute, Academy of Sciences of the USSR
Translated from Kinetika i Kataliz, Vol. 1, No. 3, pp. 345-355,
September-October, 1960
Original article submitted March 28, 1960

The oxidation of an equimolar mixture of $C_3H_6 + O_2$ containing labeled $C^{14}H_3CHO$ and $C^{14}H_3NNC^{14}H_3$ has been studied under static conditions at 315° and an initial pressure of 245 mm Hg.

It has been shown by the isotopic kinetic method that approximately 75% of the methanol is formed from the methyl group of the acetaldehyde.

It has been established that under the experimental conditions, methyl radicals react to form methyl alcohol, formaldehyde, and methane.

* * *

It is known that organic peroxides, aldehydes, and alcohols are formed during the oxidation of hydrocarbons. Although the main features of the mechanism of formation of peroxides and aldehydes are clear [1, 2], a much smaller number of papers has been devoted to the study of the mechanism of formation of alcohols.

In one of the first works devoted to this problem [3], it was suggested that the methyl alcohol is formed from methoxy radicals according to the reaction:

$$CH_3\dot{O}+RH \rightarrow CH_3OH+\dot{R}. \qquad \text{I}$$

Experimental confirmation that this elementary reaction takes place at temperatures of approximately 200°, can be found in [4]. Reaction I has been used by a number of authors [5, 6, 1] to explain the formation of alcohols during the oxidation of hydrocarbons and other organic compounds.

The formation of methyl alcohol according to the reaction:

$$CH_3O\dot{O}+RH \rightarrow CH_3OH+R\dot{O} \qquad \text{II}$$

was postulated in [7]. This elementary reaction was used by the authors of [8] to explain the formation of methyl alcohol during the oxidation of methane.

As far as the formation of peroxide radicals and methoxy radicals is concerned, the former are obtained according to the reaction:

$$\dot{C}H_3+O_2 \rightarrow CH_3O\dot{O}, \qquad \text{III}$$

which has been studied in a number of works [9-11], while the latter are formed according to the reaction:

$$\begin{matrix} CH_3{-}CH{-}R \\ \quad\;\; | \\ \quad O{-}\dot{O} \end{matrix} \longrightarrow CH_3\dot{O}+RCHO. \qquad \text{IV}$$

This last reaction, which is associated with isomerization of the peroxide radical, has been used many times in the works of N. N. Semenov and V. Ya. Shtern.

We have seen that the reaction involved in the formation of methyl alcohol during the oxidation of hydrocarbons has been insufficiently studied, although these reactions play an important part in the mechanism of oxidation of hydrocarbons in the gaseous phase, particularly at high pressures [12]. Very little work has been done on the question of the competition between the various reactions of methyl and peroxide radicals. Finally, almost no studies have been made of the elementary reactions I-IV in complex reacting systems.

The aim of the present work was to study the mechanism of formation of methyl alcohol during the oxidation of propylene in the temperature range around 300°. In this way we hoped to obtain material which would enable us to discuss some of the elementary reactions leading to the formation of CH_3OH and the competition between these reactions and reactions leading to the formation of other products.

Development of the isotopic kinetic method [13, 14] made it possible to realize this aim.

EXPERIMENTAL PROCEDURE

The experiments were carried out with an equimolecular mixture of $C_3H_6 + O_2$ at a pressure of 244 mm Hg and 315°. In several series of experiments, a small quantity of labeled acetaldehyde $C^{14}H_3CHO$ was introduced into the mixture. In other series of experiments a small quantity of labeled azomethane was added to the mixture. The conditions for the preparation and purification of the substances used in the work are given below.

Propylene was prepared by dehydrating purified isopropyl alcohol on Al_2O_3. The gas obtained was purified from higher olefins in H_2SO_4 and condensed, and the liquid obtained was distilled at low temperatures. Mass-spectrometric analysis and the vapor pressure curves proved that the propylene obtained contained no impurities.

Oxygen from a cylinder was condensed and redistilled. The middle fraction was used for the experiments.

Acetaldehyde labeled with radiocarbon in the methyl group was synthesized from $C^{14}H_3COOH$ by conversion to ethyl acetate, which was then reduced with lithium aluminum hydride to $C^{14}H_3CH_2OH$. The alcohol obtained was oxidized with chromic mixture to yield acetaldehyde.

Azomethane labeled with radiocarbon was prepared from labeled methanol by conversion to labeled dimethyl sulfate according to the reaction:

$$2C^{14}H_3OH + 2SO_3 \rightarrow (C^{14}H_3)_2SO_4 + H_2SO_4. \qquad V$$

The dimethyl sulfate was then allowed to react with tetrabenzoylhydrazine:

$$(C^{14}H_3)_2SO_4 + (C_6H_5CO)_2NN(C_6H_5CO)_2 \xrightarrow{NaOH} C_6H_5CONC^{14}H_3NC^{14}H_3C_6H_5CO \qquad VI$$

The product obtained was hydrolyzed with hydrochloric acid to yield labeled dimethylhydrazine, which was oxidized with K_2CrO_4. As a result we obtained labeled azomethane in approximately 40% yield. The azomethane was freed from moisture with $CaCl_2$ and distilled carefully. The product obtained was shown to be pure by measurement of the vapor pressure from −100° to +2°.

Our measurements showed that the relationship between the vapor pressure of azomethane (P) and the absolute temperature T can be expressed by the formula:

$$\log P = 7{,}60 - \frac{5900}{2{,}3RT}. \qquad (1)$$

The vapor pressure of azomethane at 1.5° was determined by Thiele [15]. The value 750 mm found by Thiele shows good agreement with our data.

The experiments on the oxidation of propylene were carried out on a static apparatus which differed only in details from that described in [16]. After the mixture had been introduced into the reaction vessel, an induction period, lasting approximately 260 sec was observed, after which the pressure began to increase exponentially and four cold flames appeared one after the other. When the last cold flame had been extinguished, the pressure continued to increase slowly. The reaction was stopped after different time intervals and the reaction products were transferred to an evacuated flask. The products which condensed were frozen out in traps cooled with liquid nitrogen. The gases were adsorbed on silica gel, which was also cooled with liquid nitrogen.

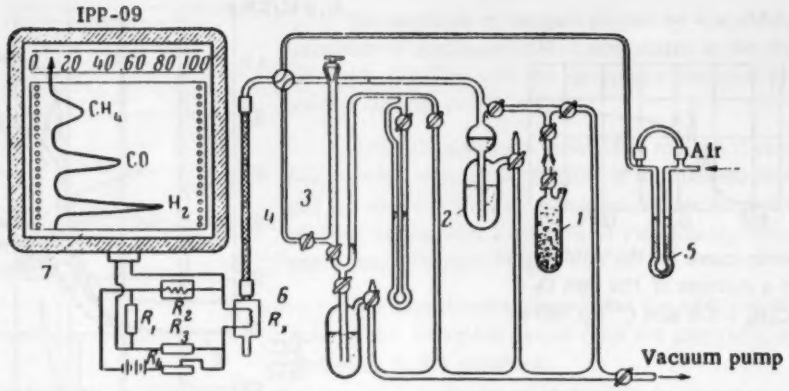

Fig. 1. Diagram illustrating the chromatographic apparatus: 1) Trap with silica gel; 2) Töpler pump; 3) measuring buret; 4) chromatographic column; 5) flowmeter; 6) outlet gas detector; 7) electronic potentiometer.

The aldehydes were determined polarographically. Acetaldehyde was separated from formaldehyde by the dimedonate method. After purification of the dimedonate by recrystallization, its specific activity was determined on an end-face counter. The concentration of methyl alcohol was determined by the isotope dilution method [17].

The carbon dioxide was absorbed in $Ba(OH)_2$ solution. The CO was oxidized with I_2O_5 to CO_2, which was also absorbed in $Ba(OH)_2$. The specific activity of the $BaCO_3$ precipitates was determined with an end-face counter. The analysis procedure has been described in more detail in [18, 19].

The methane content of the product of the oxidation of propylene is so small (10^{-6}-10^{-7} mole/liter) that up to now it has not been detected. Since it was extremely important for us to determine the methane content and its specific activity, we constructed for this purpose a special chromatographic apparatus, which is illustrated diagramatically in Fig. 1.

The trap 1 with silica gel, on which the gaseous reaction products (H_2, CO, O_2, and CH_4) were adsorbed, was connected to the apparatus by means of a ground joint. The gases were transferred from the heated trap by means of a Töpler pump 2, to a graduated buret 3 where their volume and pressure were determined. The gases were then passed into the chromatographic column 4, which was filled with activated carbon. A stream of air was passed through this column at a constant rate recorded by means of a flowmeter 5. The H_2 was eluted from the column first, followed by the CO and finally the CH_4. The gases leaving the column were detected by means of the detector 6, which recorded their catalytic oxidation. The catalyst used was a platinum wire connected in a Wheatstone bridge. The heating of the wire led to a breakdown of the equilibrium of the bridge. The current in the bridge was recorded by means of the potentiometer 7. The recording was used, in conjunction with calibration curves, to determine the concentration of hydrogen, CO, and methane with a probable error of 1-3% of the measured quantity.

The specific activity was determined by oxidizing the methane to CO_2, which was then absorbed in $Ba(OH)_2$. The $BaCO_3$ specimens were subjected to radiometric analysis.

EXPERIMENTAL RESULTS

In an earlier paper [20], it was suggested that the acetyl radical, after combining with an oxygen molecule, breaks down according to the scheme:

$$CH_3COO\dot{O} \rightarrow CH_3\dot{O} + CO_2. \qquad \text{VII}$$

The methoxy radical may be converted to methanol according to Eq. I.

In order to confirm that this mechanism is involved in the formation of CH_3OH, we carried out a series of experiments with a mixture of 122 mm O_2 + 116 mm C_3H_6 + 5.8 mm $C^{14}H_3CHO$ at 315°. The course of the reaction was followed from the increase in pressure. One of the kinetic curves is shown in Fig. 2. The peaks on the kinetic curve correspond to the formation of the four cold flames.

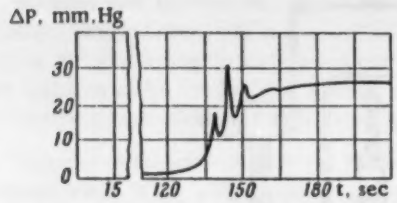

Fig. 2. Kinetic curve for the cold-flame oxidation of a mixture of 122 mm O_2 + + 116 mm C_3H_6 + 5.8 mm $C^{14}H_3CHO$ at 315°.

The results of the determination of the concentration C, the specific activity α, and the total activity I for the principal reaction products—CH_3CHO, HCHO, CH_3OH, CO, and CO_2—are given in Fig. 3. The figure shows that during the induction period, the concentration of acetaldehyde remains almost constant while the concentration of other active products is equal to zero. Starting from the moment t ≈ 100 sec, the concentrations of all the active products increase rapidly towards limiting values. The concentration of acetaldehyde reaches a maximum value and then decreases. At the end of the reaction, the rate of consumption of acetaldehyde evidently exceeds the rate of its formation, as we have shown earlier [21].

The specific activity α of the acetaldehyde decreases sharply during the rapid oxidation and then remains almost constant. This means that the rate of its formation is high during the rapid oxidation of propylene and tends towards zero at the end of the reaction. The specific activity of the methanol at the moment t = 140 sec is slightly lower than the specific activity of the acetaldehyde, from which it follows that acetaldehyde is not the only substance whose formation precedes the formation of CH_3OH. At later stages, $\alpha_{CH_3OH} > \alpha_{CH_3CHO}$, indicating a considerable increase in the proportion of alcohol formed from the methyl group of the acetaldehyde.

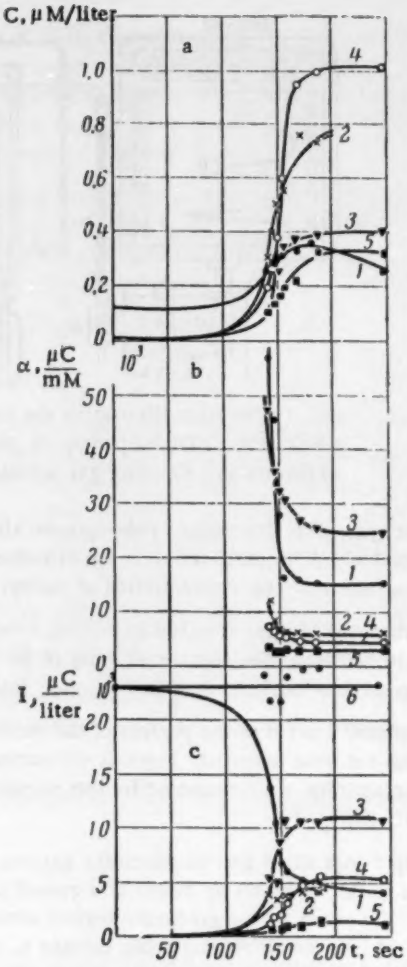

Fig. 3. Change in the concentration (a), specific activity (b), and total activity (c) of the reaction products during the oxidation of a mixture of 122 mm O_2 + 116 mm C_3H_6 + 5.8 mm $C^{14}H_3CHO$ at 315°. 1) CH_3CHO; 2) CH_2O; 3) CH_3OH; 4) CO; 5) CO_2; 6) sum of the total activities of the reaction products.

The specific activity of the formaldehyde and the oxides of carbon is slightly lower. This means that only a small proportion of these products are formed from the methyl group of the acetaldehyde.

The total activity I of the reaction products was calculated from the formula:

$$I = \alpha \cdot C. \qquad (2)$$

Calculations showed that I_{CH_3CHO} decreases sharply during the rapid reaction while the total activities of the other reaction products increase.

The results of the summation of the total activities of all the products which were isolated are shown by the points in Fig. 3, c. Within the limits of experimental error, these points lie on a horizontal straight line passing through the point corresponding to the initial activity of the acetaldehyde. The fact that the sum of the total activities is constant (± 10%) indicates that we have taken account of all the principal reaction products.

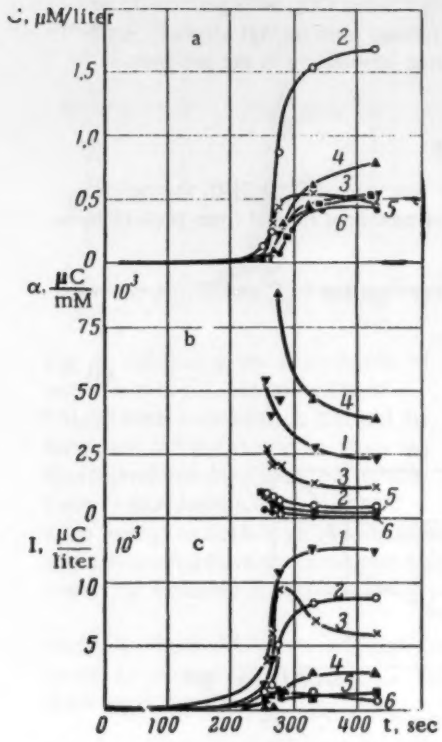

Fig. 4. Change in the concentration (a), specific activity (b), and total activity (c) of the reaction products during the oxidation of a mixture of 122 mm O_2, 122 mm C_3H_6 and 1 mm $C^{14}H_3NNC^{14}H_3$ at 315°. 1) CH_3OH; 2) CO; 3) CH_2O; 4) CH_4; 5) CO_2; 6) CH_3CHO. (The CH_4 concentration is increased by a factor of 10.)

The question of the part played by acetaldehyde in the formation of methanol will be considered in the final part of the work, together with the question of the part played by the methyl radicals in this reaction.

It has already been shown that methanol can be formed from methyl radicals as a result of the successive reactions III and II. In order to study this question, we carried out a series of experiments with a mixture of 122 mm O_2, 122 mm C_3H_6, and 1 mm $C^{14}H_3NNC^{14}H_3$ at 315°.

Out experiments showed that the addition of azomethane reduces the induction period τ for the propylene cold flame according to the equation:

$$\log \tau = \alpha - Kc \qquad (3)$$

where c is the azomethane concentration. The same relationship has been found earlier [22] in a study of the influence of added acetaldehyde and peroxide on the induction period for the butane cold flame. It was found that the value of k in Eq. (3) for the case of azomethane is approximately double that for the case of acetaldehyde [23].

By removing the reaction products after different time intervals, we determined the change in the concentration and the specific and total activities of the principal reaction products—CH_3OH, CO, HCHO, CH_4, CO_2, and CH_3CHO. The results of these determinations are given in Fig. 4. As in the previous series of experiments, the concentration of all the products isolated is close to zero during the induction period and increases sharply in the region of cold-flame oxidation.

The specific activity of the azomethane introduced into the reaction was equal to 2.14 μC/mM. Of the reaction products which we isolated, the methane showed the greatest specific activity. However, α_{CH_4} which decreased during the reaction from 0.09 to 0.04 μC/mM, was smaller than the specific activity of the azomethane by a factor of 20-50. This means that only a small percentage of the methane was obtained from azomethane. The greater part of the methane was produced from inactive intermediate products.

An unexpected feature was the detection of active acetaldehyde in the reaction products. The labeled acetaldehyde is probably formed from methyl radicals according to one of the following reactions:•

$$\dot{C}^{14}H_3 + CH_2O \longrightarrow C^{14}H_3CHO + H, \qquad \text{VIII}$$

$$\dot{C}^{14}H_3 + CH_3CHO \longrightarrow C^{14}H_3CHO + \dot{C}H_3, \qquad \text{IX}$$

The results of the calculation of the total activity of the products according to Eq. (2) are given in Fig. 4, c. Of particular interest is the rapid increase in I_{CH_2O}, which reaches a maximum value and then begins to decrease. This indicates that the formaldehyde is being used up. If it is assumed that oxides of carbon are formed in the process, their activity should increase. The curves show that I_{CO} and I_{CO_2} do in fact increase. Moreover, in the time interval 275-430 sec, the following relationship applies:

$$\Delta I_{CO} + \Delta I_{CO_2} - \Delta I_{CH_2O} = 0. \qquad (4)$$

• The question of the mechanism of formation of the acetaldehyde will be examined in more detail in a later paper.

It may be assumed that the consumption of the formaldehyde yields only CO and CO_2, with practically no HCOOH. In addition, it should be noted that practically no CO and CO_2 are formed from methyl alcohol. Analogous conclusions were reached by the authors of [24], who studied the oxidation of methane in the presence of $C^{14}H_3OH$.

DISCUSSION OF RESULTS

The data which we have obtained on the oxidation of propylene in the presence of $C^{14}H_3CHO$, in conjunction with the kinetic isotopic method, can be used to calculate the quantity of methanol formed from acetaldehyde. For this purpose we calculate first the quantity of acetaldehyde consumed.

If we denote the decrease in the activity of the acetaldehyde and its concentration by I' and C' respectively, we have the following equation

$$dI' = dC' \cdot \alpha_{CH_3CHO}. \tag{5}$$

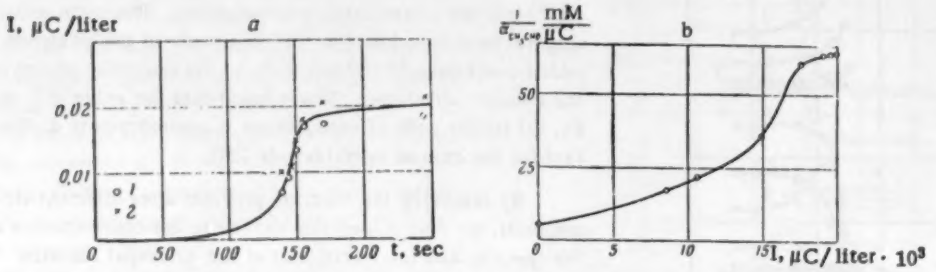

Fig. 5. Data for calculating the quantity of acetaldehyde consumed: a) Change in I with time from the decrease in $I_{C^{14}H_3CHO}$ (1) and from the activity of the products formed (2); b) relationship between $1/\alpha_{CH_3CHO}$ and I.

The value of I' can be calculated from the data given in Fig. 3, c, by two methods. Firstly, it is equal to the decrease in the total activity of the CH_3CHO (curve 1), and secondly, it can be obtained by taking the sum of the total activities of CH_2O, CH_3OH, CO, and CO_2 (curves 2-5). The results of calculations by these two methods are shown by the crosses and circles in Fig. 5, a. The solid line shows the average values of I'.

From Eq. (5) it follows that:

$$C' = \int_0^I \frac{1}{\alpha_{CH_3CHO}} \cdot dI'. \tag{6}$$

To determine the value of C', we constructed the curve giving the relationship:

$$\frac{1}{\alpha_{CH_3CHO}} = f(I'). \tag{7}$$

which is shown in Fig. 5, b. By graphical integration we found how C' changes during the course of the oxidation of propylene. The results of the calculation are given in Fig. 6 (see curve 1).

Our experiments show that CH_3OH, CH_2O, CO, and CO_2 are formed from the methyl group of the acetaldehyde. If the methanol was not consumed, then the quantity of CH_3OH formed from the methyl group of the acetaldehyde could have been calculated from the formula:

$$C_{CH_3CHO} = \int_0^I \frac{1}{\alpha_{CH_3CHO}} \cdot dI_{CH_3OH}. \tag{8}$$

The activity of the methanol in our experiments is represented by curve 3 in Fig. 3, c. As shown in [2], the consumption of alcohol during the oxidation of propylene under the conditions of our experiments is comparatively

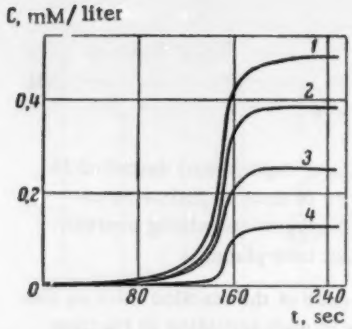

Fig. 6. Kinetics of the consumption of acetaldehyde (1), the formation of CH_3OH from acetaldehyde (2), and the formation of CH_3OH from methoxy radicals produced from the CH_3CHO (3). Curve 4 (the formation of methanol from methyl radicals from acetaldehyde) was constructed from the difference between the ordinates of curves 2 and 3.

small and amounts to 7% of the quantity of accumulated methanol at the end of the induction period and 20% of this quantity at the end of the cold-flame zone. With the introduction of this correction, we constructed the curve showing the relationship between $1/\alpha_{CH_3CHO}$ and the corrected value of I_{CH_3OH}. The values of C_{CH_3OH} found by graphical integration are shown in Fig. 6 (curve 2).

From the literature data given above, it is known that methanol can be formed either from methoxy radicals (reaction I) or from methyl radicals (reactions III and II). The oxidation of acetaldehyde may yield both methyl and methoxy radicals, according to the scheme:

$$CH_3CHO \longrightarrow CH_3C\dot{O} \begin{cases} \longrightarrow CH_3 + CO \\ \xrightarrow{O_2} CH_3COO\dot{O} \longrightarrow CH_3\dot{O} + CO_2 \end{cases} \qquad \text{X}$$

It is of interest to estimate what fraction of the methanol is obtained from methoxy radicals. Assuming that in accordance with reaction X the number of methoxy radicals formed from the methyl group of the acetaldehyde is equal to the number of CO_2 molecules formed from the carbonyl group of the acetaldehyde, and also that all the methoxy radicals are converted to methanol molecules according to reaction I, we can estimate the quantity of methyl alcohol formed from acetaldehyde via methoxy radicals, from the formula:

$$x = \int_0^I \frac{1}{\alpha_{CH_3CH^{14}HO}} \cdot dI_{CO_2}. \qquad (9)$$

Using the data given in [20], where the oxidation of propylene was studied in the presence of $CH_3C^{14}HO$, we calculated the value of x at different moments of time by graphical integration. The results obtained are given in Fig. 6 (curve 3).

The quantity y of methanol formed from acetaldehyde via methyl radicals can be estimated from the difference $C_{CH_3OH} - x$. The values of y found in this way are given in Fig. 6 (curve 4).

By comparing curves 1 and 2 in Fig. 6 we see that approximately 75% of the methyl groups of the acetaldehyde consumed are converted to methanol. Comparison of curves 1 and 3 in the same figure shows that approximately 50% of the methyl groups of the acetaldehyde form methyl alcohol via methoxy radicals.

Assuming that the consumption of acetaldehyde takes place chiefly according to reaction X, we reach the conclusion that under the conditions of our experiments, approximately 50% of the acetal dehyde decomposes to form methyl radicals. If it is assumed that the rate of reaction I can be neglected by comparison with the rate of reaction III, the methyl radicals are almost completely converted to peroxide radicals $CH_3O\dot{O}$. The peroxide radicals can form methanol according to reaction II. Since approximately 25% of the acetaldehyde consumed undergoes conversion in this way (see curves 1 and 4 in Fig. 6), an appreciable fraction of the $CH_3O\dot{O}$ radicals should form not methanol, but other products. From our analyses it follows that these products consist chiefly of formaldehyde. This is apparently formed according to the reaction:

$$CH_3O\dot{O} \longrightarrow CH_2O + OH. \qquad \text{XI}$$

The formation of formaldehyde according to this scheme was suggested in [8].

The peroxide radicals $CH_3O\dot{O}$, are formed from methyl radicals. It is therefore of considerable interest to examine the mechanism of the conversion of methyl radicals in a mixture of a hydrocarbon and oxygen. It was assumed that in the temperature range around 300°, we should have competition between the following reactions

of the methyl radical:

$$\dot{C}H_3 \begin{cases} +RH \xrightarrow{w_1} CH_4 + \dot{R} \\ +O_2 \xrightarrow{w_2} CH_3O\dot{O} \longrightarrow CH_3OH + CH_2O + CO + CO_2. \end{cases} \qquad \text{XII}$$

In order to confirm that these reactions take place, we carried out the series of experiments described in the experimental part of the work, in which labeled azomethane was added. Since in these experiments we detected the formation of considerable quantities of labeled methane and labeled oxygen-containing products, it may be assumed that competition between the radical reactions XII does in fact take place.

By using the isotopic kinetic method, we can calculate from our data the ratio of the reaction rates ω_1 and ω_2 at different moments of time. If we denote the total activity of the methane formed according to reaction XII by I_{CH_4} and the specific activity of the methyl radicals by α_{CH_3}, and neglect the rate of consumption of methane, we obtain the relationship:

$$\frac{dI_{CH_4}}{dt} = w_1 \cdot \alpha_{CH_3}. \qquad (10)$$

In exactly the same way we obtain, for the sum of the activities of all the oxygen-containing products I, the equation:

$$\frac{dI}{dt} = w_2 \alpha_{CH_3}. \qquad (11)$$

Dividing (10) by (11), we obtain:

$$\frac{w_1}{w_2} = \frac{dI_{CH_4}}{dI}. \qquad (12)$$

In order to find the derivative dI_{CH_4}/dI, we constructed the graph in Fig. 7, showing the relationship between I_{CH_4} and I, and by means of graphical differentiation we found the ratio of the rates ω_1/ω_2 at different moments of the reaction.

Time after which samples were removed, sec	264	274	330	430
ω_1/ω_2	0.035	0.3	0.9	1.2

The above data show that the value of ω_1/ω_2 increases gradually with increase in the extent of the reaction. Substituting in Eq. (12) the expressions for the rates of the radical reactions ω_1 and ω_2, we obtain

$$\frac{w_1}{w_2} = \frac{k_1 [CH_3][RH]}{k_2 [CH_3][O_2]} = \frac{k_1 [RH]}{k_2 [O_2]}. \qquad (13)$$

We tried to attribute the observed increase in the ratio ω_1/ω_2 to the decrease in the oxygen concentration. During the course of the reaction, however, the oxygen concentration decreases by a factor of 15, and the propylene concentration by a factor of 2. Thus Eq. (13) could explain an increase in the ratio ω_1/ω_2 by a factor of 7.5, whereas in actual fact this quantity increases by a factor of almost 35.

In order to explain this discrepancy, it must be assumed that during the course of the reaction there are formed intermediate products which are better hydrogen-donors than propylene. Aldehydes and methanol are possible products of this type.

It appears to us that our experiments have shown that an important part in the oxidation of hydrocarbons is played by the competition between the radical reactions of the methyl radicals with hydrogen-donors and oxygen molecules.

Let us now examine the competition between the reactions of the peroxide radicals $CH_3O\dot{O}$, which can form methanol and formaldehyde according to reactions II and XI. The reaction of the azomethane forming methyl radicals can be represented in the form of the following over-all process:

$$C^{14}H_3NNC^{14}H_3 \begin{cases} \xrightarrow{w_3} CH_3OH \\ \quad \downarrow w_5 \\ \xrightarrow[w_4]{} CH_2O \end{cases} \qquad \text{XIII}$$

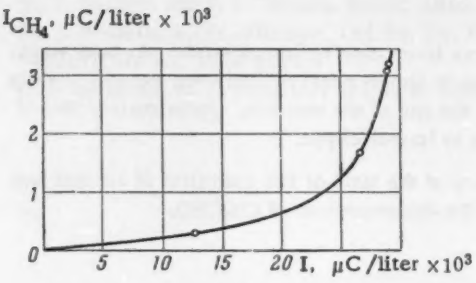

Fig. 7. The relationship between I_{CH_4} and $I = I_{CH_3OH} + I_{CH_2O} + I_{CO} + I_{CO_2}$.

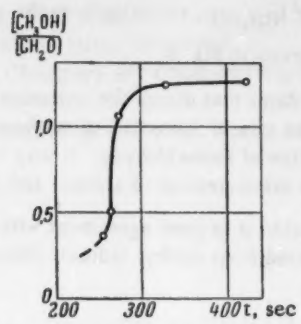

Fig. 8. Change in the ratio of the quantities of alcohol and formaldehyde formed from methyl radicals, during the course of oxidation of propylene.

The quantity of methanol formed from azomethane can be represented by the integral:

$$[CH_3OH] = \int_0^t w_3 dt \tag{14}$$

and the quantity of formaldehyde formed by the azomethane is equal to:

$$[CH_2O] = \int_0^t w_4 dt. \tag{15}$$

Using the equations of the kinetic isotopic method, we obtain:

$$w_3 = \frac{1}{\alpha}\left(\frac{dI_{CH_3OH}}{dt} + \beta\frac{d[CH_3OH]'}{dt}\right), \tag{16}$$

$$w_4 = \frac{1}{\alpha}\left(\frac{dI_{CH_2O}}{dt} - \beta\frac{d[CH_3OH]'}{dt}\right). \tag{17}$$

Here α and β are the specific activities of the azomethane and methanol; I is the total activity, and $[CH_3OH]'$ is the quantity of alcohol consumed.

Substituting the values of ω_3 and ω_4 in Eqs. (14) and (15) and integrating, we obtain:

$$[CH_3OH] = \frac{I_{CH_3OH}}{\alpha} + \frac{1}{\alpha}\int_0^C \beta d[CH_3OH]'; \tag{18}$$

$$[CH_2O] = \frac{I_{CH_2O}}{\alpha} - \frac{1}{\alpha}\int_0^C \beta d[CH_3OH]'. \tag{19}$$

Dividing (18) by (19), we obtain:

$$\frac{[CH_3OH]}{[CH_2O]} = \frac{I_{CH_3OH} + I_{CH_3OH'}}{I_{CH_2O} + I_{CH_3OH'}}. \tag{20}$$

In this formula $I_{CH_3OH'}$ is equal to the value of the integral $\int_0^C \beta d[CH_3OH]'$ and equal to the total activity of the formaldehyde formed from the labeled alcohol at a rate ω_5 according to reaction XIII. In order to calculate this integral, it is necessary to know the quantity of alcohol consumed. Taking this quantity from our earlier work [2], we found the values of $I_{CH_3OH'}$ by graphical integration of the curve $\beta = f(CH_3OH')$. Having

found the value of I_{CH_3OH}, we calculated the ratio $\frac{[CH_3OH]}{[CH_2O]}$ according to formula (20). The results of our calculations are given in Fig. 8.

The figure shows that during the induction period, azomethane forms chiefly formaldehyde. At later stages of the reaction, the rate of formation of methanol from azomethane is almost equal to, and even exceeds slightly the rate of formation of formaldehyde. It may be assumed that at the end of the reaction, approximately 50% of the methyl groups are converted to alcohol and approximately 50% to formaldehyde.

This conclusion is in good agreement with the earlier estimate of the ratio of the quantities of alcohol and formaldehyde formed from methyl radicals obtained as a result of the decomposition of CH_3CHO.

SUMMARY

1. It has been shown by means of the isotopic kinetic method that during the oxidation of propylene, approximately 75% of the CH_3OH is formed from the methyl group of the acetaldehyde.

2. In the oxidation of $C_3H_6 + O_2$ in the presence of $C^{14}H_3NNC^{14}H_3$, we detected $C^{14}H_4$, from which it follows that azomethane can act as a source for the thermal formation of methyl radicals in a medium containing oxygen.

3. It has been shown that in a mixture of $C_3H_6 + O_2$ the methyl radicals may react to form not only CH_4, but also CH_2O, CH_3OH, and CH_3CHO.

4. It has been shown that with increase in the extent of the decomposition of propylene, the ratio of the rates of formation of CH_3OH and CH_2O from the methyl radicals increases.

5. It has been shown that during the course of the reaction, the ratio of the rates of formation of CH_4 and oxygen-containing products from the methyl radicals increases.

This feature is evidently related to the accumulation, in the reaction mixture, of aldehydes and other reaction products containing mobile hydrogen.

LITERATURE CITED

1. N. N. Semenov, Some Problems of Kinetics and Reactivity [in Russian] (Izd. AN SSSR, Moscow, 1958).
2. V. Ya. Efremov, M B. Neiman, and V. N. Panfilov, Zhur. Fiz. Khim. 23, 2152 (1959).
3. R. A. Day and P. N. Pease, J. Am. Chem. Soc. 57, 2296 (1935).
4. F. F. Rust, F. H. Seubold, and W. E. Vaughan, J. Am. Chem. Soc. 72, 338 (1950).
5. E. W. R. Steacie, Atomic and Free Radical Reactions (New York, 1954).
6. S. S. Polyak and V. Ya. Shtern, Chain Reactions in the Oxidation of Hydrocarbons in the Gaseous Phase [in Russian] (Izd. AN SSSR, Moscow, 1955).
7. W. Jost, Explosion and Combustion Processes in Gases, [Russian translation] (IL, Moscow, 1952).
8. L. V. Karmilova, N. S. Enikolopyan, and A. B. Nalbandyan, Zhur. Fiz. Khim. 30, 798 (1956).
9. I. H. Raley, et al., J. Am. Chem. Soc. 73, 15 (1951).
10. G. R. Hoey and K. O. Kutschke, Canad. J. Chem. 33, 496 (1955).
11. W. C. Sleppy and J. G. Calvert, J Am. Chem. Soc. 81, 769 (1959).
12. D. M. Newitt and A. E. Haffner, Pros. Roy. Soc. A-134, 591 (1932).
13. M. B. Neiman, Zhur. Fiz. Khim. 28, 1235 (1954).
14. M. B. Neiman, Int. J. Appl. Rad. Isotopes. Lond. 3, 20 (1958).
15. J. Thiele, Ber. 42, 2575 (1909).
16. M. B. Neiman and G. I. Feklisov, Zhur. Fiz. Khim. 30, 1126 (1956).
17. V. Ya. Efremov, M. B. Neiman, and V. N. Panfilov, Proceedings of the Analytical Chemistry Commission [in Russian] (Izd. AN SSSR, Moscow-Leningrad) 9, 361 (1958).
18. M B. Neiman and G. I. Feksilov, Doklady Akad. Nauk SSSR 91, 877 (1953).
19. A. F. Lukovnikov and M. B. Neiman, Zhur. Fiz. Khim. 29, 1410 (1955).
20. M. B. Neiman and N. K. Serdyuk, All-Union Scientific and Technical Conference on the Application of Radioactive and Stable Isotopes and Radiation in the National Economy and Science [in Russian] (Izd. AN SSSR, Moscow, 1958).

21. M. B. Neiman, et al., Izvest. Akad. Nauk SSSR, Otd. Khim. Nauk. 408 (1956).•
22. M. B. Neiman and P. I. Tutakin, Izvest. Akad. Nauk SSSR, Otd. Khim. Nauk 329 (1938).•
23. M B. Neiman, V. Ya. Efremov, and Yu. Ya. Efremov, Papers on Chemistry and Chemical Technology [in Russian] (Gor'kii, 1959) p. 525.
24. R. I. Moshkina, N. L. Galanina, and A. B. Nalbandyan, Izvest. Akad. Nauk SSSR, Otd. Khim. Nauk 725 (1959).•

•Original Russian pagination. See C. B. translation.

THE ISOTOPIC EXCHANGE OF HYDROGEN ON SPECIMENS OF n- AND p-TYPE GERMANIUM

V. L. Kuchaev and G. K. Boreskov

L. Ya. Karpo Physicochemical Institute
Translated from Kinetika i Kataliz, Vol. 1, No. 3, pp. 356-364,
September-October, 1960
Original article submitted June 27, 1960

A study has been made of the adsorption of hydrogen and the rate of isotopic exchange in molecular hydrogen on specimens of n- and p-type germanium, which had been finely-ground in vacuo.

The rates of adsorption of hydrogen and isotopic exchange were found to be similar for all specimens, in spite of the fact that the concentration of free electrons and holes in the test specimens varied by 7-9 orders of magnitude. From this it follows that the free electrons or holes in the bulk of the semiconductor do not take part in the adsorption of hydrogen on germanium.

It has been shown that isotopic exchange of molecular hydrogen on a germanium surface takes place by an adsorption–desorption mechanism.

• • •

A number of theoretical and experimental works have been devoted to the study of the relationship between the activity of solid catalysts and their electrical properties [1]. For the reaction involved in the isotopic exchange of hydrogen with deuterium, these studies have been carried out chiefly with oxide catalysts. In the case of zinc oxide it has been shown that increase in the electrical conductivity leads to an increase, and decrease in the electrical conductivity to a decrease, in the catalytic activity [2, 3]. The change in the electrical conductivity of the zinc oxide in these works was brought about either by the introduction of considerable quantities of impurities (more than 0.03%) or by changing the oxygen content by heating in vacuo, hydrogen, or oxygen. An unambiguous interpretation of the results obtained in such complex systems is difficult. In this connection it is of interest to study the catalytic activity of simpler systems, for example, germanium, in which the position of the chemical potential level can be varied considerably by the introduction of very small quantities of alloying additives.

The relationship between the catalytic and semiconducting properties of germanium has been studied by G. M. Schwab and coworkers [4], with particular reference to the hydrogenation of ethylene and the dehydrogenation of formic acid, and by V. M. Frolov, O. V. Krylov, and S. Z. Roginskii with particular reference to the reactions involved in the dehydrogenation of ethanol [5] and the decomposition of hydrazine [6]. In all cases, except the reaction involved in the decomposition of hydrazine, an increase in the apparent activation energy of the reaction was observed on going from p-type germanium to n-type germanium. As a result of the existence of a compensating effect, the difference in the specific catalytic activities of different specimens of germanium for the dehydrogenation of ethanol was small. For the reaction involved in the decomposition of hydrazine [6], small concentrations ($\sim 10^{15}$ mol./cm^3) of antimony and gallium have no influence on the activity and activation energy of the reaction; at concentrations of $\sim 10^{18}$ mol./cm^3, however, the presence of antimony leads to a marked decrease in the rate of reaction.

The aim of the present work was to study the influence of the semiconducting properties of crystalline germanium on its catalytic activity, with particular reference to the reaction involved in the isotopic exchange of hydrogen with deuterium, and also to examine the ability of germanium to chemisorb hydrogen.

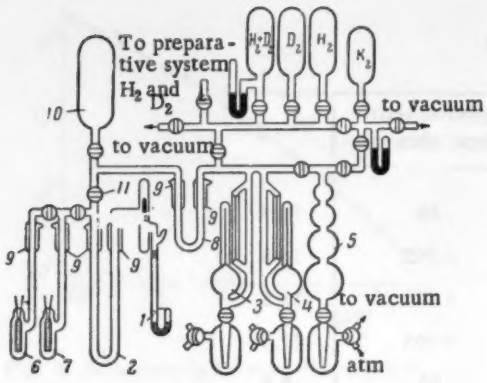

Fig. 1. Diagram of the apparatus used to study the catalytic activity and adsorption.

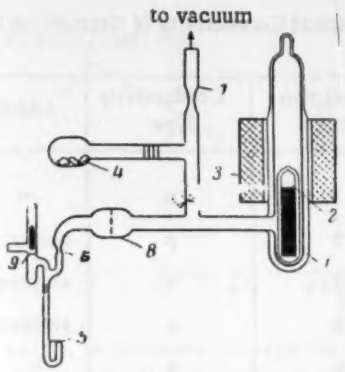

Fig. 2. Diagram of the apparatus for grinding germanium in vacuo.

EXPERIMENTAL PROCEDURE

Apparatus. A diagram of the apparatus is given in Fig. 1. A reaction vessel of quartz glass 1 was kept isolated from the rest of the system by a trap 2 immersed in liquid nitrogen, to protect the catalyst from poisoning by mercury vapor, lubricant, etc. The McLeod gauges 3 and 4 with constants $C_3 = 2.7 \times 10^{-6}$ mm^{-1} and $C_4 = 3.08 \times 10^{-5}$ mm^{-1} were used to measure the pressure from 0.11 to 1.1 mm Hg in the study of the catalytic activity and the adsorption of hydrogen and krypton. The buret 5 was used as a Töpler pump. The valves 6 and 7, containing platinum wires of diameter 20 μ and length 30 cm, were used to measure the concentration of HD by the thermal conductivity method at the temperature of liquid nitrogen. At the liquid nitrogen level, the traps 2 and 8 and the tubes leading to valves 6 and 7 were fitted with silvered vacuum jackets 9 to prevent pressure variations in the system with change in the liquid nitrogen level in the Dewar vessels. The system was evacuated by a DRN-10 mercury diffusion pump to a pressure of 2×10^{-7} mm Hg.

Gases. The hydrogen and deuterium were obtained by electrolysis. To remove water, traces of oxygen and nitrogen, the hydrogen and deuterium were passed through a trap at the temperature of liquid nitrogen and then circulated for one hour in a closed circuit containing two reaction vessels with nickel wire (surface area 4000 cm^2) at a temperature of 300° and a trap with activated carbon at the temperature of liquid nitrogen. In addition, the hydrogen was circulated for half an hour in the same circuit into a by-pass carbon trap to allow the high-temperature equilibrium between ortho- and parahydrogen to be reached. The deuterium was obtained from heavy water containing 99.6% D_2O.

Catalysts. The catalysts used consisted of powders obtained by grinding germanium monocrystals in vacuo [7]. A total of five specimens was studied and the specific resistance, conductivity type, and weight of these specimens are given in Table 1.

A diagram of the glass apparatus used for grinding the germanium in vacuo is shown in Fig. 2. The grinding was carried out in a thick-walled glass tube 1 by means of a glass pestle 2 inside which a transformer iron was sealed. The pestle was moved by alternate switching on and off the current through the solenoid 3. The system was evacuated to a pressure of 5×10^{-7} mm Hg and several pieces of germanium, each weighing 2-3 g, were treated in a quartz ampoule 4 at 600° for three hours. The reaction vessel 5 and the constrictions 6 and 7 were heated at reduced pressure with a gas burner. The constriction 7 was then sealed, the germanium was transferred to cylinder 1, where it was ground finely and then transferred to the reaction vessel 5. The coarse grains of germanium (with dimensions of approximately 1 mm and above) were retained by the pyrex glass sieve 8 and were given a further grinding treatment. When the grinding was complete, the constriction 6 was sealed off and the reaction vessel was then sealed to the working apparatus. The glass membrane 9 was then broken and the specimen was ready for study. Specimens 2, 4, and 5 were ground in vacuo as just described. Specimens 1 and 3 were ground in slightly different fashion; the coarse pieces of germanium were placed directly in cylinder 1 and were not heated before the grinding process. Before constriction 7 was sealed, an apparatus (which would pulverize titanium film acting as a getter) was sealed in place of the quartz ampoule 4.

TABLE 1

Electrical Conductivity of Germanium Specimens

Specimen No.	Conductivity type	Additive	Specific resistance, ohm·cm	Wt., g
1	n	–	50	17.0
2	p	helium	0.002	15.5
3	n	antimony	0.005	13.5
4	n	antimony	0.005	17.5
5	n	–	50	0.6

TABLE 2

The Surface Area of Germanium Specimens, cm^2

Specimen No.	Preliminary thermal treatment at			
	100°	300°	500°	630°
1	2.3	1.9	1.4	1.3•
2	2.0	1.6•	–	–
3	1.8	1.5•	1.1•	–
4	2.1•	1.8•	–	–
5	–	–	0.05	–

• See text.

When the membrane 9 was broken, the McLeod gauge 3 (Fig. 1) was used to measure the pressure, which amounted to 1-2 $\times 10^{-5}$ mm Hg.

RESULTS OBTAINED

Catalyst surfaces. The surface of the specimens was measured directly in the reaction vessel, from the adsorption of spectrally pure krypton at the temperature of liquid nitrogen.

The calculation was carried out according to the BET equation. The area occupied by one krypton atom was taken as equal to 19.4 A [8]. The measurement of the surface was carried out after the studies of the catalytic activity and the adsorption of hydrogen on the pure surface had been completed (specimens 1-3). The relative error in the measurement of the surface was approximately 5%.

Table 2 gives the surface areas of different germanium specimens, with allowance for the change in the surface during the experiments at different temperatures. The values of the surface area which were measured directly, are marked with asterisks, and the figures without asterisks represent data extrapolated by analogy with specimens for which the change in surface area under analogous temperature treatment was determined experimentally. It was assumed that the decrease in the surface area of specimen 1 treated at 630°, compared with that treated at 500°, was proportional to the decrease in the catalytic activity, i.e., amounted to 10%. The surface area of specimen 5 was calculated from its weight, with the assumption that its specific surface is the same as that of specimens 1-4.

The proportion of free volume of catalyst under the working conditions was 0.45.

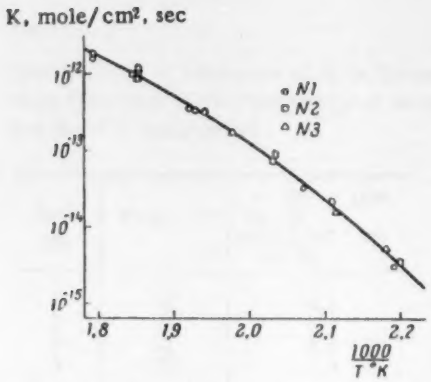

Fig. 3. Relationship between the catalytic activity of different specimens of germanium and temperature at a pressure of 0.7 mm Hg.

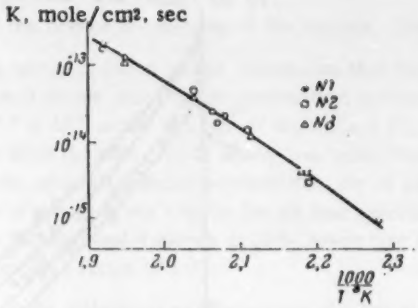

Fig. 4. Relationship between the specific activity of different specimens of germanium and temperature at a pressure of 0.1 mm Hg.

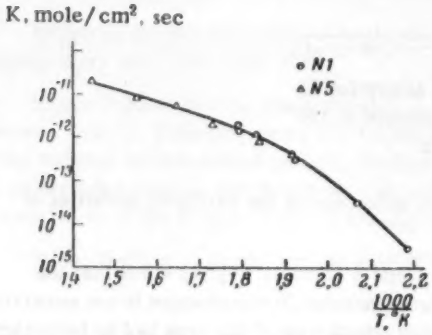

Fig. 5. Relationship between the specific catalytic activity of specimens 1 and 5, and temperature at a pressure of 0.7 mm Hg.

The catalytic activity. The study of the catalytic activity of germanium with particular reference to the reaction involved in the isotopic exchange in homomolecular hydrogen was carried out by a static method at pressures of 0.7 and 0.1 mm Hg of an equimolecular mixture of hydrogen and deuterium at 180-280°.

The HD concentration was determined by means of the analyzer valves 6 and 7 (Fig. 1), which were connected in a Wheatstone bridge. At the temperature of liquid nitrogen, an increase in the HD concentration leads to an increase in the thermal conductivity of the gas and hence to a decrease in the resistance of the wire in the valve. The breakdown of the balance in the bridge was recorded by means of a galvanometer. A standard valve 6, filled with a mixture of hydrogen and deuterium at the test pressure, was used to decrease the influence of the current strength through the bridge, and variations in the temperature of the liquid nitrogen, on the galvanometer readings.

The sequence of operations involved in the study of the catalytic activity was as follows. The reaction vessel 1 (see Fig. 1), the McLeod gauges 3 and 4, and cylinder 10, the buret 5, and the valves 6 and 7, immersed in liquid nitrogen, were filled with a mixture of hydrogen and deuterium at the test pressure, after which the current in valves 6 and 7 was switched on and the standard valve 6 was disconnected from the system. The gas was kept over the catalyst for a period of time sufficient to enable adsorption equilibrium to become established at the test temperature, and the temperature was maintained constant during this time by raising the mercury in the buret 5. The tap 11 was then closed and the partially converted gas in the McLeod gauges and the cylinder 10, was replaced by fresh gas. The tap 11 was then opened for five minutes. During this time the HD concentration became uniform throughout all parts of the system; this concentration did not differ appreciably from that of the original unconverted mixture, since the volume of the reaction vessel and analyzer valve is smaller than the volume of cylinder 10 by a factor of approximately 20. The tap 11 was then closed and the change in the HD concentration with time was recorded. The calculation of the specific catalytic activity of the exchange reaction has been described in a paper by M. A. Avdeenko, G. K. Boreskova, and M. G. Slin'ko [9].

Figures 3 and 4 give the results of the study of the specific catalytic activity (K) of germanium specimens 1, 2, and 3 in the temperature range 170-280° at pressures in the hydrogen–deuterium mixtures of 0.7 and 0.1 mm Hg, respectively. The order of the reaction with respect to pressure for all specimens was approximately 0.35 at 234° and close to zero at 180°. The activation energy is approximately 35 kcal/mole at 180° and decreases with

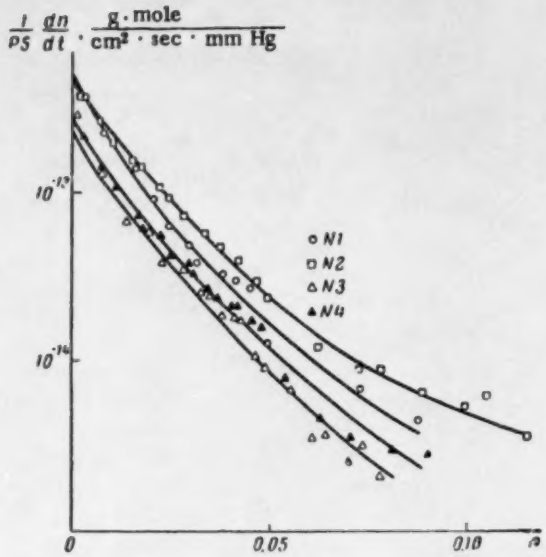

Fig. 6. Relationship between the rate of adsorption of hydrogen on different specimens of germanium at 100° and the degree of covering of the surface.

increase in temperature. The graphs show that there is no significant difference in the catalytic activities of specimens of different conductivity type.

The fact that the values of the specific activity of specimens 1 and 5 coincide (Fig. 5) shows that the decrease in the activation energy of the reaction on specimens 1-3 with increase in temperature is not associated with diffusion of the gas between the germanium particles. If diffusion retardation of this type had in fact taken place, there would have been a greater degree of utilization of the surface on specimen 5, whose weight is smaller than that of specimen 1 by a factor of approximately 30, and this would have led to greater apparent values for the specific activity of specimen 5, compared with specimen 1. The activation energy of exchange at high temperatures, as measured on specimen 5, is equal to 12 kcal/mole.

Change in the temperature of preliminary treatment of specimen 1 from 300° to 600° had no significant effect on the value of the specific catalytic activity.

Adsorption of oxygen to a degree of covering equal to 0.1, did not lead to a change in the catalytic activity of specimen 1. This is probably related to the fact that oxygen is completely absorbed by the germanium granules next to the surface and does not reach the main bulk of the powder.

The rate of adsorption of hydrogen. The study of the rate of adsorption of hydrogen was carried out on specimens 1-4 at room temperature and 100° before the study of the catalytic activity.

Over a period of 1-1.5 hr, measurements were made of the adsorption of hydrogen from the decrease in pressure at room temperature. The hydrogen was then evacuated, the temperature of the reaction vessel was raised to 100°, fresh gas was admitted, and the measurements of the rate of adsorption were continued at a pressure of 8×10^{-3} mm Hg. When an appreciable decrease in the pressure in the system had taken place, fresh gas was admitted and the measurements of the adsorption were repeated. When the rate of adsorption had decreased by a factor of 10-12 (at degrees of covering equal to 4%), the study was repeated at a pressure one order of magnitude higher.

Table 3 gives values of the specific rates of adsorption divided by the pressure $\frac{1}{PS}\frac{dn}{dt}$ at $\theta = 0$ and room temperatures for four germanium specimens. The quantity $\frac{1}{PS}\frac{dn}{dt}$ characterizes the adsorptive power of the surface

TABLE 3

Specific Rates of Adsorption of H_2 on Germanium Specimens (activation energy of adsorption 6 ± 0.5 kcal/mole)

Spec. No.	Temp., °C	$\frac{1}{PS}\frac{dn}{dt} \times 10^{14}$, mole/cm² · sec · · mm Hg
1	18	4,0
2	24	4,9
3	22	3,7
4	22	2,9

at a given temperature, if the rate of adsorption is proportional to the pressure. Figure 6 gives the relationship between $\frac{1}{PS}\frac{dn}{dt}$ and the degree of covering of the surface. The degree of covering was calculated on the assumption that the hydrogen atom is linked to one atom on the germanium surface and that there are 7.7×10^{14} atoms per cm² of the surface [7]. The above data show that the rate of adsorption, activation energy of adsorption, and relationship between the rate of adsorption and degree of covering are similar for all four specimens. The n-type specimens 3 and 4 show a slightly lower rate of adsorption (smaller by a factor of 1.5).

The slight difference in the degrees of subdivision of specimens 3 and 4 did not lead to any significant difference in the rate of adsorption on these materials.

All the specimens showed a rapid decrease in the rate of adsorption with increase in the degree of covering, even in the earliest stages of the hydrogen adsorption.

Isotherms for the adsorption of hydrogen. Isotherms for the adsorption of hydrogen were recorded at three temperatures: 210°, 244°, and 274°.

Figure 7 gives data for the adsorption of hydrogen at 244° on specimens 1-4, together with the isotherm, borrowed from K. Tamaru's work [10] for the adsorption of hydrogen at 245° on a film of germanium obtained by the thermal decomposition of GeH_4 (broken line). The graphs show that there is no significant difference in the adsorption isotherms for specimens with ordinary (1) and hole (2) conductivity. The adsorption isotherms for specimens of the n-type (3 and 4) lie slightly below these (by approximately 30%).

Figure 8 shows isotherms for the adsorption of hydrogen on specimen 1 at 274°, 244°, and 210°.

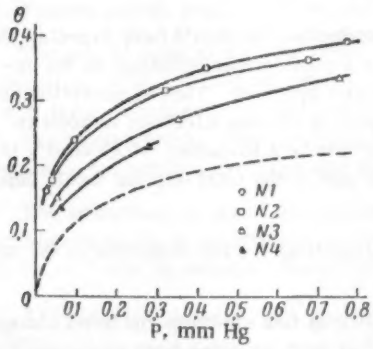

Fig. 7. Isotherms for the adsorption of hydrogen at 244° on different specimens of germanium and on a germanium film obtained by thermal decomposition of GeH_4.

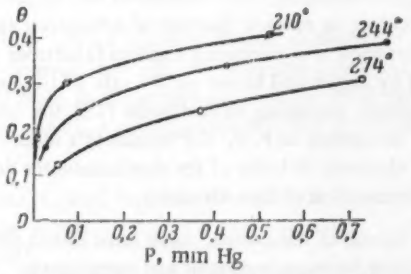

Fig. 8. Isotherms for the adsorption of hydrogen on specimen 1.

Figure 9 shows the relationship between $\frac{\theta}{1-\theta}$ and $\sqrt{P}$ for the adsorption of hydrogen on specimen 2 at 274° and 244° for low degrees of covering. At degrees of covering up to $\theta = 0.15$, the isotherms follow the Langmuir equation for adsorption with dissociation. The heat of adsorption is equal to 25 kcal/mole.

At higher degrees of covering, deviations from the Langmuir equation and a decrease in the heat of adsorption are observed. These results are in agreement with the data of K. Tamaru and M. Boudart [10, 11].

The solubility of hydrogen in germanium is so small [12] that it could have had no significant influence on the results of the adsorption measurements.

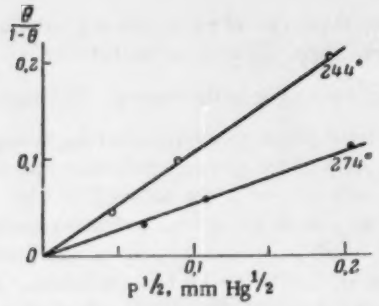

Fig. 9. The relationship between $\frac{\theta}{1-\theta}$ and $\sqrt{P}$ for the adsorption of hydrogen on specimen 1.

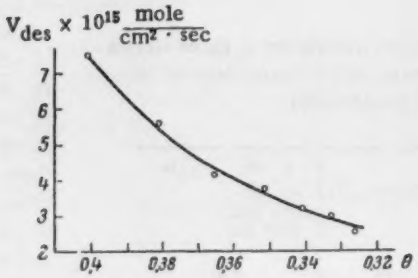

Fig. 10. Relationship between the rate of desorption of hydrogen and the degree of covering of the surface on specimen 1 at 180°.

The desorption of hydrogen. In order to study the relationship between the rate of desorption of hydrogen ($v_{des.}$) and the degree of covering of the surface, hydrogen was adsorbed on germanium (Spec. 1) to give a degree of covering of the surface $\theta = 0.40$. The hydrogen was then drawn off for a period of one minute and the increase in pressure in the system with time was recorded by means of a McLeod gauge. This operation was repeated several times. The relationship between the rate of desorption and the degree of covering of the surface at 180° is shown in Fig. 10. The graph shows that when approximately 20% of the adsorbed hydrogen had been removed from the germanium surface, the rate of desorption had decreased by a factor of three.

After carrying out the experiment on the study of the catalytic activity of specimen 1 at 180°, we determined the rate of desorption of the hydrogen–deuterium mixture from the germanium surface at the same temperature. This was found to be approximately 1.5 times greater than the rate of the isotopic exchange reaction and 1.5 times smaller than the rate of desorption of hydrogen under the same conditions.

DISCUSSION OF RESULTS

According to modern theories of adsorption and catalysis on semiconductors, we should have expected that the concentration of free current carriers (electrons and holes) would have a considerable influence on the adsorption of hydrogen and hence on the rate of isotopic exchange in molecular hydrogen. Thus in adsorption on semiconductors, according to K. Hauffe [13], the adsorbed particles are held by the free electrons or holes in the solid. According to F. F. Vol'kenshtein's theory [1], there may in addition be a so-called "weak bond", in which the electrons or holes of the semiconductor do not take part, but its part in the total sorption should depend on the concentration of free electrons.

The results of the present study have shown that these theoretical predictions are not confirmed in the case of the reaction between hydrogen and germanium.

In the germanium specimens which we have studied, the concentration of free electrons and holes changes by factors of approximately 10^9 at room temperature, 10^7 at 100°, and 10^4 at 200°, on going from specimens 3 or 4 (n-type) to specimen 2 (p-type). At the same time the adsorption of hydrogen and the catalytic activity with particular reference to the isotopic exchange reaction in the temperature range studied were found to be approximately the same for all specimens studied.

From this it may be concluded that the adsorption of hydrogen on germanium takes place without the participation of free electrons or holes from the bulk of the semiconductor, i.e., without charging of the surface.

Attempts might have been made to explain these results by suggesting that the germanium surface is "quasi-insulated" [14], i.e., that its surface properties are not related to its bulk properties. This suggestion, however, is difficult to reconcile with the results obtained by G. M. Schwab and co-workers [4], and by V. M. Frolov, S. Z. Roginskii, and O. V. Krylov [5], who observed a change in the activation energy of certain reactions catalyzed by germanium, on going from p-type specimens to n-type specimens.

It seems to us a more probable suggestion that the adsorption of hydrogen on germanium is brought about by the formation of a two-electron covalent bond involving the electrons of the hydrogen and the electrons of the surface atoms of germanium.

This suggestion is in agreement with the high degree of covering of the germanium surface by the adsorbed hydrogen (up to 40%), which we have observed in our experiments and which is difficult to explain on the assumption that the adsorption is associated with charging of the surface.

We have previously studied the catalytic activity of germanium powders obtained by grinding monocrystals in air with subsequent reduction at 500° in hydrogen [15]. At 270° the catalytic activities of specimens of pure germanium and alloyed specimens of the n- and p-type were approximately the same, but at 150° the activity of pure germanium was found to be several times greater than the activity of the n- and p-type specimens. The cause of the discrepancy is evidently related to the insufficient purity of the material under the conditions of these experiments.

Our data on the kinetics of hydrogen adsorption differ from the results obtained by other workers. R. M. Dell [16] did not detect any adsorption of hydrogen at room temperature on germanium powder obtained by reduction of GeO_2. M. Green and K. Maxwell [17] did not detect any adsorption of hydrogen at 20° or 100° on germanium powder with a surface of approximately 70 cm^2, obtained by grinding in vacuo. In contrast to the data of K. Tamaru and M Boudart [11], in our experiments the adsorption of hydrogen decreased sharply with increase in the degree of covering at very low degrees of covering. The activation energy of adsorption at low degrees of covering (6 kcal/mole) differs from the value of the activation energy obtained by K. Tamaru (14.6 kcal/mole) and is close to the value of the activation energy obtained by J. T. Law [18]. Further studies are necessary in order to explain the rapid change in the rate of adsorption with increase in the degree of covering at low degrees of covering of the surface with small change in the heat of adsorption.

The fact that the value of the rate of adsorption is close to that of the rate of isotopic exchange indicates that the reaction takes place by an adsorption–desorption mechanism. The slight difference in the rates of desorption and exchange ($v_{des.\ H_2 + D_2} = 1.5\ v_{exchange}$) can apparently be attributed to the kinetic isotopic effect of desorption, the existence of which is indicated by the difference in the rates of desorption of hydrogen and the hydrogen–deuterium mixture ($v_{des.\ H_2} = 1.5\ v_{des.\ H_2 + D_2}$). The kinetic isotopic effect was observed by K. Tamaru and M. Boudart [10, 11] for the desorption of hydrogen and deuterium from germanium film.

The rate of desorption in the range of degrees of filling $\theta = 0.4$-0.3 does not change so sharply as the rate of adsorption. When 20% of the total adsorbed hydrogen was removed, the rate of desorption decreased by a factor of three, which corresponds to an increase of 1-0.6 kcal/mole in the activation energy of desorption of the hydrogen remaining. Thus under the conditions of our experiments, a considerable fraction of the surface takes part in the isotopic exchange reaction.

The activation energy of the reaction at high temperatures is equal to 12 kcal/mole and increases to 35 kcal/mole as the temperature is decreased. The order of the isotopic exchange reaction in the pressure range 0.1-0.7 mm Hg decreases from 0.35 at 240° to zero at 180°.

At temperatures of 180-210°, approximately 30-40% of the germanium surface is covered by adsorbed hydrogen.

It is apparently only on this fraction of the surface that the adsorption and desorption of hydrogen, and hence the isotopic exchange, take place at an appreciable rate. The remaining fraction of the surface is apparently characterized by such a low value of the activation energy of adsorption and such a high corresponding value of the activation energy of desorption that the exchange which takes place on this region has no significant influence on the over-all rate of the process.

At the temperatures indicated, the "working" part of the surface is almost saturated with hydrogen, so that the activation energy of exchange is close to the activation energy of desorption and the rate of exchange in independent of the hydrogen pressure.

With increase in temperature, the degree of covering of the "working" part of the surface by hydrogen decreases, as a result of which the rate of exchange starts to become dependent on the hydrogen pressure; the activation energy of exchange decrease and at very low degrees of covering of the "working" surface it approaches the activation energy of adsorption.

LITERATURE CITED

1. F. F. Vol'kenshtein, Electronic Theory of Catalysis on Semiconductors [in Russian] (Gos. Izd. Fiz.-Mat. Lit., Moscow, 1960).
2. E. Molinary and G. Parravano, J. Am. Chem. Soc. 75, 5233 (1953).
3. F. Heckelsberg, A. Clark, and G. C. Bailey, J. Phys. Chem. 60, 559 (1956).
4. G. M. Schwab, et al., Z. Phys. Chem. Neue Folge 15, 363 (1958); G. M. Schwab, Semiconductor Surface Physics. (Ed. R. H. Kingstone) (Philadelphia, 1957) p. 283.
5. V. M. Frolov, O. V. Krylov, and S. Z. Roginskii, Doklady Akad. Nauk SSSR 126, 107 (1959)*
6. V. M. Frolov, O. V. Krylov, and S. Z. Roginskii, Collection: Problems of Kinetics and Catalysis [in Russian] (Izd. AN SSSR, Moscow, 1960) Vol. 10, p. 102.
7. M. Green, J A. Kafalas, and P. H. Robinson, Semiconductor Surface Physics (Ed. R. H. Kingstone) (Philadelphia, 1957) p. 349.
8. A. J. Rosenberg, J. Am. Chem. Soc. 78, 2929 (1955).
9. M. A. Avdeenko, G. K. Boreskov, and M. G. Slin'ko, Collection: Problems of Kinetics and Catalysis [in Russian] (Izd. AN SSSR, Moscow, 1957) Vol. 9, p. 61.
10. K. Tamaru, J. Phys. Chem. 61, 647 (1957).
11. K. Tamaru and M. Boudart, Adv. in Catal. 9, 699 (1957).
12. A. Wieringen and N. Warmoltz, Physica, 22, 849 (1956).
13. K. Hauffe, Ang. Chem. 67, 189 (1955).
14. Ph. Wolkenstein and S. M. Kogan, Z. Phys. Chem. Leipzig, DDR 211, 282 (1959).
15. V. L. Kuchaev and G. K. Boreskov, Collection, Problems of Kinetics and Catalysis [in Russian] (Izd. AN SSSR Moscow, 1960), Vol. 10, p. 108.
16. R. M. Dell, J. Phys. Chem. 61, 1584 (1957).
17. M. Green and K. H. Maxwell, J. Phys. Chem. Sol. No. 11 (1957).
18. J. T. Law, J. Phys. Chem. 59, 543 (1955).

*Original Russian pagination. See C. B. translation.

THE MECHANISM OF THE ACID DECOMPOSITION OF HYDROPEROXIDES

Yu. A. Shlyapnikov

Chemical Physics Institute, Academy of Sciences of the USSR
Translated from Kinetika i Kataliz, Vol. 1, No. 3, pp. 365-373,
September-October, 1960
Original article submitted January 28, 1960

This paper deals with the regular features of the acid decomposition of hydroperoxides and the related features of the isomerization of peroxy esters (the Criegee rearrangement).

It has been shown that the schemes previously proposed for the acid decomposition of hydroperoxides—Kharasch's scheme and the scheme of Seubold and Vaughan—are inadequate. A detailed examination has been made of the scheme suggested by the author and V. A. Shushunov, which regards the acid decomposition as a chain reaction with active centers in the form of ion pairs. Values have been given for the decomposition constants of some hydroperoxides, determined experimentally under identical conditions.

Many organic peroxides decompose under the influence of strong acids according to the following general scheme:

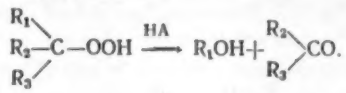

$$R_1R_2R_3C{-}OOH \xrightarrow{HA} R_1OH + R_2R_3CO. \qquad (1)$$

This type of decomposition is shown, in particular, by all alkyl aryl hydroperoxides in which hydroperoxide and aromatic groups are linked simultaneously to a central carbon atom [1]. Kharasch [2] has shown that in the decomposition products, the hydroxyl group is found to be attached to this aromatic group, and different hydroperoxides form different phenols and ketones (or aldehydes). The acid decomposition of cumene (isopropylbenzene) hydroperoxide, first studied in 1944 by Hock and Lang [3],* has formed the basis of the modern industrial method for the preparation of phenol [4]. Changes analogous to the decomposition of aryl alkyl hydroperoxides are undergone by cyclohexene hydroperoxide [2], tertiary decalin hydroperoxide [2, 5] and various other compounds, under the influence of acids.

The acid decomposition of hydroperoxides and the related reactions involving the isomerization of esters of peroxy acids (peroxy esters) have been studied by many workers. The experimental material which has accumulated up to the present time, enables us to solve the problem of the mechanism of this process.

In the present work an attempt is made to provide a detailed justification of the mechanism of the acid-catalyzed decomposition of hydroperoxides, proposed by the author and V. A. Shushunov.

The acid decomposition of hydroperoxides has been studied in most detail by Kharasch and co-workers [1, 2, 6, 7]. In their work it was shown that the process is catalyzed only by strong acids. Thus in a medium of acetic acid at room temperature, cumene hydroperoxide undergoes almost no decomposition, but when a small quantity of perchloric acid is added the decomposition is complete in a few minutes.

*This reaction was discovered independently and almost simultaneously in the USSR by P. G. Sergeev and co-workers.

In order to explain the mechanism of this reaction, Kharasch [1] proposed the following scheme:

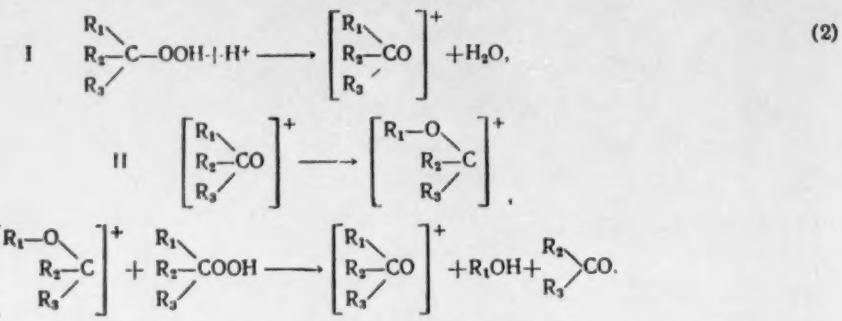

(2)

According to this scheme, the acid decomposition of hydroperoxides is an ionic chain reaction (the stage of chain rupture is omitted from the scheme).

A different scheme was first suggested by Seubold and Vaughan [8] and later by Wichterle and Cefelin [9] (the latter authors erroneously attributed this scheme to Kharasch):

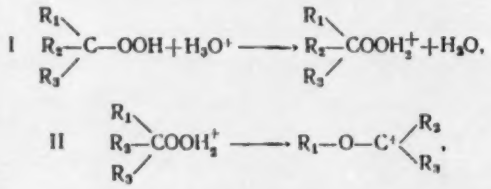

(3)

or

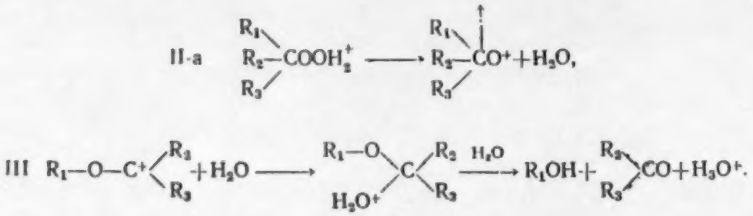

These authors gave no evidence in support of this scheme.

A feature common to both schemes is the rearrangement which takes place in the positive ion:

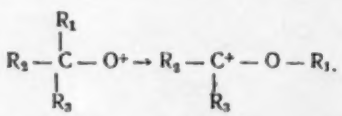

(4)

This type of rearrangement has been studied in detail for the case of the isomerization of peroxy esters.

The isomerization of peroxy esters was first observed by Wieland and Maier [10]. In an attempt to synthesize triphenylmethyl perbenzoate, these authors obtained, instead of the expected peroxy ester, a derivative of benzophenone. They attributed this phenomenon to isomerization of the peroxy ester formed:

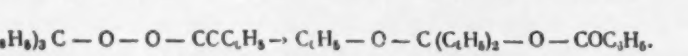

(5)

Hock and Kropf [11] succeeded in isolating the analogous peroxy ester dimethylphenylmethyl perbenzoate ("benzoyl cumyl peroxide"). After standing for several days at room temperature this peroxy ester underwent an analogous rearrangement. The authors suggested that the first stage in the process is dissociation of the peroxy ester into ions:

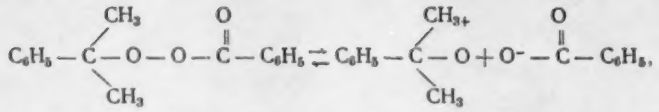

(6)

after which the positive ion undergoes rearrangement:

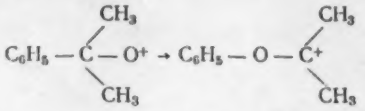

(7)

followed by recombination of the ions to form the molecule of the final product.

In a study of the rearrangement of decalyl perbenzoate

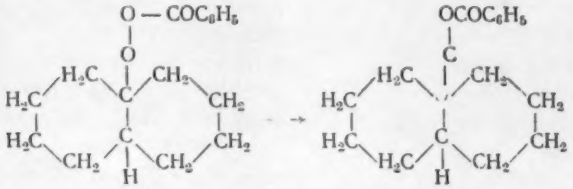

(8)

in various solvents, Criegee [12] showed that the rate of rearrangement is higher, the higher the dielectric constant of the solvent. Bartlett and Storey [13] studied the rearrangement of decalyl perbenzoate and tertbutyl p-toluenepersultonate:

(9)

and showed that the rate of these reactions in a methanol–water mixture increases with increase in the water content of the mixture (Fig. 1). It had already been shown that the rearrangement of peroxy esters is a first order reaction [14]. All these data provide evidence in support of the suggestion that the dissociation of the peroxy esters to form ions, is a necessary condition for the rearrangement. The data of other workers indicate, however, that free ions are not formed in the process. In experiments on the isomerization of decalyl perbenzoate in the presence of p-bromobenzoic acid and its salts and of decalyl p-bromoperbenzoate in the presence of benzoic acid, it was shown that the exchange of anions between the acid (or salt) and the peroxy ester during the rearrangement does not exceed 0.6% [14]. In [15] no exchange of ions was observed in the decomposition of decalyl perbenzoate in a medium of methanol in the presence of a large excess of lithium p-nitrobenzoate or during the decomposition of p-nitroperbenzoate in the presence of lithium benzoate.

In a study of the isomerization of decalyl perbenzoate labeled with O^{18} in the carbonyl group of the acid, in a medium of methanol and acetic acid, it was shown that during the reaction the oxygen atoms of the anion do not change places [16]. Thus although, the –O–O– bond in the peroxy ester may be converted to an ionic bond, the process does not lead to the formation of free ions, but proceeds only as far as the stage of formation of a firmly-held ion pair. The stronger the acid corresponding to a given anion, the higher the polarity of the –O–O– bond and hence the easier the rearrangement. This is confirmed by experiments on the isomerization of peroxy esters of substituted benzoic acids. The rate constants for the isomerization at 24.6° are: 55×10^{-5} sec^{-1} for decalyl p-nitroperbenzoate $4.9 \cdot 10^{-5}$ sec^{-1} for the unsubstituted perbenzoate, and $3.2 \cdot 10^{-5}$ sec^{-1} for the p-methylperbenzoate [14].

Work on the isomerization of peroxy esters leads to the conclusion that the rearrangement [4] accepted by the authors of both mechanisms proposed for the acid decomposition of hydroperoxides is quite possible, but that the formation of free ions is not necessary for this rearrangement to take place.

In order to solve the problem of the mechanism of a process, kinetic studies are necessary. The kinetics of the acid decomposition of cumene hydroperoxide have been studied in most detail.

The kinetics of the decomposition of cumene hydroperoxide in 50% (by weight) acetic acid under the influence of p-toluenesulfonic acid have been studied by Seubold and Vaughan [8], who established that the

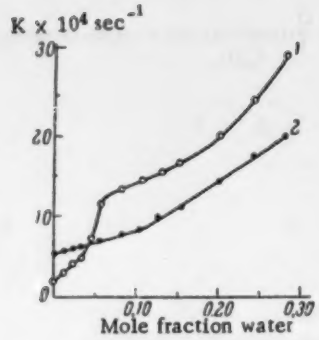

Fig. 1. Relationship between the rate constant for the isomerization of tertbutyl p-toluenepersulfonate at 4.5° (1) and of decalyl perbenzoate at 25° (2) on the composition of the methanol–water mixture (according to Bartlett's data [13]). The scale of the ordinate has been increased by a factor of 10 for curve 2.

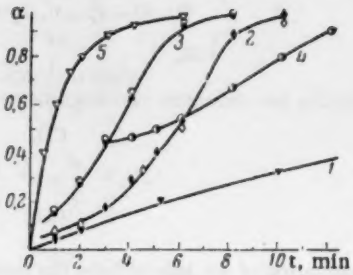

Fig. 2. Kinetic curves for the decomposition of cumene hydroperoxide in dioxane at 50°, $[H_2SO_4]$ = 0.03 mole per liter: 1) Without additives; 2-5) with the addition of 0.1 mole/liter acetic anhydride. The degree of conversion is plotted on the y axis (the black and open points represent data from parallel experiments).

decomposition is of first order with respect to the acid and of first order with respect to the hydroperoxide. The activation energy, calculated from the temperature dependence of the rate of reaction, was found to be equal to 21.3 kcal/mole. Working with the same solvent, but using sulfuric acid as catalysts, Wichterle and Cefelin [9] confirmed these observations. The activation energy in this case was equal to 20.6 kcal/mole.

The kinetics of the decomposition of cumene hydroperoxide in a medium of glacial (99.0 mole %) acetic acid under the influence of sulfuric acid was studied by Shushunov and Shlvapnikov [17]. In addition to the features already established, they found that the reaction is accelerated considerably by one of its products—acetone. At an initial hydroperoxide concentration greater than 0.02 mole/liter, the kinetic curves are autocatalytic, as a result of this phenomenon. In the absence of a strong acid, acetone does not bring about decomposition of the hydroperoxide, and its accelerating action in the presence of acid is suppressed by the addition of water. It has also been established that the reaction is retarded considerably by water and is accelerated considerably by the addition of acetic anhydride. The activation energy of the reaction is equal to 20.0 kcal per mole, but in the presence of acetone (0.1 mole/liter) this decreased to 16.1 kcal/mole.

In pure acetic anhydride, the decomposition of the hydroperoxide under the influence of sulfuric acid is again a first order reaction, both with respect to the hydroperoxide and with respect to the acid, but the rate of the reaction is much higher (by 4 orders of magnitude at 40°) than in acetic acid. The activation energy in this case amounts to approximately 12 kcal/mole.

The kinetics of the decomposition of cumene hydroperoxide and a number of its analogs have been studied by these authors in the greatest detail in a medium of dioxane [18, 19]. In the absence of dehydrating agents, the process takes place, as in the majority of solvents, according to first order kinetics with respect to both the acid and the hydroperoxide, and the activation energy is 20.7 kcal/mole. The addition of the reaction products to the reaction mixture has little influence on the rate of the reaction, but the decomposition is retarded slightly by acetone and accelerated by phenol.

It has been shown that free radicals do not take part in the acid decomposition of cumene hydroperoxide. To confirm this, use was made of the weakly-active free radical diphenylpicrylhydrazyl, which can be isolated in the free state in the form of dark violet crystals which are soluble in various organic compounds to form brightly-colored solutions.

Diphenylpicrylhydrazyl reacts readily with other free radicals, forming weakly-colored products and suppressing free-radical chain reactions [20]. In the experiments of Shushunov and Shlyapnikov, the addition

of diphenylpicrylhydrazyl to the reaction mixture had absolutely no influence on the rate of acid decomposition of the hydroperoxide and its color did not change during the course of the reaction.

Water has a marked retarding effect on the decomposition, and at low water concentrations (up to 1 mole % with respect to dioxane), the reciprocal of the rate increased linearly with increase in the water concentration. Thus the rate of the reaction in the presence of water could be expressed by the following empirical equation:

$$-\frac{d[\mathrm{HP}]}{dt}=\frac{a[\mathrm{HP}]\,[\mathrm{HA}]}{1+b\,[\mathrm{H_2O}]}=k_a\cdot[\mathrm{HP}]\,[\mathrm{HA}], \qquad (10)$$

where k_a is the rate constant calculated per mole of acid; a and b are empirical constants; and [HP] is the hydroperoxide concentration.

The addition of a small quantity of acetic anhydride brought about a sharp change in the nature of the kinetic curves. Figure 2 shows the kinetic curves for the reaction (at 50°, for $[H_2SO_4]$ = 0.03 mole/liter). Curve 1 was recorded in the absence of acetic anhydride. This is the usual kinetic curve for a first order reaction. The reaction follows the same curve in the presence of 0.1 mole/liter acetic acid.

If we start the reaction by mixing a solution of the hydroperoxide containing acetic anhydride with sulfuric acid solution containing water, the rate of decomposition increases sharply after a certain time has elapsed from the start of the reaction (Fig. 2, curve 2). If all the water is removed from the original solutions before the start of the reaction (this can be done by dividing the acetic anhydride between the original solutions), the rate of decomposition increases from the earliest stages of the reaction (Fig. 2, curve 3). In order to prove that the cause of the increase in rate is the removal of water as a result of its reaction with acetic anhydride, in one of the experiments a quantity of water (0.01 mole/liter) was introduced into the reaction mixture during the course of the reaction, which was started as in the case represented by curve 3. The addition of water led to a marked decrease in the rate of the decomposition (curve 4). Acetone, which accelerates the reaction in a medium of acetic acid, retards the process slightly in dioxane containing acetic anhydride. Thus when the last traces of water are removed, the reaction rate increases more sharply than follows from Eq. (10). The spontaneous acceleration of the process in the case where all the water was removed from the initial solutions before the start of the reaction (curve 3) can be attributed to the fact that the anhydride also removed the water which is formed during the course of the reaction. Diphenylpicrylhydrazyl has no influence on the rate of the acid decomposition of cumene hydroperoxide in the presence of acetic anhydride. The same regular features were observed for the decomposition of all the hydroperoxides studied, although their rates of decomposition varied considerably.

Shushunov and Shlyapnikov [19] put forward a scheme for the acid decomposition of hydroperoxides, which provides a qualitative and quantitative explanation of all the regular features observed experimentally:

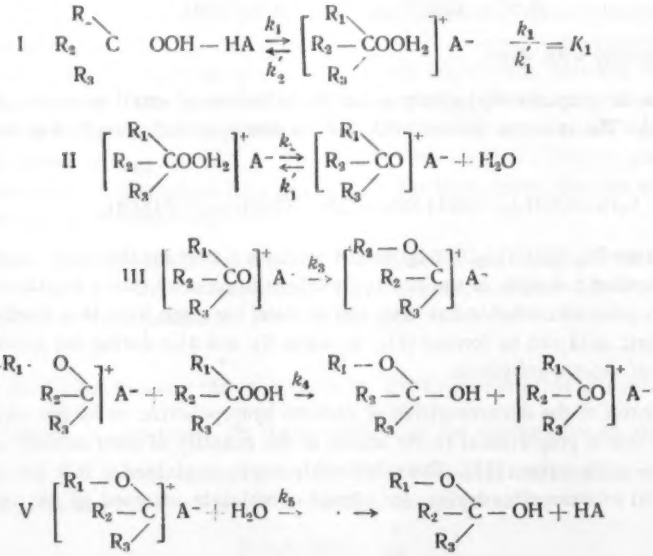

343

$$R_1-O\diagdown \\ R_2-C-OH \rightarrow R_1OH + R_2-CO-R_3. \\ R_3\diagup$$

This scheme differs from that of Kharasch [1] in that the free ions are replaced by ion pairs; this is necessary in order to explain the fact that the reaction is of first order with respect to both hydroperoxide and acid, and, which is more important, because it provides for two forms of chain rupture. Calculation carried out on the basis of this scheme by means of the method of quasi-stationary concentrations leads to the equation:

$$-\frac{d[HP]}{dt} = \frac{K_1 k_2 [HP][HA]}{1 + \frac{k_2'}{k_3}[H_2O] - \frac{k_4[HP]}{k_4[HP] + k_5[H_2O]}}. \qquad (12)$$

When the water concentration is sufficiently high ($k_5[H_2O] \gg k_4[HP]$), the third term in the denominator of Eq. (12) can be neglected. This gives the equation:

$$-\frac{d[HP]}{dt} = \frac{K_1 k_2 [HP][HA]}{1 + k_2'/k_3[H_2O]}, \qquad (12a)$$

which is identical with the experimentally-observed Eq. (10), if we put K_1k_2 = a and k_2'/k_3 = b.

Equation (12a) can be obtained from the scheme of Seubold and Vaughan [8] (with certain additional assumptions), but this scheme cannot explain the spontaneous acceleration of the reaction in the presence of acetic anhydride. This effect, however, is readily explained by Kharasch's scheme [1] (if stage I is assumed to be reversible).

The regular features of the reaction between acetic anhydride and water under the experimental conditions (extremely low concentrations of water and fairly high concentrations of sulfuric acid) are not known. Calculations show that irrespective of the order of the reaction with respect to water and the other component, the decomposition of hydroperoxide in the presence of small quantities of anhydride, if scheme (11) is accurate, should take place with a spontaneous acceleration. The best agreement with experiment is shown by the assumption that the rate of the interaction between acetic anhydride and water in the presence of sulfuric acid should be independent of the water concentration; this may be the case if the first and rate-determining stage of the interaction is the process:

$$H_2SO_4 + (CH_3CO)_2O \rightarrow SO_3 + 2CH_3COOH$$

after which the SO_3 reacts rapidly with water.

Cumene hydroperoxide decomposes explosively under the influence of small quantities of sulfuric anhydride even at low temperatures [4]. The reaction between SO_3 and the hydroperoxide can lead to the formation of cumene persulfate:

$$C_6H_5-C(CH_3)_2-OOH + SO_3 \rightarrow C_6H_5-C(CH_3)_2-OOSO_2OH,$$

which has the ion-pair structure $[C_6H_5C(CH_3)_2O]OSO_2OH$ and provides a start for the chain reaction. The same thing apparently takes place when a sample of the hydroperoxide is introduced into a solution of sulfuric acid and acetic anhydride in dioxane, after this solution has been left to stand for some time in a thermostat [19], where dehydration products of sulfuric acid can be formed (Fig. 2, curve 5), and also during the decomposition of the hydroperoxide in a medium of acetic anhydride.

In the study of the kinetics of the decomposition of cumene hydroperoxide on an ion-exchange resin, it was discovered that the reaction rate is proportional to the square of the quantity of solid catalyst in unit volume of the solution, i.e., to the square of the surface [21]. This relationship can be explained if it is assumed that traces of water remaining in the initial mixture after drying, are almost completely adsorbed on the catalyst surface. In

The Decomposition of Various Hydroperoxides in Dioxane. Catalysts H_2SO_4

Substance	$k_{obs.}$,* liter · mole^{-1} · sec^{-1}	K_1k_2, liter · mole^{-1} · sec^{-1}	k'_2/k_3 liter/mole^{-1}	E kcal/mole	A_0,** liter · mole^{-1} · sec^{-1}
	при 40°				
Cumene hydroperoxide	$8{,}7\cdot10^{-3}$	$9{,}8\cdot10^{-3}$	36	20,7	$3\cdot10^{12}$
p-Tertbutylcumene hydroperoxide	$3{,}55\cdot10^{-2}$	$3{,}9\cdot10^{-2}$	29	19,6	$4\cdot10^{12}$
p-Hydroxycumene hydroperoxide	0,38	0,6	70—130	18	$2\cdot10^{12}$
p-Diisopropylbenzene hydroperoxide	$4{,}5\cdot10^{-2}$	$4{,}8\cdot10^{-2}$	20	19,5	$2\cdot10^{12}$
Secbutylbenzene hydroperoxide	$8{,}7\cdot10^{-3}$	$1\cdot10^{-2}$	50—60	21,0	$5\cdot10^{12}$
Cyclohexylbenzene hydroperoxide	$4{,}47\cdot10^{-3}$	$5\cdot10^{-3}$	26	18,2	$1\cdot10^{9}$
p-Isopropylcyclohexylbenzene dihydroperoxide	$3{,}54\cdot10^{-2}$	—	—	—	—
Diphenylmethane hydroperoxide	$4{,}15\cdot10^{-3}$	$4{,}4\cdot10^{-3}$	19	22,8	$4\cdot10^{13}$
Diphenylethane hydroperoxide	$2{,}56\cdot10^{-2}$	$2{,}9\cdot10^{-2}$	45	18,0	$1\cdot10^{11}$

* At $[H_2O] = 3.22 \cdot 10^{-3}$ mole/liter.

** A_0 is the preexponential factor calculated on the assumption that $k_{obs.} = K_1k_2 = A_0e^{-\frac{E}{RT}}$.

*** Structure 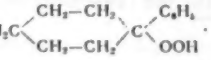 .

this case the surface concentration of water will be inversely proportional to the area of the surface. On the other hand, it follows from (12) that when $[H_2O] \gg k_4/k_5\,[HP]$, the rate of reaction (in this case on the resin surface) becomes inversely proportional to the water concentration, i.e., the specific rate of reaction (calculated per unit area of the catalyst) will be proportional to the surface of the catalyst in unit volume of the solution and the total rate will be proportional to the square of this quantity.

As already indicated, the same regular features were observed in the decomposition of the various peroxides studied by Shushunov and Shlyapnikov [18, 19].

The table gives values of the rate constants for the decomposition of these hydroperoxides under identical conditions, the constants from Eq. (12a), the activation energies, and the pre-exponential factors. In order to calculate the quantities K_1k_2 and k'_2/k_3, a study was made of the relationship between the experimental constant $k_{obs.}$ and the water concentration. The table also gives values of $k_{obs.}$ for the single water concentration ($[H_2O]$ = = 0.0032 mole/liter) at which the relationship between the rate and the temperature was studied. Since at this water concentration the value of $k_{obs.}$ is close to that of K_1k_2, the activation energy given in the table is related to the value of K_1k_2. For the case of cumene hydroperoxide it has been shown that the value of k'_2/k_3 shows almost no change with change in temperature.

The table includes p-hydroxycumene hydroperoxide, which has not been isolated in the free state, but which is an intermediate product of the decomposition of p-diisopropylbenzene dihydroperoxide. The rate constants for its decomposition were calculated from the kinetic curves for the decomposition of the dihydroperoxide.

For this purpose, the curves showing the change in the total concentration of hydroperoxide groups were plotted on coordinates $\log \frac{C_0}{C}$ versus time. On these coordinates the curves have an asymptote which cuts off an intercept θ on the x axis. It can be shown that if the dihydroperoxide decomposes much more slowly than p-hydroxycumene hydroperoxide, the decomposition constant for the latter is:

$$k = k_{II}\,[HA] = \frac{1}{2\theta}. \qquad (13)$$

The table shows that for the cumene hydroperoxide derivatives studied, including the dihydroperoxide, the pre-exponential factors are practically the same (taking account of the fact that the error in their calculation is large).

The introduction of the tertbutyl, and, more particularly, the hydroxy group, into the para position in the ring leads to a marked increase in the rate of decomposition of the hydroperoxide. On the other hand, the nitro group leads to a marked decrease in the rate of the acid decomposition [9].

In the decomposition of p-nitrophenyldiphenylmethane hydroperoxide under the influence of acid, the hydroxyl group is transferred for the most part to an unsubstituted phenyl group [22].

In the decomposition of cumene hydroperoxide under the influence of perchloric acid, the rate is higher than in the case of sulfuric acid, and increases more rapidly with increase in the acid concentration than is required by first order kinetics. It has been shown that in a medium of methyl alcohol this can be attributed to the catalytic action of the ClO_4^- [23].

SUMMARY

1. Experimental data of various authors for the acid decomposition of hydroperoxides and the isomerization of peroxy esters have been examined.

2. The mechanism of the acid decomposition of hydroperoxides, which was suggested by the author and V. A. Shushunov, and which regards the reaction as an ionic chain reaction, has been generalized. Data for the kinetics of decomposition of various hydroperoxides under identical conditions have been compared.

LITERATURE CITED

1. M. S. Kharasch, A. Fono, and W. Nudenberg, J. Org. Chem. 15, 748 (1950).
2. M. S. Kharasch and J. G. Burt, J. Org. Chem. 16, 150 (1951).
3. H. Hock and S. Lang, Ber. 77, 257 (1944).
4. B. D. Kruzhalov and P. G. Sergeev, Khim. Nauka i Prom. 1, 287 (1956).
5. H. E. Holmquist, et al., J. Am. Chem. Soc. 78, 5339 (1956).
6. M. S. Kharasch, A. Fono, and W. Nudenberg, J. Org. Chem. 16, 128 (1951).
7. M. S. Kharasch, et al., J. Org. Chem. 17, 207 (1952).
8. F. H. Seubold and V. E. Vaughan, J. Am. Chem. Soc. 75, 3790 (1953),
9. O. Wichterle and P. Cefelin, Collection Czechosl. Chem. Commun. 22, 1083 (1957).
10. H. Wieland and J. Maier, Ber. 64, 1205 (1931).
11. H. Hock and H. Kropf, Chem. Ber. 88, 1544 (1955).
12. R. Criegee and R. Kaspar, Ann. 560, 127 (1948).
13. P. D. Bartlett and B. T. Storey, J. Am. Chem. Soc. 80, 4954 (1958).
14. P. D. Bartlett and J. L. Kice, J. Am. Chem. Soc. 75, 5591 (1953).
15. H. L. Goering and A. C. Olson, J. Am. Chem. Soc. 75 5853 (1953).
16. D. B. Denney and D. G. Denney, J. Am. Chem. Soc. 79, 4801 (1957).
17. V. A. Shushunov and Yu. A. Shlyapnikov, Works on Chemistry and Chemical Technology [in Russian] (Gor'kii, 1958) p. 50.
18. V. A. Shushunov, Yu. A. Shlyapnikov, and A. A. Kvasov, Works on Chemistry and Chemical Technology [in Russian] (Gor'kii, 1959) p. 102.
19. V. A. Shushunov and Yu. A. Shlyapnikov, Doklady Akad. Nauk SSSR 128, 341 (1959).•
20. C. E. Bawn and S. F. Mellish, Trans. Faraday Soc. 47, 1216 (1951).
21. V. A. Shushunov, V. A. Yablokov, and O. A. Kolmakov, Works on Chemistry and Chemical Technology [in Russian] (For'kii, 1959) p. 24.
22. P. D. Bartlett and J. D. Cotman, J. Am. Chem. Soc. 72, 3095 (1950).
23. A. W. de Ruyter van Steveninck, J. Chem. Soc. 2066 (1958).

•Original Russian pagination. See C. B. translation.

MECHANISM OF HOMOGENEOUS CATALYTIC ACTIVATION OF MOLECULAR HYDROGEN

V. K. Bykhovskii and O. N. Temkin

M. V. Lomonosov Moscow Institute of Refined Chemical Technology and
L. Ya. Karpov Physicochemical Institute
Translated from Kinetika i Kataliz, Vol. 1, No. 3, pp. 374-378,
September-October, 1960
Original article submitted March 12, 1960

The mechanism of homogeneous activation of molecular hydrogen by different catalysts was investigated.

It is assumed that in the transitional state the molecular orbitals of the ligands can take part in the general binding (dative bond). The decisive significance of this effect in the process of activation of molecular hydrogen and unsaturated compounds is indicated.

* * *

Analysis of the accumulated experimental data concerning the homogeneous catalytic activation of hydrogen and unsaturated molecules in the addition reaction of salts of copper (Cu^{I}, Cu^{II}), silver (Ag^{I}), mercury (Hg^{I}, Hg^{II}), platinum (Pt^{II}), rhodium (Rh^{I}), and palladium (Pd^{II}), and also bases, amides, alkyls, and metal carbonyls, leads us to assume that there exists a definite analogy in the mechanism of activation of different molecules by the substances indicated. Thus, all the compounds mentioned catalyze the reduction, the isotopic exchange, and the ortho-para transformation of molecular hydrogen [1-2]. Platinum salts catalyze homogeneous hydration of ethylene [3], and platinum and palladium salts catalyze the oxidation of olefins [4, 5]. The hydrogenation and hydroformulation of olefins occur in the presence of cobalt carbonyl [6, 7], while polymerization occurs in the presence of the metal alkyls [8]. As to acetylene, it adds the HX molecule (where X can be OH, Cl, Br, I, CN, CH_3COO) in the presence of copper, silver, and mercury salts [9]; it undergoes polymerization in solutions of copper salts [10]; a carbonyl is formed and condensation occurs in the presence of nickel, cobalt, and iron cyanides [11, 12]; it adds alcohols in alkaline solutions [12, 13]. Furthermore, acetylene is hydrated in alkaline solutions [14] and is polymerized in the presence of metal alkyls [8, 15]. The analogy can be seen in the fact that the transformation of the same molecule (i.e., H_2 or C_2H_2) is catalyzed by species of different natures (e.g., Cu^{+} and Hg^{++} or OH^{-} and NH_2^{-}) and, conversely, the same catalyzing particle (e.g., Hg^{++} or R) activates completely different molecules (e.g., H_2, C_2H_2, C_2H_4). The analogy in the mechanism of the activation of H_2 and C_2H_2 was noted earlier by Ya. K. Syrkin [16]. It must be noted that in spite of the numerous investigations undertaken to clarify the mechanism of catalytic activation of the molecules investigated with respect to the addition reaction, no satisfactory explanation has yet been found. Therefore it seems of importance to attempt to find some common characteristics of the mechanism of activation of different molecules in the case of the simplest activated molecule, H_2.

The most widely accepted point of view concerning the mechanism of activation of molecular hydrogen by metal salts was developed in detail by Halpern [1]. It assumes that the complex ion in the solution possesses low energy orbitals which are used by the electrons of the H_2 molecules; the decrease of the activation energies of the processes involving H_2 is due to this removal of electrons from H_2. In accordance with this point of view Halpern relates the reaction capacity of complex ions to their affinity for the electrons, which is approximated by corresponding values for metal ions in the gaseous state. It should be noted, however, that this correlation is not always satisfactory. For example, in the fourth period the maximum affinity among the doubly charged

ions is manifested by Cu^{++} (27.9 ev), which also has the highest catalytic activity, but its neighbor, Zn^{++} (27.4 ev) is totally inactive up to 150°. Let us note that the analogous correlation for Cu^{++}, Ag^{+}, and Hg^{+}, is also unsatisfactory. Further, to explain the optimum activity of ions d^{8}-d^{10} from the point of view of the displacement of the electrons, $H_2 \rightarrow M^{+}$, Halpern must make an artificial assumption concerning $d \rightarrow sp$ promotion of electrons of the central atom, which is in this case rather improbable. This point of view is even less satisfactory because it is just the d^{10} ions which have the maximum activity. Ya. K. Syrkin [16] believes that in the activation of H_2 by the metal salt an essential role is played by the formation of three-centered bonds of the type: . This assumption, which takes into account only donor-acceptor bonds, is insufficient in our opinion, and does not satisfactorily explain the existing data. In particular, the mechanism of the activation of H_2 by the OH^{-}, NH_2^{-}, R^{-} (R alkyl) and by many other species mentioned above, remains unexplained.

There is reason to believe that the indicated defects in the interpretation of the mechanism of activation of molecular hydrogen by metal salts is due to the fact that the possibility of the participation of dative bonds in the process of activation is not taken into account. Dative bonds, particularly in recent years, have been used successfully in the description of the structure and reaction capacity of complex compounds [2, 17, 18]. The tendency to form a maximum number of bonds between the central atom (ion) and the ligands [16], (i.e., in the final analysis, by the tendency to decrease the total energy of the system), induces the creation of dative bonds. As is known, the undivided electron pairs of the central atom are brought together as the result of their transfer to the free molecular orbitals of the total system, and the orbitals of the ligands may be included in the total binding. At this point, it is necessary to note the following: In spite of the general stabilization of the system (complex) resulting from the fact that the undivided pairs are brought together, the binding within the ligand itself (H_2, C_2H_2, C_2H_4, and others) can be weakened because of the intervention of its molecular orbitals in the total binding.

Apparently this effect leads to the activation of the ligand (for example, terminal or nonterminal hydrogen) with respect to the addition reaction of different molecules. We believe that the effect of inclusion of undivided pairs in the general binding is not limited to the complex compound, but occurs much more widely (e.g., the mechanism of the configurational interaction).

The effects due to the charge transfer in the transitional state, for example in reactions of the type, $Na(^2P) + H_2 \rightarrow Na(^2S) + 2H$ or $Hg(^3P) + H_2 \rightarrow Hg(^1S) + 2H$, were treated from the quantum mechanics point of view [19], and the transitional complex was written as $Na^{+}H_2^{-}$ or $Hg^{+}H_2^{-}$. It has been suggested that dative bonds play an important role in the transitional state of the hydration of acetylene by the Kucherov method [20]. During the investigation of the catalytic addition of HX molecules to acetylene, it was noted also that metal ions capable of forming dative bonds are the most active in the activation of acetylene. It was shown that there exists a relationship between the capacity of ions to activate acetylene, with dissociation of the C-H bonds, and their tendency to form dative bonds. These data were successfully applied in choosing the catalyst for some acetylene reactions [9, 21]. The decisive significance of the effects of dative bonds was demonstrated during the investigation of the mechanism of polymerization of olefins [22, 23]. All these results indicate the necessity of taking into account the possibility of dative bonds to participate in the process of activation of molecular hydrogen.

Let us examine a few possible models of the transitional state during the process of activation of hydrogen. The concept of the dominating effect of donor-acceptor bonds in the transitional state corresponds to the complex: 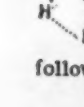 or $H_2 \rightarrow H^{+}$. Then the effects conditioned by the possibility of dative bonds can be investigated by the following models: or (corresponding respectively to the dative bonds made by an unpaired electron or an undivided pair). It is easy to see that the indicated series of complexes (H_3^{+}, H_3, and H_3^{-}) is similar to the sequence of H_2^{+}, H_2, and H_2^{-}. If the bond order (p) is defined as the corresponding combination of the number of filled connecting and molecular orbitals [24], then H_2^{+}, H_2, and H_2^{-} must be written in the bond order, $p = \frac{1}{2}$, 1, and $\frac{1}{2}$, while for H_3^{+}, H_3, and H_3^{-}, $p = \frac{2}{3}$, $\frac{1}{3}$, and 0, respectively. The binding energies and the internuclear distances in these species are in good agreement with the bond order (see table), so that for a

Characteristics of the Model Complex

Complex	Bond order (p)	Binding energy, ev	Internuclear distance, A	Lit. cited
H_3^-	0	–	–	–
H_2^+	1/2	2.73	1.07	[25]
H_2^-	1/2	2.4	0.86	[26]•
H_3	1/3	–	–	–
H_2	1	4.74	0.74	[25]
H_3^+	2/3	–	–	–

•Calculated.

complex with unknown parameters one can make certain conclusions based on the bond order. In particular, since the bond order of H_2 and H_3^+ are close to each other, one can conclude that the binding properties in H_3^+ are not weakened significantly with respect to those in H_2. This indicates that a particle of the H^+ type, which does not have electrons of its own, apparently cannot activate an H-H bond. Thus, Halpern's idea of the dominant role of the donor-acceptor bond becomes again questionable. On the contrary, if the catalyzing species has its own electrons, as in the case of H or H^-, then one would expect, according to the bond order, a certain loosening of the H-H bond in the activated state – H_3($p = 1/3$) or H_3^- ($p = 0$); it should be noted that in the symmetrical activated complex all the H-H bonds are weakened to the same degree. This consideration of the condition of binding in models of transitional complexes makes it possible to confirm the earlier assumption and to indicate the general characteristics of the mechanism of activation of saturated (H_2) and unsaturated molecules; the mechanism is apparently reduced to the participation of the molecular orbitals of molecules being activated in the general binding. This point of view makes it possible to explain satisfactorily the extensive results accumulated in this area.

As early as 1936 Wirtz and Bonheoffer [27] found that molecular hydrogen exchanges with heavy water in the presence of an alkali. In a solution of potassium amide in liquid ammonia molecular deuterium exchanges very rapidly [28]. However, no exchange of D_2 occurred in 10 M sulfuric acid (120°, 5 hr) or in a mixture of $HF-BF_3$ under analogous conditions [28]. Catalysis in these cases was ascribed to the ionized acid-base interaction. From our point of view there is no reason to ascribe such a property to molecular hydrogen. Here one can assume also that the catalytic activation is reduced to the participation of the molecular orbitals of H_2 or D_2 in the general binding of a suitable activated complex (linear or trigonal) through the intermediary of undivided pairs of OH^- or NH_2^- (so that one obtains a complex analogous to H_3^-). From this point of view, one can expect, for example, an exchange in the presence of H^- or R^- (R alkyl), i.e., in solutions of metal hydrides or alkyls in suitable solvents and also, for example, in the presence of species of the I^- type. The ease with which hydrogen is reduced in alkaline metal alkyls is explained in the same way [28]. The absence of exchange during the catalysis of H^+ (H_2SO_4, $HF-BF_3$) can be explained by the absence of the dative bond in the H_3^+ complex. Let us note that catalysis of the ortho-para transformation and of the exchange of hydrogen by paramagnetic particles fits very well in the framework of the scheme developed here (H_3 model). The activation of hydrogen by metal salts is also based on the assumption of the formation of the σ complex with a dative bond in the transitional state. Such a point of view is confirmed by the similarity between the reaction rates and activation energies during the catalysis of different transformations of hydrogen by the OH^-, NH_2^-, and some metal ions and salts [28]. Let us note that the problem of the linear or trigonal structure of the transition complex requires a special discussion in each concrete case.

During the investigation of the catalytic activation of molecular hydrogen by metal salts, it was found that the ligands affect the rate and activation energy of the process. Halpern explains this effect from the point of view of the strength of the bond between hydrogen and the ligands. Within the framework of concepts developed

in this article the effect of ligands is accounted for by the participation of the electrons of the ligand in the charge transfer within the limits of the transition complex. Ligands with low free energy orbitals (CN^-, PR_3, Cl, Br, I, and some organic anions, etc.) are capable of assembling the d electrons of the central atom. In this case one would expect a decrease in catalytic activity with respect to ligands of the H_2O, F, NH_3, and others, which is in agreement with the experimental data. In this case of the polybond ligand of the ethylendiamine type, one must also take into account the difficulty of spatial coordination of H_2.

To conclude, let us note that the mechanism by which atoms in the excited state are brought to lower states by saturated and unsaturated molecules, the mass spectrometrical reaction of hydrogen, the mechanism of rapid exchange of hydrogen in NaCl at 20-340° (activation energy, 8 kcal/mole), and other problems can be investigated from the point of view proposed here.

SUMMARY

We have investigated the mechanism of homogeneous activation of molecular hydrogen by different catalysts on the basis of the assumption that the molecular orbitals of the ligand (H_2) participate in the general binding of the transition state (dative bonds). We have indicated that this effect has a decisive importance in the activation of ligands. In view of this it has been assumed that the activation of the saturated and unsaturated molecules (H_2, C_2H_2, C_2H_4, and others) is similar, which is in accord with the experimental data concerning the reactions of the compounds. The mechanism proposed explains satisfactorily the difference in the catalytic activity of the metal ions, the effect of the ligands, and also the mechanism of activation by species of the type of R^-, OH^-, NH_2^-, and others.

The authors express their profound thanks to T. K. Rebane for discussions of this work and a number of valuable suggestions.

LITERATURE CITED

1. I. Halpern, Adv. in Catal. 9 (195); 11, 301 (1959).
2. F. Basolo and R. G. Pearson, Mechanisms of Inorganic Reaction in Solutions (New York, 1958).
3. I. H. Flynn and H. M. Hulburt, J. Am. Chem. Soc. 76, 3393, 3395 (1954).
4. I. I. Moiseev, M. N. Vargaftik, and Ya. K. Syrkin, Doklady Akad. Nauk SSSR 130, 820 (1960).*
5. I. Smidt, et al., Angew. Chem. 71, 5, 176 (1959).
6. H. Adkins and G. Krsek, J. Am. Chem. Soc. 71, 3051 (1949).
7. I. Wender, R. Levine, and M. Orchin, J. Am. Chem. Soc. 72, 4375 (1950); I. Wender, M. Orchin, and H. H. Storch, J. Am. Chem. Soc. 72, 4842 (1950).
8. N. G. Gaylord and H. F. Mark, Linear and Stereoregular Addition Polymers (Interscience Publ. Inc., New York, 1959) Chap. 7.
9. R. M. Flid, Doctoral Dissertation [in Russian] (MITKhT, Moscow, 1959).
10. A. L. Kelbanskii, I. M. Dolgonol'skii, and Z. F. Dobler, Doklady Akad. Nauk SSSR 114, 323 (1957).*
11. W. Reppe, Chimia 3, 233 (1949).
12. Chemistry of Acetylene, Collection of papers ed. by A. D. Petrov [Russian translation] (IL, Moscow, 1954).
13. M. F. Shostakovskii, Simple Vinyl Ethers [in Russian] (Izd. AN SSSR, Moscow, 1952).
14. M. Ban and T. Jamamoto, J. Chem. Soc. Japan Ind. Chem. Sect. 61, 706, 708 (1958).
15. B. Frauzus, P. I. Canterino, and R. A. Nicklitte, J. Am. Chem. Soc. 81, 6, 1514 (1959).
16. Ya. K. Syrkin, Uspekhi Khim. 28, 903 (1959).
17. I. Chatt, Cationic Polymerisations, ed by Plesh. (Cambr. Univ. Press, 1953).
18. Chemistry of the Co-ordination Compounds. A. Sympos. (Pers. Press, 1957).
19. K. I. Laidler, Chemical Kinetics of Excited States (1955) p. 23.
20. I. I. Moiseev, Candidate's Dissertation [in Russian] (MITKhT, Moscow, 1958).
21. R. M. Flid and O. N. Temkin, Zhur. Fiz. Khim. [in press].
22. V. K. Bykhovskii and K. S. Minsker, Vysokomolek. Soed. 2, 529 (1960).
23. K. S. Minsker and V. K. Bykhovskii, Vysokomolek. Soed. 2, 535 (1960).
24. G. Herzberg, Spectra and Structure of Diatomic Molecules [Russian translation] (IL, Moscow, 1949).

*Original Russian pagination. See C. B. translation.

25. Landolt-Börnstein, Physikalisch-chemischen Tabellen, Zahlenwerten und Funktionen 1, 3, 4.
26. J. Fischer-Hjalmars, J. Chem. Phys. 31, 1099 (1959).
27. K. Wirtz and K. F. Bonhoeffer, Z. Phys. Chem. A177, No. 1 (1936).
28. C. V. Weller and J. A. Mills, Some Problems of the Theory and Technology of Organic Reactions [Russian translation] (IL, Moscow, 1959) 208.

EFFECT OF CATHODIC AND ANODIC POLARIZATION ON THE CATALYST FOR AMMONIA SYNTHESIS AND ITS ACTIVITY•

L. M. Dmitrenko, S. S. Lachinov, and R. F. Sibyakova

Scientific Research Institute of the Nitrogen Industry

Translated from Kinetika i Kataliz, Vol. 1, No. 3, pp. 379-384,
September-October, 1960
Original article submitted December 22, 1959

We describe the method and the results of an investigation concerning the effect of polarization of the catalyst on its activity, and the effect of chemisorption of nitrogen and hydrogen and of the reaction of synthesis of ammonia on the intensity of the polarizing current. It is shown that the activity of the catalyst increases as the result of cathodic polarization, and decreases as a result of anodic polarization. We believe that electron transfer is the basis of the process of ammonia synthesis and that the limiting stage of the process is the transfer of electrons from the catalyst to the adsorbed particles.

• • •

During recent years the role of electrons in catalysis has been greatly emphasized [1-5]. Investigators have found a definite relationship between the catalytic activity and the electron state of solids for different reactions occurring on metals and semiconductors. There are various publications concerning the synthesis of ammonia with iron or other catalysts which attempt to show that the basis of this catalysis is to be found in the electron mechanism [6, 7]. We have investigated the relationship between the catalytic activity of iron catalysts used for ammonia synthesis and their electronic structure, using the method worked out by A. I. Krasil'shchikov and L. G. Antonova [8]. This method consists essentially in determining the effect of the polarization of the catalyst on the rate of the catalytic reaction.

The essential part of the apparatus used in this method is a glass cell reactor with two electrodes consisting of deposits on the inside and outside walls of the reactor; these electrodes are connected with a source of direct current through platinum contacts. The inside electrode consists of a deposit of the catalyst being investigated; the electrolyte is the glass, conducting current at high temperatures.

The catalyst electrode is polarized by direct current under a difference of potential of 300 v. Alternating current from an outlet is passed through a voltage stabilizer and a rectifier, then through a rheostat and microamperemeter, and finally through the electrodes of the reaction tube. As the current is switched on the difference of potential at the limit of separation, catalyst-glass, changes by a jump and induces polarization of the surface of the glass. Since the deposit of the reduced catalyst is porous, the gas has the possibility of penetrating freely to the surface of the glass and is adsorbed at the polarized surface of the catalyst. The cathodic polarization of the catalyst facilitates the passage of electrons from the solid to the adsorbed gas, and during the anodic polarization of the catalyst the electrons pass from the adsorbed gas to the solid. Consequently, if the limiting stage of the catalytic process is the transfer of electrons from the solid to the gas, then the cathodic polarization will increase the rate of the reaction while anodic polarization will decrease it. If, however, the limiting stage is the transfer of electrons from the adsorbed gas to the catalyst, then the phenomenon will be reversed.

•M. A. Petrova and N. M. Khokhlova, laboratory assistants, participated in this investigation.

EXPERIMENTAL

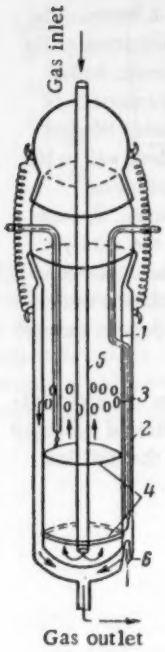

Fig. 1. Reaction vessel.

In the A. I. Krasil'shchikov reactor the inside electrode is in an atmosphere of the gas being investigated and the outside electrode is in air. The creation of the deposit of the catalyst for ammonia synthesis on the inside wall of the tube is somewhat difficult. Furthermore, as our further experiments have shown, it is important that both electrodes be in contact with the same gas. As a result of this consideration we developed another reactor (Fig. 1) composed of two tubes, 1 and 2, put one inside the other and connected through a ground glass cover. The inner tube 1, has a number of openings, 3, around the perimeter which allow the gas to pass from tube 1 into the space between the two tubes.

The catalyst was deposited in the following way: Finely ground catalyst was mixed into a 3% solution of "liquid glass" and was sprayed on the heated outer surface of tube 1. The second electrode—the deposit of nickel—was prepared by decomposing nickel nitrate on the inner surface of the same tube. The two electrodes were connected with the source of direct current through two platinum rings 4, which closely fitted the glass and the electrodes.

The reactor was welded into an apparatus in which gas could pass through and circulate. The experiments described below were performed in the part of the apparatus where the gas was passing through.

The nitrogen-hydrogen mixture of stoichiometric composition used in the experiments was collected from the high pressure purifier into a bottle, then purified at low pressure in an apparatus composed of a series of scrubbers filled with activated carbon, fused alkali, silica gel, and a furnace with a nickel-chromium catalyst and two traps with silica gel in Dewar flasks filled with liquid nitrogen. The thoroughly purified nitrogen-hydrogen mixture was admitted to the reactor along the central tube 5, and passed over the nickel electrode, the catalyst deposit, and then evacuated at the bottom. This arrangement was used to avoid heating the ground stopper (by the hot exhaust gases) when it was closed. The temperature in the area of the catalyst was measured with a thermocouple introduced in a special housing, 6. The rate of the gas leaving the reactor was measured with a gas flow meter. Samples of the gas were taken periodically to determine the concentration of ammonia in it.

In the first few experiments the nickel and the catalyst deposits were reduced simultaneously, but in later experiments they were reduced separately by the ordinary steplike method [11].

The geometric surface of each deposit was approximately 75-80 cm^2. The thickness of the catalyst deposit was not greater than 1 mm, and its weight in the reduced state was about 2 g.

Before each experiment the kinetic of the process was measured at different temperatures. The main experiments were performed essentially at temperatures of 350° and a pressure of 1 atm, with a gas flow rate of 7 liter per hr under normal conditions.

The sequence of the experiments with the reduced deposits was as follows: First the concentration of ammonia in the exhaust gas was determined under stable conditions, then cathodic and anodic polarization were alternated, each being continued for several hours. The variation in the concentration of ammonia occurring as the result of the polarizing current allowed us to determine the effect of the polarization current on the activity of the catalyst.

EXPERIMENTAL RESULTS

We performed the experiments with deposits of catalysts whose activity was promoted by the addition of potassium and aluminum oxide (K-55). In Expt. No. 14 the second electrode was a silver deposit, and in No. 16, a nickel deposit.

The results of Expt. No. 14 are shown in Fig. 2. The x axis represents time (τ) of the experiment and the y axis the percent of ammonia and the density of the polarizing current in $\mu a/cm^2$. The curve shows that in this experiment the cathodic polarization has almost no effect on the concentration of ammonia, while anodic

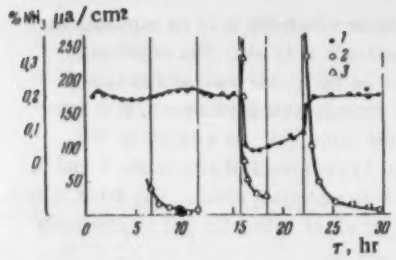

Fig. 2. Variation of the concentration of ammonia during cathodic and anodic polarization of the K-55 (second electrode, Ag). Expt. No. 14: 1) % NH_3; 2) current density during cathodic polarization; 3) current density during anodic polarization.

polarization decreases the original concentration 4-5 times. The fact that the density of current during cathodic polarization of the catalyst is considerably lower than the density of current during anodic polarization, is important. Possibly the concentration of ammonia remains constant during cathodic polarization because of the low current density. Therefore our first problem was to try to increase the current density during cathodic polarization. Investigation of the mechanism of the transfer of current through the glass shows that during cathodic polarization of the catalyst, the cations (primarily Na^+ and Ag^+) transfer from the silver deposit to the catalyst. Consequently, during anodic polarization some other cations in addition migrate from the catalyst deposit through the glass.

We have assumed that these additional cations are essentially hydrogen ions formed as the result of the dissolution of hydrogen in the electrodes, with the release of electrons into the unfilled

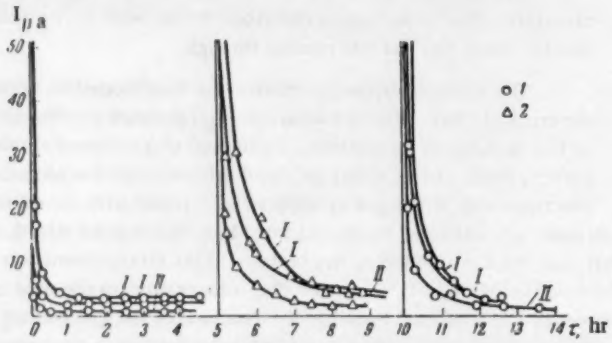

Fig. 3. Variation of the intensity of polarizing currents as a function of the composition of the gaseous medium (electrodes, nickel-nickel). 1) Current intensity during cathodic polarization; 2) current intensity during anodic polarization. I) In nitrogen-hydrogen mixture; II) in nitrogen.

d shell of the metal. The transfer of hydrogen ions through the glass in the case of aqueous solutions was shown by Kvitner [10]. It is probable that an analogous situation occurs in a gaseous medium.

We decided to check this assumption with an experiment. It is well known that metals such as palladium, nickel, and others dissolve hydrogen much better than silver; consequently, the use of deposits of these metals should increase somewhat the density of cathodic current. We deposited nickel on both sides of the walls of the reactor and measured the intensity of the polarizing current in nitrogen and in a nitrogen-hydrogen mixture. The results of the experiments are shown in Fig. 3, where the x axis represents time, and the y axis the intensity of current, I.

The figure shows that the intensity of current in the nitrogen-hydrogen mixture is somewhat higher than in nitrogen, which indicates that our assumption concerning the transfer of current through the glass by the hydrogen ion is correct.

In further experiments we used a nickel deposit as a second electrode. The results of Expt. No. 16, where the second electrode was a nickel deposit, are shown in Fig. 4.

In this experiment we alternated many times from cathodic to anodic polarization. Furthermore, we checked the concentration of ammonia when the polarizing current was off. The figure shows that the concentration of

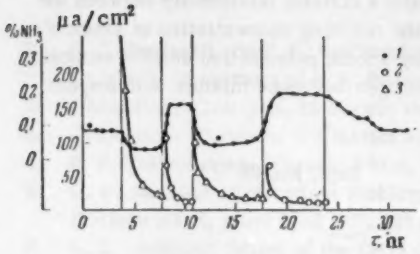

Fig. 4. Variation of the concentration of ammonia during cathodic and anodic polarization of the K-55 catalyst (second electrode, nickel). Expt. No. 16: 1) % NH_3; 2) current density during cathodic polarization; 3) current density during anodic polarization.

ammonia increases from 2 to 2.5 times during cathodic polarization and decreases about 2 times during anodic polarization. Switching from cathodic and anodic polarization and back, induces sharp changes in the concentration of ammonia, which indicates the transfer of electrons in the process of ammonia synthesis, and thus the limiting stage is the transfer of electrons from the catalyst to the adsorbed gas, most probably to the nitrogen. The slow return of the concentration of ammonia to its original value when the polarizing current is switched off is apparently explained by the gradual discharge of the system, and perhaps partially by the process of electrolysis.

In Expt. No. 16 the intensities of cathodic current are actually somewhat higher than in Expt. No. 14, but with respect to the anodic current they are still considerably lower.

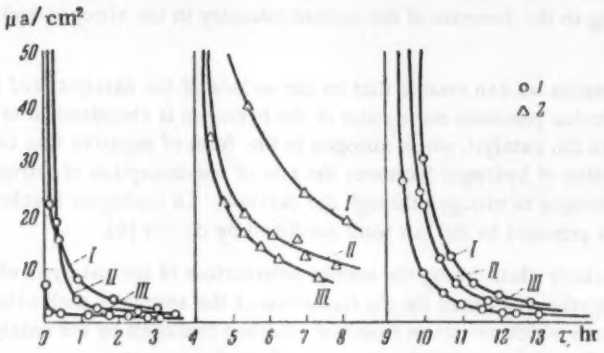

Fig. 5. Variation of the density of polarizing currents as a function of the composition of the gaseous medium (electrodes, K-55 catalyst-nickel). Expt. No. 16: 1) Current density during cathodic polarization; 2) current density during anodic polarization. I) In the nitrogen-hydrogen mixture; II) in hydrogen; III) in nitrogen.

Furthermore, comparison of the current intensities in Expt. No. 16 and in the case of two nickel deposits (Fig. 3), indicates that in the second case they are 2-3 orders lower than in the first. It is clear that the higher current intensities are due to the presence of the catalyst.

One can assume that during the passage of the current through the glass, an important role is played by the cation, created as the result of the catalytic reaction. An investigation of the polarizing current in different media (nitrogen, hydrogen, nitrogen-hydrogen mixture) (Fig. 5), allowed us to clarify this point.

The figure shows that with a nickel electrode the densities of cathodic current in different media do not differ significantly from each other; the density of anodic current in the nitrogen-hydrogen mixture is somewhat higher than in nitrogen or hydrogen. This phenomenon indicates clearly that as a result of the cathodic reaction, there is created an additional number of cations which easily penetrate the glass and transfer the current through it. It is probable that these are hydrogen ions.

Comparison of the intensities of current in nitrogen and hydrogen during cathodic and anodic polarization shows that they are lower during cathodic than during anodic polarization. Apparently this is due to the fact that, compared with nickel, the catalyst has a larger capacity for dissolving gas, with formation of ions carrying the current through the glass. Furthermore the cations of the catalyst (Na^+ and K^+) passing into the glass may also play a certain role in the transfer of current.

Analysis of the results obtained leads us to believe that there may exist a definite relationship between the current intensity, which is increased as a result of catalytic reaction, and the resulting concentration of ammonia. We give below the calculated number of ammonia molecules formed during anodic polarization and the number of electrons corresponding to the increase of the current intensity in the nitrogen-hydrogen mixture with respect to the current intensity in hydrogen.

	Expt. No. 20	Expt. No. 30
Number of NH_3 molecules formed during 1 hr of anodic polarization	$6.2 \cdot 10^{19}$	$5.4 \cdot 10^{19}$
Number of electrons corresponding to the increase of current intensity in the nitrogen-hydrogen mixture.	$1.24 \cdot 10^{19}$	$2.18 \cdot 10^{19}$

These results show that the number of ammonia molecules formed during anodic polarization and the number of electrons corresponding to the increase of the current intensity in the nitrogen-hydrogen mixture are magnitudes of the same order.

On the basis of these results we can assume that on the surface of the catalyst used for ammonia synthesis the following oxidation-reduction processes occur: part of the hydrogen is chemisorbed in the form of positive ions giving off an electron to the catalyst, while nitrogen in the form of negative ions takes an electron from the catalyst. The chemisorption of hydrogen increases the rate of chemisorption of nitrogen due to the partial transfer of electrons from hydrogen to nitrogen through the catalyst. An analogous mechanism of chemisorption of nitrogen and hydrogen was proposed in the last work published by de-Bur [9].

The situation is particularly clear during the anodic polarization of the catalyst, when the chemisorption of nitrogen in the form of negative ions, used for the formation of the ammonia molecule, occurs apparently mainly because of the electrons which are taken from the adsorbed hydrogen by the catalyst. The protons formed in this manner pass into the glass and increase the intensity of anodic current.

The increase of the concentration of ammonia resulting from cathodic polarization of the catalyst and its decrease due to anodic polarization indicate that the limiting stage of ammonia synthesis is the transfer of electrons from the catalyst to the chemisorbed particles, which under our conditions are most probably nitrogen.

The authors express their thanks to Ya. M. Kolotyrkin, F. F. Vol'kenshtein, and to the authors of the method, A. I. Krasil'shchikov and L. G. Antonova, for their valuable advice and discussions of this work.

SUMMARY

1. It was shown that during cathodic polarization of the catalyst the concentration of ammonia increases, and decreases during anodic polarization, which indicates that the process is the result of electron transfer.

2. It was shown that protons take part in the transfer of current through the glass.

3. We have compared the intensities of the polarizing current in the catalyst deposit (second electrode, nickel) in nitrogen, hydrogen, and a nitrogen-hydrogen mixture. It was found that the current intensity during cathodic polarization of the catalyst in all media does not differ significantly, and that the intensity of anodic current in the nitrogen-hydrogen mixture, i.e., during the reaction, is considerably higher than in nitrogen or hydrogen, apparently due to the protons formed during the reaction.

4. On the basis of the results and the calculations made we conclude that in the process of ammonia synthesis on iron catalysts, hydrogen is partially chemisorbed in the form of positive ions, giving off its electron to the catalyst, while nitrogen, capturing these electrons from the catalyst, is chemisorbed in the form of negative ions. The transfer of electrons from the catalyst to the chemisorbed particles (most probably nitrogen under our conditions) limits the rate of the process.

LITERATURE CITED

1. S. Z. Roginskii and F. F. Vol'kenshtein, Collection: Catalysis, (Transactions of the All-Union Meeting on Catalysis, in memory of L. V. Pisarzhevskii [in Russian] (1950) p. 9.
2. Collection: Catalysis, Electronic Phenomena [Russian translation] (IL, Moscow, 1958).
3. Collection: Problems of Kinetics and Catalysis [in Russian] (Izd. AN USSR, 1955) Vol. 8.
4. F. F. Vol'kenshtein, Uspekhi Khim. 27, 11, 304 (1958).
5. G. K. Boreskov, Collection: Problems of Physical Chemistry [in Russian] (Izd. AN USSR, 1958) No. 1, 101; Doklady Akad. Nauk SSSR 127, 591 (1959).*
6. S. S. Lachinov, Report of the OBTI GIAP (June 25, 1955).
7. S. S. Lachinov and V. A. Kurkovskii, Khim. i Khimich. Tekh. 1, 6, 610 (1956).
8. A. I. Krasil'shchikov and L. G. Antonova, Doklady Akad. Nauk SSSR 91, 291 (1953).
9. Ya. Kh. de Bur, Collection: Catalysis, Some Problems of the Theory and Technology of Organic Reactions [Russian translation] (IL, Moscow, 1959) p. 166.
10. V. A. Pchelin, Measurement of the Activity of Hydrogen Ions With Glass Electrodes [in Russian] (Izd. 1941) p. 78.
11. S. S. Lachinov, Zhur. Priklad. Khim. 10, 19, 1847 (1937).

*Original Russian pagination. See C. B. translation.

CATALYTIC ACTIVITY OF NICKEL CATALYSTS

II. EFFECT OF ADDITIONS OF TRANSITION METALS

G. D. Lyubarskii, L. N. Ivanovskaya, G. G. Isaeva, D. I. Lainer, and N. M. Kagan

L. Ya. Karpova Physicochemical Institute

Translated from Kinetika i Kataliz, Vol. 1, No. 3, pp. 385-392, September-October, 1960
Original article submitted December 26, 1959

A study has been made of the effect of adding transition metals (Cr, Mo, Ti, V, Co, and Fe) to nickel during its fusion with aluminum ("nickel skeleton") on the rate of hydrogenation of benzene in a continuous circulation system. It has been shown that the specific activity of nickel is practically constant for additions of up to 20-30 at.% metal. This is because under these conditions, the specified metals only form solid solutions with nickel, to an insignificant extent, and therefore have very little effect on the electronic structure of nickel.

* * *

In the first communication we published results for the effect which different factors have on the properties of fused "skeleton" nickel catalysts, and developed standard methods for their preparation and comparative investigation.

In that paper we also gave experimental data on a study of the effect which additions of transition metals have on the specific catalytic activity of nickel.

As we pointed out [1], fusion of the metals is a convenient means of evenly regulating their electronic structure, a change in which is associated with a change in catalytic activity.

In particular, addition of the metals to nickel and formation of solid solutions can change its electronic structure, and this should affect the catalytic activity [2]. A quantitative development of these changes should provide material for the construction of a theory for a series of catalysts. Our earlier investigations showed that addition of a small amount of chromium to nickel noticeably increased its activity towards specific hydrogenation reactions, for example, hydrogenation of sugars. There are similar results [3] for an increase in activity of "skeleton" nickel catalysts with additions of molybdenum, cobalt and chromium, in liquid phase hydrogenation reactions of safrole, furfural, etc. especially in alkaline solutions. Analogous data on the activity of nickel borides [4] etc., is well known.

It is essential to explain the effect which additions of transition group metals to nickel during its fusion with aluminium or silica have, on the specific activity of the catalysts, which are obtained when the aluminium has been leached out.

The metals we have chosen are known to form solid solutions with nickel in considerable quantities [5]: titanium—up to 9 at.%, chromium up to 30 at.% and molybdenum up to 14 at.%.

A series of nickel-aluminium melts were prepared with different concentrations of the metals—titanium, chromium, vanadium, molybdenum, iron, cobalt and copper, but with the same aluminium content (50% by weight). These three component melts were ground up, leached out, and examined by the method previously described [1].

TABLE 1

Additions of chromium to Nickel (hydrogenation at 38°)

Amt. of chromium introduced at.% in Ni	Degree of leaching out	Specific surface area, S, m^2/g	Degree of hydrogenation per g catalyst α,%	$k \cdot 10^2$ mole/g hr		$k' \cdot 10^4$ mole/m^2 hr		Activation energy E, kcal per mole
				per g catalyst	per g nickel	per m^2 catalyst	per m^2 nickel	
a) Addition of chromium to nickel-aluminium melt (50% by wt. Al)								
0	91	80	27	1,2	1,2	1,5	1,5	11,5
0*	91,5	81	32	1,43	1,43	1,78	1,78	12,5
3	93,7	94	33,5	1,50	1,54	1,60	1,7	12,6
4	90,0	87	32,5	1,45	1,51	1,66	1,81	11,2
5	93,5	86	31,5	1,40	1,47	1,63	1,8	12,4
11	81,0	85	25,7	1,14	1,28	1,34	1,7	12,3
2	63,0	83	20,5	0,92	1,18	1,11	1,82	12,7
						Average:	1,7±0,1	12,2
b) Addition of chromium to nickel-silicon melt (50% Si)								
0	85	67	30	1,34	1,34	2,0	2,0	14,0
4	92,6	62	23	1,03	1,08	1,67	1,82	13,0
22	77,2	70	20	0,9	1,15	1,28	2,1	13,8

*Nickel content in melt 56%.

The activity of the samples was determined in a continuous circulation apparatus in relation to the hydrogenation reaction of benzene, usually at three temperatures (27, 32, and 38°), with an inflow rate of hydrogen – 7 g per hr · 1 cm^3 catalyst and an initial benzene concentration of 5.5 mmole per 1 g mixture of benzene vapor and hydrogen. The surface areas were measured by the BET nitrogen adsorption method.

1a. Addition of chromium. Aluminium can be leached out by alkali fairly easily from the binary melts Ni-Al, Cr-Al.

With a gradual increase of the chromium content in the nickel–aluminium melt, the amount of aluminium which can be leached out, decreases (Table 1). Ni, Al and Cr evidently form phases which are difficult to decompose by alkali.

The table gives values of zero order rate constants for the hydrogenation reaction of benzene at 38°, calculated in moles/hour per g catalyst and per g nickel (the weight of the dry, granular catalyst was ~ 2 g/cm^3).

Specific rate constants were also calculated for 1 m^2 of measured catalyst surface and for 1 m^2 of nickel surface. To calculate the nickel surface, it was assumed that it occupied a fraction of the catalyst surface, which corresponded to the atomic content of nickel in the leached out catalyst. Such an assumption is justified, in that the surface area of the leached out chromium aluminium melt (not containing nickel) is essentially the same (91 m^2/g) as the surface area of "skeleton" nickel.

At a 3-4 at.% chromium content in the catalyst a small maximum in the activity for 1 g catalyst (an increase of 15-20%) is observed. Also, on increasing the nickel content in the initial binary melt (to 56%), the activity of the catalyst reaches a value, which was obtained for nickel plus impurity [1]. The comparative constancy of the specific activity, calculated for unit nickel surface, is very noticeable (Fig. 1).

The surface areas of the samples were 80-90 m^2/g, which means that the nickel crystals have extremely small dimensions (40-100 A); for this surface area every sixth atom of nickel, on the average, must occur on the surface. A weakening of the line in the x-ray analysis, which we carried out, also indicates a high degree of dispersion of the cubic nickel crystals obtained.

Activation energies for the hydrogenation process hardly vary from the mean value of 12 ± 0 kcal/mole. The catalysts have quite a high thermal stability (Table 3).

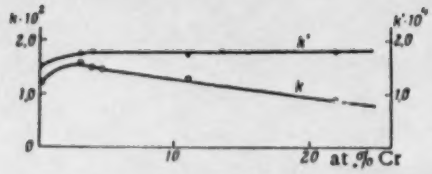

Fig. 1. Activity of nickel catalysts with added chromium: k—activity per 1 g nickel; k'—specific activity.

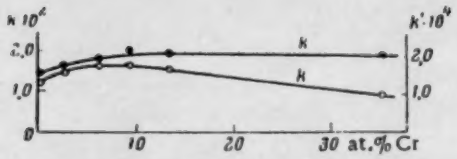

Fig. 2. Activity of nickel catalysts with added molybdenum.

1b. Nickel—silicon melts; addition of Cr. Nickel "skeleton" catalysts can also be obtained by fusing nickel with silicon, and subsequently leaching out the silicon from the melt.

In order to compare the activity of catalysts, obtained in this way, with the activity of the samples described above (with a view to explaining the possibility of a specific effect of aluminium), we prepared some nickel-silicon melts (50% by wt. silicon) with and without additions of chromium. The melts were leached out for one hour at 100° with a 20% caustic soda solution.

Section b of Table 1 shows that the activity of such catalysts (per 1 g Ni and per 1 m^2 surface) is practically the same as that of the preceeding samples, so the nature of the metal which is leached out has no specific significance.

Thus, addition of chromium hardly affects the specific activity of nickel, but improves other properties of the catalyst—its stability, mechanical stability and so on, which are important in its industrial application.

2. Addition of titanium. Analogous results were obtained in an investigation of samples of nickel catalysts containing added titanium. The amount of aluminium leached out hardly changed, and the surface area of the sample was about the same (Table 2a). There was a small maximum in catalytic activity at 5-7 at.% titanium. The specific activity did not vary more than 25% from the mean value. The activation energy was ~ 12.5 kcal per mole, as in the other cases.

TABLE 2

Addition of Titanium, Molybdenum and Vanadium (hydrogenation at 38°)

Addition (at. % in Ni)	L, %	S, m^2/g	α, %	$k \cdot 10^2$ mole/g hr		$k' \cdot 10^4$ mole/m^2 hr		E, kcal/mole
				per 1 g catalyst	per 1 g nickel	per 1 m^2 catalyst	per 1 m^2 nickel	
a) Addition of titanium								
2,2	90	85	29	1,29	1,32	1,52	1,58	12,0
7,2	89	85,6	31	1,38	1,50	1,61	1,87	12,7
12	86	79	19,8	0,88	1,0	1,12	1,44	12,3
17	85	96	20,5	0,91	1,1	0,95	1,38	13,1
						Average:	1,57±0,25	12,5
b) Addition of molybdenum								
2,4	97,5	95	31	1,38	1,41	1,45	1,53	11,0
6	97	97	34	1,51	1,61	1,56	1,79	11,5
9	93,3	92	35	1,56	1,71	1,69	2,04	12,2
13	93	99	31,5	1,40	1,61	1,41	1,86	12,2
37	99	77	14	0,62	1,0	0,80	2,05	11,5
						Average:	1,85±0,25	11,7
c) Addition of vanadium								
3	95,5	79	30	1,34	1,41	1,8	1,96	12,2
12,5	90,5	87	21,8	0,97	1,11	1,1	1,47	12,9
14,3	100	98	21,8	0,97	1,13	1,15	1,35	13,5
						Average:	1,6±0,3	12,8

TABLE 3

The Effect of Heat Treatment in a Stream of Hydrogen on the Activity at 38°

Catalyst composition (at.% of addition)	Temp. of heating, °C	α, %		k · 10², mole/g hr	
		before heat treatment	after heat treatment	before heat treatment	after heat treatment
Without addition	200	29	35,7	1,29	1,50
The same	250	32	38,0	1,42	1,69
3% Cr	200	23,5	25,5	1,05	1,13
3% Cr	250	25,5	25,5	1,13	1,13
4% Cr	200	30,0	32,5	1,36	1,44
2,2% Ti	200	20,5	26,2	0,92	1,16
2,2% Ti	250	26,2	19,7	1,16	0,88
2,2% Ti	200	23,0	29,0	1,04	1,29
7,2% Ti	250	26,2	21,7	1,16	0,97
13% Mo	200	25,7	19,6	1,41	0,87
37% Mo	200	31,0	18,5	1,37	0,82

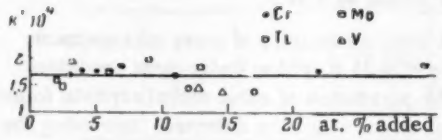

Fig. 3. Specific activity of nickel catalysts with additions of transition metals.

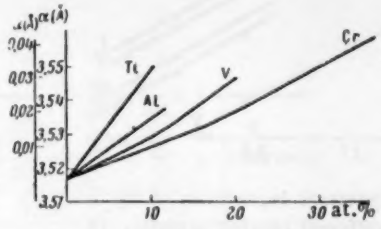

Fig. 4. Variation in the nickel parameters during its fusion with metals.

The thermal stability of the samples was quite high (see Table 3). Treatment of the samples, containing chromium or titanium, with hydrogen at 200° further increased their catalytic activity.

3. Addition of molybdenum. Similar results were also obtained for an investigation of samples of nickel catalysts, containing different amounts of molybdenum. The amounts of aluminium leached out, in contrast to the case of added chromium, did not change even at contents of 37 at.% molybdenum, and was almost 100%. The surface area was also high and approximated to 100 m^2/g, Table 2b. A small activity maximum was observed at 6-9 % Mo content per g catalyst, but the specific activity per 1 m^2 nickel surface was practically constant, and had a value similar to that for the other "skeleton" catalysts (Fig. 2). The activation energy for the hydrogenation of benzene was about 12 kcal/mole.

It should be noted that these samples are less stable after being heated in hydrogen; at 150° their activity is already considerably diminished (Table 3).

Results obtained for samples containing vanadium impurity, are generally analogous to the preceeding results (Table 2 c). The increased combustibility, particularly at high vanadium contents, and the low stability of the samples should be noted.

As can be seen from the results, especially Fig. 3, the specific catalytic activity of nickel remains approximately constant over a wide range of impurity concentration, and is on the average 1.7×10^{-4} mole/m^2 hour at 38°; the activity per 1 g catalyst has a small maximum at low impurity contents.

Boreskov and his co-workers [6] showed that the specific catalytic activity of a series of catalysts which had the same chemical composition, but had been prepared by different methods, was approximately constant. We also found that the specific activity of our samples of nickel remained approximately constant, although other metals were also present. It can therefore be concluded that nickel is the "active" metal in all our samples; added transition metals only form solid solutions with it to an insignificant extent, and therefore their presence

TABLE 4

Activity of Nickel Catalysts

Catalyst	S, m^2/g	k, (mole/hr · g Ni) at 38°	k, (mole/hr · g Ni) at 150°	E, kcal/mole
Melt with 2% Cr	86	$1,4 \cdot 10^{-2}$	3,6 (calc.)	12,2
Ni (from oxalate)	4	$3 \cdot 10^{-5}$	$8 \cdot 10^{-3}$	11,5
Ni (on Cr_2O_3)	140	$2 \cdot 10^{-3}$	0,2	12,0
Ni (on Al_2O_3)	200	$4 \cdot 10^{-4}$	0,03	13,0

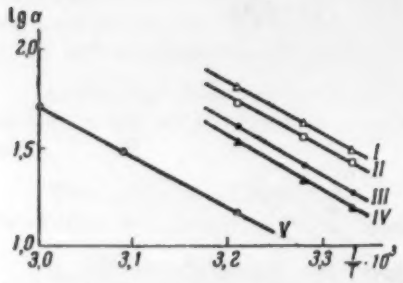

Fig. 5. Temperature dependence of the rate constant for different catalyst samples: 1) 4% Cr; II) Ni-Al; III) 12% Ti; IV) 2.5% Mo; V) 13% Cu.

has little effect on the specific activity of nickel. An x-ray investigation of the phase composition of these melts showed that formation of solid solutions between the specified metals and nickel is very restricted. Fig. 4 shows the change in the parameters of the nickel crystals during their fusion with different metals [5]. Additions of 3 at.% titanium, 6 at.% aluminium, 8 at.% vanadium, or 10 at.% chromium, only change the lattice by 0.01 A.

The usual limit of accuracy of x-ray measurements lies in the region of 0.01 A, and so under these conditions the change in the parameters of cubic nickel crystals, formed from leached out melts, cannot be detected. Increasing the accuracy to 0.002 A allowed small changes in the nickel parameters to be detected in the presence and absence of chromium and titanium. However, this change was independent of the amount of metal added, and was evidently associated with the presence of aluminium in the solid solution of nickel. From these results, and a comparison of other results (spectroscopic analysis, correlations of metal surface dissolution) it was concluded that if the investigated transition metals do form solid solutions with nickel, then they do so only in the range up to 1%, which is almost negligible.

However, in a few cases (Cr, Ti) these additions determine properties of the catalysts, which are important in their practical application, for example their stability, the mechanical stability of the granular material and so on, which evidently help to prevent sintering processes. These properties have been successfully utilized in the industrial hydrogenation of sugars.

As we have already shown, the activity of the investigated fused catalyst is very high, and enables the hydrogenation of benzene to be carried out at temperatures near to room temperature.

A comparison of the activity of these catalysts with the activity of other nickel catalysts, obtained by reduction of the oxides or nickel salts, is given in Table 4.

From the table it can be seen that "skeleton" catalysts are considerably more active per 1 g nickel for the hydrogenation of benzene than other well known nickel catalysts.

The activation energy, calculated from the temperature coefficient of the reaction, remains approximately constant at about 12 ± 1 kcal/mole (Fig. 5), and is independent of the composition of the nickel catalyst. It should be pointed out that the activation energy for the hydrogenation of benzene on other catalysts (for example Ru, Rh, Pt) was also found to be 12 kcal/mole; Herbo [8] obtained a value of E = 11.7 kcal/mole for Ni/ThO_2 catalyst.

The approximate constancy of the activation energy for the hydrogenation of benzene for all the catalysts investigated suggests that the mechanism of the reaction is probably the same; this assumption is linked with

TABLE 5

Addition of Cobalt (hydrogenation at 38°)

Cobalt content (at.%)	L, %	m^2/g	α, %	$k \cdot 10^2$, mole/g hr per 1 g catalyst	$k' \cdot 10^4$, mole/m^2 hr per 1 m^2 catalyst	E, kcal/mole
0	91	85	26	1,15	1,35	12,3
10	100	83	26	1,15	1,40	12,9
20	100	70	20,2	0,9	1,28	14,1
20*	86	73	44,5	1,98	2,70	11,0
40	100	60	12,5	0,55	0,925	12,0
40*	97,5	105	44	1,95	1,86	—
100	86,6	17	13,7	0,6	3,5	13,8
100**	96,5	—	8,7	0,4	—	—

*Leaching out at 50°

**Composition of initial melt 30 at.% Co + 70 at.% Al; leaching out at 56°.

TABLE 6

Effect of the Addition of Iron to Nickel*

At % iron (in Ni)	L, %	S, m^2/g	Temp., (°C)	α, %		$k \cdot 10^{-2}$ mole/g · hr		$k^1 \cdot 10^4$ mole/m^2 · hr		E, kcal/mole
				per 1 g catalyst	per 1 g catalyst	per 1 g catalyst	per 1 g catalyst	1 m^2 catalyst	1 m^2 catalyst	
0	91	80	38	27	27	1,2	1,2	1,5	1,5	12,5
10,4	89	96	38	25	27,9	1,11	1,24	1,16	1,44	12,9
14,7	100	120	38	14	16,2	0,62	0,72	0,5	0,68	13,6
20,8	99	88	38	8,2	11,7	0,36	0,52	0,41	0,66	13,8
20,8	99	88	60	41	52,5					
31,1	89	84	38	6	8,7	0,27	0,39	0,32	0,66	14,3
31,1	89	84	60	28	40,5					
41,5	85	59	60	10	17,1	0,08	0,138	0,136	0,40	12,0
41,5	85	59	70	16,7	28,6					
61	89	43	70	6,2	16,0	0,023	0,059	0,053	0,35	12,3
61	89	43	80	10,3	26,6					
100	93	28	140	2,0	—					

*For convenience the data in the table has been reduced to a constant velocity at 38°.

another of our observations, which will form the contents of a future communication, that the reaction kinetics are the same.

4. Addition of cobalt. Nickel–cobalt catalysts, obtained by decomposing the mixed formates, were studied in the hydrogenation reaction of benzene by Lihl [9].

Lihl's results showed unexpectedly an increased activity of cobalt compared to nickel; additions of the latter to cobalt decreased the activity of the cobalt considerably.

Our results for catalysts, prepared by leaching out aluminium from its melts with nickel and cobalt, showed that additions of cobalt had little effect on the activity of nickel; the activity of cobalt by itself was lower than that of nickel (Table 5).

20 at.% additions of cobalt to nickel lowered the activity of the nickel slightly if the standard method of leaching out was used, but if the leaching out process was carried out at a lower temperature (50°) the activity of the sample obtained was the same as that of a nickel sample, which had been treated in the same way [1].

The surface area of the cobalt catalyst was considerably lower than that of nickel, and therefore the specific activity of cobalt (per 1 m^2 surface) was higher than for nickel.

5. Addition of iron. The effect of iron on the activity of nickel catalysts, obtained by reduction of the hydroxide, has been studied by Long and his co-workers [10] and by Dowden [11].

These workers showed that additions of iron to nickel lowers the catalytic activity of the latter in the hydrogenation of benzene and styrene, for example 50% hydrogenation of benzene proceeds at 66° on pure nickel and at 108° on a nickel catalyst with 25% iron.

Dowden associated the observed decrease in catalytic activity with a decrease in the electron density.

It seemed of interest to compare these results with the action of iron on a fused nickel catalyst. To do this, we prepared samples of melts with a constant aluminium content (50% by wt.) and with varying iron and nickel contents. The melts were treated as before [1].

The results of these experiments are given in Table 6, where it can be seen that addition of iron to nickel during its fusion with aluminium hardly changes the amount of aluminium extracted from the melt, but noticeably decreases the catalytic activity of nickel at additions higher than 10 at.%. The specific catalytic activity of nickel is changed relatively little (3-4 times) even at an iron content of 60 at.%.

Unfortunately the impossibility of determining directly the fraction of the total catalyst surface occupied by nickel, means that the specific activity of nickel in the melts studied cannot be defined more accurately.

SUMMARY

1. An investigation of the specific activities of different nickel catalysts in the vapor phase hydrogenation of benzene has been carried out for the first time by a continuous circulation method, which ensures that the process proceeds isothermally and enables the rate to be determined simply.

2. Introduction of additions of the transition metals chromium, titanium, vanadium and molybdenum, to the nickel–aluminium melts appeared to have little effect on the activity of the nickel catalysts. Additions of 5-7 at.% only increased the activity of the catalysts obtained by 15-20%, and further increase in the amount added, hardly affected the activity. Analogous results were obtained for additions of cobalt and iron. This is due to the fact that the transition metals only form solid solutions with nickel to an insignificant extent, and separate out during the leaching out of the aluminium. They therefore have little effect on the electronic structure of nickel.

3. The constancy of the activation energy of the reaction indicates a common mechanism for the hydrogenation of benzene on the different catalysts.

LITERATURE CITED

1. G. D. Lyubarskii, L. N. Ivanovskaya, and G. G. Isaeva, Kinetika i Kataliz 1, 260 (1960).*
2. D. A. Dowden, J. Chem. Soc. Lond. 242 (1950); Ind. Eng. Chem. 44, 977 (1952); S. Z. Roginskii, Problems of Kinetics and Catalyses [in Russian] (Izd. Akad. Nauk SSSR, Moscow, 1955); Vol. 8; G. K. Boreskov, Problemy Fiz. Khim. 1, 101 (1958).
3. R. Paul, Bull. Soc. Chim. France 208 (1946).
4. R. Paul and P. Buisson, Ind. Eng. Chem. 44, 1066 (1952).
5. A. Taylor and R. W. Flyod, J Inst. Metal 80, 577 (1955); I. I. Kornilov and I. G. Domotkenko, Doklady Akad. Nauk SSSR 120, 311 (1958).*
6. G. K. Boreskov, Zhur. Fiz. Khim. 30, 2787 (1956); 31, 937 (1957).
7. A. Amano and G. Paravano, Adv. in Catal. 9, 716 (1958).
8. Cl. Herbo and V. Hauchard, Bull. Soc. chim. Belg. 52, 10 135 (1943).
9. F. Lihl, H. Wagner, and P. Zemsch, Z. Elektrochem. 56, 619 (1952).
10. J. H. Long, J. C. Frazer, and E. Ott, J. Am. Chem. Soc. 56, 1101 (1934).
11. D. A. Dowden and P. W. Reynolds, Disc. Faraday Soc. 8, 184 (1950).

*Original Russian pagination. See C. B. translation.

THE ACTIVATION OF FUSED IRON FISCHER-TROPSCH CATALYSTS UNDER THE INFLUENCE OF THE REACTION MIXTURE

Yu. B. Kagan, A. N. Bashkirov, E. V. Kamzolkina, and S. M. Loktev

Institute of Petrochemical Synthesis, Academy of Sciences of the USSR
Translated from Kinetika i Kataliz, Vol. 1, No. 3, pp. 393-400,
September-October, 1960
Original article submitted January 19, 1960

A study has been made of the activation, by means of the reaction mixture, of fused iron catalysts for the synthesis of hydrocarbons from CO and H_2, prereduced at a temperature of about 1000°.

Certain rules governing the activation have been established, and these rules are general for catalysts of different compositions.

* * *

It was shown in our previous work [1, 2] that fused iron catalysts for the synthesis of hydrocarbons from CO and H_2, prereduced at temperatures of about 1000°, usually acquire high activity some 20-25 hr after synthesis conditions have been established. The activation which takes place during this period is the result of the simultaneous occurrence of a series of concurrent reactions between the components of the catalyst and the components of the reaction mixture (CO, H_2, C_nH_{2n+2}, H_2O, CO_2, etc.).

These concurrent reactions include, in particular, carbide formation by the iron, hydrogenation of these carbides, oxidation of the iron by steam, and reduction of the iron oxides by carbon monoxide. As a result of the occurrence of the concurrent reactions during the course of the synthesis, surface compounds (carbides an oxides) are repeatedly formed and decomposed on the iron. At the same time, the activity of the catalyst gradually increases, the surface area increases, and there is an increase in the reactivity of the iron and the surface compounds formed; the reactivity develops during the interaction of the iron and surface compounds with components of the reaction mixture [2]. The sum total of the experimental data led to the conclusion that there exists a specific relationship between the activity of iron catalysts during hydrocarbon synthesis from CO and H_2 and the reactivities of the iron and its surface compounds [2].

In the light of the material presented above, activation of fused iron Fischer-Tropsch catalysts can be considered as the formation of a surface—a certain combination of iron and its surface carbides and oxides which possess the required reactivity. It has been shown experimentally [1, 2] that such a surface is active in hydrocarbon synthesis from CO and H_2.

In the work cited above, activation was considered complete when, during the course of the synthesis, practically complete conversion of the carbon monoxide in the feed was attained at a space rate of feed gas of the order of 1500 hr^{-1}. In addition, it was assumed that the attainment of a high degree of CO conversion in the synthesis reaction must lead to a sharp retardation of the reactions leading to interconversion of the surface compounds and the associated activation of the catalyst.

Naturally, this assumption required experimental confirmation. The present investigation was carried out with this purpose in mind and also for the purpose of obtaining additional data on the process of catalyst activation during the course of the synthesis; the problems included clarification of the effect on the indicated process of the duration of the catalyst test under synthesis conditions, the effect of catalyst composition, and the effect of the conditions under which activation is carried out.

TABLE 1

Change in Catalyst Activity During Synthesis

Catalyst	CO_2 content of effluent gas, %		Conditioning time, hours	Conditioning conditions		Synthesis conditions during different time intervals after completion of conditioning (time in hours)							
						24		80		225			
	one hour after start of expt.	after conditioning		t°	P, atm	t°	P, atm	t°	P, atm	t°	P, atm		
1	1.5	44	7-8	298	20	297	12	297	11	297	10.5		
2	1.0	42	17-18	300	20	300	12	300	11	—	—		
3	1.0	44	45-50	335	30	330	30	330	30	—	—		

The activity of a catalyst for hydrocarbon synthesis from CO and H_2 was characterized by the process conditions (pressure and temperature) required for a given productivity. The reactivity of the catalyst material was evaluated by means of its activity for the decomposition of carbon monoxide with the formation of carbide carbon $2Fe + 2CO \rightarrow Fe_2C + CO_2$ (I). This reaction was selected, because the formation of carbides is required for the creation of a surface which is active for hydrocarbon synthesis from CO and H_2 [1]. Moreover, carbide formation is apparently one of the reactions initiating this synthesis [2, 3]. The activity of the catalyst was also determined with respect to the parasitic reaction in which CO is decomposed with the formation of elemental carbon $2CO \rightarrow C + CO_2$ (II).

Changes in the Properties of Catalysts of Differing Compositions During Synthesis with CO and H_2

The following catalysts were investigated:

1. $100Fe_3O_4 + 6Al_2O_3 + 4,2SiO_2 + 1,2K_2O + 0,3Cr$,
2. $100Fe_3O_4 + 6Al_2O_3 + 4,2SiO_2 + 1,2K_2O + 0,5V$,
3. $100Fe_3O_4 + 6Al_2O_3 + 4,2SiO_2 + 1,2K_2O + 1,0B_2O_3$,

these were reduced at 1000° in a stream of hydrogen (1 atm, 2000 hr^{-1}) for a period of 1.5 hr.

Testing of the catalysts for hydrocarbon synthesis was carried out in a high-pressure laboratory apparatus [4].

The catalyst, 25 cc, was charged to the reactor under an atmosphere of CO_2. First, for each catalyst was determined the lowest temperature and pressure at which a high degree of conversion (84-86%) was attained over freshly reduced catalyst in a time commensurate for all catalysts at a space rate of synthesis gas (1 : 1 mixture of CO and H_2) of about 1500 hr^{-1}. The freshly reduced catalyst was gradually activated under these conditions.

When this conditioning treatment had been completed, i.e., when the predetermined productivity had been attained (85% CO conversion at a space rate of 1500 hr^{-1}), the productivity was maintained constant by varying the pressure and temperature. These changes in synthesis conditions permitted us to evaluate the increase or decrease in catalyst activity for hydrocarbon synthesis.

Several samples of each catalyst were tested in synthesis runs of different durations. In one series of experiments, run durations were limited for all catalysts to the time required for completion of catalyst conditioning. In the other series of experiments, the runs were continued for an additional 24 or 80 hr after completion of conditioning, and catalyst 1 was also tested for a period of 225 hr.

All tests of catalysts having the same composition were carried out under the same conditions and in the same reactor.

TABLE 2

Overall Reaction Rate for the Decomposition of Carbon Monoxide (W) as a Function of Synthesis Time on the Catalyst

Time from start of CO treatment	W, g carbon monoxide per 100 g of catalyst per min (x 10³)				
	freshly reduced	after conditioning	after conditioning and synthesis operation (t, hr)		
			24	80	225
			Catalyst 1		
0—20	6,5	15,8	44,8	61,0	56,2
20—60	6,8	8,3	10,0	15,5	18,7
60—120	4,2	4,0	4,2	5,9	5,7
120—180	3,0	2,6	2,9	4,0	3,9
			Catalyst 2		
0—20	4,7	7,5	26,8	37,3	—
20—60	2,9	4,3	12,6	18,4	—
60—120	1,6	3,4	6,2	7,0	—
120—180	1,1	2,5	4,2	4,2	—
			Catalyst 3		
0—20	0,6	16,6	16,8	25,6	—
20—60	0,3	7,2	7,5	10,7	—
60—120	0,3	4,1	4,2	5,6	—
120—180	0,3	0,3	—	4,7	—

TABLE 3

Rate of Carbon Deposition on Catalysts (W_2) During Synthesis

Catalyst	W_2, g carbon per 100 g catalyst per min ($\times 10^3$)			
	for catalyst during conditioning	for catalyst which has operated for indicated hours after conditioning		
		0-27	24-80	80-225
1	0.15	0.27	0.32	0.30
2	0	0.11	0.52	—
3	0.04	0.26	0.39	—

In this way, good reproducibility of all synthesis characteristics was obtained, which indicated that the results obtained were comparable.

After being tested in the synthesis process for the selected period of time, the catalysts were hydrogenated to remove the iron carbides and oxides formed during the course of the synthesis. Catalysts 1 and 2 were hydrogenated at 350° and a hydrogen pressure of 5 atm; catalyst 3 was hydrogenated at 370° and 10 atm. The hydrogenation was carried out over a period of 48 hr at a temperature 40-50° above the synthesis temperature at the completion of conditioning. The amount of elemental carbon formed during the experiment was determined by combustion of the hydrogenated samples; this permitted calculation of the average rate of this reaction for different intervals of time.

The hydrogenated catalyst samples were treated with carbon monoxide at atmospheric pressure, a space rate of 800 hr^{-1}, and a temperature 10° above the synthesis temperature at the completion of conditioning. The method of treatment has been described in a previous communication [5]. The rate of carbon monoxide decomposition was

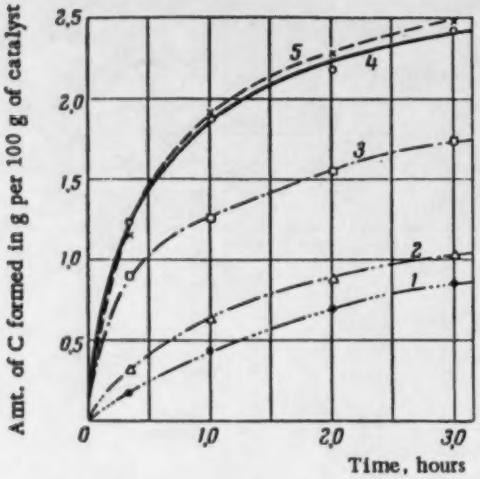

Fig. 1. Curves of over-all carbon formation for the catalyst 100 Fe_3O_4 + 6 Al_2O_3 + 4.2 SiO_2 + 1.2 K_2O + 0.3 Cr as a function of operating time in the synthesis of hydrocarbons from CO and H_2: 1) after reduction; 2) after completion of conditioning; 3) after conditioning and operation in synthesis for 24 hr; 4) 80 hr; 5) 225 hr.

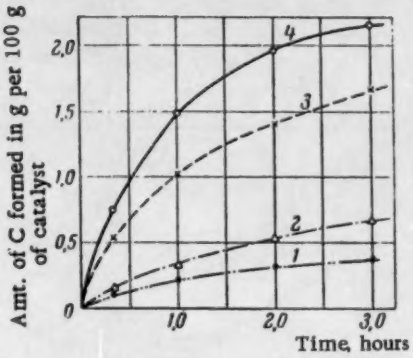

Fig. 2. Curves of over-all carbon formation for the catalyst 100 Fe_3O_4 + 6 Al_2O_3 + + 4.2 SiO_2 + 1.2 K_2O + 0.5 V as a function of operating time in the synthesis of hydrocarbons from CO and H_2: 1) after reduction; 2) after completion of conditioning; 3) after conditioning and operation in synthesis for 24 hr; 4) 80 hr.

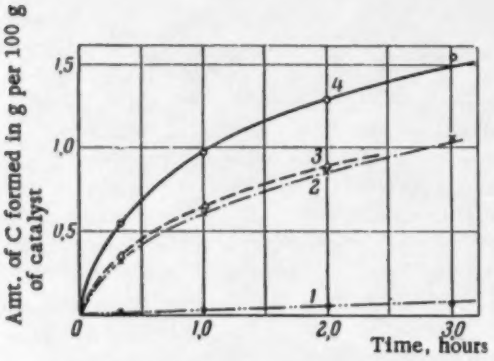

Fig. 3. Curves of over-all carbon formation for the catalyst 100 Fe_3O_4 + 6 Al_2O_3 + 4.2 SiO_2 + + 1.2 K_2O + 1.0 B_2O_3 as a function of operating time in the synthesis of hydrocarbons from CO and H_2: Legend is the same as for Fig. 2.

determined at 20, 60, 120, and 180 min from the beginning of the experiment. In conformity with data previously obtained [6], it was assumed that the amount of carbon formed during the first 20 min characterized the rate of carbide formation, and the amount of carbon deposited in the interval from 120 to 180 min characterized the rate of formation of elemental carbon. The results of the experiments are presented in Tables 1, 2, and 3 are depicted graphically in Figs. 1, 2, and 3.

The data of Table 1 relating to catalysts of different composition, once again confirm the proposal formulated above that fused iron catalyst are inactive, directly after reduction at high temperatures (1000°), for the synthesis of hydrocarbons from CO and H_2 and that they acquire activity only during the course of the synthesis. Moreover, it was found that the composition of the catalyst has an appreciable effect on the length of time required for activation under synthesis conditions. The duration of the conditioning period varied within the limits of 7 to 50 hr for the catalysts studied. Activation of the catalysts is not limited to this period, however, although its intensity decreases sharply after completion of the conditioning period. The data of Table 1 show that in all experiments, catalyst activity increased for at least an additional 24 hr after completion of conditioning. This is indicated by the decrease in the synthesis temperature and pressure required to maintain the given productivity.

In the majority of cases, some, though less intense, activation was observed over an additional 2-3 days after the first 24 hr operation with the given productivity. It follows from this that the concurrent reactions between the components of the reaction mixture and the catalyst material, which provide catalyst activation, proceed under synthesis conditions even with active catalysts, thereby providing for practically complete conversion of the

TABLE 4

Results of Hydrocarbon Synthesis Tests of the Fused Iron Catalyst 100 Fe_3O_4 + 6.0 Al_2O_3 + 4.2 SiO_2 + 1.2 K_2O + 0.3 Cr Introduced into Synthesis by Different Methods and the Effect of the Method of Introduction on the Activity of the Catalyst for the Decomposition of Carbon Monoxide with the Formation of Elemental Carbon

Expt. No.	Synthesis conditions at completion of conditioning			W_2, g C per 100 g catalyst per min. ($\times 10^3$) at indicated carbonization temperatures in °C									
				after holding at indicated space rate						after completion of conditioning			
				500 hr^{-1}		1000 hr^{-1}		290	310	330	350		
	pressure, atm	temp., °C	CO_2 conc. in effluent gas, %	290	310	290	310						
1	17-18	303-304	40	–	–	–	–	1.5	2.4	3.5	–		
2	20	300-310	40-43	–	–	–	–	4.8	9.9	–	–		
3	20	300-310	42-46	2.5	3.4	2.4	3.1	2.7	3.6	–	–		
4	17-18	302-304	40-41	–	–	–	–	1.5	1.4	1.7	3.1		
5	25	303	52.5	–	–	–	–	1.0	–	–	–		

carbon monoxide feed supplied at the rate indicated above. The experimental results presented in Table 2 and Figs. 1-3 are in good agreement with the data of Table 1. They show that the reactivities of freshly reduced catalysts differ greatly with respect to the formation of iron carbides at temperatures close to conditioning temperatures. Thus the reaction rate with Catalyst 1 was greater than that with Catalyst 3 by an order of magnitude. During the course of conditioning (and after its completion), the reactivity of all the catalysts studied with respect to carbide formation increased appreciably along with an increase in catalyst activity during synthesis, and in all cases the reactivity was of approximately the same order directly upon completion of conditioning. Moreover, the conditioning time increased regularly with the decrease in the initial reactivity of the catalyst with respect to the carbide-forming reaction (see Tables 1 and 2).

All of these facts are in good agreement with our previously developed concepts [2] of the relationship between catalyst activity for hydrocarbon synthesis from CO and H_2 and the reactivity of iron and its surface compounds in reactions with components of the reaction mixture.

Table 3 presents data on the changes occurring during synthesis in the activities of the catalysts for the decomposition of carbon monoxide with the formation of elemental carbon.

These results in conjunction with the data presented in Table 2 show that during the conditioning period and during the course of the synthesis itself, the activity of all catalysts studied gradually increased with respect to the formation of elemental carbon. However, this activation proceeded with considerably less intensity than did the reactivity of the catalysts for carbide formation during the same period. It should be noted that the differences in activity with respect to Reaction II observed during carbon formation tests with freshly reduced catalysts of different compositions, gradually leveled out with activation of these catalysts during the course of the synthesis process.

Effect of Activation Conditions on the Properties of Fused Iron Catalysts

After reduction at 1000°, fused iron Catalyst 1 was introduced into synthesis by five different methods. By "introduction of the catalyst into synthesis" is to be understood the period from the moment the inactive reduced catalyst is first contacted, with synthesis gas until the assigned productivity is attained, i.e., until completion of conditioning. The following experiments were carried out:

1. The synthesis gas (1 : 1 CO + H_2) was fed to freshly reduced catalyst under synthesis conditions (t = 300-304°, P = 20 atm, space rate of synthesis gas of 1500 hr^{-1}). In this and the remaining experiments, conditioning was considered complete when practically complete conversion of the carbon monoxide was obtained at the space rate indicated.

2. The catalyst was heated in an atmosphere of hydrogen to 200°, and synthesis gas was then fed to the catalyst at a space rate of 1500 hr^{-1} and a pressure of 20 atm. The temperature was then gradually increased (2-3° per hour) until conditioning was complete.

3. The synthesis gas mixture was initially fed to the catalyst at 20 atm and 200° with a space rate of 500 hr^{-1}. The temperature was then gradually increased until the concentration of CO_2 in the effluent gas reached 8-10%. The catalyst was maintained at this temperature for 4 hr. The space rate was then increased at 1000^{-1}, and the temperature was again increased until the concentration of CO_2 in the effluent gas was of the order of 8-10%. The catalyst was held under these conditions for four hours; the space rate was then increased to 1500 hr^{-1} and the temperature was gradually increased until conditioning of the catalyst was complete.

4. Synthesis gas was fed to the catalyst at synthesis temperature (300-304°), atmospheric pressure, and a space rate of 500 hr^{-1}. The pressure was gradually increased (1 atm per hour) until the concentration of CO_2 in the effluent gas reached 8-10%. The catalyst was maintained under these conditions for four hours; the space rate was then increased to 1000 hr^{-1}, and the pressure was again increased until the concentration of CO_2 in the effluent gas was of the order of 8-10%. The catalyst was maintained under these conditions for four hours, and the space rate was then increased to 1500 hr^{-1}. The pressure was then increased until conditioning was complete.

5. Conditions for the introduction were analogous to those described in the preceding paragraph except that the synthesis gas contained 25% CO_2 in addition to the CO and H_2.

In all of the above methods of introducing the catalyst into synthesis, catalyst activity was characterized by the synthesis conditions in effect at the time conditioning was complete.

After a catalyst had been introduced into synthesis by any one of the methods described above, it was tested for carbon formation by means of carbon monoxide. The carbon monoxide was fed to the catalyst at a space rate of 800 hr^{-1}, atmospheric pressure, and at various temperatures (including the synthesis temperature). The test was continued until the reaction rate was practically constant. The data obtained during the test characterized the reaction rate for CO decomposition with the formation of elemental carbon.

In certain experiments, this testing of the catalyst with carbon monoxide was carried out after completion of the basic intermediate stages of the conditioning treatment.

The data obtained are presented in Table 4.

It follows from a consideration of the data in the table that the conditions under which activation of a fused iron catalyst is carried out have a very appreciable effect on catalyst activity for the synthesis of hydrocarbons from CO and H_2 and also with respect to Reaction II. Catalysts which were activated by operation at synthesis temperature (Expts. 1 and 4) were the most active for synthesis. Catalysts for which activation was initiated at a temperature approximately 100° below synthesis temperature (Expts. 2 and 3) developed considerably less activity.

Catalysts which were treated with a gas containing 25% CO_2 (Expt. 5) were still less active. When the synthesis gas did not contain CO_2, the temperature at which activation was carried out was the sole factor affecting catalyst activity for synthesis, at the time conditioning was complete. Changing the pressure and space rate during conditioning had no effect on the activity of the catalyst for the synthesis reaction. This conclusion was additionally confirmed by a special experiment in which conditioning was carried out in one case under operating synthesis conditions and in another case under the same conditions, but at a lower space rate.

Catalyst activity with respect to reactions resulting in the formation of elemental carbon, like activity with respect to hydrocarbon synthesis, depended primarily on the temperature at which activation of the catalyst was carried out. However, the nature of the relationship was completely different. The highest activity with respect to this reaction was possessed by catalysts for which activation was initiated at temperatures approximately 100° below synthesis temperature. In addition to temperature, space rate also had an appreciable effect on the activity of a catalyst with respect to Reaction II. In the initial stages of activation, a decrease in space rate led to a decrease in the activity of the catalyst with respect to Reaction II.

The lowest catalyst activity with respect to Reaction II was reached in Expt. 5 in which activation was carried out at synthesis temperature with a gas containing 25% CO_2, and was initiated at a low space rate.

The above experimental results show that the use of a well-selected method of introducing the catalyst into synthesis can guarantee that the most active synthesis catalyst will be obtained and that the catalyst will simultaneously possess the lowest activity with respect to parasitic reactions in which elemental carbon is formed.

SUMMARY

1. Using catalysts of different compositions, we have shown that there is general significance to our previously formulated proposal that directly after reduction at a high temperature (about 1000°), fused iron catalysts are inactive for hydrocarbon synthesis from CO and H_2 and that the catalyst acquires activity only during the course of the synthesis process.

2. Activation of the catalyst continues during the course of the synthesis process, and it still continues even after an activity has been reached which provides practically complete conversion of the original carbon monoxide. This activation process is completed not earlier than 3-4 days after completion of conditioning.

3. Simultaneously with activation of the catalyst, the influence of the synthesis gas brings about an increase in catalyst reactivity with respect to carbide-forming reactions. Catalysts which, by virtue of their conditioning treatment, have attained equivalent activities for synthesis, simultaneously acquire close to the same reactivity with respect to carbide-forming reactions.

4. Activation of catalysts during the synthesis process is accompanied by an increase in their activity with respect to the decomposition of CO with the formation of elemental carbon.

5. The conditions under which catalyst activation is carried out have an appreciable effect on catalyst properties. Of the introduction methods studied, conditioning at synthesis temperature gives the most active catalysts, which simultaneously possess a lower activity with respect to decomposition reactions of CO, resulting in the formation of elemental carbon.

LITERATURE CITED

1. Yu. B. Kagan, et al., Khim. Tekh. Topliva i Masel 3, 14 (1958).
2. Yu. B. Kagan, et al., Izvest. Akad. Nauk SSSR, Otdel. Khim. Nauk 1274 (1958).*
3. Yu. B. Kagan, et al., Trudy Inst. Nefti Akad. Nauk SSSR 13, 167 (1959).
4. A. N. Bashkirov, et al., Trudy Inst. Nefti Akad. Nauk SSSR 10, 234 (1957).
5. A. N. Bashkirov, E. V. Kamzolkina, and Yu. B. Kagan, Trudy Inst. Nefti Akad. Nauk SSSR 12, 214 (1958).
6. Yu. B. Kagan, A. N. Bashkirov, E. V. Kamzolkina, and A. Ya. Rozovskii, Zhur. Fiz. Khim. 33, 2706 (1959).

*Original Russian pagination. See C. B. translation.

CHARACTERISTICS OF THE KINETICS OF THE ISOMERIZATION OF ALLYLBENZENE ON PLATINUM FILMS AT HIGH TEMPERATURES*

V. I. Shimulis, V. M. Gryaznov, and A. E. Cherkashin

Chemical Faculty, Moscow State University

Translated from Kinetika i Kataliz, Vol. 1, No. 3, pp. 401-407,
September-October, 1960
Original article submitted March 3, 1960

The isomerization of allylbenzene on platinum films at temperatures below 500° proceeds by a zero order reaction with an activation energy of 7 kcal/mole, while at 500-600° the reaction is first order with an apparent activation energy of 41 kcal/mole; this may be explained by an increase in the catalytically active surface as a consequence of a sharp increase in the mobility of the surface atoms of the platinum. At temperatures above 660°, the activation energy for the reaction in the presence of platinum films is close to that for the reaction in a quartz cell in the absence of a film, which indicates that a homogeneous process predominates.

It is well known that at temperatures exceeding $0.3\ T_m$, where T_m is the melting point of the crystals in °K, there is a sharp increase in the mobility of the surface atoms [1, 2]. At the same time, the magnitude of the catalytically active surface, whatever its nature may be, cannot ordinarily remain unchanged, and it would be expected that beginning at some temperature the catalytically active surface would change with temperature.

In this connection, we have studied the kinetics of the isomerization of allylbenzene on platinum films over a wide range of temperatures 250-700° C ($\frac{T}{T_m}$ = 0.27-0.47).

EXPERIMENTAL

The kinetics of the isomerization of allylbenzene to propenylbenzene were studied in a static system at pressures of 0.2-2.0 mm. The catalysts were platinum films, which were evaporated onto the walls of a completely sealed quartz cell with optical windows. Prior to each experiment, the cell was pumped for several hours at a final temperature of 700°. A platinum wire, which was suspended along the axis of the cell, was repeatedly heated to 1300° by means of an electric current until the pressure remained constant ($5 \cdot 10^{-6}$ mm) during the next heating. The platinum films were then evaporated and conditioned by pumping at a wire temperature of 1400° and under the conditions indicated in Table 1.

After completion of thermal conditioning of the film, "pure grade" krypton was passed into the cell until the pressure reached about 100 mm, the cell was cut off at the closed stopcocks, fitted into a horizontal position in front of the entrance slit of a ZMR-2 monochromator and again sealed to the high-vacuum apparatus, which was fitted with a tube containing allylbenzene** and a manometer filled with D-1 oil (d^{20}_4 = 0.8881). The krypton, with which the cell was filled in order to prevent air from being drawn into the cell through the stopcocks when the cell was sealed to the vacuum apparatus, was pumped out of the heated cell.

*Presented at the Conference on Organic Catalysis, Moscow, November 17, 1959.

**Constants of the allylbenzene used in this investigation: normal b.p. 154°, $n^{20}D$ = 1.5128; these values are close to the literature values [3]: normal b.p. 154°, $n^{20}D$ = 1.5131. The hydrocarbon was freed from dissolved gases by freezing with liquid nitrogen while pumping and melting under a static vacuum.

TABLE 1

Conditions Used in the Preparation and Thermal Conditioning of the Platinum Films

Film No.	Time, min		Cell wall temp.	
	evap.	cond.	during evap.	during cond.
1	15	70	660	660-670
2	45	120	690	670-700
3	95	90	730	720
4	120	60	720	680
5	120	90	470-480	470-480

The depth of conversion of the allylbenzene was determined by ultraviolet absorption spectroscopy [4]. The intensity, I, of radiation with a wave length of 259 mμ passing through the isomerization cell was recorded in each experiment on the strip chart of the electronic potentiometer EPP-09 of the ZMR-2 monochromator. The molar absorption coefficient of propenylbenzene vapors in the region of 259 mμ considerably exceeds that of allylbenzene. Therefore, the accumulation of propenylbenzene during the reaction increased the optical density of the reaction mixture. The kinetic experiments were carried out over a pressure interval for which the applicability of the Lambert–Bouger–Beer law has been demonstrated. It can be shown that if at a time t from the beginning of the reaction the partial pressure of the allylbenzene has decreased to a value p_1 and the partial pressure of the propenylbenzene formed is p_2, then:

$$\lg \frac{I_p}{I} = k_2 p_2 - k_1 p_1, \qquad (1)$$

where I_p is the intensity of radiation with a wave length of 259 mμ, passing through the cell filled with allylbenzene vapors at an initial pressure of p_0; k_1 is a proportionality constant which includes the cell thickness, the temperature of the allylbenzene vapors, and the molar absorption coefficient of allylbenzene vapor; k_2 is an analogous constant for propenylbenzene vapors.

The pressure during the course of the reaction remained constant in all experiments. This shows that isomerization of the allylbenzene over the entire temperature range studied was not complicated by polymerization or cracking reactions. A number of investigators have failed to detect side processes at 180-300° over a number of catalysts [3-7]. It is possible in principle that at high temperatures allylbenzene isomerizes not only to propenylbenzene, but also to indane:

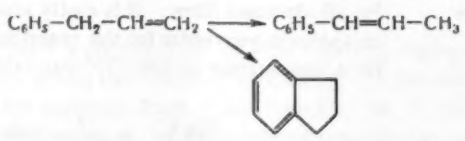

However, this second reaction has never been observed at temperatures up to 300°. On the contrary, it has been found [8] that a homolog of allylbenzene (2-methyl-3-phenyl-1-propene) is not converted to methylindane over 20% platinized carbon at a temperature of 310°, a pressure of 1 atm, and a space rate of 0.2 hr^{-1}.

A comparison of the ultraviolet absorption spectra of the products of the isomerization of allylbenzene at 250 and 600° shows no substantial difference in the courses of the reactions, and the curves showing the relationship between optical density at 259 mμ and time are similarly indicative. Therefore, it was assumed that propenylbenzene is the only product of the isomerization of allylbenzene. In this case, Eq. (1) assumes the form:

$$\lg \frac{I_p}{I} = (k_2 - k_1) p_2,$$

since $p_2 = p_1$.

TABLE 2

Dependence of the Initial Isomerization Rate of Allylbenzene in a Quartz Cell at 630° on Initial Pressure

Expt. No.	Initial pressure p_0, mm	Initial reaction rate, $V_0 \cdot 10^4$, mm · sec^{-1}	First order rate constant, $k = V_0/p_0 \cdot 10^4$, sec^{-1}
1	0.4	2.5	6.3
2	1.2	7.5	6.3
3	0.7	4.4	6.3
4	0.8	5.5	6.9
5	0.6	3.9	6.5
6	0.5	3.2	6.4

Average $k = 6.4 \cdot 10^{-4}$

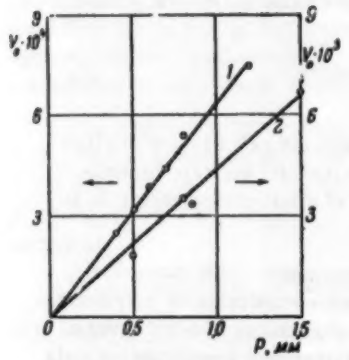

Fig. 1. Variation of the initial isomerization rate of allylbenzene in a quartz cell at 630° (1) and on platinum film No. 4 at 675° (2) with initial pressure.

It was established that the relationship between the optical density of the vaporous reaction mixture and time is described by the empirical formula

$$\lg \frac{I_\rho}{I} = \frac{t}{a + bt}, \qquad (3)$$

where t is the time from the beginning of the reaction; a and b are constants, which were determined by averaging using the linear dependence of $\frac{t}{\log I_\rho / I}$ on t. For temperatures above 500°, the initial reaction rate was calculated by the equation

$$\left(\frac{dp_2}{dt}\right)_{t=0} = \frac{1}{a(k_2 - k_1)} = \frac{1}{2{,}25a} \text{ mm·sec}^{-1}. \qquad (4)$$

At temperatures below 470°, the constant b in Eq. (3) was zero for all platinum films. It is easily seen that this corresponds to an apparent zero order for the reaction. The initial reaction rate for a temperature of 250-470° was calculated by the equation

$$\left(\frac{dp_2}{dt}\right)_{t=0} = \frac{1}{3{,}26a} \text{ mm·sec}^{-1}. \qquad (5)$$

The study of the kinetics of the isomerization of allylbenzene in the presence of platinum films was preceded by experiments designed to clarify the course of this reaction in the cell prior to the evaporation of platinum on the walls. It was found that under these conditions isomerization of allylbenzene proceeds with an appreciable rate only at temperatures above 600°. As the data of Table 2 and Curve 1 of Fig. 1 show, the initial reaction rate at 630° increased linearly with an increase in the initial pressure of the allylbenzene vapor from 0.4 to 1.2 mm. Values of the first order rate constant (Table 2) differ from the average by less than 8%.

The results of the study of the temperature dependence of the initial isomerization rate of allylbenzene in a quartz cell are presented in Table 3 (see also Fig. 3, Curve 1).

The activation energy for the isomerization of allylbenzene in a quartz cell in the absence of a platinum film was calculated from the data of Table 2 to be $E = 61 \pm 2$ kcal/mole; the pre-exponential factor was found to have a value of $A = k \cdot e^{E/RT} = 5 \cdot 10^{11}$ sec^{-1}.

TABLE 3

Dependence of the Initial Isomerization Rate of Allylbenzene in a Quartz Cell on Temperature

Expt. No.	t, °C	p_0, mm	$V_0 \cdot 10^4$ mm·sec^{-1}	$k \cdot 10^4$ sec^{-1}
1	600	0,72	1,8	2,5
2	650	0,78	13,7	18
3	715	0,85	123,0	145
4	605	0,78	2,1	2,7
5	605	0,72	2,2	3,1
6	610	0,72	2,8	3,9
7	650	0,78	14,7	19

TABLE 4

Kinetics of the Isomerization of Allylbenzene on Platinum Film No. 3 at Temperatures from 254 to 435°

t, °C	p_0, mm	$V_0 \cdot 10^4$ mm·sec^{-1}	Constants in Eq.(3)	
			a, sec	b, mm^{-1}
254	0,72	0,055	58200	0
331	0,72	0,119	27500	0
435	0,78	0,294	11200	0

TABLE 5

Dependence of the Initial Isomerization Rate of Allylbenzene on Platinum Film No. 4 at 675° on the initial Pressure p_0

Expt. No.	p_0, mm	$V_0 \cdot 10^3$ mm·sec^{-1}	$k \cdot 10^3$ sec^{-1}
1	0,45	1,77	3,9
2	0,80	3,46	4,3
3	1,50	6,80	4,5
4	0,85	3,38	4,0

Average $k = 4.2 \cdot 10^{-3}$

The isomerization of allylbenzene on platinum films prepared by the method described above is a zero order reaction at temperatures of 250 to 470°; this has previously been observed to be the case for palladium films [4]. Thus, the following values of a and b in Eq. 3, were obtained with platinum film No. 3 (Table 4).

As we have already pointed out, a value of zero for the constant b implies that the reaction has an apparent order of zero.

The isomerization on platinum films at temperatures above 500° is an apparent first order reaction, as determined from the initial rates. For example, the results presented in Table 5 and in Fig. 1 (Curve 2), were obtained on film No. 4 at 675°.

It is readily seen from the data of Table 5 and Fig. 1, that the initial reaction rate on film No. 4 increased linearly with the initial allylbenzene pressure when the latter was varied by a factor of three, and the first order rate constants differed from the average value by not more than 7%.

The results of the investigation of the relationship between the isomerization rate of allylbenzene on films Nos. 1-5 and the isomerization temperature are presented in Table 6. First order rate constants were calculated for temperatures above 500°, while at lower temperatures the value of V_0 was taken as the rate constant for the zero order reaction.

The platinum films developed a considerable catalytic activity during the first experiment, which then decreased and reached a constant level; the results of experiments carried out under equivalent conditions were in satisfactory agreement (cf., for example, Expts. 5 and 6 on film No. 3, Table 6; Expts. 10 and 11 on film No. 4, Table 6). The activity of film No. 2, which decreased considerably after the first experiment, increased and stabilized after the film had been held for five hours under vacuum at 570°.

DISCUSSION

Our study of the kinetics of the isomerization of allylbenzene on platinum films has shown that the reaction is zero order at temperatures up to 470°, and the activation energy, 7 kcal/mole, is the same for films of different catalytic activities, as may be seen upon examination of Table 7. Apparent activation energies calculated for temperatures of 500 to 660° were in agreement, within experimental error, even when the catalytic activity of the individual films used in the experiments differed by a factor of ten (cf. Curves 2 and 5, Fig. 2). However, the apparent activation energy in this temperature interval (41 kcal/mole) was almost six times greater than the apparent activation energy at temperatures up to 500°. Isomerization of allylbenzene in a quartz cell in the absence of a platinum film was observed to occur at 600°, and the reaction was zero order as in the case of platinum films at temperatures below 500°.

TABLE 6

Dependence of the Initial Isomerization Rate of Allylbenzene on Platinum Films on Temperature

Film No.	Expt. No.	t, °C	p_0, mm	$V_0 \cdot 10^4$ mm·sec^{-1}	$k \cdot 10^4$ sec^{-1}	Film No.	Expt. No.	t, °C	p_0, mm	$V_0 \cdot 10^4$ mm·sec^{-1}	$k \cdot 10^4$ sec^{-1}
1	4	507	0,65	0,29	0,45	4	2	405	0,75	0,28	
	5	579	0,65	2,76	4,25		3	468	0,78	0,42	
	6	648	0,70	15,1	21,5		4	534	0,85	0,67	0,79
	7	656	0,80	22,9	28,6		5	582	0,85	2,63	3,10
2	2	315	0,65	0,20			6	582	0,85	2,45	2,88
	3	407	0,65	0,47			7	582	0,82	2,34	2,86
	4	472	0,72	0,75			8	617	0,78	6,40	8,20
	5	564	0,65	3,20	4,9		10	663	0,78	18,0	23,1
	6	600	0,65	8,50	13,1		11	663	0,85	19,5	23,0
							14	675	0,85	33,8	39,8
3	2	254	0,72	0,055			17	701	0,78	61,0	78,2
	3	331	0,72	0,119			18	701	0,85	70,0	82,3
	4	435	0,78	0,294		5	1	587	0,92	37,2	40,4
	5	469	0,78	0,336			2	587	0,85	33,8	39,8
	6	469	0,78	0,349			3	654	0,85	209	246
	7	557	0,78	1,12	1,44						
	8	608	0,85	4,44	5,22						
	9	693	0,85	54,7	64,4						
	10	693	0,78	53,7	68,8						

TABLE 7

Apparent Activation Energies and Pre-exponential Factors for the Isomerization of Allylbenzene on Platinum Films and in a Quartz Cell

Film No.	Temp. range, °C	Order of reaction	E, kcal/mole	$A = k \cdot e^{E/RT}$
2	315—472	Zero	7±1	$7 \cdot 10^{-8}$ mole/sec.
3	254—469		7±1	$4 \cdot 10^{-8}$ "
4	405—468		7±1	$4 \cdot 10^{-8}$ "
1	507—656	First	40±2	$8 \cdot 10^{6}$ sec^{-1}
2	564—600		41±2	$2 \cdot 10^{7}$ "
3	557—608		39±2	$3 \cdot 10^{7}$ "
4	534—663		40±2	$5 \cdot 10^{6}$ "
5	587—654		43±2	$3 \cdot 10^{8}$ "
4	675—701	The same	60±10	$6 \cdot 10^{9}$ "
Quartz cell	600—715	" "	61±2	$5 \cdot 10^{11}$ "

The relationship between logarithm of the initial isomerization rate, log V_0, at constant initial allylbenzene pressure and 1/T is shown in Fig. 3. It is readily apparent that plotting the data in terms of these coordinates permits a comparison of the data for the entire temperature range studied in spite of the fact that the order of the reaction changes as the temperature passes through the region 470-500°.

For films Nos. 3 and 4, which had almost the same catalytic activity, the relationship between log V_0 and 1/T, can be represented by a broken line consisting of three sections, as shown in Fig. 3, Curve 1, which represents the results of experiments in the quartz cell in the absence of a platinum film, parallels the upper section of broken line 2. The apparent activation energy for the isomerization of allylbenzene on film No. 4, at 660-700° does not differ from that found for the isomerization in the quartz cell in the absence of a platinum film, which suggests that the reaction is chiefly homogeneous under these conditions. Such an interpretation is in agreement with the values of the pre-exponential factor, which was $6 \cdot 10^{9}$ sec^{-1} for films No. 4 and $5 \cdot 10^{11}$ sec^{-1} for isomerization in the quartz cell.

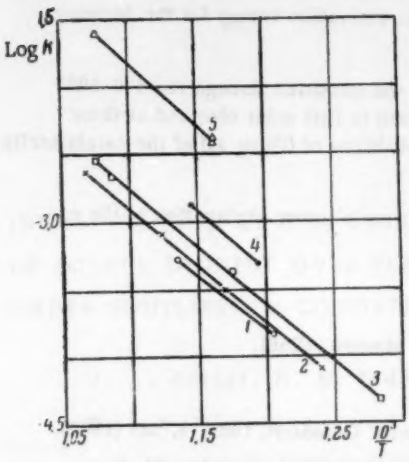

Fig. 2. Dependence of the logarithm of the rate constant for the isomerization of allylbenzene, log k, on platinum films on the reciprocal of the absolute temperature: 1) film No. 3, 2) film No. 4; 3) film No. 1; 4) film No. 2; 5) film No. 5.

The isomerization of allylbenzene at 500-660° (central section of broken line 2) cannot be represented as a combination of a catalytic reaction with an activation energy of 7 kcal/mole and a homogeneous reaction with an activation energy of 60 kcal/mole, since in such a case the central section of the graph would be curved and located below the straight line corresponding to the experimental data. For example, at 582° the sum of the initial rates calculated by extrapolation of the upper and lower sections of the broken line comprises only 60% of the experimental value of the initial rate of isomerization of allylbenzene on film No. 4. This discrepancy is even more significant in the case of film No. 2 (see broken line 3) and the highly active film No. 5, for which the initial reaction rate at 587° was 25 times higher than in the quartz cell in the absence of platinum films.

All of the data obtained show that with the transition through the region of 470-500°, the catalytic activity of the platinum films increased, the apparent activation energy for isomerization of allylbenzene increased by 34 kcal/mole, and the order of the reaction changed. Inasmuch as all of these changes take place at temperatures 0.36-0.38 times the melting point of platinum, they may be explained by an

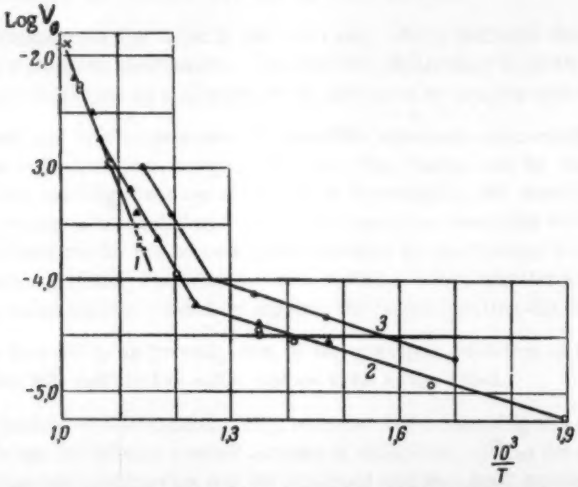

Fig. 3. Dependence of the logarithm of the initial rate of isomerization of allylbenzene in a quartz cell (1) and on platinum films No. 3 and No. 4 (2) and No. 2(3) on 1/T.

increase of the catalytically active surface as a consequence of a sharp increase in the mobility of the surface platinum atoms. The magnitude of the catalytically active surface does not depend on temperature at the lower temperatures, which would be expected from the considerations discussed at the beginning of the article. Therefore, the activation energy of 7 kcal/mole characterizes the catalytic reaction alone. When the experiments were carried out at temperatures which provided mobility of the surface atoms of the metal, the magnitude of the catalytically active surface becomes a function of temperature. The absence of a smooth transition between the lower and central sections of the broken line suggests that in the present case an equilibrium is attained between the catalytically active surface and the catalyst lattice, and the experimentally determined activation

energy includes both the activation energy of the catalytic reaction and the activation energy for the increase in the catalytically active surface.

This concept of the increase in the catalytically active surface with the transition through the 470-500° region is in agreement with the change in the order of the reaction from zero to first order observed at these same temperatures. At the rather low allylbenzene pressures used, the probability of filling all of the catalytically active centers would decrease with an increase in the number of them.

This point of view is not the only one possible; however, it provides a satisfactory explanation of the experimental results and seems to us to be the most probable one.

LITERATURE CITED

1. A. Rees, Chemistry of the Defect Solid State [Russian translation] (IL, Moscow, 1956).
2. W. Seith, Diffusion in Metallen [Russian translation] (IL, Moscow, 1958).
3. R. Ya. Levina, Zhur. Obshch. Khim. 9, 2287 (1939).
4. V. I. Shimulis, V. D. Yagodovskii, and V. M. Gryaznov, Vestniki Moskov. Gosudarst. Univ. 4, 237 (1957).
5. R. Ya. Levina, Zhur. Obshch. Khim. 7, 1587 (1937).
6. R. Ya. Levina, and F. F. Tsurikov, Zhur. Obshch. Khim. 4, 1250 (1934).
7. K. V. Topchieva, A. I. Pletyushkina, and I A. Zen'kovich, Zhur. Obshch. Khim. 28, 624 (1958).•
8. O. V. Vragin, Candidate's Dissertation, Institute of Organic Chemistry [in Russian (Izd. AN SSSR, Moscow, 1959).

•Original Russian pagination. See C. B. translation.

INVESTIGATION OF THE KINETICS OF THE OXIDATION OF SULFUR DIOXIDE OVER PLATINUM CATALYST UNDER EQUILIBRIUM CONDITIONS

V. A. Roiter, N. A. Stukanovskaya, G. P. Korneichuk, N. S. Volikovskaya, and G. I. Golodets

L. V. Pisarzhevskii Institute of Physical Chemistry, Academy of Sciences of the USSR

Translated from Kinetika i Kataliz, Vol. 1, No. 3, pp. 408-417, September-October, 1960
Original article submitted March 12, 1960

The kinetics of the oxidation of sulfur dioxide over platinum screen under equilibrium conditions have been investigated by means of a tracer technique using radioactive sulfur. The kinetics were also investigated under nonequilibrium conditions by the ordinary circulation–flow method.

It was found that the kinetics are the same in the two cases, which indicates that the mechanism is general. Basis was provided for a reaction mechanism. The observed differences in heats of activation and rate constants in the two cases are explained by poisoning of the platinum by oxygen under equilibrium conditions.

The rates of the forward and reverse processes of reversible reactions under equilibrium conditions and the dependence of these rates on concentrations, temperature, and other factors can be studied by means of radioactive tracer techniques. Such investigations are of interest in determining the mechanism of a process. Inasmuch as when the over-all process is in equilibrium all of its stages are reversible and are also in equilibrium, the selection of possible mechanisms for the process from a number of mechanisms which formally satisfy the observed kinetic laws, becomes limited. Furthermore, a comparison of the kinetics under equilibrium conditions with those observed under nonequilibrium conditions suggests the stages limiting the rates of the processes.

The present work was devoted to an investigation of the catalytic oxidation of sulfur dioxide by oxygen over platinum screen with the S^{35} radioactive sulfur isotope used as the label.

The principle of the method was as follows. To a reaction cell containing the catalyst and an equilibrium mixture of SO_2, SO_3, and air, was introduced a small amount of radioactive $S^{35}O_2$; the amount introduced was sufficiently small that the reaction equilibrium was not disturbed and that good mixing with the reaction mixture was obtained. The rate of transfer of radioactive sulfur from the SO_2 to SO_3 was determined.

Assuming that the transfer was associated with the process

$$2S^*O_2 + O_2 \rightleftarrows 2S^*O_3,$$

it is easy to connect the observed rate of isotope exchange with the rate of the chemical process in which SO_2 is oxidized or with the equivalent rate of the reverse process in which sulfur trioxide dissociates (W).

Let V_{SO_2} be the amount of SO_2 in the reaction vessel, V_{SO_3} is the amount of SO_3; y and x are the mole fractions of S^{35} in the SO_2 and SO_3, respectively, at time t, and y_0 is that at the start (x = 0).

Then

$$-\frac{dy}{dt} V_{SO_2} = W(y - x)$$

or, since

$$x = (y_0 - y) \cdot \frac{V_{SO_3}}{V_{SO_2}},$$

$$\frac{dy}{dt} = \frac{W}{V_{SO_2}} [y_0 - y(\lambda + 1)], \text{ где } \lambda = \frac{V_{SO_3}}{V_{SO_2}}.$$

Integrating from y_0 to y and from 0 to t, we obtain

$$\ln \frac{\lambda y_0}{(1+\lambda) y - y_0} = \frac{W(\lambda+1)}{V_{SO_2}} \cdot t, \text{ whence } W = \frac{2{,}3 V_{SO_2}}{t(\lambda+1)} \lg \frac{\lambda y_0}{(1+\lambda) y - y_0}.$$

Since in the experiments we did not directly measure the mole fractions of radioactive sulfur in the SO_2 and SO_3, but instead measured the specific radioactivities of the $BaSO_4$ precipitates formed, respectively, from SO_2 or SO_3 (I_{SO_2} and I_{SO_3}), we must replace y by the proportional αI_{SO_2}, and y_0 by the proportional $\alpha(I_{SO_2} + I_{SO_3}) = \alpha I_0$. Then

$$W = \frac{2{,}3 V_{SO_2}}{t(\lambda+1)} \lg \frac{\lambda I_0}{(1+\lambda) I_{SO_2} - I_0}$$

Use of the dimensionless parameter $I' = I_{SO_2}/I_{SO_3}$, is still more satisfactory. In this case, the equation assumes the form

$$W = \frac{2{,}3 V_{SO_2}}{t(\lambda+1)} \lg \frac{\lambda}{(1+\lambda)\frac{I'}{I'+1}}$$

By changing the initial ratio of SO_2 and air and, consequently, the equilibrium ratio of SO_2 and SO_3, it was possible to investigate the dependence of W on reactant concentrations and to calculate the rates of the forward and reverse processes (k_1 and k_2); by changing the temperature, it was possible to determine the corresponding heats of activation.

APPARATUS

The investigation was carried out in the circulation apparatus shown schematically in Fig. 1. The circulation system consisted of a quartz reactor, a circulation pump with a capacity of 5 liters per minute, a block furnace, a dosing apparatus for the introduction of the labeled SO_2, and a system for collecting samples of the reaction mixture for analysis. The sulfur dioxide and air were passed through their respective purification trains into the mixer, from which they entered the circulation system. The technical sulfur dioxide was dried with sulfuric acid, and the air was passed through a column containing fused alkali and calcium chloride and then to a trap cooled with liquid air.

The catalyst— a platinum screen weighing about 0.2 g—was securely fixed to the thermocouple well, which extended along the axis of the reactor. The geometric surface area of the wire forming the screen was 16 sq cm/g. In order to accelerate attainment of equilibrium, an auxiliary catalyst prepared from the same screen (weight, about 2 g) was also used; this was removed to the cold part of the apparatus by means of an attached platinum wire after equilibrium had been attained. Introduction of the radioactive SO_2 into the circulation system was carried out as follows: buret 7 (Fig. 1) was filled with radioactive SO_2, the mercury was brought to the same level in the buret and the leveling bulb, and the SO_2 was introduced into the circulation system by rotation of control stopcock "K". Bulb 13 was then raised to bring mercury up to stopcock 14, thereby forcing all of the SO_2 into the circulation system, and the stopcock was then closed.

The radioactive SO_2 was prepared by burning radioactive sulfur in a stream of air. The resulting $S^{35}O_2$ was condensed in a liquid air-cooled glass trap, and it was then transferred to a steel cylinder for storage and use.

The corrosiveness of the medium and its sensitivity to traces of moisture made it necessary to work without lubricants in the dry, carefully ground joints and stopcocks. The metal spring in the circulation pump was replaced by a pad of broken glass, 11, and the current in the coil was so chosen that the piston did not, as a rule, reach the pad, but was stopped in a lower position from which it was raised by an increase in the current.

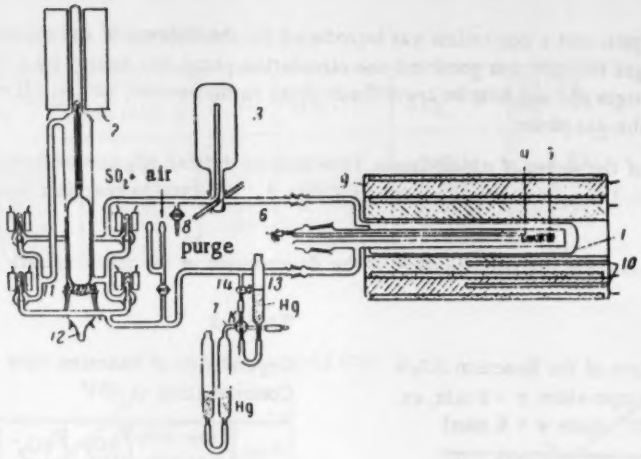

Fig. 1. Circulation apparatus for studying the kinetics under equilibrium conditions. 1) Quartz reaction tube; 2) glass circulation pump; 3) sampling devide; 4) auxiliary platinum catalyst; 5) platinum catalyst; 6) wire for shifting the auxiliary platinum catalyst; 7) buret containing radioactive SO_2.

The mixture of SO_2 and SO_3 was forced from the sample collector by a ten-fold volume of dry air and passed successively through a tube containing NaCl to tie up the SO_3 [1] and then through a trap containing a titered iodine solution to combine with the SO_2. The $NaCl \cdot SO_3$ formed in the first tube was dissolved in water, and the resulting solution was titrated with NaOH solution; the I solution was back-titrated with sodium thiosulfate. In this manner, the amounts of SO_2 and SO_3 in the sampling system were determined. The SO_2 and SO_3 were separately converted to SO_4^{--} and precipitated with barium chloride; the $BaSO_4$ precipitate was filtered, washed, removed by means of a small brush to previously weighed glass plates having a diameter of 1.9 cm, dried, and weighed, and the radioactivity was then determined by means of an end-window counter.

The usual flow–circulation apparatus was used to study the kinetics under nonequilibrium conditions.

Kinetic Investigation Under Equilibrium Conditions

The reactor was heated to the desired temperature, and the system was then purged with reaction mixture for an hour. The system was then closed in for 1-2 hr (depending on the temperature of the experiment) in order to establish equilibrium. The time required at each temperature was determined by preliminary experiments. After equilibrium was established, the auxiliary catalyst was shifted to the cold part of the apparatus, and 0.3 ml of radioactive SO_2 was introduced from the dosing apparatus (the overall volume of the circulation system was 1650 ml). After a given time, the stopcock of the sampling system was turned 90°, and the sample was analyzed for SO_2 and SO_3 by the method described above. The temperature of the sampling system was

TABLE 1

Dependence of the Rate of Oxidation of Sulfur Dioxide on SO_2 Content of the Original Mixture (α_{SO_2}) at 650°

α_{SO_2}, %	τ, min.	P_{SO_2}, atm	P_{SO_3}, atm	P_{O_2}, atm	$\lambda = \frac{P_{SO_3}}{P_{SO_2}}$	I_{SO_3}	I_{SO_3}	$I' = \frac{I_{SO_2}}{I_{SO_3}}$	W, ml per min·g
3,60	10	0,0114	0,0246	0,191	2,14	14,0	10,3	1,36	1,051
3,71	8	0,0117	0,0254	0,189	2,17	38,0	17,2	2,20	0,844
3,89	8	0,0120	0,0269	0,189	2,24	28,2	11,7	2,40	0,800
6,13	8	0,0184	0,0429	0,176	2,33	15,7	9,3	1,69	1,72
6,19	8	0,0184	0,0435	0,175	2,36	18,7	8,6	2,17	1,33
7,33	9	0,0223	0,0510	0,169	2,29	15,8	9,2	1,71	1,83
8,40	10	0,0234	0,0606	0,163	2,59	8,5	5,1	1,66	1,73
9,04	10	0,0280	0,0624	0,161	2,23	8,3	5,5	1,51	2,32

determined for each analysis, and a correction was introduced for the volume of gas mixture contained in it. Since circulation of the gas mixture was good and the circulation pump was heated by a small electric lamp, the temperature in the system did not drop below 30° anywhere in the system, so that all components of the mixture were maintained in the gas phase.

The results of one of the series of experiments, in which the initial SO_2 concentration was varied while the temperature was maintained constant, are presented in Table 1. All data on reaction rates are referred to 1 g of catalyst.

Table 2 presents data from the investigation of the dependence of the reaction rate on temperature.

TABLE 2

Dependence of the Rate of the Reaction $SO_2 + \frac{1}{2} O_2 \rightleftharpoons SO_3$ on Temperature τ = 8 min, except in Expt. 8 at 650° where τ = 6 min)

t, °C	P_{SO_2}, atm	P_{SO_3}, atm	I'	W, ml per min·g
600	0,0105	0,0377	4,40	0,375
606	0,0115	0,0382	3,98	0,450
625	0,0151	0,0356	2,74	0,846
625	0,0145	0,0386	2,50	0,889
650	0,0169	0,0276	2,50	1,44
655	0,0172	0,0267	1,82	1,56
674	0,0205	0,0289	1,43	2,47

TABLE 3

Dependence of Reaction Rate on Initial SO_2 Concentration at 587°

α_{SO_2}, %	Flow rate, ml/min	P_{SO_2}, atm	P_{SO_3}, atm	P_{O_2}, atm	W_1-W_2, ml/min·g
2,69	204	0,0114	0,0155	0,197	3,32
3,46	206	0,015	0,0197	0,194	4,27
3,39	206	0,0150	0,0189	0,194	4,08
5,74	210	0,0258	0,0316	0,182	6,98
6,26	210	0,0289	0,0346	0,180	7,65

Investigation of the Reaction Kinetics Under Nonequilibrium Conditions

The investigation was carried out in the same type of apparatus as used for the investigation under equilibrium conditions; a flow–circulation method was used. The circulation rate was maintained at 4-5 liter/min, and the fresh feed rate was 0.2 liter/min. The weight of the catalyst–platinum screen–was 0.9512 g.

The reactor was heated to the predetermined temperature, and a mixture of SO_2 and air was passed into the system; the composition of the mixture was determined from gas meter readings. After 20-30 min, the effluent mixture was subjected to chemical analysis. For this purpose, to the effluent end of the system was connected, successively, a trap containing sodium chloride to tie up the SO_3, a wash bottle containing a titered iodine solution, and a Mariotte bottle for determination of the total volume of mixture taken for the analysis. The prescribed conditions (temperature, concentration of SO_2 in the feed) were maintained until constant conversion was attained, which required from 1.5 to 2 hr.

Variation of the concentrations in the circulation system was carried out by changing the initial SO_2 concentration (α_{SO_2}). The observed conversion rate, which was calculated as the product of the SO_3 concentration in the effluent times the flow rate, represented the difference in the rates of the forward and reverse reactions (W_1-W_2).

The results of one of the series of experiments are presented in Table 3; the degree of conversion in this series was 70%.

Table 4 presents the results of an investigation of the effect of temperature on reaction rate.

DISCUSSION

The oxygen concentration changed very little in our experiments, and, to a first approximation, it may be considered constant. In order to determine the form of the dependence of W on the concentration of SO_2 and SO_3, the calculated value of W (Table 1) was plotted as a function of these concentrations (Figs.2 and 3).

As may be seen from the graphs, W may be satisfactorily represented by either the equations $W = k' P_{SO_2}$ or $W = k'' P_{SO_3}$. It is evident that the first of these equations corresponds to the forward and the second to the reverse reaction. Thus, one molecule of SO_2 takes part in the elemental act of SO_2 oxidation on platinum, and

TABLE 4

Dependence of Reaction Rate on Temperature

t, °C	P_{SO_2}, atm	P_{SO_3}, atm	W_1-W_2, ml/min · g	t, °C	P_{SO_2}, atm	P_{SO_3}, atm	W_1-W_2 ml/min · g
600	0,0237	0,0355	7,68	500	0,0342	0,0214	4,62
600	0,0233	0,0339	7,32	510	0,0338	0,0216	4,66
575	0,0242	0,0324	6,97	450	0,0465	0,0109	2,36
550	0,0254	0,0320	6,91	450	0,0438	0,0109	2,36
550	0,0252	0,0316	6,80	420	0,0410	0,0070	1,42

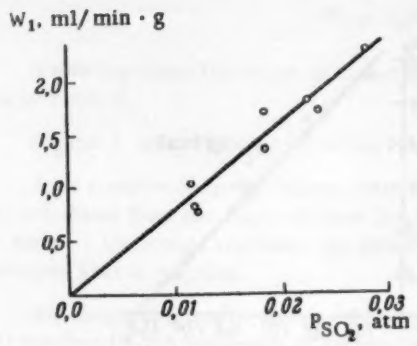

Fig. 2. Dependence of the rate of the forward reaction on the partial pressure of SO_2.

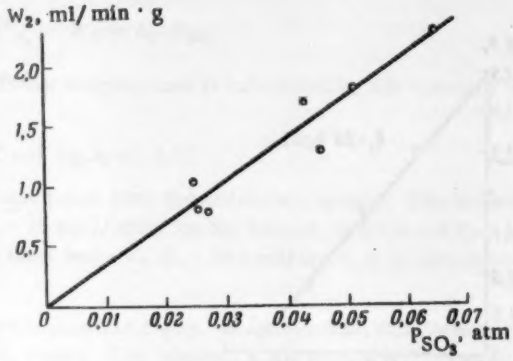

Fig. 3. Dependence of the rate of the reverse reaction on the partial pressure of SO_3.

one molecule of SO_3 takes part in the reverse reaction. This is in conformity with the conclusion of G. K. Boreskov [2] that the molecularity of the process is $\nu = 1$.

The linear relationship indicates that SO_2 and SO_3 are weakly adsorbed (Henry's law region).

In considering the kinetics of the reaction which takes place under equilibrium conditions from the point of view of one assumed mechanism or another, one should, as already indicated at the beginning of this paper, discard all of those mechanisms which assume the absence of equilibrium in even one of the reaction steps. Thus, it is evident that the approach of M. I. Temkin (principle of semi-equilibrium is unsuitable, though this approach was used by G. K. Boreskov to deduce the kinetic equation of this process [3]. In this case it was assumed that there is no equilibrium between the gaseous and the adsorbed SO_2. Indeed, the expressions for the forward and reverse reactions proposed by the latter author,

$$w_1 = k_1 P_{O_2}^{0,25} \cdot P_{SO_2} \cdot P_{SO_3}^{-0,5},$$

$$w_2 = k_2 P_{O_2}^{-0,25} \cdot P_{SO_3}^{0,5}$$

do not conform to the linear dependence of reaction rate on P_{SO_2} and P_{SO_3}, which our data indicate. It is also evident that a chain mechanism cannot be assumed for this process, since the basis of such a mechanism is the assumption that active radicals accumulate in concentrations exceeding equilibrium concentration.

On the other hand, under equilibrium conditions when there is no restriction as to time, SO_3 can be formed by all possible parallel routes, even if certain of these routes have high activation energies.

The observed oxidation kinetics will, in this case, be determined by that particular reaction which proceeds more rapidly than the other parallel reactions and, therefore, produces the major amount of SO_3.

TABLE 5

Temperature Dependence of the Rate Constants for the Reaction $SO_2 + {}^1/_2 O_2 \rightleftharpoons SO_3$ Under Equilibrium Conditions

t, °C	600	606	625	625	650	655	674
k_1	82,5	92,0	132,0	144,0	196,8	209,0	279,0
k_2	9,95	11,80	23,80	23,00	52,30	58,25	85,60

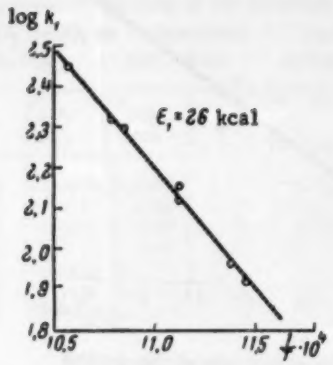

Fig. 4. Graph of log k_1 vs 1/T.

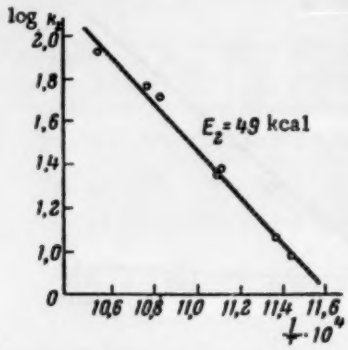

Fig. 5. Graph of log k_2 vs 1/T.

Of the possible reaction mechanisms which correspond to our experimental data and which, at the same time, conform to the principle of detailed equilibrium, the following may be proposed:•

I	II
1. $O_2 \rightleftarrows 2O$	1. $SO_2 + O_2 \rightleftarrows SO_3 + O$
2. $O + SO_2 \rightleftarrows SO_3$	2. $O + SO_2 \rightleftarrows SO_3$
	3. $2O \rightleftarrows O_2$

In order to choose between these variants on the basis of kinetic data, a detailed investigation of the relationship between reaction rate and oxygen concentration would be necessary, since these two variants are indistinguishable on the basis of the form of the relationship between rate and SO_2 and SO_3 concentrations. Therefore, our data are of no avail for this purpose. We conditionally assumed variant I in our further calculations, since it is the simplest and since, moreover, it conforms to literature data [2] regarding the high rate of adsorption of oxygen on platinum accompanied by partial or complete dissociation.

Scheme 1 for the overall process of SO_2 oxidation on a platinum surface, which corresponds to variant I, is presented below.

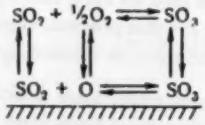

Scheme 1

•All substances in the adsorbed state.

The kinetic equations for the rates of the forward and reverse reactions corresponding to this variant are:

$$W_1 = k'\theta_{SO_2} \cdot \theta_O,$$
$$W_2 = k''\theta_{SO_3},$$

where θ is the fraction of the catalytically active surface covered by a given component.

Assuming on the basis of our experimental data that

$$\theta_{SO_2} = a_{SO_2} \cdot P_{SO_2}; \quad \theta_{SO_3} = a_{SO_3} \cdot P_{SO_3}$$

and, conditionally, that $\theta_O \sim \sqrt{a_{O_2} P_{O_2}}$, we obtain

$$W_1 = k_1 P_{SO_2} \sqrt{P_{O_2}}; \quad W_2 = k_2 \cdot P_{SO_3}.$$

Table 5 presents the values of k_1 and k_2 at different temperatures as calculated by this equation from the data of Table 2.

Figures 4 and 5 show graphs of log k_1 vs. $1/T$ and log k_2 vs. $1/T$.

As is apparent from the figures, there is good agreement with the Arrhenius equation. The heats of activation calculated from the slopes of these lines are E_1 = 26 kcal/mole for the forward reaction and E_2 = 49 kcal per mole for the reverse reaction; the difference in these heats, $E_2 - E_1$ = 23 kcal/mole, is in agreement with the known heat of reaction.

An energy diagram for the proposed mechanism is shown in Fig. 6. It follows from this diagram that the heat required for the conversion of gaseous molecular oxygen to an adsorbed atom is $Q_d = -(E_1 - \epsilon_0) = -(26 - \epsilon_0)$. Since, considering the radical character of O_{ads}, the value of ϵ_0 cannot be large (not more than 10 kcal/mole [4]), the value of Q_d can be approximately evaluated as 20 kcal/mole. Taking into account the fact that the heat of dissociation of O_2 into gaseous atoms is 59 kcal/g atom, the energy of the bond of an adsorbed oxygen atom with the platinum should be about 40 kcal/g atom; this is a reasonable value.

Under nonequilibrium conditions, equilibrium will be disturbed first in the slower steps. If this is an elementary reaction on the surface, the rate of the over-all process will be determined by the difference in the rates of this surface reaction, and the equilibrium between the adsorbed and gaseous participants in the reaction will be maintained. In this case (Langmuir–Schwab kinetics), it should be expected that the over-all kinetics would be described by the difference in rates W_1 and W_2, where each of these rates may retain the same form of dependence on concentration as observed in the equilibrium state. If the slowest step is adsorption of one of the reactants, equilibrium will be maintained on the surface, and the reaction rate will be determined by the rate of adsorption of this substance (Temkin kinetics). In this case, the kinetic expression will be different from, for example, the corresponding Boreskov equation.

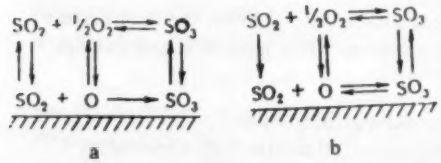

Scheme 2: a) Langmuir–Schwab kinetics; b) Temkin–Boreskov kinetics.

For comparison with equilibrium Scheme 1, both of these cases are presented in a similar manner in Scheme 2.

Table 6 represents values of k_1, calculated from the data on W_1-W_2 of Table 3 by (a) the equation for kinetics in the equilibrium state; and (b) an equation corresponding to that of Boreskov.

It is evident from these data that the Boreskov equation leads to a significant systematic increase in k_1, while the values of K_2 calculated by the second equation, exhibit practically no dependence on SO_2 or SO_3 concentration.

Thus, the mechanism and kinetics of the equilibrium state are apparently retained under nonequilibrium conditions.

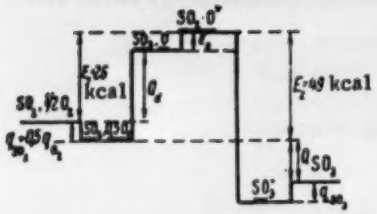

Fig. 6. Energy diagram of the reactions: E_1 and E_2) observed heats of activation; Q) heat of the reaction $SO_2 + 0.5\,O_2 \rightarrow SO_3$; q_{SO_2}, q_{SO_3}, q_{O_2}) heats of adsorption of SO_2, SO_3, and O_2; Q_d) heat of the reaction $0.5\,O_2 \rightarrow O$; ϵ_0) height of the energy barrier. An underline under a formula indicates that the substance is in the adsorbed state.

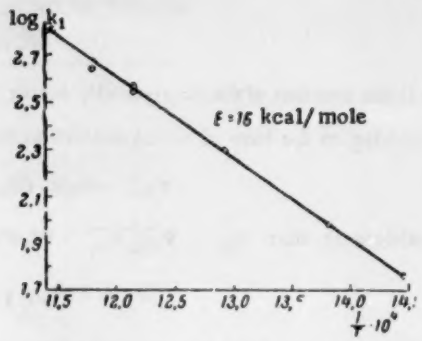

Fig. 7. Graph of log k_1 vs. 1/T (equilibrium conditions).

TABLE 6

Comparison of Rate Constants Calculated by the Equation for Equilibrium Conditions with Those Calculated by the Boreskov Equation for a Temperature of 587°

a_{SO_3}, %		2,69	3,46	3,39	5,74	6,26
$k_1 = \frac{W_1 - W_2}{P_{O_2}^{0,5} \cdot P_{SO_2} - \frac{P_{SO_3}}{K_p}}$	(a)	894	880	824	844	860
$k_1 = \frac{W_1 - W_2}{P_{SO_2} \cdot P_{O_2}^{0,25} \left(1 - \frac{P_{SO_3}}{K_p \cdot P_{SO_2} \cdot P_{O_2}^{0,5}}\right)}$	(b)	73,4	81,5	75,4	97,8	104,0

Table 7 presents values of the rate constant k_1 for different temperatures as calculated by Eq. (a) using the data of Table 4.

Figure 7 presents graphically the dependence of log k_1 on 1/T, from which it is seen that the temperature dependence of the rate constant is in good agreement with the Arrhenius equation. The heat of activation calculated from the slope of the line is E_1 = 16 kcal/mole.

Upon comparing the results of the treatment of the data obtained under equilibrium and nonequilibrium conditions, it is deserving of attention that, with retention of the same kinetic relationships and, apparently, the same mechanism, there is a sharp difference in the absolute rate constants; the rate constants in the equilibrium state are much lower and the values of the heats of activation are significantly higher than those calculated for the reaction under nonequilibrium conditions.

These conflicting results can be explained if it is assumed that in the reaction of the oxygen with the platinum, in addition to reactive O_{ads} atoms, there is also formed some other surface compound, which we shall provisionally denote by Pt. . . O_2; this reacts slowly with the sulfur dioxide. Consequently, an additional equilibrium step must be added to the equilibrium processes as represented by the mechanisms of variants I and II:

$$O_2 + Pt \rightleftarrows Pt \ldots O_2,$$

$$Pt \ldots O_2 + 2SO_2 \rightleftarrows Pt + 2SO_3.$$

If it is assumed that these processes proceed very slowly in comparison to the process considered previously, the amount of SO_3 formed by this route is insignificant and can be disregarded. However, the presence of these steps leads to a decrease in the free surface of the platinum and, thereby, to a decrease in the values of k_1 and k_2.

TABLE 7

Dependence of the Rate Constant on Temperature.

t, °C	600	575	550	550	450	420
k_1	686 635	440 —	362 358	200 202	97,8 97,8	58,9 —

If it is further assumed that, as is usual for surface compounds, the chemical potential of the Pt . . .O_2 depends on the degree of surface coverage, the ratio Pt/Pt. . .O_2 will increase with an increase in temperature (the process Pt + O_2 → Pt . . .O_2, is obviously exothermic) and the rate constant for the oxidation of SO_2 will increase not only due to an increase in the probability of the interaction of SO_2 with O_2 on the available surface of the active platinum, but also owing to an increase in the fraction of free surface, which is apparent as an increase in the observed heats of activation.•

As already noted above, as the process is removed from equilibrium conditions, the first equilibria to be disturbed are those of the slowest individual parallel reactions, one of which is the interaction of oxygen with the platinum as considered above. The equilibrium is shifted far to the left, there is an increase in the free surface of the platinum, and the rate constants sharply increase. An increase in the temperature cannot now bring about an increase in the free surface of the platinum, and, therefore, the observed heats of activation can assume normal values——values which are lower than under equilibrium conditions.

The poisoning effect of oxygen on platinum catalysts has been noted by numerous investigators, particularly in the work of G. K. Boreskov and co-workers [6]. Nevertheless, we carried out a special experiment in order to confirm the hypothesis presented here. An active platinum catalyst was treated with air at 550-600° (in the presence of SO_2); the treatment was for 2 hr. The activity of this catalyst was then determined at this same temperature. It was found that, in fact, the activity of this catalyst sharply decreased after this treatment; the degree of conversion prior to this treatment was 57.9-51.2%, while after the air treatment it was 9.2-8.8%. A three-hour treatment of the catalyst with the gas-air mixture was required to increase the activity gradually to its original value. Thus, some such type of interaction of oxygen with the platinum actually exists, which leads to poisoning of the catalyst, and both this process and the process by which the catalyst surface becomes free during catalysis, are very slow processes.

SUMMARY

1. A radioactive tracer technique was used to measure the rates of the forward and reverse reactions in the oxidation of SO_2 over a platinum screen as functions of the SO_2 and SO_3 concentrations at different temperatures. It was shown that the molecularity of the process is $\nu = 1$. Kinetic equations were determined which are in agreement with the experimental data, and possible mechanisms have beeen proposed for the process; these mechanisms satisfy the observed kinetic relationships and the principle of detailed equilibrium. The heats of activation of the forward and reverse reactions were calculated.

2. The kinetics of the process under nonequilibrium conditions were investigated over this same catalyst. The data satisfied the same kinetic equations that were found to hold under equilibrium conditions. This permits extension of the proposed mechanism to the process under nonequilibrium conditions and leads to the conclusion that the limiting step is the surface reaction of SO_2 with oxygen, and not the interaction of any of the components of the reaction mixture with the catalyst.

3. In addition, it was established that the reaction rate constants for the equilibrium state are considerably less in absolute value and the observed heats of activation are higher than those found when the reaction was carried out under nonequilibrium conditions. This fact is explained by the presence of a slow, reversible interaction of oxygen with the platinum, which leads to the formation of surface compounds of low reactivity, and these, in turn, decrease the active platinum surface available. It was shown that this poisoning must occur chiefly under equilibrium conditions and has practically no connection with the nonequilibrium process. The assumption of a poisoning effect of oxygen on platinum and the slowness of this process were confirmed by a special experiment.

• The concept of the dependence of rate constants of catalytic processes on the composition of the gas mixture and on temperature has been developed in detail by G. K. Boreskov [5].

LITERATURE CITED

1. F. N. Kel'man, Zavodskaya Lab. 11, 1316 (1952).
2. G. K. Boreskov, Catalysis in the Production of Sulfuric Acid [in Russian] (Goskhimizdat, Moscow–Leningrad, 1954).
3. G. K. Boreskov, Zhur. Fiz. Khim. 19, 535 (1945).
4. N. N. Semenov, On Some Problems of Chemical Kinetics and Reactivity [in Russian] (Izd. AN SSSR, Moscow, 1958).
5. G. K. Boreskov, Zhur. Fiz. Khim. 32, 2739 (1958); 33, 1969 (1959).
6. G. K. Boreskov, M. G. Slin'ko, and V. S. Chesalova, Zhur. Fiz. Khim. 30, 2786 (1956).

A STUDY OF ORTHOHYDROGEN – PARAHYDROGEN CONVERSION UNDER SOLID CATALYSTS

II. REACTION IN THE LIQUID PHASE

R. A. Buyanov

United Institute for Nuclear Investigations at Dubna

Translated from Kinetika i Kataliz, Vol. 1, No. 3, pp. 418-420,
September-October, 1960
Original article submitted March 16, 1960

The activities of a number of catalysts for the conversion of orthohydrogen to parahydrogen in the liquid phase (21-22°K) at pressures of from 2 to 150 atm have been measured.

A comparison has been made of these activities with those obtained at 78°K. Catalysts for use in the reactors of hydrogenliquefiers and optimum conditions for their operation are recommended.

• • •

1. EXPERIMENTAL METHOD AND CONDITIONS.

The results of work on the selection of a series of catalysts and the determination of their activities with respect to orthohydrogen–parahydrogen conversion at temperatures of 78-64°K have been reported previously [1].

In the present work the catalysts were tested in a flow apparatus at a temperature of 21-22°K, i.e., in the liquid phase at pressures of from 2 to 150 atm.

Specially prepared hydroxides, $Cr(OH)_3$, $Mn(OH)_4$, $Fe(OH)_3$, $Co(OH)_3$, and $Ni(OH)_2$ (without carrier), and also a chrome-nickel catalyst were tested.

To the experimental reactor were charged samples of 1-3 cc, the size depending on the catalyst activity. All samples had a particle size of 0.7-1.0 mm diameter. The liquid hydrogen flow rate was varied within the range of 50-240 liters/hr calculated as a gas under standard conditions. The initial composition of the hydrogen was 25% parahydrogen. The flow apparatus and the method of catalyst preparation have been described in some detail in the first communication [1]. As before, analysis of the gas was carried out in a continuous recording thermal conductivity gas analyzer [2].

The reactor was cryostatted with liquid hydrogen. With the exception of the chrome-nickel catalyst, all catalysts were activated, as before, by pumping the reactor to a pressure of $1 \cdot 10^{-2}$ mm Hg, while heating for 24 hr. The heating was carried to 135°C in the case of the ferric hydroxide. All of the remaining catalysts were heated to 90-100°C. At the end of the activation, the reactor heater was turned off, and the reactor was filled with pure hydrogen. The chrome-nickel catalyst was activated by heating to 140°C in a stream of hydrogen at a space rate of 4000 hr^{-1}.

2. METHOD OF CALCULATION AND EXPERIMENTAL

As previously [1], calculation of the rate constants was carried out by means of the equation for a first order reaction:

$$k = \frac{n_c}{V_k} \ln \frac{1 - C_n/C_e}{1 - C/C_e} .$$

Here, k is the reaction rate constant in moles/cc · sec; n_c is the hydrogen consumption in moles/sec; V_c is the volume of catalyst in the reactor in cc; C_0, C_e, and C are, respectively, the initial and equilibrium concentrations and the concentration of parahydrogen in the stream (from the liquefier) in %.

A simple transformation of this equation to one applicable for the conditions under which the hydrogen liquifier was operated leads to the expression:

$$v_H = \frac{44{,}7 V_c k}{\lg \frac{1 - C_n C_e}{1 - C/C_e}},$$

where v_H is the productivity of the hydrogen liquefier (liters of liquid parahydrogen with a concentration C per hour).

Thus, knowing the rate constant for a given catalyst and the concentration of parahydrogen which is desired from the liquefier, it is easy to find the ratio v_H/V_c, which is required for hydrogen liquefier calculations.

The experimentally determined values of the rate constants for the various catalysts are shown in the table.

Values of k at T = 22°K and of the ratio $k_{22°K}$ per $k_{78°K}$.

Catalyst	$k_{22°K} \cdot 10^3$ moles/cc/sec	$k_{22°K}/k_{78°K}$
Chrome-nickel	1,6—2,1	1,05—1,25
$Cr(OH)_3$	0,9—1,6	1,8—2,2
$Mn(OH)_4$	1,6—2,1	1,75—2,2
$Fe(OH)_3$	0,9—2,1	0,92—0,93
$Co(OH)_3$	0,32—0,34	1,2—1,4
$Ni(OH)_2$	0,5—0,8	1,1—1,5

As previously reported [1], the apparent activation energies of all of the catalysts tested over the temperature interval 78-64°K were small and varied within the limits 0-250 cal/mole. However, it was found that the decrease in the values of the rate constants with temperature takes place only down to the critical temperature of hydrogen. liquefaction of the hydrogen in the reactor was accompanied by a substantial increase in the rate constants, and this increase was so great that at a temperature of 21-22°K the rate constant usually became even greater than at 78°K. For illustrative purposes, the table presents ratios of these constants $k_{22°K}/k_{78°K}$.

As may be seen from the table, the ratio $k_{22°K}/k_{78°K}$ is different for various catalysts. It characterizes the change in the relative activity with temperature, which must be taken into account in practical applications of the catalysts.

The equilibrium concentration of parahydrogen depends on temperature. Therefore, provision of an isothermal process at the lowest possible temperature is an important condition for good operation of the catalyst in the liquid-phase reaction. Such a process can be provided by submerging the reactor and the condensation coil of the hydrogen liquifier, which precedes the reactor, in a liquid-hydrogen bath.

The liquified ordinary hydrogen from the condensation coil contains 75% orthohydrogen. Its conversion to parahydrogen involves the liberation of 235 cal/mole of hydrogen. Under these conditions, the absorption of heat from the reactor can be accomplished by taking advantage of the simultaneous operation of two factors—by taking maximum advantage of the heat of evaporation of the hydrogen and by providing the best possible heat exchange with the reactor. With an increase in pressure, the heat of evaporation of liquid hydrogen gradually decreases and becomes zero at the critical pressure (12.8 atm). However, a decrease in the pressure in the coil can be permitted only down to specific limits at which there is still retained a certain temperature gradient for heat transfer from the condensing hydrogen in the reactor to the boiling hydrogen in the liquefier bath. If a pressure of 0.8 atm is maintained in the liquefier bath, then these two conditions will best be realized at a pressure of 1.8-2.5 atm in the reactor.

SUMMARY

1. Catalysts were found for carrying out the conversion of orthohydrogen to parahydrogen in the liquid phase. The best catalysts for liquid-phase operation are chrome-nickel, $Mn(OH)_4$, $Fe(OH)_3$, and $Cr(OH)_3$.

2. It was shown that there is an increase in catalyst activity with a decrease in temperature to below the critical point.

3. A method for calculating the required amount of catalyst for a given productivity of the liquefier is recommended, and optimum conditions for operation of the reactor are discussed.

In conclusion, we desire to express our sincere appreciation to Corresponding Member of the Academy of Sciences USSR, G. N. Boreskov, for guidance in the course of the work.

LITERATURE CITED

1. R. A. Buyanov, Kinetika i Kataliz 1, 306 (1960).•
2. D. I. Vasil'ev and A. I. Shal'nikov, Pribory i Tekh. Eksp. 4, 106 (1958).

•Original Russian pagination. See C. B. translation.

AN ISOTOPIC STUDY OF THE SURFACE HETEROGENEITY OF OXIDE CATALYSTS FOR DECOMPOSITION OF ISOPROPYL ALCOHOL

I. CALCIUM OXIDE

O. V. Krylov and E. A. Fokina

Institute of Physical Chemistry, Academy of Sciences of the SSSR
Translated from Kinetika i Kataliz, Vol. 1, No. 3, pp. 421-430,
September-October, 1960
Original article submitted March 23, 1960

The decomposition of marked (with C^{14}) and unmarked isopropyl alcohol in the adsorption layer on calcium oxide, has been studied by the differential isotopic method and the isotopic exchange method with subsequent desorption. The differential isotopic method indicated a uniform isotopic composition of all the desorbed decomposition products of the alcohol. A study of molecular isotopic exchange between adsorbed iso-C_3H_7OH and iso-C_3H_7OH in the gas phase, and subsequent desorption of the alcohol, indicated the presence of three groups of active centers on calcium oxide: 1) centers which facilitate exchange of iso-C_3H_7OH, but are inactive in the decomposition reaction of alcohol, 2) centers which are catalytically active in the dehydrogenation reaction of alcohol and 3) centers on which exchange is difficult, but which are catalytically active in the dehydration reaction. It has been proposed that dehydration proceedes on active CaO centers which are associated with $CaCO_3$ impurity.

* * *

A few years age we carried out experiments on the adsorption of marked and unmarked molecules of phenol, cresol and aniline on a series of adsorbents having acidic and basic natures [1], and also on the adsorption of CO_2. A differential isotopic investigation by Keier and Roginskii [2] showed that in all cases, mixtures of molecules having different isotopic compositions, which had been adsorbed separately, had the same isotopic composition on desorption, i.e., the composition had been made uniform by the acid-base properties of the surface. It was of interest to examine this result for catalytic reactions.

There are numerous references in the literature to investigations of catalytic reactions of the acid type: cracking of hydrocarbons, dehydration of alcohols and HCOOH, isomerism, etc. One author pointed out the constancy of the unit surface activity of catalysts prepared by different methods [3-7], others have indicated surface heterogeneity [8-12].

Heterogeneity has been studied very little by direct methods. Keier [13] made a differential isotopic study of the decomposition of ethyl alcohol on ZnO and Al_2O_3. Fractions of alcohol of the same isotopic composition were adsorbed, and during desorption, both desorption products—CO_2 and ethylene, had the same isotopic composition, indicating surface homogeneity. Adsorbed alcohol undergoes complete exchange with alcohol from the gas phase at 20°. However, if the adsorbent (ZnO) is heated with a fraction of adsorbed alcohol and then cooled, and more alcohol of another isotopic composition is adsorbed, only part of the alcohol undergoes exchange and the isotopic composition of the fraction changes during desorption.

To establish the nature of the active surface of oxide catalysts we took the decomposition reaction of isopropyl alcohol in the adsorption layer, which we had studied earlier [14]. In contrast to the case of ethyl

TABLE 1

A Differential Isotopic Study of the Catalytic Decomposition of Isopropyl Alcohol in the Adsorption Layer on CaO.

No. of Expt.	Sequence of alcohol adsorption	% surface coverage of CaO	Dehydrogenation products		Dehydration products	
			%	mean activity, counts/min at 0.1 mm CO_2	%	mean activity counts/min at 0.1 mm CO_2
4	Marked-unmarked	5.03	56	3300	44	3450
5	Unmarked-marked	3.77	51.5	3720	48.5	3520
6	Marked-unmarked	4.32	48	3410	52	3390
7	Unmarked-marked	5.70	54	3170	46	2900

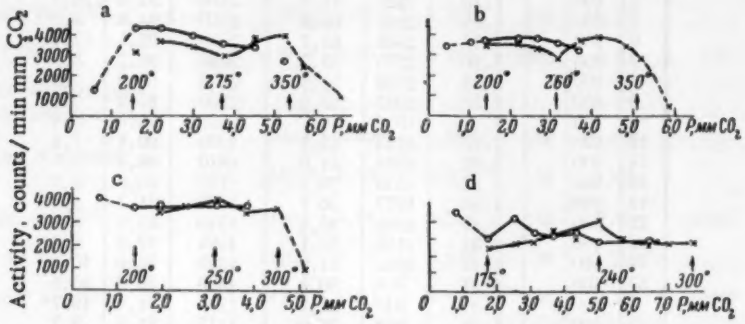

Fig. 1. Differential isotopic study of the decomposition of isopropyl alcohol on CaO. a,b) Adsorption sequence: marked alcohol-unmarked alcohol Expt. 4 and 6); c,d) adsorption sequence: unmarked alcohol-marked alcohol (Expt. 5 and 7.

alcohol, this reaction proceeds in the adsorption layer by two distinct routes: dehydrogenation, with the formation of acetone, and dehydration with the formation of propylene. Secondary products such as ether, CO_2, and CH_4 are hardly formed. It is often assumed [15] that dehydrogenation proceeds by an electronic mechanism, but it proceeds by an acid-base mechanism.

A typical acidic oxide Al_2O_3, a typical basic oxide CaO and a typical electronic semiconducter oxide ZnO were used for the investigation.

Differential Isotopic Study of the Decomposition of Alcohol on Calcium Oxide

The weighed quantity of calcium oxide was 3 g, the surface area 33 m^2/g and the adsorption temperature 150°. At this temperature the decomposition of isopropyl alcohol proceeds very slowly in the layer. The desorbed decomposition products of the alcohol were frozen out in special traps, which were cooled with solid normal propyl alcohol (mainly acetone and unreacted alcohol) and liquid nitrogen (propylene and "cracked" products). Each fraction was combusted and the activity of the CO_2 formed was determined spectroscopically.

Results of this study are given in Table 1.

Figure 1 a,b shows the results for Expts. 4 and 6, in which a fraction of marked alcohol was adsorbed first, and then ordinary, unmarked alcohol. Figure 1 c,d gives the results for Expts. 5 and 7, in which this adsorption sequence was reversed.

TABLE 2

A Study of Exchange Between Marked Isopropyl Alcohol Adsorbed on CaO, and Isopropyl Alcohol in the Gas Phase, with Subsequent Desorption (Expt. 10)

Operation	Duration of operation, min	Amt. of alcohol remaining on the surface, % of initial	Amt. of CO_2 in 159 cm^3 after combustion, mm Hg	Activity, counts/min at 0.1 mm CO_2	Total activity of material remaining on the surface % of initial	Specific activity on the surface at 0.1 mm CO_2	Percentage of exchange for equal distribution	Percentage of fraction not undergoing exchange
1	2	3	4	5	6	7	8	9
Adsorption at 30°		100		4414	100	4414	—	—
Exchange at 30°								
1	1	100	1,83	3973	92,7	4100	97,2	28,8
2	2	100	1,92	3609	85,8	3790	95,6	22,4
3	3	100	2,60	3458	76,0	3400	100	6,4
4	4	100	1,70	2920	71,7	3170	92,5	16,8
5	5	100	1,66	2805	66,8	2950	94,8	9,0
6	6	100	1,47	2566	63,2	2790	92,1	12,1
7	7	100	3,10	2275	55,7	2460	92,2	8,9
8	8	100	1,75	2192	52,3	2310	94,3	5,3
9	9	100	1,55	2083	49,8	2200	95,2	5,1
10	10	100	1,70	1952	46,7	2060	95,3	4,4
11	12	100	1,75	1733	43,7	1930	90,4	7,4
12	14	100	1,67	1594	41,0	1810	88,7	7,7
13	16	100	1,51	1538	38,7	1710	90,6	6,0
14	19	100	1,50	1477	36.7	1620	91,7	4,9
15	22	100	1,47	1264	34,4	1540	83,0	8,8
16	26	100	1,44	1196	33,1	1465	82,3	8,4
17	31	100	1,47	1043	31,6	1395	76,0	10,4
18	37	100	1,57	966	30,1	1330	73,8	10,5
19	5	100	2,57	849	27,9	1230	71,4	10,7
20	5	100	1,51	828	26,6	1175	71,7	9,7
21	10	100	1,32	779	25,4	1120	70,2	9,4
22	5	100	1,75	696	24,2	1070	66,3	10,0
23	10	100	1,75	654	23,1	1020	65,4	9,7
24	6	100	1,96	638	22,0	970	67,4	8,8
25	5	100	1,70	511	21,1	930	56,8	10,4
26	5	100	1,91	493	20,1	890	57,3	10,1
27	5	100	1,82	483	19,2	850	58,6	9,3
Desorption at 100	120	63,0	8,52	693	13,46	943	—	—
The same	90	58,2	1,085	626	12,78	968	—	—
" "	60	56,3	0,43	708	12,38	971	—	(5,05)
Adsorption	0,5	67,0	—	—	12,38	840	—	9,1
Exchange at 100°								
1	1	67,0	5,44	370	10,40	713	51,0	8,5
2	2	67,0	3,92	307	9,25	608	48,7	7,3
3	3	67,0	5,08	200	8,21	540	38,2	8,1
								(5,42)
4	5	67,0	5,82	159	7,29	480	35,4	7,6
Desorption at 100°	120	56,3	2,47	191	6,83	536	—	—
Desorption at 140°	120	36,3	4,60	309	5,43	658	—	—
	120	35,4	0,814	440	5,07	682	—	—
Desorption at 160°	30	23,5	2,23	439	4,11	785	—	(5,2)
Desorption at 190°	125	17,3	1,325	582	(3,34)	—	—	(3,67)
Dehydrogenation at 190°	125	14,4	0,680	781	2,82	868	—	—
Desorpt. and dehydrog. at 200°	180	13,4	0,217	430	(2,73)	—	—	—
Dehydration at 200°	180	11,9	0,350	702	2,49	923	—	—
Desorpt. and dehydrog. at 200°*	140	11,6	0,070	341	(2,46)	—	—	—
Dehydration at 200°*	140	10,43	0,264	977	2,21	935	—	(1,88)
Dehydrogenation at 250°	70	9,92	0,117	593	(2,15)	—	—	—
Dehydration at 250°	70	8,71	0,280	1141	1,83	929	—	—
Dehydrogenation at 275°	190	8,33	0,037	189	(1,81)	—	—	—

*As in original (Publisher's note).

TABLE 2 (Continued)

Operation	Duration of operation, min.	Amt. of alcohol remaining on the surface, % of initial	Amt. of CO_2 in 159 cm^3 after combustion, mm Hg	Activity, counts/min at 0.1 mm CO_2	Total activity of material remaining on the surface % of initial	Specific activity on the surface at 0.1 mm CO_2	Percentage of exchange for equal distribution	Percentage of exchange not undergoing exchange
1	2	3	4	5	6	7	8	9
Dehydration at 275°	190	7,51	0,189	1645	1,51	886	—	—
Dehydrogenation at 300°	180	6,88	0,145	231	(1,48)	—	—	—
Dehydration at 300°	180	6,23	0,151	2245	1,14	810	—	—
Dehydrogenation at 325°	60	5,47	0,176	100	(1,13)	—	—	(1,79)
Dehydration at 325°	60	4,95	0,117	2310	0,87	771	—	(0,83)
Reaction at 350° with formation of products, which were not frozen out	135	4,68	0,062	578	(0,83)	—	—	—
Dehydrogenation of residue at 350°	135	4,53	0,035	33	(0,83)	—	—	—
Dehydration etc., at 350°	135	3,44	0,249	145	0,80	(1020)	—	—
Cracking, etc. at 375°	120	3,37	0,015	36	(0,79)	—	—	—
Dehydration, etc. at 375°	120	3,30	0,155	256	0,75	(1035)	—	—
Cracking, etc. at 400°	60	2,07	0,280	20	(0,74)	—	—	—
Dehydration, etc. at 400°	60	1,32	0,176	647	0,63	(2100)	—	(0,56)
Residue		1,32			0,63			

As Table 1 and Fig. 1 show, the products of isopropyl alcohol decomposition in the adsorption layer have an approximately constant specific activity, the mean activities of the dehydration and dehydrogenation products being the same. Occasionally differences are found between the desorbed fractions. The first fraction, frozen out in solid n-propyl alcohol, always has an isotopic composition which approximates to that of the last fraction of alcohol adsorbed. In addition to containing acetone it also contains unreacted isopropyl alcohol. The last fraction, which contains a small fraction of the total alcohol adsorbed (46%), always has a reduced radioactivity which is independent of the adsorption sequence.

A possible reason for this phenomenon could be the unequal distribution of C^{14} in the C_3H_7OH molecules. Although we do not know the method of preparation of the marked alcohol, the C^{14} most probably enters the center of the molecule: $CH_3C^*HOHCH_3$. Then, during high temperature cracking of the alcohol, the CaO is either enriched with radioactive hydrocarbon or impoverished, and this determines the activity of the desorbed products. Another possible reason is dilution of the desorbing fraction with CO_2, which occurs in the catalyst. Special experiments on the adsorption of $C^{14}O_2$ showed that under these conditions it would only separate from CaO at temperatures above 350°. However, the fact that this decrease in activity of the desorbed fraction at high temperatures, is also found with other catalysts (Al_2O_3, ZnO), which do not have alkaline properties and do not entrap CO_2, makes the first reason more plausible.

It should also be noted that in the region of mean coverage in all four experiments, the radioactivity of the dehydrogenation products differs somewhat from the activity of the dehydration products. In Expts. 4 and 6, where marked alcohol was adsorbed first, a minimum was observed in the activity of the dehydration products desorbed at 260-275°; in Expts. 5 and 7, where unmarked alcohol was adsorbed first, there is a corresponding maximum for

the fraction desorbed at 240-260°. However, the data available is insufficient to decide whether this extreme reflects the actual catalytic properties of the surface or whether it is just coincidence.

Thus, a differential isotopic study of the decomposition of isopropyl alcohol on CaO does not give a clear answer to the question of the heterogeneity of the catalyst surface. It indicates this at very low percentage surface coverages, and we therefore turned to an isotopic exchange study of surface heterogeneity

A Study by Isotopic Exchange and Subsequent Desorption of the Surface Heterogeneity of Calcium Oxide

Isopropyl alcohol of one isotopic composition was adsorbed on the catalyst surface until adsorption saturation was reached, and then alcohol of a different composition was introduced into the system and its change in activity studied during the exchange process. Table 2 contains results for one such experiment involving exchange and subsequent desorption.

In all 0.071 m moles $C^{14}C_2H_7OH$ were adsorbed i.e., 17% of the CaO surface was covered, assuming the area of an isopropyl alcohol molecule to be 40 sq A^2 [16]. This was also the value taken for the 100% value in column 3 of the table.

The exchange process was studied at 30°, and 27 experiments of different durations (P = 2 mm) were carried out (col.2). Both the alcohol in the gas phase and the alcohol physically sorbed (chemisorbed with a small heat of adsorption) took part in exchange. The alcohol was then frozen out, combusted and tested for radioactivity. The amount of CO_2, formed during the combustion, in 159 cm^3, is given in column 4. The total amount of adsorbed alcohol would correspond to 23 mm CO_2 in the same volume.

We were not able to measure the kinetics of the isotopic exchange between adsorbed alcohol and alcohol from the gas phase under the experimental conditions. During the course of successive exchange processes the activity in the gas phase decreased (see column 5). This suggests that during exchange all the radioactivity is in an equilibrium distribution between the surface and the gas phase. Then, if it as assumed that the fraction of alcohol, which was introduced afterwards for the exchange process, is constant, the activity can be determined from the formula for a geometric progression

$$a = \frac{a_0}{(1+m)^n}, \tag{1}$$

where n is the number of exchange operations (see column 1), and α_0 is the initial activity. In our experiments $m_{cr} = 0.0737$. However, the curve calculated from this formula lies above the experimental points (Fig. 2). This suggests that there is a quantity of adsorbed alcohol, which does not participate in exchange. If we denote this fraction y, then

$$a = \frac{a_0(1-y)^n}{(1-y+m)^n}. \tag{2}$$

In order to test this assumption we calculated the specific activity of the alcohol remaining on the surface after each exchange (column 7) (the total residual activity for total coverage) and the percentage of exchange for equal distribution (column 8). It can be seen from Table 2 that the percentage of exchange for equal distribution, decreases systematically, but this is not due, however, to a gradual poisoning (lowering of the catalytic activity) of the surface, since interruptions of several days in the course of the experiments (between Expts. 5 and 6, 11 and 12, 18 and 19—see arrows on Fig. 2) did not result in any kind of change in the form of the curve.

It is impossible to calculate y from Eq. (2), since the experiment is not sufficiently accurate. Therefore, we calculated it from

$$y = \frac{a_{sur} - a_{ex}}{a_{in} - a_{ex}} \cdot 100\%, \tag{3}$$

where α_{sur} is the specific activity of the alcohol on the surface, α_{ex} is the specific activity of the alcohol remaining in the n'th experiment and α_{in} is the initial activity. The results of this calculation are given in the last column of the table, and it is easy to see that the higher the value of n, the more accurately y can be determined. If the radioactivity can be measured to ± 20 counts/min, then, in Expt. 1, y can be determined to ± 0.12 or about 100% of the determined value, and in Expt. 27 y can be determined to ±0.01 or about 10% of the

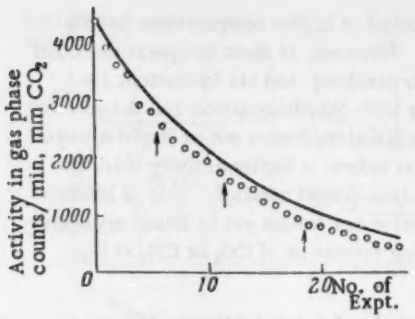

Fig. 2. Dependence of the radioactivity of isopropyl alcohol on the number of exchange operations between iso-C_3H_7OH on the CaO surface and iso-C_3H_7OH in the gas phase. Points—experimental results; line—theoretical curve for equidistribution.

determined value. Thus with increasing n the divergence of y decreases. The average value from 27 experiments is 9.7%, and if this value is substituted in Eq. (2), the curve obtained lies on the experimental points.

Thus, 9.7% of the total alcohol adsorbed does not participate in exchange. This should be apparent in the desorption kinetics, and during desorption the activity of the alcohol should increase with increasing temperature.

In fact at 100° (Table 2) the activity of the fraction being desorbed is already considerably higher than the activity of the last fraction of alcohol to undergo exchange. This indicates that desorption has begun at regions where the "nonexchanging" alcohol occurs (we will term this alcohol "firmly bound").

At 100° exchange proceeds in the same way as at 30°, i.e., a portion of alcohol on the surface (with an initial ac-

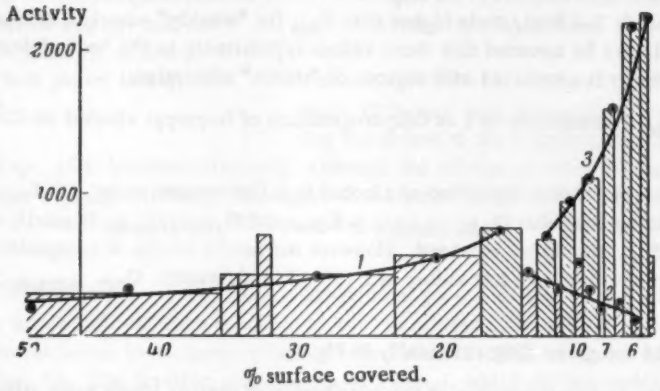

Fig. 3. Dependence of the radioactivity of the fraction being desorbed from CaO on the surface coverage, after partial exchange of marked alcohol with unmarked alcohol: 1) Desorption of iso-C_3H_7OH; 2) dehydrogenation; 3) dehydration.

tivity of 483 counts/min) can be completely exchanged, and another portion (with an activity of 4414 counts per min) hardly undergoes exchange at all. The fraction y of "nonexchanging" alcohol is about 8.1 to 5.42% of that initially sorbed. Separate experiments showed that no poisoning of the surface was observed, nor any acceleration of exchange with increased time of contact.

Further desorption at 140-190° proceeded at both kinds of centers (Table 2). There was a continuous increase in the activity of the alcohol being removed, i.e., a relative increase in the fraction of "firmly bound" alcohol during desorption. This amount of "firmly bound" alcohol, as a fraction of that initially adsorbed, is given in parenthesis in the last column of the table.

At 190° a catalytic reaction begins in the layer. As the radioactivity measurements show, the activity of the dehydrogenation fraction decreases somewhat, but the dehydration fraction increases systematically. This indicates that dehydrogenation proceeds preferentially on centers of "weak" adsorption, and dehydration on centers of "stable" adsorption. At 325° the dehydrogenation products possess an extremely low radioactivity (100 counts per min) and the dehydration products, a very high one (2210 counts/min).

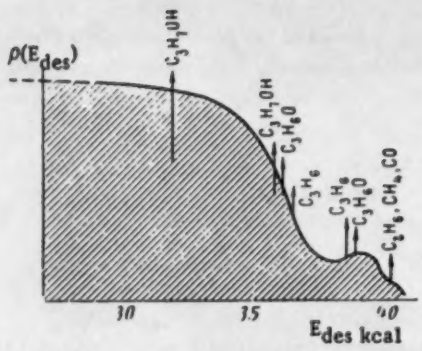

Fig. 4. Rough scheme of decomposition regions on CaO surface with respect to desorption activation energies of alcohol and its decomposition products.

Fractions desorbed at higher temperatures have a lower radioactivity. However, at these temperatures other reactions of alcohol: cracking and tar formation, etc., proceed side by side with dehydrogenation and dehydration on the surface. The fraction, frozen out in liquid nitrogen (dehydration), has, as before, a higher activity than the fraction, frozen out in n-propyl alcohol. It is of interest to note that the fraction not frozen out in liquid nitrogen was active, indicating formation of CO_2 or CH_4 at high temperatures.

From the formula of Polyani-Wigner [17]

$$u = \nu \cdot n_\alpha e^{-E/RT}, \qquad (4)$$

where u is the desorption rate for 1 cm^2 surface, n_α is the number of molecules adsorbed per cm^2 and $\nu = 10^{13}$ sec^{-1}, the desorption activation energy can be evaluated E_{des}. This evaluation shows that at 100° alcohol is desorbed with E_{des} of the order of 27-31, at 140° with E_{des} about 31-33, at 160° with E_{des} 33-35, and at 190-200° with E_{des} 35-37 kcal/mole. Calculation also shows that E_{des} for "stable" adsorbed alcohol is 3-4 kcal/mole higher than E_{des} for "weakly" adsorbed alcohol. Since adsorption proceeds very quickly, it can be assumed that these values approximate to the heat of desorption (Q_{des}). Some adsorption activation energy is associated with regions of "stable" adsorption.

The values for E_{des} approximate to E of dehydrogenation of isopropyl alcohol on CaO (32-36 kcal/mole at 180-200° [18]).

The activation energy for decomposition of alcohol in a flow system is $E_{flow} = E_{layer} - Q_{ads.\ alcohol} + Q_{ads.\ acetone}$. If it is assumed that $Q_{ads.\ alcohol} \sim E_{des.}$ and $Q_{ads.\ acetone}$ is small, very low values of E_{flow} ($E_{flow} = E_{layer} - E_{des}$) should be obtained. However our results for the decomposition of isopropyl alcohol in a flow system [19] do not give such low values of E (10-16 kcal/mole). $Q_{ads.\ acetone}$ probably has some effect on E_{flow}.

Results for Expt. 10 are given diagramatically in Fig. 3.

Figure 4 is a schematic representation of the distribution of regions which have different desorption activation energies. If $E_{des} \sim Q_{ads.}$, this diagram would also correspond to the distribution with respect to heats of adsorption. The relative lengths of the arrows correspond approximately to the relative discharge of desorption products and the decomposition of alcohol.

In order to save space, tables of results for the other experiments have not been given, but these results have been represented by graphs analogous to Fig. 3. Figure 5 contains the results of three consecutive experiments, carried out on the same sample of CaO; Expt. 10 (discussed in detail above, Fig. 3 and Table 2), and Expts. 11 and 12, carried out under similar conditions, i.e., with the following scheme: adsorption-exchange desorption-reacton. In Expt. 11 as in 10, the adsorbed marked alcohol underwent exchange with unmarked alcohol in the bulk phase, but in Expt. 12 unmarked alcohol, which was adsorbed on the CaO surface, underwent exchange with marked alcohol from the bulk phase. More unmarked alcohol underwent exchange than in Expt. 10 (48-65% of that initially adsorbed, instead of 5-11% as in Expt. 10). However, there were no substantial differences between the two experiments. As before, part of the alcohol on the surface does not participate in exchange (11-13% as opposed to 9.7%—the average figure for Expt. 10). Thus increasing the pressure of the alcohol by factors of 5-10, does not bring about a corresponding change in the nature of exchange.

It can be seen from Fig. 5 that the activity of the desorbed fraction increases during the desorption process (or decreases, as in Expt. 12, where unmarked alcohol was adsorbed initially). This indicates some surface heterogeneity. Dehydrogenation proceeds on centers, which have approximately the same activity as centers upon which the last fraction of alcohol to be desorbed was adsorbed. The activity of different sections of the dehydrogenation fraction is approximately the same, which suggests that the dehydrogenation of alcohol proceeds on a relatively

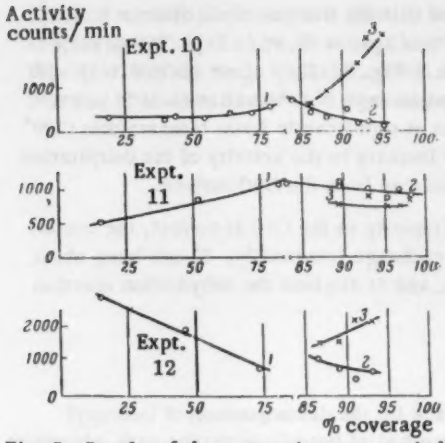

Fig. 5. Results of three experiments, carried out successively on the same CaO sample, on desorption and reaction in the layer after partial isotopic exchange of the isopropyl alcohol: 1) desorption; 2) dehydrogenation; 3) dehydration; in Expts. 10 and 11, marked alcohol on the surface underwent exchange with unmarked in the bulk phase; in Expt. 12 this order was reversed.

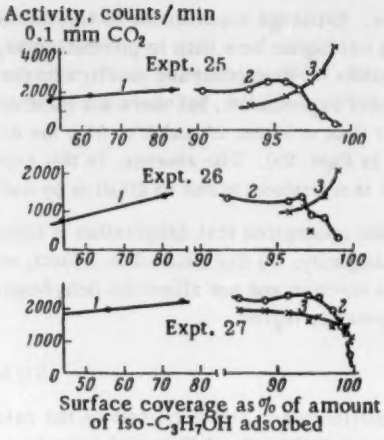

Fig. 6. Results of three experiments, on different CaO samples, on the desorption and reaction in the layer after partial isotopic exchange of the iso-C_3H_7OH: 1) desorption; 2) dehydrogenation; 3) dehydration.

uniform CaO surface. The dehydration products in Expt. 10 have a very high activity, which increases during the course of the reaction; in Expt. 12 it stays approximately constant, but in Expt. 11 it increases similarly, although the adsorption and exchange sequence is the reverse of that in 10. These experiments therefore, suggest a variation in the distribution of active centers on CaO during the course of the reaction. To test this conclusion we carried out additional experiments on fresh samples.

Figure 6 gives the results for three experiments. Experiment 25 was carried out on a fresh CaO sample, which had been heated in air at 800° and then in vacuo at 500° to remove CO_2 and H_2O. Marked alcohol was first adsorbed and was then subjected to exchange with unmarked alcohol. The exchange kinetics were approximately the same as in Expt. 10. The fraction of stable bound alcohol, which did not undergo exchange [calculated from Eq. (3)] was 12.3 ± 1.1% of the total amount adsorbed. The initial activity was 7500 counts/min at 0.1 mm CO_2; the average activity on the surface after exchange was 1820 counts/min. The activity of the fractions after desorption and reaction in the layer is given in Fig. 6. These experimental results agree qualitatively with those of Expt. 10 (see Fig. 5). The total amount of dehydrogenation products (5.11%) is approximately equal to the amount of dehydrogenation products in Expt. 10 (5.22%), but the amount of dehydration products is several times smaller (8.68% in Expt. 10 and 1.45% in Expt. 25). This makes our earlier assumption probable [19], that dehydration is brought about on CaO by $CaCO_3$ impurity. After careful treatment, $CaCO_3$ was removed from the CaO and the percentage of dehydration products of the alcohol decreased. Since the amount of $CaCO_3$ decreases during the course of the experiments when only one sample is used, the percentage of dehydration decreases and the distribution of active dehydration centers varies (see Expt. 10-12, Fig. 5).

In Expt. 26 (Fig. 6), 13.4 mm marked isopropyl alcohol and 4.64 mm unmarked alcohol were adsorbed on a freshly prepared CaO sample. This alcohol was then subjected to exchange with marked alcohol from the gas phase ("differential kinetic" method, first developed by Sinyak [20]). Then desorption and reaction in the adsorption layer were carried out, as in the previous experiments. As Fig. 6 shows, the picture obtained is similar to that for the preceeding experiments. Alcohol, adsorbed in the first few moments, i.e., with low E adsorption, undergoes exchange less readily and desorbs at higher temperatures than alcohol, which is adsorbed later. The dehydration reaction proceeds preferentially on these regions.

In Expt. 27, 6.6 mm CO_2 was adsorbed on freshly prepared CaO, corresponding to about 5% coverage. Then adsorption of marked isopropyl alcohol, exchange with unmarked alcohol, desorption and reaction in the

layer took place. Exchange experiments on this calcium oxide showed that the fraction of alcohol not undergoing exchange was higher here than in preceeding experiments; 16.7% as against 12.3% in Expt. 25 and 9.7% in Expt. 10. Results for desorption and reaction in the layer are shown in Fig. 6. They agree qualitatively with the results of other experiments, but there are some differences; the percentage of dehydration (5.75%) is considerably higher than in Expts. 25 and 26. Also the dehydration begins at significantly lower temperatures (200° instead of 280° in Expt. 25). The absence, in this experiment, of any increase in the activity of the dehydration fraction at high temperatures is due to dilution by carbon dioxide, produced from the CaO surface.

Thus, if the assumption that dehydration is linked with $CaCO_3$ impurity in the CaO is correct, the centers formed by this impurity: 1) link alcohol in a form, which undergoes exchange less readily, 2) can bring about the dehydration reaction and not affect the dehydrogenation reaction, and 3) displace the dehydration reaction to a lower temperature region.

SUMMARY

1. The distribution of active centers on the calcium oxide surface for the decomposition of isopropyl alcohol has been studied by the differential isotopic method and the method of isotopic exchange with subsequent desorption.

2. During the investigation of calcium oxide by the differential isotopic method, a constant specific radioactivity of all the desorbed decomposition products of isopropyl alcohol was observed.

3. During the isotopic exchange study of adsorbed iso-C_3H_7OH and iso-C_3H_7OH in the gas phase, two types of centers were observed on CaO: centers, on which alcohol underwent exchange almost instantaneously, and centers, on which alcohol hardly underwent exchange at low temperatures (30-100°).

4. After partial isotopic exchange the isotopic composition of isopropyl alcohol changes during the desorption process, indicating a heterogeneous catalytic surface.

5. Dehydrogenation and dehydration proceed on different active centers on CaO. The distribution of active dehydration centers changes during the course of the reaction. It has been proposed that dehydration proceeds on active centers of CaO, which are linked with the $CaCO_3$ impurity.

The authors would like to thank S. Z. Roginskii for his valuable advice.

LITERATURE CITED

1. O. V. Krylov and E. A. Fokina, Problems of Kinetics and Catalysis [in Russian] (Izd. AN SSSR, Moscow, 1957) Vol. 9, p. 304.
2. H. P. Keier and S. Z. Roginskii, Doklady Akad. Nauk SSSR 57, 157 (1947).
3. A. Kh. Bork and A. A. Tolstopyatova, Zhur. Fiz. Khim. 12, 227 (1937).
4. A. V. Frost and T. V. Antipina, Zhur. Fiz. Khim. 24, 860 (1950).
5. L. Kh. Freidlin and A. M. Levit, Zhur. Obshch. Khim. 21, 1255 (1951).*
6. P. A. Tesner, E. Ya. Robinovich, and T. D. Sneg'reva, Doklady Akad. Nauk SSSR 88, 95 (1953).
7. D. P. Dobychin and T. F. Tsellinskaya, Doklady Akad. Nauk SSSR 109, 351 (1956).*
8. M. M. Egorov, T. S. Egorova, V. F. Kiselev, and K. G. Krasil'nikov, Doklady Akad. Nauk SSSR 114, 579 (1957).*
9. K. G. Krasil'nikov, V. F. Kiselev, and E. A. Sysoev, Doklady Akad. Nauk SSSR 116, 940 (1957).*
10. T. S. Egorova, V. F. Kiselev, and K. G. Krasil'nikov, Doklady Akad. Nauk SSSR 123, 1059 (1958).*
11. K. V. Topchieva and I. F. Moskovskaya, Doklady Akad. Nauk SSSR 101, 517 (1955); 123, 891 (1958).*
12. A. A. Babushkin and A. V. Uvarov, Doklady Akad. Nauk SSSR 110, 581 (1956).*
13. N. P. Keier, Problems in Kinetics and Catalysis [in Russian] (Izd. Akad. Nauk SSSR, Moscow, 1955) Vol. 8, p. 224.
14. O. V. Krylov and E. A. Fokina, Izvest. Akad. Nauk SSSR, Otdel. Khim. Nauk 266 (1958).*
15. S. Z. Roginskii, Doklady Akad. Nauk SSSR 67, 97 (1949).
16. A. M. Rubinshtein, Yu. A. El'tekov, and K. M. Slovetskaya, Doklady Akad. Nauk SSSR 122, 86 (1958).*

*Original Russian pagination. See C. B. translation.

17. B. Trapnell, Chemisorption [Russian translation] (IL, Moscow, 1955).
18. O. V. Krylov and E. A. Fokina, Zhur. Fiz. Khim. 33, 2555 (1959).
19. O. V. Krylov, S. Z. Roginskii, and E. A. Fokina, Izvest. Akad. Nauk SSSR Otdel. Khim. Nauk 668 (1956).
20. Yu. E. Sinyak, Candidate's Dissertation Inst. Phys. Chem. [In Russian] (Izd. AN SSSR, 1960).

•Original Russian pagination. See C. B. translation.

MODIFYING OF CATALYSTS FOR HYDROCARBON OXIDATION*

É. Kh. Enikeev, O. V. Isaev and L. Ya. Margolis

Institute of Physical Chemistry, Academy of Science, USSR
Translated from Kinetika i Kataliz, Vol. 1, No. 3,
pp. 431-439 (1960)
Original article submitted April 6, 1960

We have determined the sign of the charge which the reactants and the products have in the oxidation of propylene on copper oxide and in that of ethylene on silver. A stage scheme for these processes has been specified. The work function of CuO and Ag modified by acceptor and donor admixtures has been measured. The oxidation of hydrocarbons on semiconductors and metals, which proceeds via a series of parallel and consecutive stages, is regulated differently (as depends upon the reaction mechanism) by the work function. The repression of complete oxidation at raised work function is a characteristic feature of this process.

• • •

Previously [1] it has been shown that the activation energy of oxygen chemisorption on modified zinc oxide and the rate of ammonia synthesis on modified iron are connected with the work function. The rates are determined by the activation energies (E) and the adsorption heats of the reactants (Q). The heat of adsorption is linked up with the work function by the relation:

$$Q = Q_0 + \Delta\varphi \qquad (1)$$

where Q_0 is the heat of adsorption on the original catalyst; $\Delta\varphi$ the change in work function, when admixtures are added to the catalyst.

According to Brønsted, the activation energy is coupled with the heat of adsorption by means of the relation $E = E_0 - \gamma Q$. The change in activation energy for a catalytic reaction depends upon the change in work function [2].

$$\Delta E = \alpha \Delta\varphi \qquad (2)$$

The work function depends upon admixtures introduced into the catalyst [3]. On the other hand, it is known for a long time [4] that the selectivity of hydrocarbon oxidation may be enhanced by modifying the oxidic contacts. For this reason it was of interest to investigate the relation between the work function of a modified catalyst and the rates and the activation energies of the main reactions: the formation of oxygen containing products (acrolein, ethylene oxide, acetaldehyde and so on) and carbon dioxide.

The Oxidation of Propylene into Acrolein on Cu_2O

On the semiconductor: cupric-cuprous oxide the oxidation of propylene into acrolein proceeds according to a parallel-consecutive scheme. By the oxidation a series of products is formed, namely, acrolein, carbon dioxide, water, traces of acetaldehyde and carbon monoxide.

The catalysts were prepared by impregnating the carrier (pumice, carborundum, etc.) with a copper nitrate solution followed by drying at 70-80° and firing at 600°. The admixtures were introduced into the catalyst by mixing the original solutions with nitrates of the corresponding metals and the SO_4^{2-} and Cl^- ions by adding ammonia sulfate and chloride.

* Laboratory worker S. M. Vilenkina took part in this research.

The catalysts were put into the reactor of a flow system and brought to a stationary activity by passing a gas mixture containing 40% propylene, 10% oxygen, and 50% nitrogen at atmospheric pressure. For each sample of copper oxide catalyst with admixtures the activation energy and the pre-exponential factor (k_0) of the acrolein and carbon dioxide formation were determined.

The work function was found from the difference in contact potential measured by the vibrating condensor method [5]. The modified samples in the form of powders were outgassed in vacuum at 400° until reproducible values of the contact potential were obtained. Under the conditions of the catalytic reaction the modified CuO samples were reduced to cuprous oxide. Pure CuO and Cu_2O differ little in work function. Therefore, upon modifying them the changes in φ are comparable.

On account of experimental data on oxygen and propylene adsorption and results obtained when investigating the nature of the intermediary products by an isotope method, a stage scheme has been proposed for the oxidation of propylene on semiconducting metal oxides [4, 6, 7]. For the oxidation of propylene into acrolein on a copper oxide catalyst this scheme may be presented in the following way: oxygen is adsorbed in the form of a molecular or atomic ion; propylene is adsorbed with its methyl group on the molecular oxygen ion without breaking the double bond and gives a hydroperoxide, which decomposes into acrolein and water. The adsorbed acrolein interacts with oxygen from the gas phase giving a charged intermediary complex, which decomposes into CO_2, H_2O and a hydrocarbon radical adsorbed on the surface. The latter reacts again with oxygen (chain reaction). As S. Z. Roginskii [8] has shown, such closed chains on the surface are characteristic for many catalytic processes. Propylene may also be adsorbed on the Cu_2O surface under breaking of the double bond and be converted into a radical, which reacts with an adsorbed oxygen ion. The intermediary complex formed by this reaction decomposes into CO_2, H_2O and a hydrocarbon radical with a smaller number of carbon and hydrogen atoms. Probably, just as in the oxidation of acrolein, a chain reaction takes place on the surface of the contact.

The surface of cuprous oxide is charged, when oxygen, propylene and acrolein are adsorbed. The change in work function caused by the adsorption enables us to determine the sign of the charge on the adsorbed molecules. As most of the organic substances, propylene and acrolein are electron donors on the Cu_2O surface and oxygen an acceptor. Water lowers insignificantly the work function and is also a donor. When the various gases and vapors are adsorbed on a Cu_2O surface, the following processes take place.

1. $O_2 + e \longrightarrow (O_2)^-$
2. $O + e \longrightarrow (O)^-$
3. $C_3H_6 - e \longrightarrow (C_3H_6)^+$
4. $CHO-CH=CH_2 - e \longrightarrow (C_3H_4O)^+$, (acrolein)
5. $H_2O - e \longrightarrow (H_2O)^+$.

These results allow us to specify the series of stages and to explain the character of the electron transitions in adsorption. Probably, the oxidation of propylene into acrolein on cuprous oxide proceeds according to the following scheme:

1a. $O_2 \rightleftarrows 2O$

1b. $O + e \longrightarrow (O)^-$,

2. $O_2 + e \longrightarrow (O_2)^-$,

3. $C_3H_6 + (O_2)^- \pm ne \longrightarrow (C_3H_5OOH)$ (charged complex 1),

4. $(C_3H_5OOH) \xrightarrow{\pm ne} (C_3H_4O)^+ + (H_2O)^+$,

5. $(C_3H_4O)^+ + e \longrightarrow C_3H_4O$ gas,

6. $(C_3H_4O)^+ \pm ne + O_2 \longrightarrow (C_3H_4O \cdot O_2)$ (charged complex 2),

7. $(C_3H_4O \cdot O_2)^+ \xrightarrow{ne} CO_2 + H_2O + (R_1H)^+$, etc.,

8. $(R_1H)^+ + O_2 \longrightarrow CO_2 + H_2O + (R_2H)^+$ etc.,

9. $C_3H_6 - e \longrightarrow (C_3H_6)^+$,

10. $(C_3H_6)^+ \pm ne + (O_2)^- \longrightarrow (C_3H_6 \cdot OO)$ (charged complex 3),

11. $(C_3H_6 \cdot OO)^{\pm} \xrightarrow{ne} (CH_2OO) + (R'H)$,

12. $(R'H) + O_2 \longrightarrow CO_2 + H_2O + (R''H)$ etc.

An investigation of the kinetics has shown that the oxidation rate of propylene into acrolein and carbon dioxide is proportional to the oxygen concentration in the gas phase [6]. On the modified catalysts the kinetic law has not changed.

Under the conditions of the process three main reactions take place:

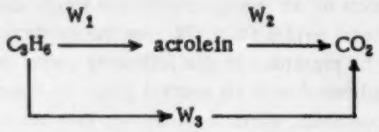

In first approximation, when neglecting the change in actual activation energy resulting from the surface charge, the rate of the acrolein formation may be represented by the following relation:

$$W_{acr} = W_1 = k_{01} C_{O_s} \exp\left(\frac{E_{01} + Q_0 - \Delta\varphi}{RT}\right), \tag{3}$$

where C_{O_s} is the surface concentration of oxygen; E_{01} the actual activation energy of acrolein formation; Q_0 the heat of oxygen adsorption on pure Cu_2O; the indexes 1,2,3 indicate which reaction of the scheme is meant.

The rate of CO_2 formation from acrolein and propylene is changed by the surface charge in a way which may be represented by the following equations:

$$W_2 = k_{02} C_{acr} \exp\left(-\frac{E_{02} + Q_2 + \Delta\varphi}{RT}\right). \tag{4}$$

$$W_3 = k_{03} C_{O_s} \exp\left(-\frac{E_{03} + Q_0 - \Delta\varphi}{RT}\right), \tag{5}$$

where Q_2 is the heat of acrolein adsorption on pure Cu_2O.

The way in which E_{0i} and k_{0i} depend upon $\Delta\varphi$ must be established experimentally.

TABLE 1

Activation Energies and Logarithms of the Pre-Exponential Factor for the Formation of Acrolein and CO_2 on Modified Copper Oxide.

Admixture to Cu_2O	Reaction giving				$\Delta\varphi$
	acrolein		carbon dioxide		
	E, kcal/mole	lg k_1	E, kcal/mole	lg k_0	
—	12	3,0	26	8,7	0
Fe_2O_3 2% at. Fe	15	4,0	24	8,0	—0,15
Cr_2O_3 2% at. Cr	18	5,0	20	7,0	—0,35
Li_2O 2% at. Li	22	4,0	16	5,0	—0,6
SO_4^{2-} 2% at. S	7	1,2	28	8,4	+0,25
Cl^- 2% at. Cl	10	2,5	27	8,5	—

In Table 1 are given the activation energies and the logarithms of the pre-exponential factor for the acrolein and CO_2 formation on Cu_2O to which chromic, iron or lithium oxide, SO_4^{2-} or Cl^- ions had been added.*

The activation of energies and k_0 for the CO_2 and acrolein formation change, when admixtures are introduced into the copper oxide. The work function is raised, when acceptor impurities (SO_4^{2-} and Cl^-) are added to copper oxide and is lowered, when the cations Cr, Fe, Li are introduced. In Fig. 1 the change in activation energy of the CO_2 and acrolein formation is plotted versus the change in work function of the modified copper oxide; for both properties pure copper oxide was taken as the reference point. An increase in work function lowers the activation energy of acrolein formation and raises that of carbon dioxide formation.

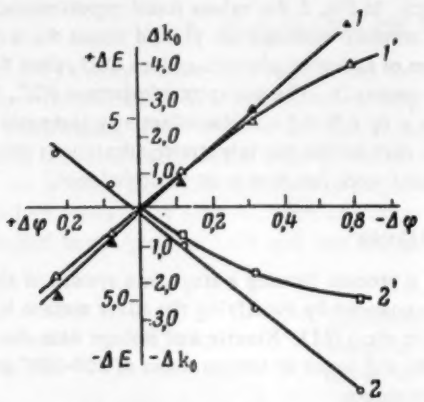

Fig. 1. The change in activation energy and logarithm of the pre-exponential factor for acrolein and carbon dioxide formation plotted versus the change in work function: acrolein—E (1), k_0 (1'); CO_2—E(2), k_0 (2').

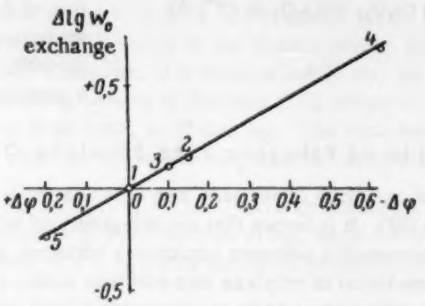

Fig. 2. The change in rate of oxygen isotope exchange on modified copper oxide plotted versus the change in work function: 1) CuO; 2) $CuO + Cr_2O_3$; 3) $CuO + Fe_2O_3$; 4) $CuO + Li_2O$; 5) $CuO + CuSO_4$.

The activation energies of acrolein and CO_2 formation change linearly with the work function

$$\Delta E_{acr} = \alpha' \Delta\varphi$$

$$\Delta E_{CO_2} = \alpha'' \Delta\varphi$$

In the oxidation of propylene on modified contacts, just as in other catalytic reactions, a compensation effect is found [9]. In Fig. 1 it is shown how k_0 depends upon the work function φ. For the formation of acrolein the activation energy E_{acr} increases at raised φ, but, in spite of that, W_1 becomes somewhat greater. Obviously, this is caused by the compensating influence of k_0 Experimental data on oxygen isotope exchange on modified copper oxide show that the exchange rate increases, when the work function is lowered and drops at raised φ (Fig. 2), in accordance with equation (4). This dependency indicates that the concentration of O_2 on the surface is regulated by the work function.

For the formation of CO_2 it is important how the rates W_2 and W_3 depend upon the surface potential. The rate (W_2) of CO_2 formation in the consecutive reaction is proportional to the acrolein concentration and must decrease as φ is raised. But the rate (W_3) of CO_2 formation directly from propylene in a parallel reaction bypassing acrolein is proportional to CO_2 and must increase as φ is raised. The experimental data (see Fig. 1) show that the activation energy E_{CO_2} is raised, when φ increases, and, consequently, the consecutive oxidation of acrolein determines the formation of CO_2. Previously it has been established by isotope methods [7] that on

* Introduced in the form of $(NH_4)_2SO_4$ or NH_4Cl.

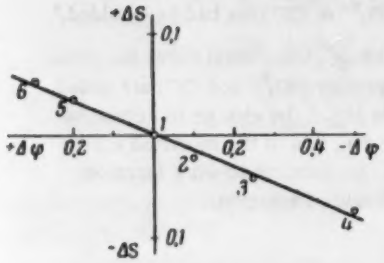

Fig. 3. The change in selectivity of propylene oxidation plotted versus the change in work function: 1) O; 2) Fe_2O_3; 3) Cr_2O_3; 4) Li_2O; 5) Cl^-; 6) SO_4^{2-}.

pure Cu_2O too carbon dioxide is mainly formed from acrolein. The fact that CO_2 formation is of first order with respect to oxygen, probably, results from the chain reactions taking place on the catalyst surface (see the scheme mentioned above).

The selectivity (S) of the process can be defined as the ratio between the rate W_1 and the sum of the rates W_1+W_2:

$$C = \frac{W_1}{W_1 + W_2}.$$

When φ is raised, the rate of acrolein formation increases and that of CO_2 formation drops. In Fig. 3 the values found experimentally for the selectivity of acrolein synthesis are plotted versus the work function. Introduction of acceptor admixtures into CuO raises S and that of donor ones decreases it. The acceptor admixtures (Cl^-, SO_4^{2-}) we have studied raise φ by 0.2-0.3 and the selectivity increases by 15-20%. To enhance still further the selectivity, admixtures giving a considerably increased work function must be introduced.

Oxidation of Ethylene into Ethylene Oxide on Silver

The oxidation of ethylene into ethylene oxide is typically a process forming a stage in a system of side reactions [10]. It is known that the selectivity of this process is enhanced by modifying the silver surface by various nonmetallic acceptor admixtures (chlorine, sulfur, fluorine etc.) [11]. Kinetic and isotope data show that the oxidation of ethylene into ethylene oxide, carbon dioxide and water at temperatures of 200-250° proceeds along two independent paths via nonisolated labil intermediary products:

$$C_2H_4 + O_2 \begin{cases} \nearrow x \rightarrow C_2H_4O \\ \searrow y \rightarrow CO_2 + H_2O. \end{cases}$$

According to data in literature [10], on a silver surface oxygen is adsorbed in the form of molecular and atomic ions. The adsorption of ethylene and the reaction products: ethylene oxide, CO_2 and water has been scarcely studied. Twigg [12], Trapnell [13] and others have shown that ethylene is not adsorbed on a reduced silver surface. On a silver surface covered with oxygen C_2H_4 is adsorbed irreversibly and the adsorption rate is described by the Roginskii-Zel'dovich' equation. Ethylene oxide in part is adsorbed reversibly (heat of adsorption about 10 kcal/mole). According to isotope data, strong adsorption of C_2H_4O gives rise to the formation of an organic layer on the surface [4]. The literature does not contain data on the sign of charge which the adsorbed gases (C_2H_4, C_2H_4O, CO_2 and H_2O) get on a silver surface. The change in work function found in our experiments when adsorbing these substances on silver showed that ethylene and ethylene oxide are electron donors and oxygen and CO_2 acceptors. Water gives a small lowering of φ. On the Ag surface the following reactions take place:

1. $C_2H_4 - e \longrightarrow (C_2H_4)^+$, 3. $CO_2 + e \longrightarrow (CO_2)^-$,

4. $C_2H_4O - e \longrightarrow (C_2H_4O)^+$, 4. $H_2O - e \longrightarrow (H_2O)^+$.

Carbon dioxide is adsorbed only on a surface covered with oxygen and, probably, forms a $(CO_3)^-$ complex. At temperatures of about 200-250° ethylene oxide on a silver surface partly decomposes into ethylene and adsorbed oxygen [12]. The changes in contact potential, found when adsorbing ethylene oxide at these temperatures, showed that the work function is raised.

Earlier, on account of kinetic and isotope data, a stage scheme had been proposed for the oxidation of ethylene into ethylene oxide [4]. Because the signs of the charges on the various components have been measured during the catalytic reaction and adsorption, the sequence of stages can be specified. The oxidation of ethylene into ethylene oxide can be represented by the following scheme:

1. $O_2 + e \longrightarrow (O_2)^-$,

2a. $O_2 \rightleftarrows 2O$,

2b. $O + e \longrightarrow (O)^-$,

3. $C_2H_4 - e \longrightarrow (C_2H_4)^+$,

4. $(O_2) + C_2H_4 \pm ne \longrightarrow (C_2H_4O_2)$ (charged complex 1),

5. $(O)^- + C_2H_4 \pm ne \longrightarrow (C_2H_4{\cdot}O)$ (charged complex 2).

5a. $(C_2H_4)^+ + (O_2)^- \pm ne \longrightarrow (C_2H_4O_2)$ (charged complex 3),

6. $(C_2H_4{\cdot}O_2)^+ \xrightarrow{ne} (C_2H_4O)^+ + (O)^-$,

7. $(C_2H_4O_2) + O_2 \xrightarrow{\pm ne} (CH_2O)^+ + (CO_2)^- + (H_2O)^+$,

8. $(C_2H_4{\cdot}O) + 2O_2 \xrightarrow{+ne} 2CO_2 + 2H_2O$.

Zimakov [14] and Lyubarskii [15] assume that the molecular oxygen ion is involved in the formation of ethylene oxide on silver and the atomic one in that of CO_2. The formation energies of these ions differ by 1.1 ev (more than 23 kcal/mole). From these data it can be supposed that the binding energy of the atomic oxygen ion to the surface is considerably higher than that of the molecular one. Therefore, it is more probable that the molecular O_2^- ion is involved in the formation of ethylene oxide. According to data of Kummer [16], adsorption of oxygen on silver raises φ by 0.25 ev, when the O_2 pressure is varied from 0.001 to 10 mm Hg. The work function we measured in air (pressure 1-70 mm Hg) changed by 0.3 ev, when the silver was outgassed in vacuum at 250°.

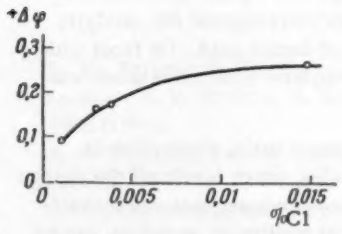

Fig. 4. Change in work function of silver by introducing chlorine.

Acceptor admixtures (Cl, I, S, Se, etc.) have an analogous influence upon φ. The change in work function of Ag, found when introducing various amounts of chlorine ions during its preparation is shown in Fig. 4.

A similar change in φ of silver catalyst was observed in the study [17] when introducing the nonmetals: chlorine, sulfur and phosphorus; the greatest increase in φ did not surpass 0.3 ev.

The fact that φ changes, when the reaction components of ethylene oxidation are adsorbed, shows that on the catalyst surface these substances occur in a charged state. Consequently, the adsorption heat of acceptor gases (O_2, CO_2) on modified silver samples is lowered and that of ethylene raised. According to equation (1), this change in heat may attain at most 7-8 kcal/mole (0.3 ev/molecule). So, the oxygen concentration is decreased on catalysts modified by nonmetals and that of ethylene increased. Actually, data on oxygen isotope exchange on silver samples modified by chlorine ions have shown [18] that upon raising the chlorine concentration in Ag (raising φ) the amount of O_2 on the surface decreases.

The kinetic data, as found in literature, are often conflicting [10]. The rates of C_2H_4O and CO_2 formation depend upon the oxygen and ethylene concentration but the order with respect to these components varies between zero and one. More often the exponents in the dependency of the rate upon the C_2H_4 and O_2 are found to be fractions. M. I. Temkin and coworkers [19] think that this diversity in the kinetic laws is caused by a different oxygen content in the layer adjacent to the surface.

The above mentioned dependency between the O_2 and C_2H_4 concentration on the catalyst surface and the change in φ, obviously, may explain the said differences in kinetics. Still more, it may be expected that upon introducing acceptor admixtures the reaction order with respect to oxygen is raised and that to ethylene is lowered. Corresponding experimental data are missing in literature and it is desirable to investigate experimentally the reaction kinetics on modified silver. The zero order with respect to oxygen, as found by Temkin and coworkers [19] for the formation of C_2H_4O and CO_2, obviously, can also be explained in the following way.

The work function is connected with admixed oxygen by $\Delta\varphi = \gamma \lg C_{O_2}$. Substituting "$\varphi$" this in equation (5) we obtain:

$$W_{C_2H_4O} = k_{01} C_{O_2} \exp\left\{\frac{E_{01} + Q_0 + \gamma \lg C_{O_2}}{RT}\right\} = k_{01} \frac{C_{O_2}}{C_{O_2}^{1}} \exp\left\{-\frac{E_{01} + Q_0}{RT}\right\},$$

at $\gamma = 1$ the reaction rate does not depend upon the oxygen concentration. The influence of the reaction products upon the kinetics must also be taken into account [19]. It is known that the formation of ethylene oxide is retarded by ethylene itself as well as by CO_2. We have measured the φ shifts caused by the adsorption of these substances on silver and they show that C_2H_4O at low temperatures is a donor and at high temperature an acceptor, while the shift of φ is much higher (0.15 ev) for C_2H_4O adsorption than it is (0.07 ev) for the adsorption of carbon dioxide. These effects cannot be explained satisfactorily by blocking of the surface. Water gives a very small lowering of φ at the reaction temperatures and, probably, only blocks some parts of the surface. When adsorbed the said substances influence the work function in an analogous way as do oxygen and nonmetal admixtures. Therefore, they must decrease the activity of the catalysts and enhance the selectivity. However, the influence of these products on the work function is smaller than that of nonmetal admixtures and, therefore, it is hardly possible to enhance notably the selectivity by admixing CO_2 to the reactant mixture.

Introduction of small amounts of sulfur results in an increased yield of ethylene oxide but upon raising further the sulfur concentration in Ag, poisoning is found, just as is the case for samples modified by chlorine [20]. We have not measured the work function of silver samples containing sulfur. However, it may be supposed that the activity maximum is determined by the ratio between ethylene and oxygen concentration. The reaction order with respect to ethylene will decrease, when the sulfur concentration is raised (increased φ) and that to oxygen increase. At a certain φ value the rate $W_1 = kC_{O_2}^{n} \cdot C_{C_2H_4}^{m}$ must be greatest at n=m. When chlorine is added to silver, an enhanced yield of ethylene is not found, which means that "pure" silver contains a certain amount of chlorine ions exceeding the optimum value.

As has been shown above, the activation energy is related to the work function φ.

In literature there are almost no data on the connection between φ and the activation energies and catalytic reaction rates on silver. From data of Haynes [21] the activation energy of N_2O decomposition on silver alloyed with various metals is found to be lowered, when φ increases. Sosnovsky [22] investigated the catalytic activity (E and k_0) on various faces of silver single crystals in the decomposition of formic acid. On faces with a higher index (lowered φ) E and k_0 increase. In the oxidation of ethylene into ethylene oxide no relation was found between φ and the reaction rate [23].

The activation energy for the oxidation of ethylene into ethylene oxide changes little, when silver is modified, since the increase in φ raises the surface concentration of donor molecules, which levels off the change in φ effected by the nonmetal admixtures. According to data in [10], the activation energies obtained by various authors differ only by 4 kcal/mole. The difference in reaction rate found upon modifying, probably, can be explained by the changed surface concentration of the reaction components.

The selectivity is defined by the following relation between the rates of C_2H_4O (W_1) and CO_2 (W_2) formation

$$C = \frac{W_1}{W_1 + W_2}.$$

The relation between the work function and the selectivity and the total acitivity is shown in Fig. 5. Upon raising the work function the activity of silver decreases and the selectivity increases.

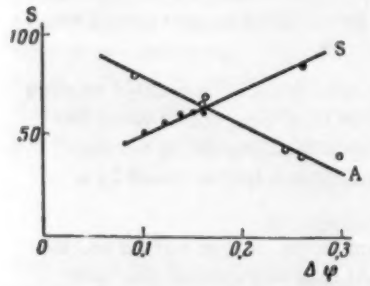

Fig. 5. The activity (A) and the selectivity (S) for the oxidation of ethylene into ethylene oxide plotted versus the change in work function.

The rates of the mild and the complete oxidation do not change equally with the work function.

W_1 is proportional to the 0.4-0.7 power of the oxygen concentration and W_2 is proportional to the 1.1 power. Therefore, W_1 and W_2 will be lowered in a different way, when the work function is raised. The higher the reaction order with respect to oxygen the more the rate is lowered upon changing φ. Therefore, raising φ results in an enhanced selectivity.

Thus, there has been revealed experimentally a relation between the work function and the catalyst activity and selectivity in the oxidation of unsaturated hydrocarbons.

The oxidation of hydrocarbons proceeds via a system of parallel and consecutive stages and is regulated differently (depending upon the reaction mechanism) by the work function.

The repression of the complete oxidation by raising the work function is a characteristic feature for the oxidation of propylene on the semiconductor Cu_2O and ethylene on the metal Ag. This relation, probably, may be explained by the fact that on different catalysts the reaction mechanism is nearly the same. Obviously, chain processes on the surface play a great role in the formation of CO_2.

The regularities found facilitate the choice of modifying admixtures, which will provide the optimum ratio between activity and selectivity.

SUMMARY

1. The work function of CuO and Ag modified by admixtures has been measured.

2. The sign of the charge on the reaction components or hydrocarbon oxidation (ethylene into ethylene oxide on silver and propylene into acrolein on copper oxide) has been determined.

3. A relation has been established between φ and the activation energies and the rates of acrolein, ethylene oxide and CO_2 formation.

4. It has been shown that the work function regulates the activity of oxidized catalysts and the selectivity in hydrocarbon oxidation.

5. By comparing the values of $\Delta\varphi$ with isotope and kinetic data a detailed mechanism could be proposed for these complicated catalytic processes.

LITERATURE CITED

1. E. Kh. Enikeev, L. Ya. Margolis and S. Z. Roginskii, Doklady Akad. Nauk SSSR, 131, 172 (1959); É. Kh. Enikeev, A. V. Krylova, A. Kuznetsov, S. S. Lachinov and S. Z. Roginskii, Doklady Akad. Nauk SSSR 131, 1126 (1960).
2. S. Z. Roginskii, Doklady Akad. Nauk SSSR 126, 817 (1959); F. F. Vol'kenshtein, Uspekh. Khim. 27, 1304 (1958).
3. É. Kh. Enikeev, L. Ya. Margolis and S. Z. Roginskii, Doklady Akad. Nauk SSSR 130, 807 (1960).
4. S. Z. Roginskii, Zhur. Fiz. Khim. 21, 1143 (1947); L. Ya. Margolis and O. M. Todes, Doklady Akad. Nauk SSSR 52, 519 (1946); L. Ya. Margolis, PhD Thesis [in Russian] (Institute of Physical Chemistry, Academy of Sciences USSR, Moscow, 1959).
5. V. F. Bogolyubov, Radiotekh. i Elecktron. 1, 557 (1957).
6. O. V. Isaev and L. Ya. Margolis, Kinetika i Kataliz, 1, 237 (1960).
7. O. V. Isaev, L. Ya. Margolis and I. S. Sazonova, Doklady Akad. Nauk SSSR, 129, 141 (1959).
8. S. Z. Roginskii, Collection: Problems in Kinetics and Catalysis, 10 [in Russian] (Moscow Acad. Sci. USSR Press, 1960).
9. E. Cremer, Adv. in Catal. 7, 152 (1955).
10. L. Ya. Margolis, Uspekh. Khim. 28, 615 (1959).
11. V. A. Pokrovskii, Uspekh. Khim. 25, 1446 (1956).
12. G. H. Twigg, Proc. Roy Soc. A188, 93, 113 (1946).
13. B. M. W. Trapnell, Chemisorption [Russian translation] (Moscow, IL, 1958).
14. P. V. Zimakov, Uspekh. Khim. 28, 1342 (1959).
15. G. D. Lyubarskii, Doklady Akad. Nauk SSSR, 110, 112 (1956).
16. J. T. Kummer, J. Phys. Chem. 63, 400 (1959).
17. J. N. Wilson, et al., Phys. Chem. 63, 463 (1959).
18. L. Ya. Margolis and V. A. Kiselev, Doklady Akad. Nauk SSSR 130, 1071 (1960).
19. A. I. Kurylenko, N. V. Kul'kova, N. A. Rybakova and M. I. Temkin, Zhur. Fiz. Khim. 32, 797, 1043 (1958).
20. A. I. Kurylenko, N. V. Kul'kova, V. I. Ostrovskii and M. I. Temkin, Doklady Akad. Nauk SSSR 123, 878 (1958).
21. K. E. Hayes, Canad. J. Chem., 37, 583 (1959).
22. H. M. C. Sosnovsky, Phys. Chem. Sol., 10, 304 (1959).
23. Ya. B. Gorokhovatskii, Collection: Problems in Kinetics and Catalysis 10 [in Russian] (Moscow Acad. Sci. USSR Press, 1960), p. 193.

DECOMPOSITION OF FORMIC ACID AND ESTERIFICATION OF ACETIC ACID IN THE VAPOR PHASE ON THE ION-EXCHANGE RESIN KU-2

T. I. Andrianova and B. P. Bruns

Institute of Physical Chemistry, Academy of Sciences, USSR
Translated from Kinetika i Kataliz, Vol. 1, No. 3,
pp. 440-446 (1960)
Original article submitted April 27, 1960

On the ion-exchange resin KU-2 the kinetics of two reactions in the vapor phase: decomposition of formic acid and esterification of acetic acid has been investigated. It has been established that this resin is stable up to 165-170°; at higher temperatures it decomposes and loses its catalytic activity.

Several kinetic regularities have been established for the course of these reactions on the sulfonated cation-exchanger. It has been shown that, under the conditions studied, the diffusion of the reacting substances has no effective influence on the kinetics of the reaction.

• • •

The first papers on the application of ion-exchange resins in organic catalysis were published between 1940 and 1950 [1-3].

At present many reactions are known to be catalyzed by ion-exchangers, which are typical catalysts of the acid-base type. Most of the processes described in the literature are carried out at low temperatures in solutions and only few of them in the vapor phase [4, 5]. Carrying out reactions in the vapor phase is limited to a certain extent by the instability of the contemporary ion-exchangers. The aim of the present study is to investigate two simple reactions on a sulfonated cation-exchanger: the decomposition of formic acid and the formation of esters from ethyl and n-butyl alcohols with acetic acid. As a catalyst we used the resin KU-2, which is a sulfonation product from the copolymer of styrene and divinylbenzene. The resin had a static specific exchange capacity (SEC) equal to 5 meq/g. The experiments were done in a flow type apparatus consisting of a vertical glass tube with a diameter of 12 mm and a height of 600 mm ending in a cooler and having a device to supply acid. On top of the tube a saturator was placed for the evaporation of the reactants and the heating of their vapors.

Decomposition of Formic Acid

The decomposition of formic acid on a sulfonated cation-exchanger proceeds according to the equation $HCOOH \rightarrow CO + H_2O$; CO_2 is not formed.

The first series of experiments was carried out at various feed rates of acid. The results obtained are given in table 1.

When calculating the contact time between the vapor and the resin from the rate of feeding vapor we used the volume occupied by the resin in the dry state. Thus, this value of the contact time is to a certain extent only a provisory one. The rate constant was determined by means of the formula for a first-order reaction:

$$k = \frac{1}{\tau} 2{,}3 \lg \frac{100}{100 - x},$$

TABLE 1

Kinetics of HCOOH Decomposition on the Resin KU-2 at 150° (Resin particle diameter 1-2 mm; weight of sample 7 g)

Contact time, τ, sec	Yield of CO, ml (STP)	Degree of HCOOH conversion, x, %	k, sec^{-1}
0,84	114	7,2	0,088
1,58	165	10,4	0,070
3,11	325	20,5	0,073
5,18	499	31,5	0,073
8,54	779	49,2	0,079

where τ is the contact time, sec; $\underline{x}$ the degree of acid conversion, %.

In the experiments given in Table 1 (and also in the other tables) we used an 85% solution of formic acid.

The data in Table 1 show that the decomposition of formic acid is a first-order reaction.

The cation-exchanger has no porosity in the usual sense of this term. During reactions in solution it swells and increases in volume. Here the SO_3H-groups it contains become accessible to the reacting molecules, which diffuse through the gel-like mass of the swollen cation-exchanger. It was of interest to reveal to which extent the total volume of the resin particle is used during the vapor phase reaction. For this purpose from the resin preparation KU-2 after it had been brought to the hydrogen form, dried and sieved over sieves with 0.25- and 1-mm meshes, two fractions were taken: one with particle size 1 mm and greater, the other 0.25 mm and less. The decomposition of formic acid was measured on both samples at 150°. From the results of these experiments, given in Table 2, it follows that the rates in both cases are nearly the same. This indicates that all SO_3H-groups of the resin are accessible to the reactants.

It was also determined how the rate depends upon temperature and the activation energy was calculated. The data obtained are given in Table 3 and in Fig. 1.

TABLE 2

Influence of Particle Size of KU-2 Resin upon the Reaction Rate

Reaction rate	KU-2 particle size	
	< 0.25 mm	> 1 mm
W, $\frac{\text{ml CO}}{\text{min-g KU-2}}$	25	20
k, sec^{-1}	0,118	0,089

As can be seen in Table 3 and Fig. 1, Arrhenius' equation describes the way in which the reaction rate depends upon temperature. The apparent activation energy calculated from these data is 25 kcal/mole. It should be remarked that the value obtained for the activation energy is an approximate one, since we had only three points in a small temperature range. This had its origin in the fact that the resin KU-2 begins to decompose at 180° and so we were limited by an upper bound of temperature. The lower bound of temperature was connected with the boiling point of the substance fed. Literature data [6] on the decomposition of formic acid can be used for a comparison. Depending upon the kind of glass used, in glass vessels this reaction proceeds in two directions:

$$HCOOH \rightarrow H_2O + CO,$$

$$HCOOH \rightarrow H_2 + CO_2.$$

The activation energy of the first reaction is 12 kcal/mole, that of the second 24.5 kcal/mole. When catalyzed by a sulfuric acid solution, the decomposition of formic acid gives CO and H_2O. The activation energy is a function of the H_2SO_4 concentration: in 97% H_2SO_4 E = 18.52 kcal/mole; in 91% H_2SO_4 E = 19.72 kcal/mole.

All previous experiments were done with seven g of resin. In the flow system the working conditions of the catalyst change along the length of the bed. Therefore, in order to find the initial rate, we carried out experiments with a smaller amount of resin. This allowed the conversion of the acid to diminish to 4-6% and the concentration of the products to become reduced in the mixture of reactants. By this the reaction rate is increased (Table 4).

As can be seen in the table, the reaction rate is greater at low conversion where the amount of water in the reactant mixture is small. To confirm this observation we have done experiments with formic acid containing various amounts of water (2-72 weight %). The results obtained are given in Table 5. As is obvious from Table 5, the mean reaction rate drops, when the H_2O content in formic acid increases. Here, upon going over from acid containing 2.55% water to acid containing 15% water the rate drops sharply, but after that a further increase in water content lowers the reaction rate approximately proportional to the decrease in the acid

TABLE 3

Influence of Temperature on the Decomposition Rate of HCOOH. (Particle size 0.25 mm, sample weight 7 g)

Temperature, t°	Amount of HCOOH fed, ml	τ, sec	Yield of CO, ml (STP)	x, %	k, sec^{-1}
134,5	3,2	2,85	185	11	0,042
150	3,1	2,69	423	27,2	0,118
167	3,2	2,20	888	56,0	0,379

TABLE 4

The Reaction Rate Constant of HCOOH Decomposition as a Function of the Amount of KU-2 Resin

Amount KU-2, g	τ, sec	x, %	k, sec^{-1}
6,30	3,8—4,5	32—41	0,12
3,69	3,6—4,5	33—36	0,10
0,38	0,21—0,26	4,6—6,4	0,25

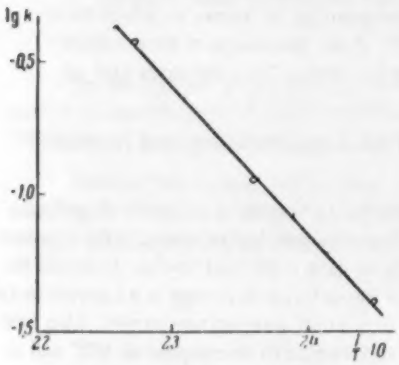

Fig. 1. The temperature dependence of the rate constant for formic acid decomposition in the vapor phase on the resin KU-2.

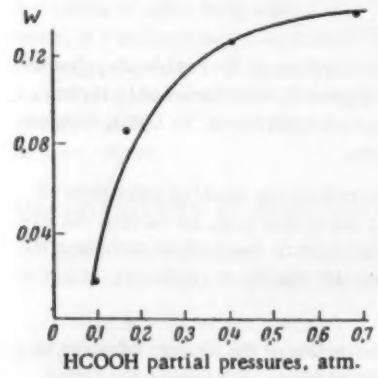

Fig. 2. Influence of the HCOOH partial pressure (in a mixture with nitrogen) upon the reaction rate.

partial pressure. This result is in accordance with those of the experiments carried out with various amounts of resin where the partial pressure of water in the mixture also varies.

To settle the question whether water vapor acts only as an inert diluent or has a retarding influence on the reaction rate we have done experiments in which water was replaced by nitrogen. The data obtained are shown in Fig. 2 and they indicate that a small dilution of formic acid vapor by nitrogen (up to 1 : 1) has a negligible influence upon the reaction rate, but a great dilution gives an approximately proportional lowering of the rate. So, the different way in which small additions of water and nitrogen act upon the rate of formic acid decomposition is connected with the retarding influence of water; this latter effect obviously is caused by the solvation of the functional groups in the resin and the resulting decrease in their acid strength. This conclusion is in agreement with the data given above on the catalyzing of the said reaction by sulfuric acid where a decrease in sulfuric acid concentration results in a lowered reaction rate and a raised activation energy. A certain analogy can be drawn between our results and data of N. M. Chirkov [7] on the polymerization of isobutylene under the action of sulfuric acid; this author has shown that the decrease in rate occurring when the partial pressure of water vapor over the catalyst is raised is connected with the lowered acid strength.

Formation of Esters

We attempted to use the cation-exchange resin KU-2 for investigating the kinetics of another vapor phase reaction, namely, the esterification of acetic acid with alcohols. At first we studied the esterification of acetic acid with ethyl alcohol. The experiments were done in the same apparatus as was used for formic acid decomposition. The first series of experiments was done at molar ratios of acid and alcohol varied between 2 and 0.12. The concentration of both components appeared to have influence upon the reaction rate. The reaction is described by the second order equation. The results obtained are shown in Table 6.

TABLE 5

The Influence Which the Water Content of Formic Acid has Upon the Rate of Decomposition at 150° (Amount of resin 2.7 g; particle size 1-2 mm)

H_2O content of the acid, weight, %	τ, sec	x, %	k, sec^{-1}
2,55	1,3	29	0,26
15,00	1,3	21	0,18
25,80	1,0	15	0,16
40,40	0,8	13	0,15
72,40	1,0	10	0,15

TABLE 6

The Influence Which the Molar Ratio Between Acetic Acid and Ethyl Alcohol has Upon the Rate of Esterification at 149°

Molar ratio $\frac{CH_3COOH}{C_2H_5OH}$	τ, sec.	x, %	W, $\frac{\text{gram acid}}{\text{sec·g KU-2}}$	k_1 (first order) sec^{-1}	k_2, (second order) liter $mole^{-1} sec^{-1}$
2:1	0,67	35,9	0,57	0,67	50
1:1	0,59	44,8	0,63	1,01	41
0,46:1	0,75	74,6	0,54	1,83	55
0,26:1	0,56	70,2	0,44	2,16	49

TABLE 7

Reaction Kinetics of Esterifying Acetic Acid with Ethyl Alcohol on the Resin KU-2 at 150° (Molar ratio CH_3COOH/C_2H_5OH = 0.12 : 1)

τ, sec	x, %	K, sec^{-1}	W, $\frac{\text{g acid}}{\text{sec·g KU-2}}$	τ, sec	x, %	K, sec^{-1}	W, $\frac{\text{g acid}}{\text{sec·g KU-2}}$
0,47	62,7	2,1	0,25	0,21	34,5	2,1	—
0,37	53,3	2,0	0,26	0,16	26,8	1,9	0,31

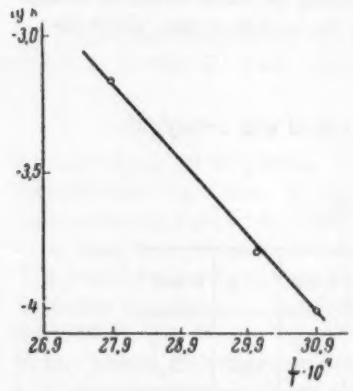

Fig. 3. The temperature dependence of the rate constant for the esterification of acetic acid with ethyl alcohol on the resin KU-2 in liquid phase.

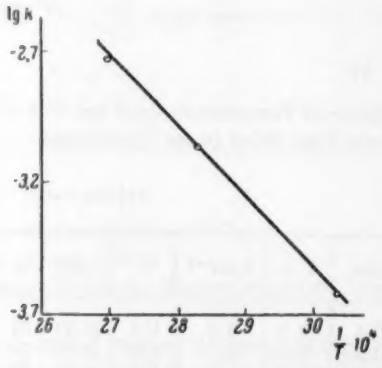

Fig. 4. The temperature dependence of the rate constant for the esterification of acetic acid with n-butyl alcohol on the resin KU-2 in liquid phase.

TABLE 8

The Influence of Temperature Upon the Rate of Esterifying Acetic Acid in the Vapor Phase with Ethyl Alcohol on the Resin KU-2

$t°$	τ, sec	x, %	k, sec^{-1}	$t°$	τ, sec	x, %	k, sec^{-1}	$t°$	τ, sec	x, %	k, sec^{-1}
134	0,41	84,3	4,5	146	0,43	73,9	3,1	171	0,23	36,8	2,0
135	0,30	72,6	4,4	146	0,26	57,6	3,3	170	0,28	34,5	1,5
				146	0,26	51,3	2,8	170,5	0,31	47,2	2,1
		average 4,4		146	0,23	49,1	2,9	170	0,18	32,8	2,2
				146	0,21	40,2	2,4	170,5	0,19	26,7	1,7
						average 2,9				average 1,9	

TABLE 9

The Influence of Temperature Upon the Rate of Esterifying Acetic Acid with Ethyl Alcohol on the Resin KU-2 in the Liquid Phase

$$\frac{CH_3COOH}{C_2H_5OH} = 0,12:1)$$

$t°$	τ, sec	x, %	$k \cdot 10^4$, sec^{-1}
51	600	5,7	1,0
60	600	9,4	1,6
85	600	33,5	6,8

When alcohol greatly exceeds the stoichiometric amount so that the change of its concentration during the reaction can be neglected, the reaction is satisfactorily described by the first order equation. Upon raising the time of contact by three times the rate constant practically does not change (Table 7).

We have also determined how the rate of esterifying acetic acid in mixtures containing excess ethyl alcohol depends upon temperature. As can be seen in Table 8, the first order rate constant decreases when the temperature is raised.

The apparent activation energy calculated from the temperature dependency of the reaction rate has a negative sign and is about -8.5 kcal/mole. Such a negative activation energy may be explained, as we propose, in the following way. Upon raising the temperature the amount of reactants sorbed by the resin decreases, which in-

TABLE 10

The Influence of Temperature Upon the Rate of Esterifying Acetic Acid with n-Butyl Alcohol on the Resin KU-2 in the Vapor Phase

(Molar ratio $\frac{CH_3COOH}{n\text{-}C_4H_9OH} = 0,15:1)$

$t°$	τ, sec	x, %	k, sec^{-1}	$t°$	τ, sec	x, %	k, sec^{-1}	$t°$	τ, sec	x, %	k, sec^{-1}
170	0,4	12,6	3,6	150	0,49	87,2	4,2	135	0,59	84,6	3,1
170	0,3	79,3	4,1	150	0,51	78,0	3,0	134,5	0,52	80,7	3,1
170	0,27	66,9	4,1	150	0,65	85,6	3,0				
170,5	0,30	60,6	3,1								
		average 3,7				average 3,4				average 3,1	

TABLE 11

The Influence of Temperature on the Rate of Esterifying Acetic Acid with n-Butyl Alcohol in Liquid Phase on the Resin KU-2

(Molar ratio $\frac{CH_3COOH}{n\text{-}C_4H_9OH} = 0,14:1$)

$t°$	τ, sec	x, %	$k \cdot 10^4$, sec^{-1}
58	615	13,8	2,4
81	605	41,7	8,8
97,5	600	67,3	18,7

evitably results in a lowered rate. Consequently, the activation energy observed will be smaller than the actual value. In the simplest case where the reaction rate in the solid phase is mainly determined by the amount of reactants, the difference between the apparent and the actual activation energy will be equal to the sorption heat of the reactant mixture on the cation-exchanger. To confirm this assumption we did a series of experiments in the liquid phase, which provided a practically constant concentration of the reaction components in the resin. When carrying out the reaction in the liquid phase in the presence of resin a positive temperature coefficient is found, as can be seen in Table 9 and Fig. 3.

Under these conditions the activation energy is 13 kcal/mole, which lies in the range of the values generally found, when similar reactions proceed in a homogeneous medium [8]. We have also done a series of experiments on the reaction between acetic acid and n-butyl alcohol on the same catalyst in the vapor phase. Just as in the case of ethyl alcohol, the reaction rate is very high: during a contact of a fraction of a second acid conversion attained 80%. At the same time the reaction rate, which was measured in the range 135-170°, appeared to depend little upon temperature. The apparent activation energy had the small positive value of about 1.6 kcal/mole. The data obtained are given in Table 10.

For a comparison we also investigated the esterification of acetic acid with n-butyl alcohol in liquid phase in the presence of the resin KU-2. In this case the reaction proceeds analogously to the esterification by ethyl alcohol, that is, the rate is nearly the same and the activation energy is 12 kcal/mole. The results of these experiments are shown in Table 11 and in Fig. 4.

The authors seize the opportunity for expressing their gratitude to S. Z. Roginskii for proposing the subject and his constant interest in the study.

SUMMARY

1. It is shown that the ion-exchanging resin KU-2 in the temperature region 135-170° can be used for the catalytic decomposition of formic acid and the esterification of acetic acid with alcohols in the vapor phase.

2. Some regularities for these reactions are established.

3. The kinetic characteristics of acetic acid esterification in the vapor and in the liquid phase on the cation-exchanging resin KU-2 are compared.

LITERATURE CITED

1. Dierichs Report, PB 866, Office of Technical Service, Dept. of Commerce, (Washington, 1945).
2. Sussman, Ind. Eng. Chem. 38, 1228 (1946).
3. Austerweil, Ind. Parf. 142 (1949).
4. L. M. Reed, L. A. Wenzel and J. B. O'Hara, Ind. Eng. Chem. 48, 205 (1956).
5. G. E. Hamilton and A. B. Metzner, Ind. Eng. Chem. 49, 836 (1957).
6. Technical Encyclopedia. Handbook of Physicochemical Values [in Russian] (Moscow, "Soviet Encyclopedia" Press, 1933), Vol. 10, pp. 299-308.
7. N. M. Chirkov, PhD Thesis [in Russian] (Institute of Chemical Physics, Academy of Sciences USSSR, 1957).
8. E. A. Moelwyn-Hughes, The Kinetics of Reactions in Solution [Russian translation] (Moscow, IL, 1938), p. 71.

SELECTIVE HYDROGENATION OF BUTYNEDIOL INTO BUTENEDIOL ON A NICKEL SKELETON CATALYST

L. Kh. Freidlin, A. A. Balandin, and I. F. Zhukova

N. D. Zelinskii Institute of Organic Chemistry, Academy of Sciences of the USSR
Translated from Kinetika i Kataliz, Vol. 1, No. 3, pp. 447-454,
September-October, 1960
Original article submitted April 28, 1960

The hydrogenation of butyne-2-diol-1,4 on a nickel skeleton catalyst has been studied. It is shown that in the adsorbed phase butenediol is displaced by butynediol. Therefore, the reaction proceeds step-wise. In the presence of pyridine it is stopped spontaneously in the stage of butenediol formation. In the process investigated both components—hydrogen and the compound to be hydrogenated—require an activation on the catalyst.

In water butynediol and butenediol are hydrogenated at a considerably lower rate than in alcohol.

The selective catalytic hydrogenation of butyne-2-diol-1,4 has been the subject of many investigations.

When hydrogenating on Pt-black in alcohol or ether, butynediol is converted quantitatively into butanediol [1].

On skeleton nickel the second mole of hydrogen is taken up faster than the first one. By stopping the reaction after one mole of hydrogen is consumed, butenediol can be obtained [2].

When hydrogenating under a pressure of 3 atm the yield of butenediol was 80% after a mole of hydrogen had been taken up [3].

When hydrogenating on a little active nickel skeleton catalyst which had been stored for along time (4.5 years) under alcohol, in the reaction products obtained after consuming a mole of hydrogen, were found 11% butanediol, 52% cis- and 14% trans butenediol, and 10% products of the dehydration side reaction [4].

On a Pd-$CaCO_3$ catalyst in methyl alcohol the rate also increases after a mole of hydrogen has been added. After half-hydrogenating, in the product, there was found about 80% butenediol [5, 6].

It has been established [7] that on a nickel skeleton catalyst at 100° and 50 atm the triple bond in hydrocarbons and esters of acetylenic acids is selectively hydrogenated to a double bond. However, upon hydrogenating butynediol on a nickel skeleton catalyst [8], the reaction does not stop at any temperature or pressure after a mole of hydrogen has been consumed. If it is interrupted, then the yield of butenediol attains 80%. When hydrogenating a 33% solution of butynediol in water at 50° and 100 atm on an iron catalyst obtained by decomposing iron carbonyl, the reaction also does not stop after a mole of hydrogen has been taken up.

On a nickel-copper catalyst used for the conversion of butynediol into butanediol selective hydrogenation of butynediol could not be accomplished [9]. In order to enhance the selectivity of catalysts in the hydrogenation of butynediol Reppe and co-workers [8] recommend to reduce the activity by various admixtures, to use weakly acidic carriers or to add 3-5% carbon monoxide to the hydrogen. For instance, when using Pt on charcoal 0.15% sodium biphosphate, 0.1% boric acid or 1.5% piperidine must be added. A cobalt catalyst is poisoned by 0.1% potassium thiocyanate.

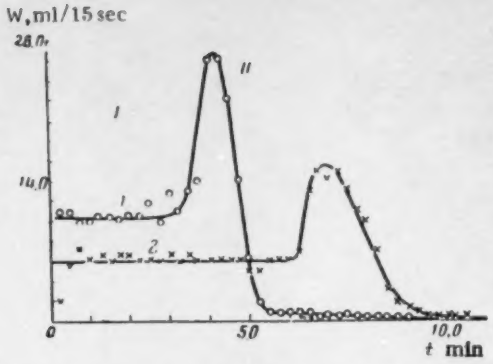

Fig. 1. Hydrogenation of butynediol: 1) in ethyl alcohol; 2) in dioxane.

Many other investigators also have used the method of half-hydrogenating for the purpose of obtaining ethylene compounds from acetylenic ones. The catalyst selectivity in this case is explained by the fact that the acetylenic compound expells the ethylenic one from the catalyst surface and is hydrogenated first. However, the ethylenic bond formed is also hydrogenated with a high rate, often higher than that for the original acetylenic compound. Therefore, the hydrogen consumption must be taken into account and watched during the course of the reaction in order to interrupt it at the right moment. Moreover, the selectivity can be upset after half-hydrogenation is completed, since then the concentration of the acetylenic compound strongly decreases and that of the ethylenic one grows.

More promising is the method of selectively hydrogenating in the presence of an alien reagent which is able to block the active catalyst surface and to depress the adsorption of the ethylenic compound. Under these conditions it is easier to control the reaction, since the surface which is partially set free by the lowering of the acetylenic compound concentration is covered by the alien reagent. It blocks the entire active surface, when the acetylenic compound is completely used up. In both cases the ethylene compound formed cannot be hydrogenated and in the reaction only one hydrogen molecule is consumed per $-C \equiv C-$bond.

In the present study the consecutive addition of hydrogen to the unsaturated bonds of butynediol and butenediol and the selective hydrogenationof butynediol on a nickel skeleton catalyst in the presence of pyridine were studied.

EXPERIMENTAL PART

The Consecutive Hydrogenation of the Unsaturated Bonds in Butynediol and Butenediol

We used an active nickel catalyst prepared by leaching out a Ni-Al alloy (1 : 1) during two hours at 100° with 20% solution of sodium hydroxide in water, rinsing with distilled water until the latter remained neutral; the catalyst was stored under water.

The experiments were carried out in a rocked vessel, which was stirred vigorously (700 one-sided strokes per minite). Each catalyst sample, 0.29 g, was used only once. The butynediol taken had a melting point 56-57°, and its boiling point at 7 mm was 137°. The products obtained in experiments carried out in the presence of pyridine with greater amounts of butynediol were fractionated in vacuum. After the solvent and the low boiling impurities (products of side reactions) had been distilled off, at 110-111° and 5 mm Hg, a constant boiling butenediol fraction with $n^{20}D$ 1.4770-1.4778 came over. According to data in literature [4, 10], the boiling point at 13 mm is 135° and $n^{20}D$ 1.4780. Upon hydrogenating samples of the butenediol obtained, the theoretical amount of hydrogen was consumed. By means of infrared spectrometry it was established that the half-hydrogenated product consisted of a mixture of cis- and trans-butenediol and a small amount of by-product. Butanediol was absent.

The conditions and the results of the experiments are given in Table 1. It can be seen from Table 1 that in ethyl and methyl alcohol at room temperature, and normal pressure butynediol is hydrogenated with a high rate into butanediol: 1.79-1.87 mole hydrogen, are taken up (Expt. 1-2). Curve 1 in Fig. 1 characterized the hydrogenation rate of butynediol in ethyl alcohol. Two sharply different regions can be distinguished in this curve: in the first it is horizontal (I) and in the second it has a maximum (II). The inflexion on the curve corresponds with the moment at which one mole hydrogen is consumed. This may be taken as an indication for the step-wise character of the hydrogenation on nickel: at first to butenediol and thereafter to butanediol. The rate in both stages is characterized by the half-period ($\tau/2$) of the reaction and that in stage I also by the rate of hydrogen consumption.

TABLE 1

Hydrogenation of Butynediol in Various Solvents

Expt. No.	Taken for the reaction: butynediol, g	Taken for the reaction: solvent, ml	Hydrogen consumption: theoretical, ml	Hydrogen consumption: found experimentally, ml	Hydrogen consumption: found experimentally, mole	Hydrogen consumption rate (W): for the first mole, ml/15 sec	for the first mole, τ/2, min	for the second mole, τ/2, min
1	0,5106	13 ethyl alcohol	266	248	1,87	10,9	1,7	1,0
2	0,5006	6 methyl alcohol	260	233	1,79	10,5	2,0	0,7
3	0,5206	10 dioxane	260	238	1,78	5,9	3,1	1,5

TABLE 2

Hydrogenation of Butynediol, Butenediol and Mixtures of Them

Expt. No.	Taken for the reaction: butynediol, g	Taken for the reaction: butenediol, g	Hydrogen consumption, ml: theoretical value for stage I	Hydrogen consumption, ml: theoretical value for stage II*	Hydrogen consumption, ml: found experimentally up to the inflexion point in kinetic curve	W, for the first mole: ml/15sec	W, for the first mole: τ/2, min	W, for the second mole, τ/2 min
4*	—	0,5336	—	135	—	—	—	1,7
5	0,5367	—	139	139	139	6,8	2,4	2,0
6	0,5323	0,5336	139	273	140	4,3	4,5	5,7**
7	—	1,0408	—	265	—	—	—	1,7
8	0,5021	—	131	131	126	7,4	2,4	1,3
9	0,5021	1,0416	131	396	131	6,3	3,0	3,0**

* Experiments 4-6 and 7-9 were done with two different samples of the Ni-catalyst.

** For the sum of the butenediols taken and formed.

Curve 2, which characterizes the rate of hydrogen addition to butynediol in dioxane, has a similar shape.

In this solvent the rate in both stages is about two times lower than in ethyl alcohol (Table 1, Expt. 3). Since the second stage proceeds at a higher rate than the first one, the observed consecutive addition of hydrogen to butynediol and butenediol, cannot be explained by the relative rates of these reactions.

Hydrogen of Butenediol Alone and in a Mixture With Butynediol

It was of interest to compare the hydrogenation rates of butenediol, butynediol (stage I) and a mixture of the diols. The experiments were carried out under the previously described conditions on 0.29 g nickel skeleton catalyst in 10 ml methyl alcohol. The results obtained are shown in Table 2 and Figs. 2 and 3. From Fig. 2 it is obvious that, under equal conditions, butenediol (curve 2, Expt. No. 4 actually is hydrogenated with a higher rate than does butynediol in stage I (horizontal part of curve 1, Expt. No. 5). From comparing the results of Expts. Nos. 5 and 6 (Fig. 2, curves 1 and 3) it follows that in the presence of butenediol, the hydrogenation rate of butynediol in stage I is lowered. An analogous result was obtained in the Expts. 7, 8 and 9 for other ratios between butynediol and butenediol (Fig. 3, curves 1-3). Butenediol is not able to expel butynediol from the catalyst, which fact is confirmed by the step-wise character of butynediol hydrogenation. Therefore, it may be supposed that the lowered rate in the first stage of butynediol hydrogenation, as is found when adding butenediol, results, because adsorbed hydrogen is expelled by the latter diol. So, in a mixture with butynediol, butenediol is not hydrogenated on nickel, but only occupies that part of the surface where hydrogen is activated.

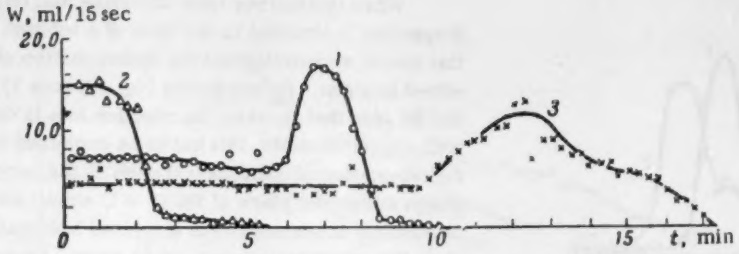

Fig. 2. The hydrogenation of 0.5 g butynediol (1), 0.5 g butenediol (2) and mixtures of them (3) in methyl alcohol.

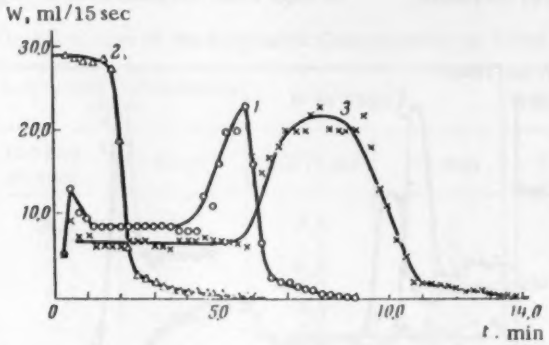

Fig. 3. The hydrogenation of 1.0 g butynediol (1), 0.5 g butenediol (2), and mixtures of them (3) in methyl alcohol.

Upon hydrogenating a mixture of butynediol and butenediol, of course, the concentration of the latter is raised, because the former is hydrogenated. By comparing the results of experiments 4 and 6, and also 7 and 9, it is obvious that by raising the final butenediol concentration in the alcohol solution from 5 to 10% or from 10 to 15% the half-period of the reaction increases from 1.7 to 5.7 min or from 1.7 to 3.0, respectively, that is, the rate drops. This also agrees with the assumption that adsorbed hydrogen is expelled by butenediol.

A calculation shows that upon hydrogenating mixtures with various butynediol-butenediol ratios the amount of hydrogen, which is consumed in the horizontal part of the curve corresponds to that required for hydrogenating the weight of butynediol in the butenediol taken for the reaction (6 and 9). The hydrogen volume consumed in the region with the maximum closely corresponds to the sum of the amounts required for hydrogenating the butenediol taken for the reaction and that formed from butynediol. So, the triple bond of butynediol is hydrogenated first even in the presence of an equal (Expt. 6) or two times greater (Expt. 9) amount of butenediol. These data confirm the results which indicate that in the adsorbed phase butenediol is expelled by butynediol.

Curves, which characterize the influence of butanediol (0.5 g) upon the hydrogenation rate of 0.5 g of butynediol, are shown in Fig.4. As is obvious from the graph, the reaction rate is also somewhat lowered in the presence of butanediol (curve 2).

The Influence Which Water and the Concentration of the Component to be Hydrated Have Upon the Reaction Rate

When studying the influence of the butynediol concentration in alcohol, we found that, if it is lowered from 26.6 to 10.7 or 5.4% (Fig. 5, curves 1-3, Expts. 10-12, Table 3), the reaction rate in both stages does not decrease, as might be expected, but increases. Probably, this can be explained by the fact the expulsion of adsorbed hydrogen is greater, when the diol concentration is raised: in stage I this is effected by butynediol and in stage II by butenediol. When the solution is diluted still more, the reaction rate practically does not change (Fig. 5, curves 4 and 5, Expts. 13-14, Table 3).

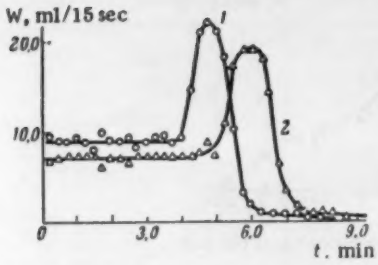

Fig. 4. Influence of butanediol upon the hydrogenation rate of butynediol
1) butynediol; 2) a mixture of butynediol and butanediol.

When synthesized from acetylene and formaldehyde butynediol is obtained in the form of a solution in water. For this reason we investigated the hydrogenation of butynediol dissolved in water. By comparing Fig. 1 (curve 1) with Fig. 6, it can be seen that in water the reaction rate is sharply lowered in both stages. Possibly, this has to be explained by a change in the orientation of the different parts in the butynediol (the OH-groups taking the place of the C ≡ C atoms) and also by an insufficient concentration of activated hydrogen on the catalyst, when the reaction is carried out in water. Upon raising the concentration of the compound to be hydrogenated, the reaction rate in water is also lowered (Table 3). In the experiment with a butynediol concentration of 10.3%, the reaction rate is small in stage I and the maximum in stage II is hardly visible (Fig. 6,

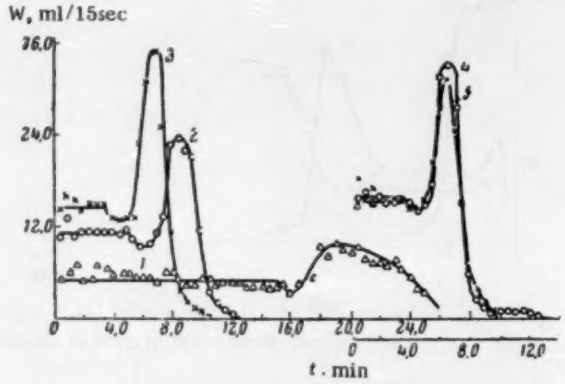

Fig. 5. The hydrogenation rate of butynediol in methyl alcohol as a function of its concentration, in %: 1) 26.6; 2) 10.7; 3) 5.4; 4) 2.7; 5) 1.8.

curve 1, Expt. 15). In more diluted solutions (5.2 and 1.7%) the reaction rate increases, while in stage II the maximum is developed clearly (Fig. 6, curves 2 and 3, Expts. 16 and 17).

The results obtained enable us to discuss in more detail the complicated character of the kinetic curves for the hydrogenation of butynediol. Obviously the shape of the kinetic curves for butenediol hydrogenation is very similar to that part of the kinetic curve for butynediol hydrogenation, where the maximum is found and which part is characteristic for the consumption of the second mole of hydrogen (Figs. 2 and 3). This confirms the correctness of the interpretation given above for the two parts of the kinetic curve for butynediol hydrogenation.

Butynediol is able to displace hydrogen from the catalyst surface. This just explains the lowering in the hydrogenation rate in stage I found upon increasing the concentration above 2.7%. However, as butynediol is consumed in the course of the hydrogenation, the reaction rate in stage I does not increase (the kinetic curve in this region is parallel to the abscissa). Obviously, the catalyst surface freed from butynediol in that region is occupied by the butenediol formed. Therefore, the amount of active hydrogen on the catalyst is not raised and the reaction rate does not increase.

Hydrogenation of Butynediol in the Presence of Pyridine

Previously it has been shown that on nickel in the presence of pyridine an acetylenic bond is selectively hydrogenated to an ethylenic one [11]. It was of interest to examine whether it is possible to hydrogenate selectively butynediol under similar conditions. In the series of experiments carried out for this purpose, the catalyst rinsed with alcohol was saturated with hydrogen, shaken in a mixture of alcohol and pyridine, and then

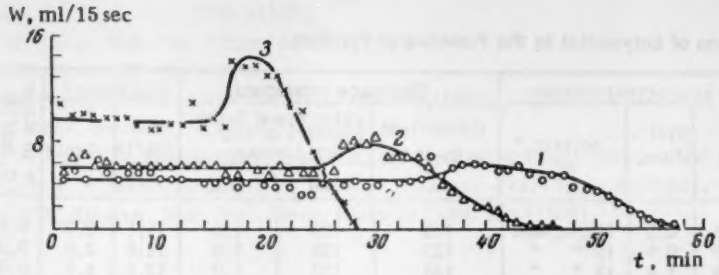

Fig. 6. The hydrogenation rate of butynediol in water as a function of its concentration, in %: 1) 10.3; 2) 5.15; 3) 1.7.

TABLE 3

The Hydrogenation Rate as a Function of the Butynediol Concentration in Water and Alcohol

Expt. No.	Weight of butynediol, g	Butynediol concentration in ml		W in stage I		W in stage II
		in ethyl alcohol	in water	ml/15 sec	$\tau/2$ min	$\tau/2$ min
10	0,5323	26,6	—	3,0	7,5	6,0
11	0,5367	10,7	—	5,4	3,6	2,0
12	0,5367	5,4	—	6,8	2,7	1,5
13	0,5367	3,5	—	7,0	2,5	1,4
14	0,5367	2,7	—	7,4	2,5	1,5
15	0,5147	—	10,3	1,1	16,7	15,5
16	0,5147	—	5,2	1,5	13,2	8,7
17	0,5147	—	1,7	2,5	7,7	5,5

the sample of butynediol in alcohol was added after which the hydrogenation was started. It turned out that, if small pyridine concentrations were used, only one mole of hydrogen was consumed. The entire part of the curve (above) where a maximum was found (stage II) has disappeared, while in stage I the rate of hydrogen consumption is not lowered, but even somewhat increased (Fig. 7; Table 4, Expts. 18-21).

The fact that treating the catalyst with pyridine has a very different influence on the addition rate for the first mole of hydrogen, in comparison with that for the second mole, also proves that on a nickel catalyst butynediol is hydrogenated in two consecutive stages. Pyridine when taken in a small concentration does not lower the rate of hydrogen addition to the triple bond of butynediol, but completely suppresses the hydrogenation of the double bond in the butenediol formed. Since at small pyridine concentrations the reaction rate in stage I is not decreased, it has to be considered that, under these conditions, neither butynediol nor hydrogen is displaced by pyridine from the catalyst surface. Therefore, the fact that the reaction proceeds selectively and the stage II is suppressed, may be explained by the adsorptive expulsion of the butenediol formed effected by the pyridine. The adsorption equilibrium is established rapidly, for if the duration of the preliminary treatment with pyridine is shortened from one hour (Expt. 20) to 20 min (Expt. 19) or ten minutes (Expt. 18), the amount of hydrogen consumed does not increase. Upon raising the pyridine concentration in the alcohol (Expt. 22) or in pure pyridine (Expt. 23), the consumption of the first mole of hydrogen is even retarded. This fact indicates that butynediol and, possibly, also hydrogen in the adsorbed phase is displaced by pyridine at higher concentrations of the latter.

When our first communication was in the press [12] and the present paper was being prepared for publication, an investigation of Fukuda and Kusama appeared [13], in which the selective hydrogenation of butynediol in water (concentration 1.7%) using Pd on carrier catalysts was also studied in the presence of catalytic poisons. On all Pd-catalysts stage II proceeds at a higher rate than does stage I, especially on Pd-$CaCO_3$ and Pd-charcoal. Just as on a nickel catalyst, on Pd the rate in stage I was found to be lowered, when the butynediol concentration was raised, which, in our opinion, points out that adsorbed hydrogen is displaced by butynediol. Upon poisoning

TABLE 4

Hydrogenation of Butynediol in the Presence of Pyridine

Expt. No.	Taken as reactant mixture: butynediol, g	pyridine, ml	solvent,* ml	Hydrogen consumed: theoretical value,** ml	value found from region I of the kinetic curve: ml	mole	W in stage I: ml/15 sec	τ/2 min	W in stage II, ml/15 sec
18	0,5095	0,5	13 eth. alc.	133	133	1,0	11,1	2,0	0,3
19	0,5095	0,5	13 " "	133	133	1,0	11,5	2,0	0,3
20	0,5114	1,0	13 " "	133	133	1,0	12,8	1,7	0,3
21	0,5006	0,5	6 m. alc.	130	130	1,0	7,2	2,7	0,3
22	0,5006	5,0	6 " "	130	130	1,0	3,1	6,1	0,0
23	0,5075	5,0	Pyridine	132	142	1,1	3,1	6,0	0,0

* eth. alc. – ethyl alcohol; m. alc. – methyl alcohol.
** Calculated for half-hydrogenation.

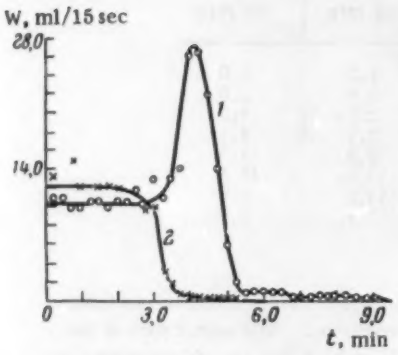

Fig. 7. Hydrogenation of butynediol: 1) in ethyl alcohol; 2) in ethyl alcohol in the presence of pyridine.

the Pd-$CaCO_3$ catalyst by lead acetate its activity in the hydrogenation of butynediol as well as that of butenediol is lowered almost at the same extent, but the latter is not completely suppressed. It is evident that on this catalyst selective hydrogenation of butynediol cannot be achieved. In the presence of quinoline the hydrogenation rate of butynediol in stage I is lowered little, but that in stage II is decreased sharply. When pyridine or piperidine are present, the opposite effect is found: the hydrogenation rate is depressed in stage I, but does not change in stage II.

SUMMARY

1. It has been found that on a nickel skeleton catalyst butyne-2-diol-1,4 is hydrogenated step-wise: at first to butene-2-diol-1,4 and then to butanediol-1,4, while the second stage proceeds at a higher rate than the first one. The step-wise character of the process results, because in the adsorbed phase the butenediol formed is displaced by butynediol.

2. When pyridine is present, butynediol is hydrogenated selectively to butenediol: after the first mole of hydrogen has been consumed, the reaction stops spontaneously. The selectivity is explained by the fact that in the adsorbed phase butenediol is displaced by pyridine.

3. When dissolved in water butynediol is hydrogenated 5-10 times more slowly than in an alcoholic solution.

4. Upon raising the butynediol or butenediol concentration the hydrogenation rate is lowered, which indicates that adsorbed hydrogen is displaced by the diols. So, for both components of the reaction studied, that is, for the compound to be hydrogenated and for hydrogen, an activation on the catalyst is required.

5. The results obtained allowus to propose that in the presence of butynediol the butenediol formed by the hydrogenation is adsorbed on the catalyst surface under displacement of hydrogen, but is not hydrogenated.

LITERATURE CITED

1. M. Lespieau, Compt. rend. 150, 1761 (1910).
2. A. Valette, Ann. Chim. 3, 644 (1948).
3. C. S. Marvel and Ch. H. Young, J. Amer. Chem. Soc. 73, 1066 (1951).
4. R. Romanet, Compt. rend. 236, 1044, 1176 (1953).

5. I. N. Nazarov, et. al., Zhur. Obshch. Khim. 28, 1132 (1958).*
6. A. W. Johnson, J. Chem. Soc. 1009, (1946).
7. R. Paul and G. Hilly, Bull. Soc. Chim. 6, 218 (1939).
8. W. Reppe, Lieb. Ann. 596, 39 (1955).
9. Acetylene Chemistry [Russian translation] (IL, Moscow, 1954) p. 280.
10. D. O. Curme and F. Johnston, "Clycols", (New York, 1953).
11. L. Kh. Freidlin and B. D. Polkovnikov, Izvest. Akad. Nauk SSSR Otdel. Khim. Nauk 1052 (1956).*
12. L. Kh. Freidlin, A. A. Balandin and I F. Zhukova, Doklady Akad. Nauk SSSR 124, 598 (1959).*
13. T. Fukuda and T. Kusama, Bull. Soc. Chim. Japan 31, 339, 343 (1958).

*Original Russian pagination. See C. B. translation.

INVESTIGATION OF THE ADSORPTION CHARACTERISTICS OF CHROMIA – ALUMINA – POTASSIUM PARAFFIN DEHYDROGENATION CATALYSTS

A. M. Rubinshtein, K. I. Slovetskaya, and T. R. Brueva

N. D. Zelinskii Institute of Organic Chemistry, Academy of Sciences of the USSR
Translated from Kinetika i Kataliz. Vol. 1, No. 3, pp. 455-463,
September-October, 1960
Original article submitted May 13, 1960

This article presents the results of an investigation of the adsorption of isopentane, water, and isopropyl alcohol at various temperatures on a catalyst consisting of 84.6 wt. % Al_2O_3, 13% Cr_2O_3, and 2.4% K_2O. An increase in the chemisorption of isopentane with an increase in temperature was observed over the range of 205 to 325°. Very appreciable chemisorption of isopropyl alcohol occurred at temperatures close to room temperature. The relationship between physical adsorption and chemisorption of water is considered.

The study of the adsorption characteristics of solid catalysts is of undoubted interest in connection with questions on the kinetics and the mechanism of heterogeneously catalyzed reactions. Of particular interest is the activated adsorption of water and hydrocarbons—substances which take part in many practically important reactions—and also of alcohols, since such compounds are used not only in catalytic reactions, but also as adsorbates in the determination of the texture of catalysts. Because of their practical significance, chromia—alumina catalysts for the dehydrogenation and dehydrocyclization of paraffins, particularly those promoted with K_2O, are suitable objects for studies of adsorption characteristics.

There has been very little study of the adsorption characteristics of these catalysts, and this is particularly true of the selective adsorption of the vapors of various substances. Those investigations which have been carried out have chiefly concerned the adsorption of H_2, O_2, CO, and CO_2 on Cr_2O_3, $Cr_2O_3 - ZnO$ and $Cr_2O_3 - Al_2O_3$ [1-9], and two forms of the chemisorption of H_2 and CO have been observed: a low-temperature, reversible adsorption probably taking place at the metal ions and a high-temperature irreversible adsorption which has been considered to be chemisorption at the oxygen ions. In the latter case, the H_2 and CO can be removed from the catalyst surface only at high temperatures and only in the form of H_2O and CO_2, respectively [10]. It has been shown that the adsorption of O_2 on Cr_2O_3 decreases with an increase in temperature over the range –100 to +100°; it then begins to increase, and it becomes irreversible at higher temperatures [4-7]. The chemisorbed oxygen can be removed only by reduction or, as our experiments showed, by heating to a temperature at which higher chromium oxides dissociate (this takes place at 500° under vacuum).

A reversible poisoning effect of water on the activity of chromium and chromia–alumina catalysts has been observed in a number of investigations [11-14], and it has also been shown [4-7] that the following reactions take place when these catalysts are alternately treated with H_2 and O_2 at 500°:

$$Cr_2O_3 + {}^3/_2O_2 \rightarrow 2CrO_3 + 6{,}1 \text{ kcal}$$
$$2CrO_3 + 3H_2 \rightarrow Cr_2O_3 + 3H_2O + 170 \text{ kcal}$$

There are indications [6] that during treatment with hydrogen, more water is removed from the oxidized surface of pure Cr_2O_3 than would be expected on the basis of iodometric determination of the amount of oxygen; this has

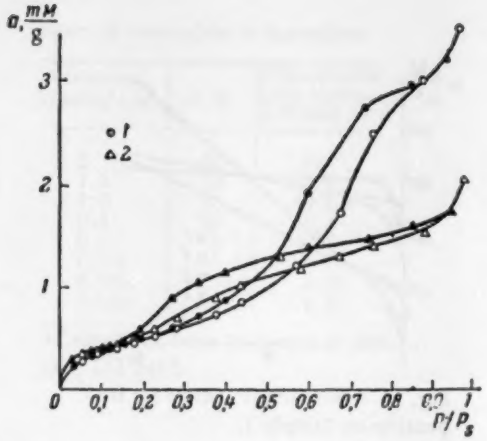

Fig. 1. Adsorption isotherms of benzene vapor at 20° on Sample 1 (1) and Al_2O_3 (2). (On all figures solid points represent desorption.)

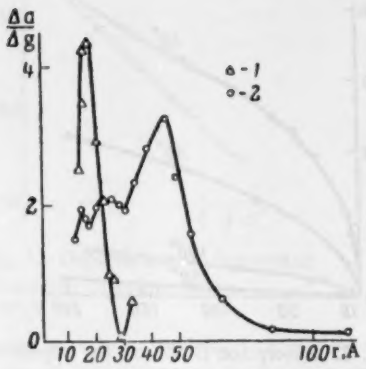

Fig. 2. Distribution of pore volume with effective radii: 1) sample; 2) carrier (Al_2O_3).

been explained as due to the removal of part of the structural water during reduction of the surface. The amount of water removed by thermal treatment of chromia–alumina catalysts is approximately that calculated from the amount of oxygen [7]. At room temperature and low pressures, the surface of either oxidized or reduced Cr_2O_3 is approximately $\frac{1}{3}$ covered by adsorbed water [15, 16].

There has been no study of the adsorption of hydrocarbons on pure C_2O_3, but hydrocarbon adsorption has been studied on mixed catalysts. The adsorption of benzene and toluene on a series of chromia–alumina catalysts of differing composition has been studied over the temperature interval of 0 to 500° by means of an approximate method [17]; the authors observed a decrease in the adsorption of these substances with an increase in temperature. Nevertheless, they proposed that the slowest step in the dehydrogenation of paraffins is chemisorption of the hydrocarbon from the layer of physically adsorbed material. A similar proposal had previously been made in reference [18], in which chemisorption by a dissociation mechanism was postulated. In a study of the adsorption of CH_4, C_2H_6, C_3H_8, and C_2H_4 on Cr_2O_3–MnO catalysts at temperatures of from 0 to 450°[19], activated adsorption of C_2H_4 was observed at temperatures above 0°, while that of the saturated hydrocarbons occurred at temperatures above 300°. The authors of this paper did not study the relationships between the amount of chemisorbed hydrocarbons and temperature and pressure. It has been proposed [10] that chemisorption of saturated hydrocarbons at high temperatures is a reversible process proceeding with a low heat of chemisorption and by a dissociation mechanism.

The aim of the present investigation was to study the adsorption characteristics of an active chromia–alumina paraffin dehydrogenation catalyst, with respect to water, isopropyl alcohol, and isopentane vapors; these catalysts had the composition 13% Cr_2O_3, 84.6% Al_2O_3, and 2.4% K_2O [20]. We are currently studying the adsorption of isoamylenes–products of the dehydrogenation of isopentane at 500-550°–on this same catalyst. The phase composition and catalytic activity of the chromia–alumina–potassium catalysts have been described previously [21].

1. Catalyst texture. Two samples of catalyst of the same composition, but from different batches were investigated in this work. They differed somewhat in texture, but had approximately the same activity with respect to isopentane dehydrogenation and isopropyl alcohol decomposition, as was confirmed by special experiments. Sample 1 was used in the isopentane adsorption study, while the adsorption of water and of isopropyl alcohol was studied on Sample 2.

Catalyst texture was determined (with the aid of A. L. Klyachko-Gurvich) by benzene vapor adsorption at 20°; the apparatus included a McBain balance. The surface areas were determined by argon (Sample 1) and krypton (Sample 2) adsorption. From the adsorption isotherm for benzene vapor on Sample 1 (Fig. 1) and the curve showing the distribution of pore volume with respect to radius (Fig. 2), it can be seen that the texture of

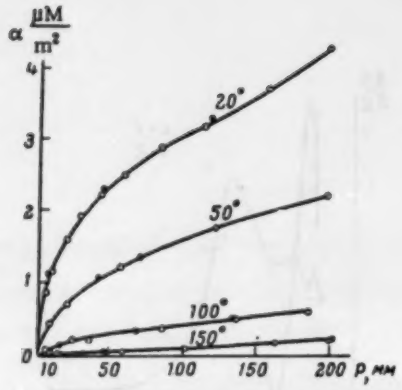

Fig. 3. Adsorption isotherms for isopentane on Sample 1.

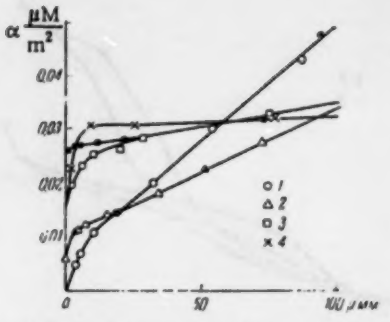

Fig. 4. Adsorption isotherms for isopentane on Sample 1.

the catalyst differed greatly from that of the carrier (Al_2O_3) and from that of Cr_2O_3 calcined at the same temperature. Chromium oxide prepared under the same conditions had S = 7 sq m/g; the Al_2O_3 had S = 110 sq m/g, and an effective pore radius of 45 A. Sample 1 has S = 120 sq m/g and an effective pore radius of the order of 20 A. A determination of S for this catalyst by the volume method using Ar adsorption at liquid nitrogen temperature gave a value of 135 sq m/g, which is in agreement with the value obtained by benzene adsorption.

Sample 2, which was used for the adsorption measurements with H_2O and C_3H_7OH, had S = 160 sq m/g by both benzene vapor and Kr adsorption measurements. The surface area calculations were carried out by means of the BET equation. The difference in the surface areas of Samples 1 and 2 was probably due to certain differences in the texture of the original Al_2O_3. A study of the texture of catalysts of this type in different stages of preparation (oxidized and reduced), operation, and regeneration, and also a study of the texture as a function of calcination time at 550° (up to 1000 hr) showed that such catalysts are highly temperature stable, and these studies also established that reduction and regeneration in air has almost no effect on the texture of the catalyst (cf. reference [21]). It is understandable that coking of the catalyst occurs during isopentane dehydrogenation; the evidence mentioned above shows that burning off the coke has practically no effect on texture.

2. Isopentane adsorption. The adsorption of isopentane on Sample 1 was studied by the capillary method described in reference [22]. The amount of isopentane adsorbed was measured with an accuracy of 0.001 mM The adsorption isotherms, which were measured at 20, 50, 100, 150 (Fig. 3), 205, 241, 297, and 325° (Fig. 4), were readily reproducible in independent measurements. The catalyst sample was pumped at 470-500° to a pressure of the order of $1 \cdot 10^{-4}$ mm Hg before the beginning of each series of experiments. With an increase in temperature from 20 to 150°, the amount of isopentane adsorbed at the same pressure decreased, and in the neighborhood of 150° the form of the isotherm changed. Thus, the isotherm at 20° was a normal isotherm of the type associated with polymolecular adsorption, and it obeyed the BET equation, by means of which the experimental data were calculated. Calculations based on this isotherm showed that a monolayer on 1 sq m of catalyst surface contains 3.02 μmoles of isopentane and that the surface occupied by one molecule of isopentane is 56 sq A. With an increase in the temperature to 150°, the process takes place in the Henry's law region—the region of low surface coverage in which adsorption depends linearly on pressure, and the isotherm is a straight line passing through the origin. Such an isotherm is one criterion of homogeneity of surface of any given adsorbent with respect to physical adsorption. Another necessary criterion of homogeneity of surface for physical adsorption is independent of the heat of adsorption, Q, with respect to degree of surface coverage θ. In the present case, this latter criterion was also approximately satisfied. Calculation of isosteric heats of adsorption by the Clausius-Clapeyron equation and based on data from the isotherms at 20 and 50° (Table 1) showed that the heat of adsorption remained almost unchanged with an increase in surface coverage from 6 to 66%. There was a small decrease in Q, which may be associated with interaction of the adsorbed molecules with each other. At low values of θ, the heat of adsorption determined from the isotherms at 150, 205, and 241° (Table 1) also remained constant with an increase in surface coverage, but it was lower than the heat of adsorption determined from the isotherms at 20 and 50° by extrapolation to these lower coverages. Similar phenomena have previously been noted in other

TABLE 1

Heats of Adsorption of Isopentane

Adsorption, μmoles/cm²	θ, %	Q, kcal/mole (from isotherms at 20 and 50°)
2	66	9,6
1,5	49	9,9
1,0	33	10,4
0,5	16	10,5
0,2	6	10,7
0,075		7,5*
0,050		7,2*
0,025		7,5*

*Calculated from isotherms at 150, 205, and 241°.

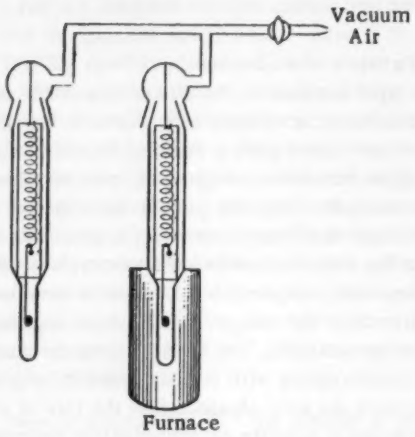

Fig. 6. Schematic diagram of the apparatus used for the study of the adsorption of water vapor.

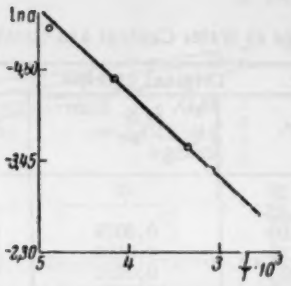

Fig. 5. Dependence of isopentane adsorption on temperature.

cases, and they have been explained chiefly by a small increase in the distance between the catalyst surface and the adsorbed molecules with increasing temperature [23]. Above 150° there was an increase in the amount of isopentane adsorbed with an increase in the temperature of the experiment in the initial part of the isotherm, up to a pressure of 10-15 mm Hg (Fig. 4). The isotherm changed from a linear and reversible type (at 150°) to a convex and irreversible Langmuir type isotherm (205-325°) which reached saturation. The adsorption process proceeded very slowly in this region. The isotherms of Fig. 4 show that between 150 and 205° there appears another type of interaction of isopentane with the surface of the catalyst—an activated adsorption which is completed at pressures of 10-15 mm Hg. Above these pressures, the isotherm continues linearly and is reversible; equilibrium was established rapidly at pressures exceeding 15 mm Hg, and adsorption decreased with an increase in temperature. As may be seen from Fig. 4, decomposition of the chemisorbed isopentane did not occur at temperatures up to 300°; however, it did occur very slowly and to an extremely slight extent at 325°, at which temperature it was not possible to determine the desorption branch of the isotherm accurately. That the 325° isotherm was linear at pressures above 15 mm, showed that a very small amount of isopentane reacted. An isotherm could not be determined at 350°, since reaction occurred to a considerable extent—a fact which was apparent from the increase in the pressure in the system. Products from the decomposition of isopentane on the catalyst were collected in this experiment, and these were analyzed (by Yu. A. Fedyunin, to whom we express our appreciation) with an MI-1035 mass spectrometer. This analysis showed that not only cracking of the isopentane, but also a series of consecutive reactions including some leading to the formation of small amounts of aromatic hydrocarbons occurred under static conditions such that the isopentane contacted the catalyst under vacuum for very prolonged periods of time.

The amount of chemisorbed isopentane varied exponentially with temperature (Fig. 5). At 241, 297, and 325° it was, respectively, 0.33, 0.9, and 1.2% of the amount of isopentane adsorbed in a monolayer on the catalyst surface at 20°. The linear relationship between the logarithm of the amount of chemisorbed isopentane and the reciprocal of the temperature can be explained by an increase in the number of chemisorption centers on the catalyst surface with an increase in temperature and by an increase in the reactivity of the isopentane itself with an increase in temperature. For technical reasons, the rate of chemisorption in our experiments could be evaluated only approximately by dividing the amount of chemisorbed isopentane by the time required to establish equilibrium. Thus, at 297°, α = 0.036 mM (on the entire catalyst sample) was reached after 96 hr,

TABLE 2

Change in Water Content and Catalyst Weight with an Increase in Temperature

Original catalyst			Reduced catalyst		
t°,	H_2O, g/g, from $Mg(ClO_4)_2$ wt. change	change in cat. wt.	t°,	H_2O, g/g from $Mg(ClO_4)_2$ wt. change	change in cat wt.
20	0	0	20	0	0
52		0,0022	54	0,0014	0,0032
100	0,0039	0,0079	100	0,0045	0,0075
150	0,0110	0,0144	150	0,0104	0,0135
200	0,0150	0,0180	200	0,0104	0,0194
250	0,0172	0,0204	250	0,0122	0,0220
300	0,0194	0,0230	300	0,0144	0,0270
350	0,0190	0,0246	350	0,0149	0,0293
400	0,0190	0,0263	400	0,0149	0,0323
450	0,0190	0,0275	450	0,0163	0,0355
500	0,0190	0,0283			
Pumped at 500°		0,0352			

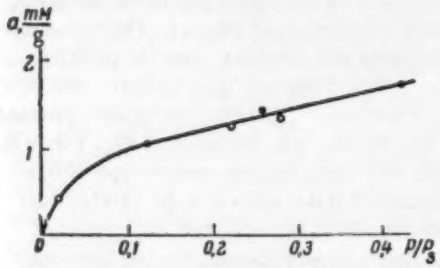

Fig. 7. Adsorption isotherm for water vapor on reduced Sample 2 at 20°.

while this same amount was adsorbed in 31 hr at 325°. These data indicate a rapid increase in the rate of isopentane chemisorption with an increase in temperature. Calculations based on the data presented above gave a value of E ≅ 15 kcal/mole for the approximate activation energy for isopentane chemisorption on this catalyst. Thus, the present investigation represents the first time that chemisorption of a paraffinic hydrocarbon on a paraffin dehydrogenation–dehydrocyclization catalyst and its change with temperature and pressure have been measured, the first time the energy of such chemisorption has been approximately evaluated, and the first time the change in rate of such chemisorption with temperature has been measured. It follows from the data obtained that the rate of chemisorption of isopentane at paraffin dehydrogenation temperatures (500° and above) must be high. Furthermore, from the rapid increase in the number of chemisorption centers with increasing temperature (500-550°), it follows that a significant fraction of the catalyst surface – up to 0.2 of the surface as measured by monolayer adsorption at 20°, according to our calculations – must take part in chemisorption (and, probably, in the reaction).

3. Adsorption of water. The adsorption of water was investigated by (a) adsorption of water on reduced Sample 2 at room temperature, (b) removal of water from both the original and reduced Sample 2 by heating and (c) adsorption of water on original and reduced Sample 2 at 440°. The experiments were carried out gravimetrically in the apparatus shown in Fig. 6. This apparatus was also used for reduction of the catalyst. In the (b) series of experiments, a desiccant – magnesium perchlorate – was placed on the second McBain balance, and the change in weight of the magnesium perchlorate was taken as a measure of the amount of water evolved.* The second balance was not used in the experiments of Series (a) and (c).

*The amount of water evolved from the catalyst could not be determined in the present case by measuring the change in weight of the catalyst during heating, because some other gas besides water was evolved when both the original and the reduced catalyst was heated (this was apparent upon comparison of the change in weight of the perchlorate and that of the catalyst; Table 2). It is possible that O_2 was evolved from the original catalyst and adsorbed CO_2 from the reduced catalyst, which had been in contact with air. The amount of gas in the first case was 0.9% and in the second case 1.9%. The somewhat different behavior of the original and reduced catalyst samples was clearly associated with the difference in phase composition [21] and, possibly, with an increase in the acidity of the AlOOH (displacement of CO_2 from K_2CO_3) with an increase in temperature.

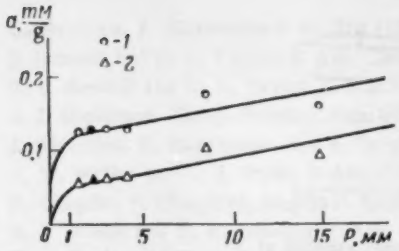

Fig. 8. Adsorption isotherms for water on Sample 2 at 440°: 1) reduced; 2) original.

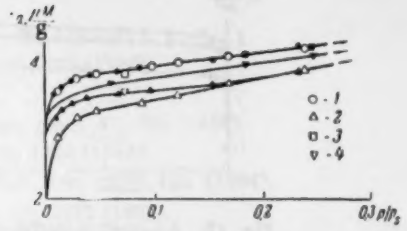

Fig. 9. Adsorption isotherms for isopropyl alcohol on Sample 2 at 30°; 1) reduced; 2) original; 3) repeat experiments on reduced sample; 4) repeat experiments on original (oxidized) sample.

The original catalyst (calcined in air at 550° during preparation) was reduced with hydrogen in the same apparatus at 500°, until evolution of water vapor had completely ceased. The reduced sample was evacuated by pumping, and the weighed catalyst sample was cooled under vacuum. Undried air was then passed into the apparatus, and the catalyst sorbed water. After 2 hr, the system was pumped at room temperature to a pressure of $1 \cdot 10^{-3}$ mm Hg, and the amount of water vapor physically adsorbed on the catalyst at room temperature was measured. The isotherm (Fig. 7) was completely reversible, and the amount of physically adsorbed water was 1.11 mM/g of catalyst. The measurements of Series (b) were then carried out on this same catalyst sample. In this series, the magnesium perchlorate was at room temperature, and the catalyst container and catalyst were heated until the catalyst attained a constant weight at each given temperature. In this series of measurements, both the original and reduced catalyst samples were pumped for removal of physically adsorbed water ($1 \cdot 10^{-3}$ mm Hg), and successive measurements at the temperatures indicated in Table 2 were then carried out. The unreduced (original) catalyst contained somewhat more chemisorbed water than did the reduced catalyst. All of the chemisorbed water could be removed from the unreduced catalyst (within the limits of accuracy of the determinations) at temperatures up to 300°. It was evolved more slowly from the reduced catalyst, and could be completely removed at temperatures up to 450°. The amount of water chemisorbed by the reduced catalyst amounted to 0.905 mM/g of catalyst.

It may be pointed out that the amount of physically adsorbed water (1.11 mM/g) comprised only 54% of the amount of water (2.04 mM/g) required for a monolayer on this catalyst (S = 160 sq m/g), if it is assumed that the area of a water molecule is 13 sq A in accordance with the literature [23]. However, the sum of the chemisorbed (0.905 mM/g) and physically adsorbed water is precisely 2.01 mM/g. It follows from this that at room temperature approximately half of the catalyst surface is covered by strongly adsorbed water which can be removed only by heating to high temperatures under vacuum. Since reduction of the catalyst and removal of water in this stage was carried out at 500°, it is clear that chemisorption of water occurred during contact of the catalyst with undried air (see above).

Adsorption of water on both the reduced and original catalyst at 400° [Series (c)] was rapid and reversible within the limits of sensitivity of the method used (0.01 mM/g in the present case). It depended only slightly on pressure and amounted to about 0.13 mM/g on the reduced catalyst, or 0.8 μmole/sq m (Fig. 8). This value is approximately 15-20 times greater than the value for chemisorbed isopentane at high temperatures (see above) on this catalyst.* The reversibility of water adsorption is evidently due to the reversible poisoning of chromia—alumina catalysts noted in a number of investigations [11-13].

4. Adsorption of isopropyl alcohol. Adsorption of isopropyl alcohol was studied by the gravimetric method at 30° on Sample 2 (reduced and original), on a catalyst of the same composition, but prepared by coprecipitation, and on a catalyst which did not contain K_2O. Before beginning the experiments, all catalyst samples were pumped at 440° to constant weight at $1 \cdot 10^{-3}$ mm Hg. Prior to this treatment, the coprecipitated catalysts were reduced with H_2 at this same temperature.

*Since the amount of chemisorbed material is expressed here in terms of a square meter of surface, the difference in the surface areas of Samples 1 and 2 need not be considered.

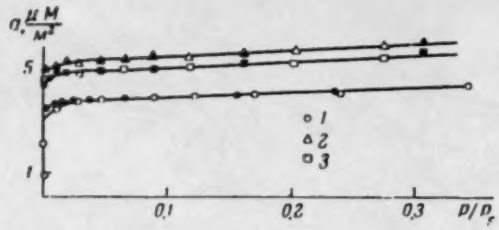

Fig. 10. Adsorption isotherms for isopropyl alcohol at 30°: 1) reduced sample; 2) coprecipitated catalyst; 3) catalyst without K_2O.

The initial adsorption on the reduced catalyst was reproducible, and in this respect it differed from adsorption on the oxidized catalyst (Fig. 9). The surface areas of the reduced and original catalyst were equal, as was established by determining S by nitrogen adsorption; moreover, it also follows from the fact that the isotherms of Fig. 9 intersect at $P/P_s \cong 0.5$. The isotherm on the original (oxidized) catalyst was not reproducible, probably owing to reduction of the surface (Cr^{+6}); as may be seen from the figure, the isotherm on the original catalyst more closely approached that of the reduced sample with each succeeding experiment. Both isotherms were irreversible, and the amount of alcohol chemisorbed on the samples prepared for the measurements of pumping under vacuum at 30° to a pressure of $1 \cdot 10^{-3}$ mm was 2.08 μ moles/sq m for the original catalyst and 2.68 μmoles per sq m for the reduced catalyst. The area occupied by a molecule of isopropyl alcohol on the surface of the reduced catalyst was 46 sq A. In the case of the coprecipitated catalysts, both with and without K_2O, the isotherms were very similar (Fig. 10). The area occupied by a molecule of iso-C_3H_7OH was 50 sq A, and the amount of alcohol chemisorbed at 30° was about 4.3 μ moles/sq m. This value is close to the amount of isopropyl alcohol (about 4 μ moles/sq m) chemisorbed on ferro-alumina gelcatalysts, which we determined in a previous investigation [24].

Thus, chemisorption of alcohol on chromia–alumina and chromia–alumina–potassium catalysts takes place to a significant extent and at a high rate even at room temperature and low relative pressures. Therefore, the use of alcohols, including methyl alcohol, for the determination of the surface area of these catalysts is hardly permissible.

In conclusion, the authors desire to acknowledge their indebtedness to O. D. Sterligov and A. P. Belen'keya for the gift of the catalyst samples used in the investigation.

SUMMARY

The adsorption of isopentane, water vapor, and isopropyl alcohol on chromia–alumina–potassium paraffin dehydrogenation catalyst was investigated, and it was established that:

1) Only physical, completely reversible adsorption of isopentane takes place at temperatures up to 150°. Chemisorption of isopentane takes place at 205-325° and pressures of 10-15 mm Hg, and the amount of chemisorbed isopentane increases with an increase in temperature. Cracking of isopentane accompanied by consecutive reactions occurs during prolonged contact with the catalyst at 350° and 10-15 mm Hg. The rate of chemisorption of isopentane, which has an activation energy of about 15 kcal/mole, increases rapidly with increasing temperature.

2. At room temperature, about 50% of the catalyst surface was covered with strongly adsorbed water which could be removed only by heating at 300-450°. At 440°, the adsorption of water was reversible, and the amount adsorbed amounted to about 0.13 mM/g of catalyst or 0.8 μ mole/m^2 on the reduced catalyst.

3. The chemisorption of isopropyl alcohol on both, the original and the reduced catalyst occurred to a significant extent at temperatures as low as 30° and at relative low pressures. During adsorption on the original (oxidized) catalyst, reduction of the hexavalent chromium compound occurred at temperatures as low as 30°. Alcohols are unsuitable for use as adsorbates for the determination of surface areas of chromia–alumina catalysts.

LITERATURE CITED

1. G. Neuman, Z. Electrochem 40, 754 (1934).
2. J. Howard and H. S. Taylor, J. Am. Chem. Soc. 56, 2259 (1934).
3. R. L. Burwell and H. S. Taylor, J. Am. Chem. Soc. 58, 697 (1936).
4. E. J. Dickinson, Trans. Faraday. Soc. 40, 70 (1944).
5. J. Givandon, E. Nagelstein, and K. Leygoing, J. chim. phys. 47, 304 (1950).
6. S. W. Weller and S. E. Voltc, J. Am. Chem. Soc. 76, 4695 (1954).
7. R. Chaplin, P. Chapman, and R. H. Griffith, Proc. Roy. Soc. A224, 412 (1954).
8. R. A. Beebe and D. A. Dowden, J. Am. Chem. Soc. 60, 2912 (1938).
9. R. A. Beebe and D. A. Dowden, J. Am. Chem. Soc. 59, 1627 (1937).
10. J. H. deBoer, Catalysis Coll.: Some Questions of the Theory and Technology of Organic Reactions [Russian translation] (IL, Moscow, 1959) p. 62.
11. A. A. Balandin, N. D. Zelinskii, M. N. Marushkin, and L. N. Pavlov, Doklady Akad. Nauk SSSR 32, 136 (1941).
12. G. D. Lyubarskii, Uspekhi Khim. 27, 316 (1958).
13. A. B. C. Dague and J. W. Myers, U. S. Pat. 2,500, 220; Chem. Abs. 44, 4668.
14. D. S. Salley, H. Fechrer, and H. S. Taylor, J. Am. Chem. Soc. 63, 1131 (1941).
15. E. H. Harbard and A. King, J. Chem. Soc. 19 (1940).
16. S. E. Voltz and S. Weller, J. Am. Chem. Soc. 75, 5231 (1953).
17. P. R. Chapman, R. H. Griffith, and J. D. Marsh, Proc. Rov. Soc. A224, 419 (1954).
18. E. C. Herington and E. R. Rideal, Proc. Roy. Soc. A190, 289 (1947).
19. J. Turkevich and H. S. Taylor, J. Am. Chem. Soc. 56, 2254 (1934).
20. B. A. Kazanskii, M. N. Marushkin, O. D. Sterligov, and A. P. Belen'kaya, Doklady Akad. Nauk SSSR 117, 619 (1957).*
21. A. M. Rubinshtein, N. A. Pribytkova, V. A. Afanas'ev, and A. A. Slinkin, Kinetika i Kataliz 1, 129 (1960).*
22. A. V. Kiselev and Yu. A. El'tekov, Zhur. Fiz. Khim. 31, 250 (1957).
23. S. Brunauer, The Adsorption of Gases and Vapors [Russian translation] (IL, Moscow, 1948) p. 352.
24. A. M. Rubinshtein, Yu. A. El'tekov, and K. I. Slovetskaya, Doklady Akad. Nauk SSSR 122, 86 (1958).*

*Original Russian pagination. See C. B. translation.

THE EFFECT OF RESTRICTION OF INTERNAL DIFFUSION ON THE KINETICS OF ETHYLENE HYDROGENATION•

A. Ya. Rozovskii, V. V. Shchekin, and E. G. Pokrovskaya

Institute of Petrochemical Synthesis, Academy of Sciences of the USSR
Translated from Kinetika i Kataliz, Vol. 1, No. 3, pp. 464-470,
September-October, 1960
Original article submitted March 22, 1960

An experimental evaluation of the effect of restriction of internal diffusion on the kinetics of the hydrogenation of ethylene over Ni/Al_2O_3 catalyst was carried out by studying the kinetics of the reaction with catalyst pellets of different dimensions. A comparison is presented of the experimental data with values obtained by a previously proposed method of calculation, and the comparison shows that the method is applicable in the present case.

Previously [1], some of us proposed an equation describing the kinetics of heterogeneous catalytic first order reactions taking place in a flow system and inhibited by reaction products and processes transferring material into the catalyst pellets; a method was also proposed for evaluating the effect of restriction of internal diffusion on the kinetics of the reaction by means of calculations based on data on the activity and structure of the catalyst.

This equation had the form:

$$\alpha = v_0 \ln \frac{1}{1-y} - \beta v_0 y, \tag{1}$$

where

$$\alpha = \frac{\sqrt{K_0 \bar{r} D_c'} S_g}{L \sqrt{2}(1+n+\delta)} = \frac{K_0 S_g f}{1+n+\delta}; \qquad \beta = \frac{n - \frac{1}{4} B}{1+n+\delta}, \tag{2}$$

v_0 is the specific feed rate in moles/g · sec; y is the conversion; K_0 is the observed rate constant for the heterogeneously catalyzed first order reaction [1] in moles/cm^2 · sec; $\bar{r}$ is the average pore radius in cm; D_c' is the diffusion coefficient (nominal) in moles/cm · sec; S_g is the catalyst surface area in cm^2/g; L is the distance from the outer surface of the catalyst pellet to the center measured along the pore, cm; n is the change in the number of moles due to the reaction; δ is the degree of dilution; B is a parameter which establishes the observed order of the reaction when the latter takes place in the kinetic region [1]; f is the internal retardation factor, the ratio of the observed reaction rate to the reaction rate in the absence of internal retardation (see [1]).

The region in which the reaction takes place is determined by the value of the dimensionless parameter

$$h = L \sqrt{\frac{2K_0}{\bar{r} D_c'}} = \frac{2\alpha^2 (1+n+\delta) L^2}{S_g \bar{r} D_c'}.$$

When $h \geq \sqrt{4 + 2BP}$ (P is the dimensionless partial pressure of the reacting substance expressed as a fraction

•Presented at the All-Union Conference on Organic Catalysis held in Moscow, November 18, 1959.

TABLE 1

Structural Characteristics of Samples 5, 6, and 7

Sample	S_g, m^2/g	Specific pore Vol. V_g, cc/g	r, Å	Bulk density, d_c, g/cc	Dimension of cylindrical pellets, cm	
					H	R
$Ni(NO_3)_2/Al_2O_3$ (initial)	122	0,383	63	—	0,52	0,22
Ni/Al_2O_3						
5	91	0,345	75	0,9	0,52	0,22
6	—	—	—	0,9	0,25	0,22
7 (after expts.)	98	0,356	73	0,9	0,135	0,22

of the total pressure), the reaction takes place in the internal diffusion region. In actual cases, especially when the reacting substance is fed to the reaction zone as a mixture with a diluent, the term BP is generally small, and the approximation $h \geq 2$ may be used.

The concepts developed in reference [1] have been applied to the evaluation of the effect of internal diffusion retardation on the kinetics of the dehydration of ethyl alcohol on aluminum oxide [2], and have now been applied to the hydrogenation of ethylene on a Ni/Al_2O_3 catalyst, which is the subject of the present communication.

Selection of this reaction was dictated by its high rate, so that internal diffusion retardation would be expected to be significant when a porous catalyst is used. This is indicated by the large difference in the values of apparent activation energies (3.1-10.7 kcal/mole) obtained by different authors [3-5]. The reaction is practically irreversible over the temperature range of 0 to 200° [6].

Method of investigation. The kinetics of the hydrogenation of ethylene were studied in a flow system, the basic details of which have been described previously [7]. The feed rate of the initial gas mixture was maintained constant with a precision of 0.1-0.3%; as a rule, variations in the temperature of the catalyst bed did not exceed a few tenths of a degree, and the temperature was measured with an accuracy of 0.1°. The concentration of ethylene in the feed gas and the degree of conversion were determined by means of an interferometer, and the determinations were accurate to 0.01% and 0.001%, respectively.

The ethylene was prepared by dehydration of ethyl alcohol over calcined commercial aluminum oxide at 380°. From the reactor, the ethylene was passed through a water-cooled receiver and then through a 30% solution of KOH. The liquid products were frozen out in a trap cooled with a mixture of solid carbon dioxide and methyl alcohol. The ethylene was passed through a column containing copper on asbestos (at 300°) to remove traces of oxygen. The hydrogen, which was fed from a cylinder, was passed through 30% KOH and a column containing copper on asbestos (at 300°).

Before entering the reactor, the feed gas (ethylene and hydrogen) was dried in columns containing calcined chloride and anhydrone. The ethylene content of the feed gas was 7.8 ± 0.3% by volume.

The Ni/Al_2O_3 catalyst was prepared by impregnation of calcined commercial aluminum oxide (with nickel nitrate). Prior to the experiments, the catalyst was repeatedly oxidized and reduced at 500° and, finally, at 700° in a stream of hydrogen for two hours. During the course of the experiments, the catalyst was also periodically oxidized with air and then reduced at 500° for two hours. Three samples of catalyst were used, and these differed in pellet dimensions (cylindrical pellets). Structural characteristics of these samples are shown in Table 1.•

As may be seen from the table, the structural characteristics of the catalyst did not change during the course of the experiments (within the limits of accuracy of the BET method).

• The adsorption measurements were carried out by F. V. Korenevskii, for which the present authors express their appreciation.

TABLE 2

Kinetics of the Hydrogenation of Ethylene over Ni/Al_2O_3 Catalyst (catalyst weight, 0.7 g)

t°	v_0, moles/hr	y	$v_0 y$	$k_1 = v_0 \ln \frac{1}{1-y}$
		Sample 5		
100	0,56	0,775	0,43	0,84
	0,76	0,660	0,48	0,82
	1,33	0,467	0,62	0,84
	1,75	0,378	0,66	0,83
110	0,56	0,826	0,46	0,98
	0,76	0,715	0,54	0,95
	1,33	0,518	0,69	0,97
	1,44	0,476	0,69	0,93
	1,76	0,416	0,73	0,95
	1,96	0,371	0,73	0,91
	2,35	0,312	0,73	0,88
	3,51	0,237	0,83	0,95
		Sample 6		
100	0,6	0,825	0,50	1,05
	0,86	0,726	0,62	1,11
	2,1	0,385	0,81	1,02
	0,61	0,875	0,53	1,27
	0,86	0,775	0,67	1,28
	1,23	0,630	0,77	1,22
	2,08	0,429	0,89	1,17
		Sample 7		
100	0,6	0,935	0,56	1,64
	0,85	0,853	0,73	1,63
	1,2	0,759	0,91	1,71
	1,6	0,629	0,99	1,60
	2,0	0,557	1,11	1,63
	2,78	0,440	1,22	1,61
120	0,85	0,915	0,78	2,10
	1,2	0,820	0,98	2,06
	1,5	0,749	1,12	2,08
	1,6	0,704	1,13	1,93
	2,0	0,640	1,28	2,04
	2,78	0,500	1,39	1,93

Results. The experiments were carried out at temperatures of 80-140° and feed gas rates of 0.8-5.0 moles per g · hr. The conversions at a given feed gas rate and temperature (t) were determined in the experiments. The resulting data were plotted to show y as a function of t (at constant feed rates), and values of y at different values of v_0 and equal t were then obtained by graphical interpolation (Table 2).

It is apparent from Table 2 that the values of $k_1 = v_0 \ln \frac{1}{1-y}$ for all catalyst samples remained constant when the conversion changed over a broad interval; i.e., the experimental data are described by Eq. (1) with $\beta = 0$.

The catalyst activity was characterized by the value of $\alpha(1 + n + \delta) = K_0 S_g = K_g$, which is the observed rate constant (without taking into account any retardation by internal diffusion) and referred to unit weight of the catalyst [1]. Data showing the relationship between the values of K_g and temperature for Sample 5 are presented in Table 3 and Fig. 1 (each point is an average of several experiments). Similar data for Samples 6 and 7 are presented in Figs. 2 and 3.* (The apparent scattering of the points was due to variations in the activity of the catalyst after regeneration.) As is apparent from the figures, the experimental data are satisfactorily described by the Arrhenius equation.

*For the sake of brevity, the corresponding numerical data are not presented in the present paper.

TABLE 3

Kinetics of the Hydrogenation of Ethylene over Sample 5 (relationship between the values of K_g and temperature)

No. of Expts.	t°	K_g, moles/g · hr	$1/T \cdot 10^3$, degrees^{-1}	$\log K_g$	$\frac{E}{2,3RT} + \log K_g$
11	82,3	0,845	2,813	—0,073	2,43
7	87,6	0,871	2,772	—0,060	2,41
12	92,5	0,944	2,735	—0,025	2,41
13	97,4	1,024	2,698	+0,010	2,41
5	101,6	1,057	2,668	0,024	2,40
12	107,6	1,173	2,626	0,069	2,41
8	112,2	1,245	2,595	0,095	2,40
6	116,4	1,279	2,567	0,107	2,40
7	122,3	1,426	2,528	0,154	2,40
6	128	1,496	2,493	0,175	2,39
5	136,6	1,80	2,440	0,255	2,42

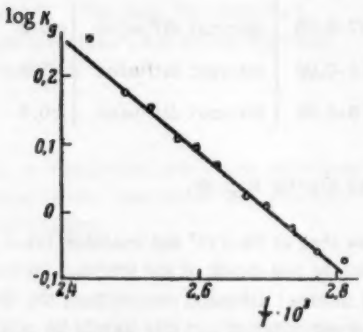

Fig. 1. Activation energy for the hydrogenation of ethylene over Sample 5.

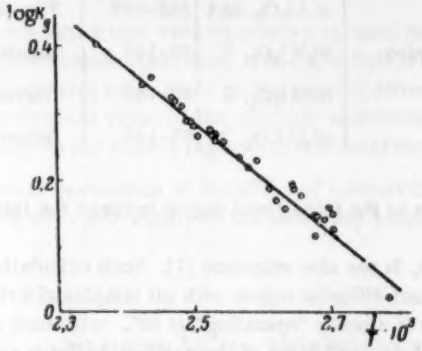

Fig. 2. Activation energy for the hydrogenation of ethylene over Sample 6.

TABLE 4

Effect of Internal Diffusion Retardation on the Kinetics of the Hydrogenation of Ethylene Over Ni/Al_2O_3 Catalyst

Sample	t°	$K_g \cdot 10^4$ moles/g	L, cm	h	θ
5	80	2,1	0,15	15	0,07
6	80	2,8	0,09	7	0,14
7	80	4,2	0,06	5	0,19
5	110	3,4	0,15	25	0,04
6	110	4,4	0,09	12	0,08
7	110	6,5	0,06	9	0,12
5	140	5,0	0,15	38	0,03
6	140	6,4	0,09	18	0,06
7	140	9,5	0,06	13	0,08

The values of the apparent activation energy calculated for the three samples from the data of the figures were very close and average E = 4.1 ± 0.2 kcal/mole. The values of the logarithm of the pre-exponential factor (last column in Table 3) calculated from this value of the apparent activation energy were constant over a broad temperature interval.

In addition to the above, the activity of the catalyst depended substantially on the dimensions of the catalyst pellets (Table 2 and Figs. 1-3); i.e., there was considerable retardation due to restriction of internal diffusion. Experiments carried out with changes in the linear gas velocity showed that the effect of external diffusion retardation was insignificant over the temperature range studied. Consequently, the dependence of catalyst activity on pellet dimensions was due to internal diffusion retardation.

The effect of restrictions of internal diffusion on the kinetics of the reaction, can be evaluated by calculations

TABLE 5

Experimental and Calculated Evaluation of the Effect of Internal Diffusion Retardation on the Kinetics of the Dehydration of Ethyl Alcohol over α- and γ-Al_2O_3 and on the Kinetics of Ethylene Hydrogenation Over Ni/Al_2O_3 Catalyst

Reaction	Catalyst	t°	Calculated data		Experimental data	
			region in which reaction occurs	f	region in which reaction occurs	f
Dehydration of ethyl alcohol	γ-Al_2O_3, 1	400	Internal diffusion	0.2	Internal diffusion	0.2
		425	Internal diffusion	0.1	Internal diffusion	0.2
	γ-Al_2O_3, 2	400	Transition*	0.7	Transition	0.8
		425	Transition	0.6	Transition	0.7
	α-Al_2O_3, 3&4	386-426	Kinetic	1.0	Kinetic	1.0
Ethylene hydrogenation	Ni/Al_2O_3, 5	80-140	Internal diffusion	0.07-0.03	Internal diffusion	< 0.5
	Ni/Al_2O_3, 6	80-140	Internal diffusion	0.14-0.06	Internal diffusion	<0.5
	Ni/Al_2O_3, 7	80-140	Internal diffusion	0.19-0.08	Internal diffusion	<0.5

*This refers to the transitional region between the internal diffusion and kinetic regions.

based on Eq. 3; see also reference [1]. Such calculations (Table 4) show that at 80-140° the reaction takes place in the internal diffusion region with all samples of catalyst. Approximately one-tenth of the internal surface of the catalyst is already "operating" at 80°. With such a strong effect of internal diffusion retardation, the thickness of the "working" layer of the catalyst pellet is small, and the observed catalyst activity should be proportional to the external area of the pellet. This is an advantage for present purposes, since equations for the calculation of L for granules having different forms, are only approximate.

On the basis of the above and taking into account data on the kinetics of ethylene hydrogenation over Sample 5, the expected activities of Samples 6 and 7 were calculated (Fig. 4). The lines shown in Fig. 4 for Samples 6 and 7 are calculated, and the points represent experimental data. Figure 4 shows that there was good agreement between the calculated and experimental values, which confirms that the reaction actually does proceed in the internal diffusion region with low values of the internal diffusion retardation factor. In this connection, the observed value of the apparent activation energy for the reaction in the kinetic region was 8.2 kcal/mole, which is in agreement with the data of other authors [4, 5].

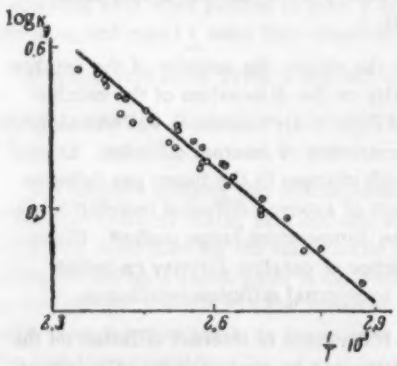

Fig. 3. Activation energy for the hydrogenation of ethylene over Sample 7.

The data presented here provide qualitative confirmation of the applicability of the proposed scheme to a description of the effect of internal diffusion retardation on the kinetics of ethylene hydrogenation. These results of our experimental and calculated evaluation of the effect of internal diffusion retardation on the kinetics of ethylene hydrogenation are presented in Table 5 along with previously published [2] data on the dehydration of ethyl alcohol over aluminum oxide.

The data of Table 5 show that the proposed method of calculation allows one to determine the region in which

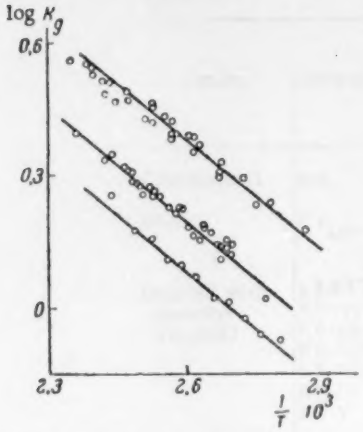

Fig. 4. Temperature dependence of the observed reaction rate constants for the hydrogenation of ethylene over Samples 5-7. (The lines for Samples 6 and 7 are calculated; the points represent experimental data.)

a given reaction takes place and to evaluate approximately the value of the internal diffusion retardation factor.

We may also point out that in recent work by R. D. Obolentsev and A. V. Mashkina [8], the applicability of Eq. (1) to a description of the reaction kinetics of the hydrogenolysis of dibenzothiophene complicated by internal diffusion retardation was demonstrated.

SUMMARY

1. The reaction kinetics of ethylene hydrogenation over three samples of Ni/Al_2O_3 catalyst differing in pellet dimensions, were studied at 80-140°.

2. It was shown that under the conditions studied, the kinetics of the reaction are described by the equation for a first order reaction (without "retardation" by reaction products); the observed value of the apparent activation energy was 4.1 kcal per mole for all catalyst samples.

3. It was shown that with all catalyst samples under the experimental conditions used, there is strong diffusion retardation, and the reaction takes place in the internal diffusion region. The observed value of the apparent activation energy for the reaction in the kinetic region was 8.2 kcal/mole.

4. A comparison was made of calculated and experimental evaluations of the effect of internal diffusion retardation on the kinetics of the reaction. The results confirm the applicability of the previously proposed method of calculation.

LITERATURE CITED

1. A. Ya. Rozovskii and V. V. Shchekin, Kinetika i Kataliz, 1, 313 (1960); *A. Ya. Rozovskii and V. V. Shchekin, Trudy Inst. Nefti Akad. Nauk SSSR 10, 286 (1957).
2. V. P. Prokov'eva, A. Ya. Rozovskii, and V. V. Shchekin, Trudy Inst. Nefti Akad. Nauk SSSR 12, 253 (1958).
3. E. K. Rideal, J. Chem. Soc. 309 (1922); C. Schuster, Z. phys. Chem. B 14, 240 (1931); Trans. Faraday Soc. 28, 406 (1932); E. K. Rideal and T. Tucholski, J. Chem. Soc. 1701 (1933); O. Toyama, Proc. Imp. Acad. Tokyo 11, 319 (1935); Rev. Phys. Chem. Japan 11, 153 (1937); 12, 115 (1938); O. Beech, Rev. Modern Physiks 17, 61 (1945).
4. G. M. Schwab and H. Z. Zorn, Z. phys. Chem. A 171, 421 (1935); Z phys. Chem. B 32, 169 (1936).
5. E. K. Rideal and G. H. Twigg, Proc. Roy. Soc. A 171, 55 (1939).
6. A. V. Frost, Khim. Tverd. Topliva 4, 171 (1933); R. N. Pease, Equilibria and Kinetics of Gas Reactions (Princeton, 1942).
7. S. A. Gol'din, A. Ya. Rozovskii, and V. V. Shchekin, Trudy Inst. Nefti Akad. Nauk SSSR 12, 246 (1958).
8. R. D. Obolentsev and A. V Mashkina, Proceedings of the Fourth Scientific Session on the Chemistry of Organosulfur Compounds [in Russian] (Ufa, 1958); Coll.: The Chemistry of Organosulfur Compounds Contained in Petroleum and Petroleum Products [in Russian] (1960) Vol. 4; A. V. Mashkina, Candidate's Dissertation, Institute of General Chemistry, Academy of Sciences USSR [in Russian] (1959).

THE EFFECT OF THE PORE STRUCTURE OF CATALYSTS ON CATALYTIC ACTIVITY AND ON THE KINETIC PARAMETERS OF CRACKING REACTIONS

K. V. Topchieva, T. V. Antipina, and Li He-Suyan

Moscow State University

Translated from Kinetika i Kataliz, Vol. 1, No. 3, 471-477,
September-October, 1960
Original article submitted March 23, 1960

The present work was devoted to a study of the kinetics of cumene cracking over silica–alumina catalysts having widely differing pore radii.

It was established that the activity and kinetic parameters depend on the magnitude of the pore radii, and the reaction takes place in the kinetic or internal diffusion range depending on the temperature and pore radii of the silica–alumina catalyst. The ratio of the activation energy in the kinetic range to that in the internal diffusion range is approximately 2.

* * *

The majority of catalysts used in industry are porous bodies having widely differing internal surfaces. The physical structure of these catalysts and the accessibility of their internal surface to molecules of the reacting substance and reaction products can have a substantial effect on catalyst activity, selectivity, and, in addition, on the regularities involved in the course of heterogeneous catalytic reactions. The determination of the kinetic parameters of chemical reactions have great significance in the design of reactors and in the creation of scientific bases for the selection of catalysts. The occurrence of reactions on catalysts with a highly developed internal surface is frequently complicated by the processes by which the material is transported into the catalyst pores; i.e., internal diffusion retardation appears, and this makes it difficult to study the actual kinetic regularities, to evaluate correctly the activity of the catalyst, and to establish the macrokinetic mechanism of the reaction.

The effect of restriction of internal diffusion on the kinetic course of heterogeneous catalytic reactions has been considered in a number of papers [1-8]. However, the literature contains no data concerning the experimental evaluation of the effect of internal diffusion retardation on the kinetics of a reaction, as it depends on pore radii and other structural characteristics of porous catalysts.

It seemed expedient to seek a solution to this problem in three basic directions: 1) a study of the kinetic regularities over a broad temperature range in order to establish the range, kinetic or diffusion, in which the reaction proceeds; 2) a study of processes over catalysts of a single chemical composition, but differing with respect to pore radii; 3) an investigation of kinetics over samples of catalysts with the same pore structure, but having different concentrations of active centers on their surface.

The present communication presents the results of an investigation along the first two routes. The effect of various structural parameters (total porosity, specific surface, pore radius, the volume of the intermediate pores, etc.) of the catalyst on catalyst activity and on the course of the reaction were studied. Particular attention was given to the preparation of homogeneously porous catalysts having large pore radii. The latter requirement is extremely important for processes which are retarded by internal diffusion effects, and it permits elimination or limitation of its effect on the process.

TABLE 1

Series	Sample	Degree of replacement of water in hydrogel, %	Surface area, sq m/g		Total pore vol., cc/g	Vol. inter. pores, cc/g	Predominant pore radius, A	$\alpha_{475°}$, moles/g per hr	$\frac{\alpha}{S} \cdot 10^3$, mM/sq m per hr
			S (BET)	S' (CC)*					
Commercial	KP_1	0	420	Initial	0,24	0,03	12	0,5	1,1
Initial	KP_{init}	0	280	210	0,44	0,26	22	3,3	11,8
I									
(treated with isobutyl alcohol)	KB-P	35	420	310	0,52	0,29	19	3,3	7,9
	KB-VI	51	420	400	0,52	0,47	21	—	—
	KB-IX	60	400	380	0,51	0,29	19	—	—
	KB-VIII	69	490	390	1,00	0,70	42	5,9	12,0
	KB-VII	81	480	390	1,31	0,94	46	8,1	16,8
	KB-IV	97	460	430	1,96	1,62	80	11,6	25,2
	KB-V	100	450	430	2,42	2,08	110	—	—
II									
(treated with isoamyl alcohol)	KA-III	55	430	230	0,50	0,25	19	—	—
	KA-I	83	500	360	1,65	1,26	61	—	—
	KA-II	95	520	410	1,92	1,52	100	—	—
	KA-IV	100	460	440	2,25	1,93	115	19	42
III									
(treated with cumene)	CC-I	34	480	240	0,55	0,25	19	3,8	7,9
	CC-II'	63	440	300	0,51	0,32	19	3,9	8,9
	CC-II	90	400	380	0,79	0,49	27	4,3	10,7
	CC-III	96	420	310	0,95	0,61	39	6,4	15,2
Houdry	KH	0	230	140	0,36	0,25	23	2,6	10,9

The study of the effect of diffusion retardation on cumene cracking kinetics was carried out with a special series of silica–alumina catalysts having the same chemical composition (12% Al_2O_3 and 88% SiO_2), but widely differing pore radii (12-115 A).

The preparation of catalysts of differing porosity was accomplished by varying the degree of replacement of intermicellar water in raw commercial silica–alumina spheres, obtained prior to the stages of syneresis, activation, and washing free of salt [9]. Isobutyl alcohol (Series I), isoamyl alcohol (Series II), and cumene (Series III) were used as replacement liquids.

In addition to these series of catalysts, a fine-pore commercial catalyst produced in this country (KP_1) and a Houdry-type catalyst,* were studied in this work.

Data on the structures of these samples are presented in Table 1; the data were calculated from adsorption isotherms for methyl alcohol vapor at 20°. Curves showing the distribution of pore volume with respect to pore radius are presented in Fig. 1.

The cracking kinetics were studied at 350-500° (measured with an accuracy of ±2°) in a flow-type apparatus with automatic control of the cumene feed with an accuracy of ±0.5 mM/hr. The degree of conversion was determined from the volume of propylene formed with an accuracy of ±1% [10, 11]. The equation of Frost [12], as derived for a monomolecular, irreversible, heterogeneous reaction in a flow system, was used to describe the reaction kinetics:

$$v_0 \ln \frac{1}{1-y} = \alpha + \beta v_0 y,$$

where v_0 is the space rate of the feed, mM/g · hr; y is the degree of conversion; α is the apparent reaction rate constant, mM/g · hr; and β is a constant.

*The kinetics of cumene cracking over this catalyst were studied by B. V. Romanovskii, S. V. Ven'yaminov, and one of us [10].

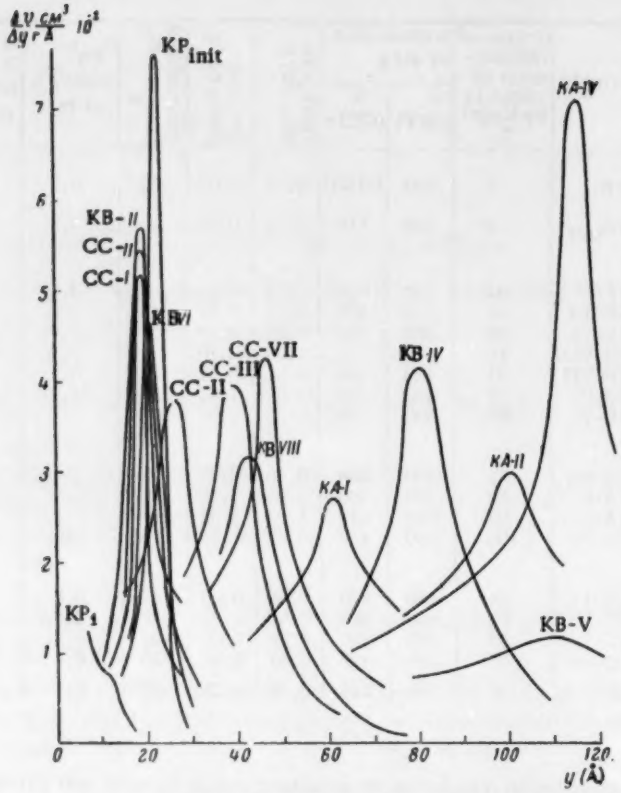

Fig. 1. Pore volume distribution with respect to pore radius for silica–alumina catalysts.

In accordance with Eq. (1), plotting $v_0 \ln \frac{1}{1-y}$ as a function of $v_0 y$ gives a straight line.

The results of the kinetic investigations with catalysts having different pore radii are presented in Figs. 2-5 and Table 2.

As can be seen from these graphs, the experimental data are completely satisfactorily described by Eq. (1), and the straight lines obtained from plots of $v_0 \ln \frac{1}{1-y}$ vs. $v_0 y$ have a slope of 1, i.e., the value of β is in agreement with the data of references [13, 14], and it indicates that the reaction proceeded by the same mechanism in the two cases. As has previously been shown [15], the value of β does not change when the reaction takes place in the internal diffusion range; however, the break in the lines representing log α as a function of $1/T$, which is quite evident in these cases, indicates the effect of diffusion processes on the kinetics of cumene cracking. This provided us with the possibility of using the relationship between the value of α and temperature to establish the region in which the reaction takes place.*

The kinetic data undoubtedly indicate a specific dependence of catalytic activity on the structural parameters of the catalysts. Moreover, the magnitude of the pore radius and the volume of the intermediate pores have the greatest effect, and these parameters parallel the course of catalytic activity (Fig. 6 and Table 1).

Indeed, in the case of catalyst KP_{init}, an increase in surface area (S) by 140 m^2/g without a simultaneous increase in pore radius (Table 1, Series I, II, and III) had practically no effect on the apparent reaction rate

*The physical significance of α under conditions such that material transport processes have an effect on reaction kinetics, will be discussed in a separate article.

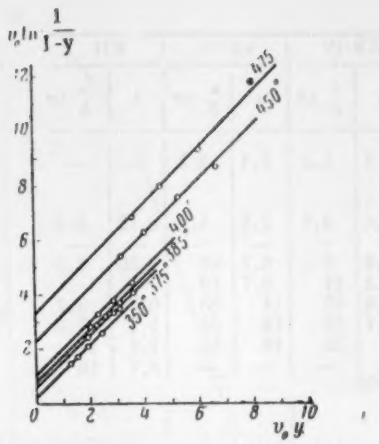

Fig. 2. Kinetics of cumene cracking over KP_{init} catalyst at different temperatures.

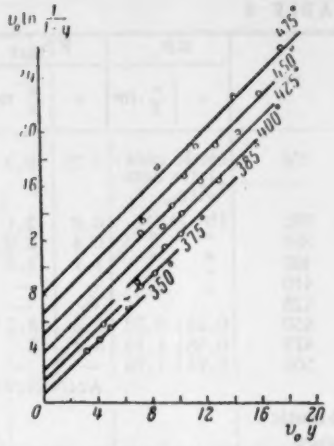

Fig. 3. Kinetics of cumene cracking over KB-VII catalyst at different temperatures.

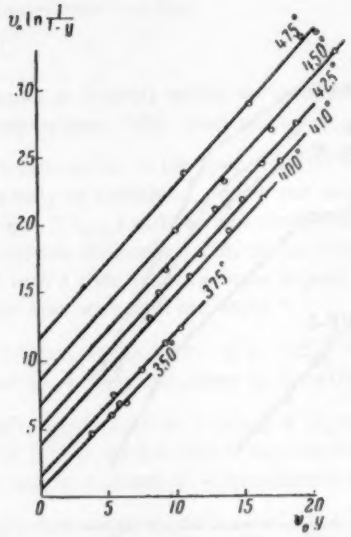

Fig. 4. Kinetics of cumene cracking over KB-IV catalyst at different temperatures.

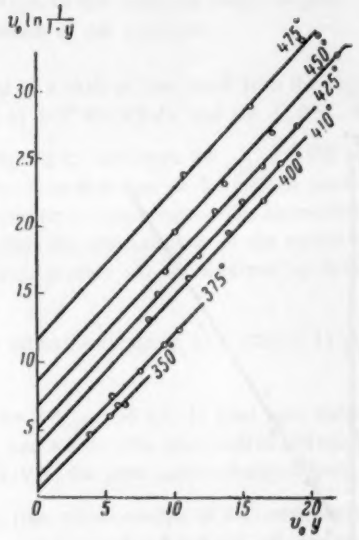

Fig. 5. Kinetics of cumene cracking over KA-IV catalyst at different temperatures.

constant. In those cases where an increase in surface area was accompanied by a simultaneous increase in pore radius and volume of the connecting pores, the rate constants increased appreciably, and the limits of the range, kinetic or diffusion, in which the reaction occurred, changed with temperature (Fig. 7). (The kinetics of cumene cracking over a Houdry-type catalyst at 375-500° are shown in Fig. 8).

As may be seen from the figures, the lines resulting from Arrhenius plots of the kinetic data have characteristic breaks which depend on temperature and pore radius, and the portions of the curves before and after the breaks correspond to the different regions of the reaction. Judging from the values of the activation energy as given by the different portions of the kinetic curves (before and after the break), it is possible to establish three ranges for the reactions studied: a kinetic range for which E_k = 28-30 kcal/mole, and a range for which $E_D \cong$ $\cong$ 15 kcal/mole, and a range for which E = 10-11 kcal/mole.

TABLE 2

T°	KP		KP_{init}		KB-VIII		KB-IV		KA-IV		KH	
	α	$\frac{\alpha}{S}\cdot10^5$	α	$\frac{\alpha}{S}\cdot10^5$	α	$\frac{\alpha}{S}\cdot10^5$	α	$\frac{\alpha}{S}\cdot10^5$	α	$\frac{\alpha}{S}\cdot10^5$	α	$\frac{\alpha}{S}\cdot10^5$
350	Little catalytic activity		0,25	0,9	0,7	1,5	0,7	1,5	1,1	2,3	—	—
375	The same		0,6	2,1	1,6	3,3	1,6	3,4	2,6	5,7	0,12	0,5
385	"	"	0,8	2,9	2,3	4,8	—	—	—	—	—	—
400	"	"	1,1	3,8	3,8	7,9	3,9	8,5	6,7	15	0,30	1,3
410	"	"	—	—	—	—	5,2	11	8,7	19	—	—
425			—	—	5,1	11	6,8	15	11	25	0,85	3,7
450	0,33	0,79	2,3	8,2	6,6	14	8,7	19	15	33	1,7	7,5
475	0,48	1,14	3,3	12	8,1	17	12	25	19	42	2,6	11
500	0,74	1,76	—	—	—	—	—	—	—	—	3,7	16
Activation energy, kcal/mole												
In kinetic range	—		29,0		28,0		28,0		29,8		36,9	
In diffusion range	15,8		15,3		10,4		10,5		11,1		17,7	

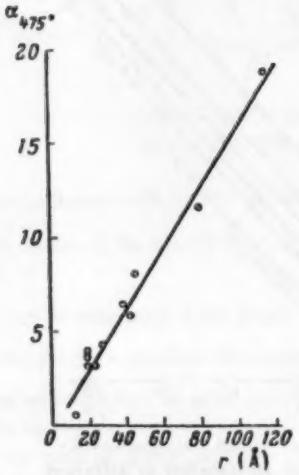

Fig. 6. Dependence of apparent reaction rate constants at 475° on pore radius of the catalyst.

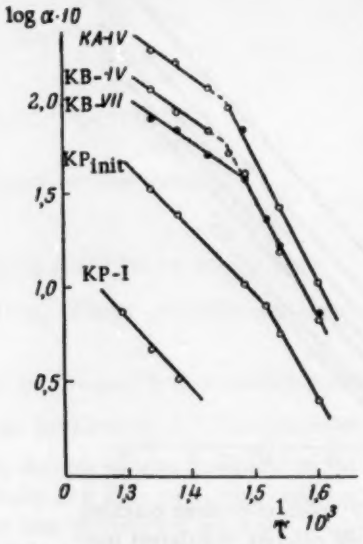

Fig. 7. Dependence of log α on 1/T for catalysts with different pore radii.

Two ranges were established for the Houdry-type catalyst: a kinetic range for which E_k = 37 kcal/mole and an internal diffusion range for which E_D = 18 kcal/mole. In the latter case, the ratio of the activation energies is 2.1. Let us consider with greater attention the effect of pore radius on the range in which the reaction takes place. In the case of a low activity catalyst with fine pores (KP), the reaction takes place in the internal diffusion range with an activation energy of 16 kcal/mole. The catalyst with a pore radius of 22 A (KP_{init}) had high activity, and there was a break in the line obtained by an Arrhenius plot of the kinetic data. This break characterized the presence of two ranges in which the reaction proceeded—a kinetic range with E_k = 29 kcal/mole and an internal diffusion range with E_D = 15 kcal/mole; the ratio of the activation energies is 1.9 . A further increase in the pore radii of the catalysts from 46 to 115 A (KB-VII, KB-IV, and KA-VII) led

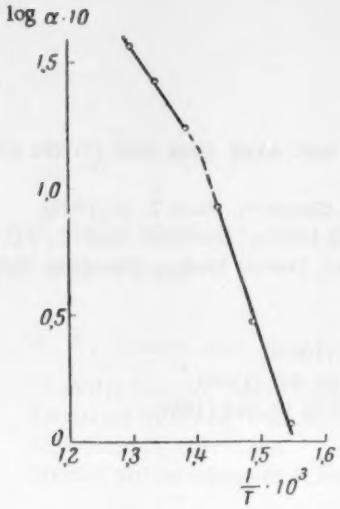

Fig. 8. Kinetics of cumene cracking at different temperatures over a Houdry-type catalyst.

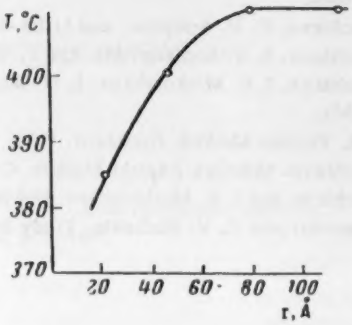

Fig. 9. Dependence of the temperature of transition from the kinetic range to the diffusion range on pore radius of the catalysts.

to an increase in activity within the temperature range studied and to a shift of the break into the region of higher temperatures. This break occurred at 400° for KB-VII, and at 415° for KB-IV and KA-II (Fig. 9).

The differences in the specific rates in the kinetic range (Fig. 8) for catalysts KP_{init}, KB-VII and KB-IV can apparently be explained, on the one hand, by the fact that the determination of the surface area of the fine pore catalyst (KP_{init}) with methyl alcohol was not sufficiently accurate to characterize the accessibility of its pores to cumene molecules, and, on the other hand, it is possible that the accessibility of the active centers increases with a significant increase in pore radius. A more accurate picture can be obtained by determining the surface area with benzene vapor.•

In comparing the values of α and $\frac{\alpha}{S}$ for the reaction in the diffusion range at 475° (Table 1) as functions of pore radius, a sharp difference in the values was noted.

Thus, α increased by a factor of approximately four to six for KP_{init} and KA-IV (the pore radius changed from 22 to 115 A), by a factor of approximately three for KP_{init} and KB-IV (the pore radius changed from 22 to 80 A), and by a factor of approximately two for KP_{init} and KB-VII (the pore radius changed from 22 to 46 A).

Upon comparing the values of α and $\frac{\alpha}{S}$ for a low-activity, fine-pore catalyst (KP-I) with the corresponding values for KA-IV (r = 115 A), it becomes apparent that there was a forty-fold increase.

Such a difference in the rate constants and the decrease in the differences between them with an increase in pore radius indicates that for the fine-pore samples there was an appreciable superposition of the diffusion processes which is limited or completely removed with an increase in pore radius of the catalysts.

Thus, this investigation of the kinetics of cumene cracking over a broad temperature interval has permitted us to establish experimentally the different ranges in which the reaction takes place and the dependence of the temperature of the transition from the kinetic to the diffusion range on pore radius of the catalyst.

LITERATURE CITED

1. Ya. B. Zel'dovich, Zhur. Fiz. Khim. 13, 163 (1939).
2. S. Ya. Pshezhetskii, Zhur. Fiz. Khim. 19, 376 (1945); 21, 1019 (1947).

•This work is currently in progress.

3. G. K. Boreskov, Khim. Prom. 8, 221 (1947); 9, 256 (1947).
4. A. Wheeler, Adv. in Catal. 3, 249 (1951).
5. P. B. Weisz and C. D. Prater, Adv. in Catal. I, 143 (1954).
6. A. I. Rastrenenko and I. E. Neimark, Zhur. Fiz. Khim.
7. K. V. Topchieva, Doklady Akad. Nauk SSSR 80, 635 (1951).
8. V. P. Prokov'eva, A. Ya. Rozovskii, and V. V. Shchekin, Trudy Inst. Nefti Akad. Nauk SSSR 10, 293 (1957); 12, 253 (1958).
9. K. V. Topchieva, T. V. Antipina, and Li He-Suyan, Vestnik Moskov. Gosudarst. Univ. 2, 13 (1960).
10. K. V. Topchieva, B. V. Romanovskii, and S. V. Ven'yaminov, Vestnik Moskov. Gosufarst. Univ. 1, 3 (1960).
11. K. V. Topchieva, I. F. Moskovskaya, L. G. Bodrova and E. I. Krupenya, Vestnik Moskov. Gosudarst. Univ. 2, 225 (1959).
12. A. V. Frost, Vestnik Moskov. Gosudarst. Univ. 3-4, 111 (1946).
13. K. V. Topchieva, Uchenye Zapiski Moskov. Gosudarst. Univ. 174, 75 (1955).
14. K. V. Topchieva and I. F. Moskovskaya, Doklady Akad. Nauk SSSR 123, 891 (1958).*
15. A. Ya. Rozovskii and V. V. Shchekin, Trudy Inst. Nefti Akad. Nauk SSSR 10, 286 (1957).

*Original Russian pagination. See C. B. translation.

ON THE QUESTION OF THE WALL HEAT TRANSFER COEFFICIENT IN PACKED TUBES

M. É. Aerov and Ya. F. Batishchev

Scientific Research Institute for Synthetic Alcohols, Novocherkassk Polytechic Institute
Translated from Kinetika i Kataliz, Vol. 1, No. 3, pp. 478-482,
September-October, 1960
Original article submitted February 20, 1960

On the basis of a treatment of published experimental data, a relationship is proposed for the determination of wall heat transfer coefficients in packed tubes. It is shown that the overall and the wall thermal resistance in packed tubes are commensurate.

In a paper by one of the present authors [1], the concept was introduced that heat transfer in a tube containing a granular bed (packing) may be divided into two stages: 1) the transfer of heat from the body of the flowing fluid to the wall of the tube (or the reverse), and 2) the transfer of heat through the boundary layer at the wall of the tube. Moreover, the thermal resistance of the stream is characterized by an effective coefficient of thermal conductivity γ kcal/m · hr · deg, and the concept of a wall (film) coefficient of heat transfer, α_w kcal/m^2 · hr · deg, was introduced to characterize the thermal resistance of the film at the wall.

The correctness of this representation of heat transfer has been confirmed by the work of other authors [2-7].

Additional resistance to heat transfer at the walls of packed tubes arises in the region of higher Reynolds numbers as a result of attenuation of turbulence at the solid walls, and it also occurs in the region of low Re_e owing to the fact that, as shown in the work reported in [8], the layer of spheres at the wall are arranged in regular cubic packing with a minimum number of contacts between the spheres in the direction of heat transfer (along the radius of the tube), and, consequently, there is a sharp decrease in the heat transfer coefficient in this layer, the thickness of which is two sphere diameters, according to [8].

The values of the transfer coefficients reported in reference [1] were determined from the overall heat transfer coefficients measured by different authors and were calculated using the thermal conductivity values reported in [9]. The experimental material available at the time of publication of [1], was not sufficiently accurate, not did it encompass the region of low Reynolds numbers. The experimental data of one of the authors of the present article on over-all heat transfer coefficients in a packed tube [10] have filled this gap.

The conditions of the experiments reported in [10] were briefly the following. Air was pumped by a compressor downward through a tube having a diameter of 31.5 mm and filled with spherical steel packing (bed height, 518 mm). The tube was externally heated by boiling water.

The air flow was measured by means of a double edge orifice plates. Average air temperatures over the inlet and outlet cross-sections of the tube were measured with platinum resistance thermometers connected to bridge circuits. Copper–constantan thermocouples were used to measure the wall temperatures. All measuring apparatus were carefully calibrated prior to the experiments.

All experiments were carried out under steady state thermal conditions. The error in the measurements of the heat transfer coefficient did not exceed ± 5%.

The experimental data were treated by means of the equation (see [1])

$$\frac{Nu_{e.w}}{Pr^{1/3}} = f(Re_e), \tag{1}$$

where

$$Nu_{e.w.} = \frac{\alpha_w \cdot d_e}{\lambda_g}, \tag{2}$$

$$Pr = \frac{\nu}{a}, \tag{3}$$

$$Re_e = \frac{G \cdot d_e}{\mu \cdot \varepsilon} \tag{4}$$

$$d_e = \frac{4\varepsilon}{a^1}. \tag{5}$$

In Eqs. (1-5): $Nu_{e.w.}$ is the wall Nusselt number; Pr is the Prandtl number; Re_e is the Reynolds number; d_e is the equivalent diameter of the voids in the packed tube, meters; λ_g, ν, α, and μ are, respectively, thermal conductivity, kcal/m/hr · deg, kinematic viscosity, m^2/sec thermal diffusivity, m^2/sec and dynamic viscosity of air, kg · sec/m^2, which is related to the logarithmic average temperature gradient; g = 9.81 m/sec^2; G is the actual mass air flow rate kg/m^2 · sec; e is the voidage in the packed tube m^3/m^3; α^1 is the surface of the packing and tube per unit volume of bed m^3/m^3.

The wall heat transfer coefficients, α_w were calculated by the method described in reference [1]. The effective coefficients of thermal conductivity required for the calculations were taken from reference [11].

The minimum value of the Nusselt number at the tube wall in the region of low Reynolds numbers, where turbulance has practically died out through the entire bed, can be evaluated from the following considerations: As already indicated above, the thickness of the low-conductivity layer can be taken as $\delta = 2d$. The thermal conductivity in this region cannot be lower than the value of λ_g. The value of the wall heat transfer coefficient will be:

$$\alpha_{w.min.} = \frac{\lambda_g}{\delta}. \tag{a}$$

Substituting (a) in $Nu_{e.w.}$, we obtain:

$$Nu_{e.w.min} = \frac{\alpha_{w.min} \cdot d_e}{\lambda_g} = \frac{d_e}{\delta}. \tag{b}$$

Under our conditions

$$d_e = \frac{4\varepsilon}{a^1} \cong 0{,}33\ d.$$

Substituting these values of d_e and δ in (b), we obtain:

$$Nu_{e.w.\ min} = 0.165. \tag{c}$$

This value must be too low, since the true heat transfer coefficient in the layer at the wall must be higher than λ_g.

Part of the data on $Nu_{e.w.}$, the data obtained in the region $Re_e < 40$, proved to be below the values of $Nu_{e\ w.\ min}$. This can apparently be explained on the basis that the longitudinal thermal conductivity, the value of which increases with the appearance of convection currents in the packing• [12], begins to exert a considerable effect on temperature distribution in the bed in the region where $Re_e < 40$. We did not include data on $Nu_{e.\ w.}$ in the region of $Re_e < 40$ (for $\underline{d}$ = 2.1 mm, five points; for $\underline{d}$ = 4 mm, three points) in the general graph.

The results of our treatment of the experimental data are shown graphically in Fig. 1. The parameter Z in this figure is the ratio of tube and sphere diameters.

•Downward movement of the gas with simultaneous heating.

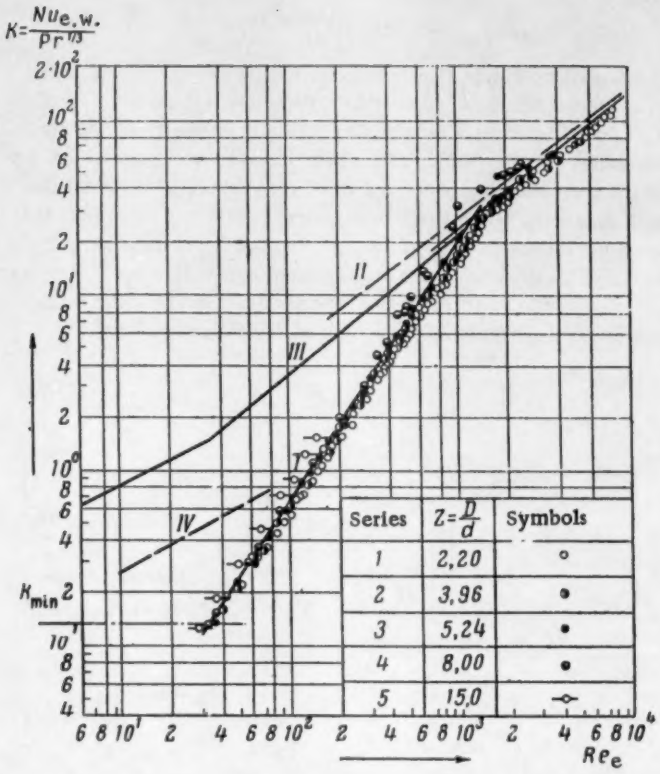

Fig. 1.

It can be seen from Fig. 1 that the experimental points satisfactorily fall along two lines (I) which have different slopes. The equations of these lines can be put in the following forms:

first zone ($Re_e = 40 - 1250$)

$$Nu_{e.w.} = 0{,}000685 \cdot Pr^{1/3} \cdot Re_e^{1{,}50}; \tag{6}$$

second zone ($Re_e = 1250 - 10{,}000$)

$$Nu_{e.w.} = 0{,}100\, Pr^{1/3} \cdot Re_e^{0{,}8}. \tag{7}$$

The relationship $Nu_{e\ w.}/Pr^{1/3} = f(Re_e)$, taken from [1], is also plotted in Fig. 1 (II).

In the region of $Re_e > 1250$, the lines for these two relationships lie close together; the change in the nature of the curves at $Re_e = 1250$, found in the earlier work [1], was not observed.

Shortly after the conclusion of the present work, the investigation of Yagi and Wakao relative to the determination of wall heat and mass transfer coefficients was published [13]. The heat transfer coefficients were determined from the temperature distribution along the height of the bed, and the mass transfer coefficients were determined from the rate of solution in water of a layer of β-naphthol coated on the wall of the tube. Different shapes of packing, chiefly of irregular shape, were used. Calculations based on the results of these measurements showed that heat and mass transfer are analogous in this case. The relationship proposed in reference [13] for the region $Re_e = 2000 - 6$ is plotted in Fig. 1 in our coordinates [III]. In the recalculation of the data of reference [13], the value of ϵ was taken as $\epsilon = 0.4$. Out recalculation of the proposed relationship [13] gave the following:

$Re_e = 38 - 2000$,

$$Nu_{e.w.} = 0{,}082\, Re_e^{0{,}8} \cdot Pr^{1/3} \tag{8}$$

and $Re_e = 6 - 38$

$$Nu_{e.w.} = 0{,}253\, Re_e^{1/3} \cdot Pr^{1/3}. \qquad (9)$$

As may be seen upon comparison of Eqs. (7-8) and from the figure, agreement of the results of the two investigations in the region of 2000-600 are in complete satisfactory agreement, especially when it is recalled that the values of the transfer coefficients were obtained by different experimental methods and methods of calculation. Equation (7) gives transfer coefficient values, which are averages between the data of references [1] and [13] it can be considered that the equation has been confirmed for packing of different shapes. In the region of $Re_e < 600$, the divergence of the results of the two investigations becomes greater, and it is impossible to explain the divergence by experimental error. In particular, at $Re_e = 30$, the difference in the values of $Nu_{e.w.}$ exceed one order of magnitude. This difference can be explained by a difference in the boundaries between the tube wall and the packing [6, 8]. Equations (6), (8), and (9) correspond to two extreme packing structures resulting from smooth metallic spheres and other forms of packing with different surfaces.

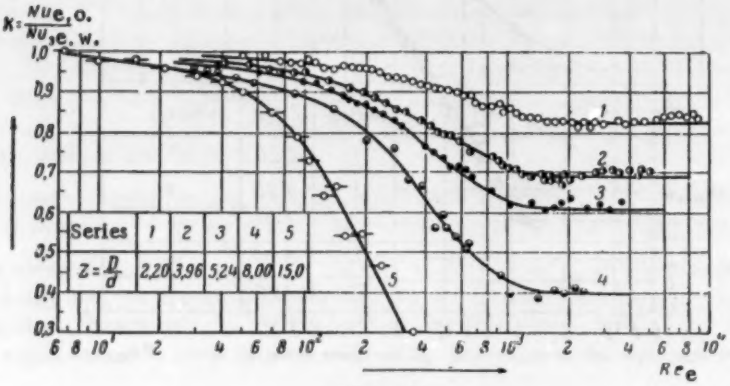

Fig. 2.

For comparison, the data of Fal'kovskii [14] on heat transfer coefficients for transfer from a bed of glass spheres to the tube in the low Re_e region are plotted in Fig. 1. Inasmuch as in this case practically all of the resistance is concentrated at the walls of the tube (see Fig. 2), the values of $Nu_{e\ w.}/Pr^{1/3}$ plotted in Fig. 1 were calculated from the over-all heat transfer coefficients. The data of Fal'kovskii [14] lie close to our values, although they do exceed them (IV).

On the basis of the data on over-all and wall heat transfer in packed tubes, it is easy to determine the fraction of the over-all resistance to heat flow present in the region of the wall, particularly for tubes having the diameter of the one tested:

$$K = \frac{Nu_{e.o.}}{Nu_{e.w.}}, \qquad (10)$$

where $Nu_{e.o.}$ is the Nusselt number calculated from the over-all heat transfer coefficient in the packed tube.

The relationship $K = \varphi(Re_e)$ has been plotted in Fig. 2 using the data of reference [10]. This figure shows that the resistance of the wall film in tubes must not be neglected in calculations of heat transfer in contacting apparatus. Since in the region of high Re_e $\lambda \cong f(Re_e)$, and $Nu_{e\ w.} \cong f'(Re_e)^{0.8}$, the value of K must pass through a minimum.

SUMMARY

1. The existence of general rules for heat transfer at the walls of tubes filled with spherical packing has been shown, and these rules hold over the range Re_e = 600-10,000 for gases with physical constants close to those of air. Moreover, two heat exchange zones and the boundary between them have been established.

2. In the region of $Re_e < 600$, the single relationship $Nu_e = f(Re_e, Pr)$, which holds for the investigations of other authors was not found to hold in the present investigation; this is apparently associated with the different bed structure in the region directly adjoining the wall of the apparatus.

3. It was shown that the over-all and wall resistances to heat flow in packed tubes are commensurate over the entire range of packing properties and hydrodynamic conditions investigated.

LITERATURE CITED

1. M. E. Aerov, Doctorate Dissertation, Moscow Institute of Chemical Machinery (1951); M. E. Aerov and N. N. Umnik, Zhur. Tekh. Fiz. 21, 1364 (1951).
2. W. Brötz, Chem. Eng. Techn. 23, 408 (1951).
3. C. A. Coberly and W. R. Marschall, Chem. Eng. Progr. 47, 141 (1951).
4. Y. R. Felix, Ph. D. Thesis. Univ. Wise (1951).
5. D. Plautz, Ph. D. Thesis. Univ. of Illn. (1953).
6. T. Y. Hanratty, Chem. Eng. Sci. 3, 209 (1954).
7. I. H. Quinton and I. A. Storrow, Chem. Eng. Sci. 5, 245 (1956).
8. L. H. S. Roblie, R. M. Baird, and I. W. Sierney, A. I. Ch. E., J., 4, 460 (1958).
9. M. E. Aerov and N. N. Umnik, Zhur. Tekh. Fiz. 21, 1351 (1951).
10. Ya. F. Batishchev, Trudy Novocherkassk. Politekh. Inst. 70/84, 33 (1957).
11. Ya. F. Batishchev, Trudy Novocherkassk. Politekh. Inst. 70/84, 45 (1957).
12. M. E. Aerov and N. N. Umnik, Zhur. Tekh. Fiz. 21, 1009 (1951).
13. S. Yagi and N. Wakao, A. I. Ch. E., J. 5, 79 (1959).
14. V. B. Fal'kovskii, Zhur. Tekh. Fiz. 23, 2176 (1953).

REPORT

SECOND EUROPEAN SYMPOSIUM ON THE PROCESSES OF CHEMICAL TECHNOLOGY

G. K. Boreskov and M. G. Slin'ko

Translated from Kinetika i Kataliza, Vol. 1, No. 3, pp. 483-487
September-October, 1960
Original article submitted June 30, 1960

The Second Symposium of the European Federation of Chemical Engineers was held between April 26 and April 29, 1960 in Amsterdam, on processes of chemical technology.

The European Federation of Chemical Engineers is an association of the technical and scientific chemical societies of Europe. It was established in Paris in 1953. The chemical societies of Great Britain, France, The Federal German Republic, Italia, Spain, Luxemburg, The Netherlands, Belgium, Greece, Portugal, Sweden, Norway, Yugoslavia and Switzerland.

The technical secretariat on the processes of chemical technology directs the Division of Chemical Technology of the Royal Institute of Engineers, and the Section of Technical Technology of the Royal Netherlands Chemical Society in Amsterdam. These two societies have arranged the convening of the symposium reported here.

About 400 persons took part in the work of the Symposium, including 172 from the Netherlands. The remaining participants were drawn from 13 European countries which are members of the European Federation of Chemists. West Germany was represented by 86 persons, Great Britain by 46, France by 27, Switzerland by 10, Belgium by 8, etc. In addition, delegates from non-European countries were also present, including 10 persons from the USA, 1 from India, 1 from the United Arab Republic, together with a delegation of 3 members from the Soviet Union.

During the Symposium, 12 sessions were held and 29 communications were presented. The major trend of the Symposium was toward the working out of methods of calculating the rate of industrial chemical processes, and the determination of optimum conditions for carrying out these processes. The problem was considered in the case of catalytic processes, as well as of reactions between gas and liquid, between two liquids, and between liquid or gas and solid.

In this survey we shall be mainly concerned with the communications on catalytic processes.

In a short introductory communication, Rijtem (The Netherlands, Eindhoven), referred to the important part played by the kinetics of chemical reactions in the investigation and development of chemical processes.

In the second communication, Kuhler (West Germany, Frankfurt), under the heading "Micro and Macrokinetic Methods of Increasing Yield" dealt generally with the value of micro- and macrokinetic factors for technological processes, but also considered specifically two problems having some slight connection with each other.

The first of these problems concerned the possibility of predictive regulation of the properties of semiconductor catalysts. This problem is of considerable interest, but is not directly connected with the major theme of the Symposium. Kuhler used the data provided by experimental work in his own laboratory on nickelous oxide

to which lithium and gallium oxides have been added to support the conclusion that the connection between the concentration of the current carrier in semiconductors and their catalytic activity is not as simple as might be expected on the basis of contemporary theoretical assumptions. At present it is not possible to predict the effect of definite additives on the activity of a catalyst. This conclusion is in agreement with the new works of Soviet scientists of which the contributor was unaware. The second part of the communication was devoted to a consideration of the optimum heat removing capacity of the apparatus from the catalyst, during the course of a reversible exothermic reaction. There were no general conclusions in the form of equations presented during the communication, but numerical data were presented for a hypothetical second order reaction characterized by definite values for the energy of activation and heat of reaction. In the work of Soviet scientists of which the contributor seemed to be unaware, there is given a general, rigid solution of the problem of the optimum temperatures and the optimum heat removing power from the contact mass.

In two sessions devoted to selectivity and optimum conditions, six communications were presented:

Denbigh (Great Britain, Edinburgh), in a paper entitled, "The Differential and Total Yield of Reactions," considered in detail the formal relationships which determine the differential and total yield of complicated reactions, for processes carried out in a reactor without stirring, in a reactor with thorough mixing, and in cascade reactors with thorough mixing. He showed that if the differential selectivity diminished with increase in the degree of conversion, then an ideal tubular reactor gives the maximum over-all sensitivity, in comparison with a single, or several series apparatuses with thorough mixing. If the differential yield in any region of concentration change increases with increase in the degree of conversion, then it may be possible to attain a higher total selectivity in cascade apparatuses with thorough mixing, in comparison with the tubular apparatus. In all cases the division of a process into stages ought to be performed with a view to providing conditions for maximum total selectivity of the process. The relationships discovered were illustrated by means of two examples: successive reactions of the first order (chlorination), and a process with unknown kinetic relationships (the nitration of hexamethylenetetramine). The methods of calculation which were set out were concerned, primarily, with isothermal processes, and so have only a limited application.

Schenemann (West Germany: Darmstadt), in a paper entitled, "The Consecutive Application of Chemical Kinetics for the Working Out of New Processes with Complex Reaction Mechanisms," described experiments on the working out of a process for the preparation of furfurol from xylose by removal of the elements of water in the presence of acids. The kinetics of this process have been investigated, which is complicated by the subsequent conversion of the furfurol into a resin, and also by its interaction with the intermediate products of the dehydration. With the object of improving the furfurol yield, use was made of the extraction of the furfurol by means of tetramine during the course of its formation. Possible types of reactor were considered in detail: a flow reactor equipped with a stirrer; cascade reactors with a stirrer for direct and counter movement of the xylose and the tetramine. The contributor suggests that the succession of stages in this process may be employed also to determine the optimum conditions for performing other processes.

Chermin and Krevelen (The Netherlands, Galeen, in a paper entitled, "Selectivity in Successive Reactions," estimated the selectivity for a process consisting of the two successive reactions:

$$aA \xrightarrow{k_1} B \text{ (mth order)} \qquad (1)$$

$$eB \xrightarrow{k_2} L \text{ (nth order)} \qquad (2)$$

The selectivity of the process is determined by the dimensionless parameter:

$$s = a^{n-1} C_{A_0}^{m-n} \frac{k_1}{k_2} .$$

The selectivity increases with increase in the parameter s. The results of calculating on electronic mathematical machines of change in concentration of intermediate product B, and its maximum value in relation to the selectivity parameter and the dimensionless time, $\tau = k_1 C_{A_0}^{m-1} t$, were presented by the contributor in the form of tables and graphs. Thus, as an example, for reaction of the first order when s = 10, the maximum possible selectivity is equal to 0.77.

In the first part of a communication entitled, "The Optimum Change of Temperature and Concentration," Gorn (West Germany, Frankfurt), carried out an analysis of the optimum temperature conditions for the carrying

out of reversible exothermic reactions. This analysis has no particular value, since the work of Soviet scientists provides more convenient equations for the determination of the optimum temperatures. Very much greater interest attaches to that part of the communication which was concerned with the determination of the optimum conditions for carrying out complex reactions. Original conclusions were given for the optimum conditions for the case of parallel reactions of any order when the process is carried out in a cyclic manner, and also for the case of a more complex combination of four parallel and successive reactions.

Veuse and Voeter (The Netherlands, Amsterdam), in a paper entitled, "The Optimum Concentration Gradients and Pressure Gradients in a Tubular Reactor," considered the effect of pressure on the rate of reactions occurring with increase in volume, and the optimum distribution of concentrations for two parallel reactions.

The rate of reactions taking place with increase of volume (for example, the reaction for the removal of the elements of water) is increased by increase in pressure, as a consequence of the growth in the number of molecules, and is diminished by the diminution in the equilibrium degree of transformation. There must therefore, for a given degree of conversion, exist an optimum pressure for which the maximum velocity is attained. This optimum pressure is reduced with increase in the degree of conversion. Thus, for example, for a reaction of the type $A \rightleftharpoons 2B$, the optimum pressure is approximately proportional to the instantaneous concentration of the initial component. If alteration of the pressure is carried out in accordance with the optimum curve, the volume of the reactor need only be a half to one third of the volume of a reactor in which constant pressure is maintained.

The authors also considered the optimum distribution of concentrations for a process consisting of two parallel reactions:

$$A + B \xrightarrow{k_1} C,$$
$$A + A \xrightarrow{k_2} D,$$

where C is the desired product.

The optimum yield under these conditions is obtained if there is maintained in the reaction mixture a minimum concentration of the component A, which will be possible if this component is introduced in stages along the reaction tube according to the increase in the degree of conversion of the component B. The results of calculating the optimum yield, in relation to the length of the reactor, the sensitivity parameter k_1F_B/k_2F_A, and the type of reactor, have been obtained with the help of electronic mathematical machines, and were given in the form of tables and graphs.

Grutter and Messikommer (Switzerland: Basle), in a paper entitled, "A Systematic Calculation of the Yield for Isothermal Reactors in the Case of Complex Reactions," described a general method for setting up the initial equations for the estimation of complex processes, using a range of parallel and consecutive reactions.

On the basis of stoichiometric relationships, equations for mass balance and equations for the rate of chemical transformations, calculated formulas were produced for the differential and total yields in a complex process. The records of the relationships were provided in the form of a short matrix arrangement. The method of calculation worked out was illustrated on the example of the oxidation of naphthalene on vanadium pentoxide as catalyst. At the conclusion of the paper, methods of calculation of the maximum total yield for an isothermal process for two parallel first order reactions were considered.

Four papers were devoted to the general problem of the evaluation and planning of chemical reactors:

1. Hoffmann (West Germany, Darmstadt), in a paper entitled, "The Present Condition of Calculations of the Distribution of Lifetimes in Technical Reactors."*

2. Hofftejzer and Zwitering (The Netherlands, Geleen), in a paper entitled, "The Characteristics of a Homogeneous Reactor for the Polymerization of Ethylene."

3. Youle (Great Britain, Harrogate, Imperial Chemical Industries Ltd.), in a paper entitled, "The Modelling of Chemical Reactors."

4. G. K. Boreskov and M. G. Slin'ko (USSR), "The Evaluation of Catalytic Processes in Industrial Reactors."

* "Lifetimes" signifies here the time during which the reaction mixture remains in the apparatus—Translator.

The first paper provided a review of work devoted to the time during which the reaction mixture remained in the apparatus. It is usually supposed that every part of the stream entering the apparatus remains for the same time. This premise is in many cases not realized since, because of the non-uniform flow of the gas, longitudinal diffusion and other causes, mixing takes place between the new stream and the reaction mixture in the apparatus. The magnitude of the reverse mixing depends on the type of apparatus. The determination of the concentration distribution along the reactor in relationship to the time, is performed by integration of the mass balance equation:

$$dC/dT = -\mathrm{div}(Cu) + \mathrm{div}\,(D\,\mathrm{grad}C),$$

where C are the concentrations, $\underline{u}$ is the linear velocity, and D is the mixing coefficient.

The paper included a solution of this equation for different types of apparatus, in both single phase and two phase systems. Three physical models were considered for the course of the gas through a tubular reactor provided with a nozzle—a diffusion model, a cellular model, and a channel model—and criterial equations were given for the calculation of the mixing coefficient in relation to constructural and technological parameters. The author believes that reverse mixing in the apparatuses is considerably greater than has hitherto been supposed.

The paper by Hofftejzer and Zwitering on the determination of the region of stable conditions, and the regulation of the process for the preparation of polyethylene at high pressure, aroused great interest. These authors believe that the rate of polymerization is proportional to the square root of the concentration of the initiator, and that the consumption of the initiator is proportional to the first power of its own concentration. By carrying out an analysis of the equations for mass and heat balance by the method of Lyaponov, the authors have found the limits of stability, and have found that the process is carried out in an unstable region in the industrial process. The condition that $(dQ_T/dT) > (dQ_p/dT)$ is not fulfilled, but the condition that $(dQ_T/dT) > [Q_p/(RT^2E)] - c_V\lambda P_m$ is observed. For certain values of the initial inhibitor concentration and the temperature, five stationary states of the system are possible. At the conclusion of the communication, the conditions were set out for the automatic regulation of the process of polymerization in the nonstationary region.

In the communication by Youle, the general principles and problems of modelling were described, for the working out of new methods of obtaining chemical products for various stages of the investigation. At the laboratory stage, the basic task of calculating and modelling is the determination of the mechanism of the reaction. Physical and engineering factors enter into the following stages, and these depend on the scale of operations. Simultaneously with this, modelling is of importance in the determination of the optimum conditions when the process is projected into pilot, and then into industrial, plants; and in the controlling of the work in the operating factory; and in automatic control of the processes.

In the communication by G. K. Boreskov and M. G. Slin'ko, there was described a general method of evaluating catalytic exothermic processes, and contact apparatuses with adiabatic layers of the catalyst, internal heat exchange and pseudoliquid layer. The general propositions were illustrated by examples of calculations for the oxidation of cerium dioxide and ethylene, made with the aid of cipher and other types of calculating machines. In addition, this communication contained a consideration of the stability conditions for contact processes.

The following communications were submitted to the division on catalytic processes:

1. Stirmen, Karsmeiner and Hofftejzer (The Netherlands, Geleen), on "An Investigation of the Oxidation of Cyclohexane by Air under Pressure in an Experimental Plant."

2. Kobel (West Germany, The Institute of Technical Chemistry in Berlin), on "Heterogeneous Gaseous Catalysis in an Apparatus containing the Catalyst in the Form of a Suspension."

3. Grotuis (The Netherlands, Amsterdam), "The Reaction Kinetics of the Shell Process for the Purification of Gasoline."

4. Schutil and Schwalb (West Germany, Frankfurt), "The Relationship between the Rate of Oxidation of Cerium Dioxide in Stationary and Pseudoliquid Layer of Catalyst, and the Size of the contact area.

5. Mars (The Netherlands, Geleen), on "The Factors Controlling the Operation of an Adiabatic Reactor for the Conversion of Water Gas."

The authors of the first of these communications used the example of the oxidation of cyclohexane by air under a pressure of 8 to 10 atm and at a temperature of 150 to 160° in the presence of a dissolved cobalt salt at a

concentration of 0.5 to 2.5 ppm, to provide a plan for the creation of a new process, from its origination in laboratory studies to its projection as an industrial enterprise.

Great interest attaches to the new methods of carrying out heterogeneous catalytic processes in the liquid phase using a suspended catalyst, illustrated by Kolbel by means of the example of the interaction of carbon monoxide with water vapor. The catalysts consisted of metals of the VIIIth group of the Mendeleev Periodic Table. Kolbel has investigated in detail the course of the process in a contact apparatus, using a suspended catalyst in the liquid phase. The process consists of two stages:

$$CO + H_2O \rightleftarrows H_2 + CO_2$$

$$\frac{CO + 2H_2 = (-CH_2-) + H_2O}{3CO + H_2O = (-CH_2-) + 2CO_2 + 58{,}4\ \text{kcal/mole}(-CH_2-)}.$$

The process is carried out at a pressure of 10-20 atm; the gas passes through the liquid in the form of fine bubbles, the liquid consisting of a synthetic hydrocarbon containing the suspended catalyst. The change from a suspended layer of catalyst in the gas phase to the process using liquid has made it possible to obtain higher selectivity in the process, a reduction in the quantity of methane formed, and an extension of the period in which the catalyst can be used.

The Shell process for the purification of gasoline consists in the oxidation of the mercaptans by means of the oxygen of the air into disulfides, according to the reaction:

$$4RSH + O_2 \rightarrow 2RSSR + 2H_2O$$

in the presence of potassium hydroxide solution and with the addition of organic compounds. The mercaptan and the air, dissolved in the hydrocarbons, pass into the alkaline solution, where the mercaptan is oxidized into the disulfide. This compound is insoluble in the alkali, and is again transferred to the gasoline. In order to increase the solubility of the mercaptans in the alkaline phase, special additives ("solutizers") are used. The fatty acids appear to be very effective in this capacity. It is found that the rate of the heterogeneous reaction between oxygen and the mercaptan is proportional to the concentration of the oxygen, and to that of the mercaptan to the power of 0.25. The over-all rate of the process is determined by the rate of transfer of the oxygen from the gaseous phase into the solution.

In the communication of Schutil and Schwalb, the problem was discussed of the effect of the process of transfer of the reacting gases within the granule on the rate of oxidation of cerium dioxide on industrial vanadium catalysts. The work was not original, and is of no particular interest.

Mars, in his communication, provided experimental data on the kinetics of the conversion of carbon monoxide on an iron-chromium catalyst. These data consisted in the results of analysis of two successive adiabatic reactors for the preparation of hydrogen; and the results of the calculation (which was carried out on electronic machines) on an industrial apparatus under variable initial conditions. According to the data produced by Mars the rate of the carbon monoxide conversion is proportional to the difference between the actual and the equilibrium concentrations of the carbon monoxide. Under industrial conditions the kinetic conditions correspond to the region of internal diffusion. The activity of the catalyst depends on the concentration of hydrogen sulfide in the gas. Increase of this caused diminution of activity. The results of measuring the catalytic activity under laboratory conditions, and the magnitudes calculated from the data on an industrial reactor, are found to agree well among themselves. On the basis of the results obtained with the help of calculations made on electronic machines, estimates have been made of the effect of the dimensions of the particles, the temperature of the gas entering the apparatus, and the hydrogen sulfide content, on the nature of the process whereby carbon monoxide is converted in the adiabatic layer of the catalyst.

In addition to the contributions mentioned, the following communications were heard:

1. Andrew and Henson (Great Britain, Billingham, Imperial Chemical Industries Ltd.), on "The Dynamics of the Adsorption of Oxides of Nitrogen."

2. Kramers and Shoek (The Netherlands, Delft), on "The Adsorption of Nitrogen Tetroxide by Water Sprays."

3. Hemond (France, Nancy), on "The Adsorption of Gas by a Liquid Layer During the Course of a Chemical Reaction Under Laminar Conditions."

4. Trambouse (France, Petroleum Institute), on "Evaluation of Reactors for the Carrying Out of Reactions Involving the Participation of Two Liquid Phases."

5. Teresen, Erga, Sorsen and Ve (Norway, Trondheim), on "Processes Whose Over-All Rate is Determined by the Rate of Interaction of a Liquid with a Solid."

6. Le Hoff, Bonnetin and Letort (France, Nancy), on "The Control of Physical Factors in the Laboratory Investigation of the Chemical Reaction Between Gas and Solid."

7. van Geld (The Netherlands, Delft), "The Reaction Between Carbon and Oxygen."

8. Hedden (West Germany, Munster), on "The Value of the Reactivity of a Fuel for Shaft Furnaces Working on Coke."

9. Bekker-Bost (West Germany, Bochum), "The Planning of Apparatus for Ion Exchange."

10. Kupper and Lloyd (The Netherlands, Limburg), on "The Reaction Between Solids and Gases in the Treatment of Uranium."

11. Villars (France, Nantes), on "A Study of a Reaction, Whose Total Rate is Determined By a Physical Stage."

12. Asbjornson (Norway, Trondheim), on "The Distribution of the Time of Delay in a Flowing, Thin, Liquid Film."

• • •

The work of the Second Symposium on the Processes of Chemical Technology has shown that during recent years and in all foreign countries, much importance is being attached to the development of methods of evaluating chemical reactors. Large groups of investigators have been organized, and are engaged on the evaluation of apparatus by means of electronic mathematical machines. Scientific investigations on the kinetics and mechanism of reactions, and their engineering development are closely connected to each other. The methods which have been worked out permit of more complete and more accurate estimation of complex, multistage processes, and of the discovery of the optimum conditions for the attainment of maximum yields. For the solution of these problems, use has been made both of modern calculating machines, and of modern mathematical methods.

In the intervals between the sessions, meetings and private scientific discussions took place, thus making it possible to make contact with scientists of various countries where work is going on in the fields of catalysts and the theory of chemical processes.

The contributions to the symposium, as well as conversations with scientists from the different countries, have shown that the studies of kinetics and catalysts carried out in the Soviet Union are little known outside our boundaries, and the foreign scientists showed great interest in the work of Soviet scientists.

It should be added in conclusion that the work of the Symposium was well organized by the Organizing Committee, lead by Professor Kramers (The Netherlands, Delft).

SIGNIFICANCE OF ABBREVIATIONS MOST FREQUENTLY ENCOUNTERED IN SOVIET PERIODICALS

FIAN	Phys. Inst. Acad. Sci. USSR.
GDI	Water Power Inst.
GITI	State Sci.-Tech. Press
GITTL	State Tech. and Theor. Lit. Press
GONTI	State United Sci.-Tech. Press
Gosenergoizdat	State Power Press
Goskhimizdat	State Chem. Press
GOST	All-Union State Standard
GTTI	State Tech. and Theor. Lit. Press
IL	Foreign Lit. Press
ISN (Izd. Sov. Nauk)	Soviet Science Press
Izd. AN SSSR	Acad. Sci. USSR Press
Izd. MGU	Moscow State Univ. Press
LEIIZhT	Leningrad Power Inst. of Railroad Engineering
LET	Leningrad Elec. Engr. School
LETI	Leningrad Electrotechnical Inst.
LETIIZhT	Leningrad Electrical Engineering Research Inst. of Railroad Engr.
Mashgiz	State Sci.-Tech. Press for Machine Construction Lit.
MEP	Ministry of Electrical Industry
MES	Ministry of Electrical Power Plants
MESEP	Ministry of Electrical Power Plants and the Electrical Industry
MGU	Moscow State Univ.
MKhTI	Moscow Inst. Chem. Tech.
MOPI	Moscow Regional Pedagogical Inst.
MSP	Ministry of Industrial Construction
NII ZVUKSZAPIOI	Scientific Research Inst. of Sound Recording
NIKFI	Sci. Inst. of Modern Motion Picture Photography
ONTI	United Sci.-Tech. Press
OTI	Division of Technical Information
OTN	Div. Tech. Sci.
Stroiizdat	Construction Press
TOE	Association of Power Engineers
TsKTI	Central Research Inst. for Boilers and Turbines
TsNIEL	Central Scientific Research Elec. Engr. Lab.
TsNIEL-MES	Central Scientific Research Elec. Engr. Lab.– Ministry of Electric Power Plants
TsVTI	Central Office of Economic Information
UF	Ural Branch
VIESKh	All-Union Inst. of Rural Elec. Power Stations
VNIIM	All-Union Scientific Research Inst. of Metrology
VNIIZhDT	All-Union Scientific Research Inst. of Railroad Engineering
VTI	All-Union Thermotech. Inst.
VZEI	All-Union Power Correspondence Inst.

Note: Abbreviations not on this list and not explained in the translation have been transliterated, no further information about their significance being available to us. – Publisher.